Integration of Spatial and Motion Information in Amblyopia

Behzad Mansouri M.D.

Department of Neurological Sciences

McGill University

Montreal, Quebec, Canada

April 2005

Supervisor

Robert F. Hess Ph.D., D.Sc.

A thesis submitted to the

Faculty of Graduate Studies and Researches

In partial fulfilment of the requirements for the degree

Doctor of Philosophy

To my wife, Mandana

Who taught me love

To my son Parsa

Who taught me the joy of every second of life

To my supervisor, Robert

Who taught me patience and good science

Abstract

It has been shown that the amblyopic visual system is similar to that of the normal visual system at the levels before the visual cortex (i.e. retina and lateral geniculate body). The visual deficiency in amblyopia is thought to involve the primary visual cortex (V1), which can explain some of the known deficiencies (e.g. contrast sensitivity at high spatial frequencies) in amblyopia. However, recent studies suggest global processing deficits in amblyopia that are either independent of V1 cells or are beyond the striate cortex, suggesting an abnormality at the extra-striate cortex. We set out to study the nature of such global deficiencies.

We used a psychophysical approach to study how the amblyopic visual system integrates moving and static elements across space, compared to the control fellow fixing eye and normal observers' eyes. We used an equivalent noise model, which provided us with two independent variables of internal noise and number of samples. Each factor in the model, theoretically, captures a quota of the overall performance of the visual system. On one hand, an abnormality in internal noise is as if the internal representation of the stimuli is abnormal, at local or global stages. On the other hand, an abnormal number of samples is as if the processing efficiency is defective.

Our results show that the global functioning in both ventral and dorsal pathways is abnormal in amblyopia. However, the nature of this deficiency appears to be different from what was suggested before. The amblyopic visual system can integrate global motion or orientation, be it either luminance- or contrast-modulated, information when all

Résumé

Il a déjà été démontré que le système visuel amblyopique manifeste les effets similaires à ceux d'un système visuel normal quand étudié à des endroits avant le cortex visuel (i.e. 'retina' et 'lateral geniculate body'). On croit que la défaillance visuelle dans l'amblyopie prend racine dans le premier cortex (V1), ce qui explique certaine défaillances connues dans l'amblyopie comme la sensibilité au contraste dans les hautes fréquences spatiales . Cependant les études récentes suggèrent que le manque de traitement global dans l'amblyopie est soit indépendant des cellules V1 ou bien au-delà du cortex striate et, en conséquence, suggèrent l'anomalie dans le cortex extra-striate. Nous étudions la nature de telles défaillances.

L'approche psychophysique est choisie dans ce travail afin d'observer comment le système visuel amblyopique intègre les éléments statiques et mobiles dans l'espace. Il est compare au bon oeil de la personne avec amblyopie et celui d'on observateur normal. Le modèle choisi est le modèle 'Equivalent Noise Model' ce qui nous fourni 2 variables indépendantes, soit les bruits internes et le nombre d'échantillons. Chacunes de ces variables, en théorie, visent un aspect de la performance globale du système visuel. D'un coté, l'anomalie dans les bruits internes est comme l'anomalie dans la représentation interne du stimuli. D'autre part, un nombre anormal d'échantillons et comme la panne d'efficacité.

Nos résultats expérimentaux démontrent que le fonctionnement global dans les chemins ventraux et dorsaux est anormal dans amblyopie. Cependant, la nature d'un tel

défaut est différente de celle proposée dans les études posteriori. Le système visuel amblyopique est capable d'intégrer les informations globales du mouvement ou de l'orientation, luminance ou 'contrast-modulated', quand tous les éléments contenaient les informations utiles. Autrement dit, les personnes amblyopique peuvent intégrer aveuglément les informations globales. Elles ont démontre la même performance que celle des cas normaux et seulement leurs bruits internes sont augmentée aux hautes fréquences. Malgré ceci, dans la présence de bruits aléatoires pédestals, là où la combinaison aveugle des informations pour un observateur idéal a échoué de stimuler leurs résultats, le système visuel amblyopique a fortement été détérioré. Les bruits internes représentent ce phénomène, ces résultats contredisent les résultats obtenu dans les études anciennes. En effet, les anciens résultats qui suggéraient le fonctionnement global anormal dans l'amblyopie, appliquait les tâches où le signal et le bruit étaient présents simultanément. Pour effectuer ces tâches-la, le système visuel doit posséder une ségrégation efficace ainsi qu'un fonctionnement d'intégration. Notre approche systématique vers le fonctionnement global dans l'amblyopie montre la différence entre ces fonctions séparées et démontre que la défaillance est localisée dans la ségrégation plutôt que dans l'intégration.

Note to the examiners

This thesis consists of 6 manuscripts, 3 published, 1 in press and 2 submitted. The author of this thesis is the main researcher and first author in 4, and co-author in 2 manuscripts. The original publisher and co-authors have given their written consents that these manuscripts be included in this thesis. The manuscripts citations are:

1. Allen, H. A., Hess, R. F., **Mansouri, B.** & Dakin, S. C. Integration of first- and second-order orientation. Journal of Optical Society of America A: Optics, Image Sciences, and Vision 20, 974-986 (2003).

2. **Mansouri, B.,** Allen, H. A., Hess, R. F., Dakin, S. C. & Ehrt, O. Integration of orientation information in amblyopia. Vision Research 44, 2955-69 (2004).

3. **Mansouri, B.,** Allen, H. A. & Hess, R. F. Detection, discrimination and integration of second-order orientation information in strabismic and anisometropic amblyopia. Vision Research (in press).

4. Hess, R. E., **Mansouri, B.,** Dakin, S. & Allen, H. Integration of local motion is normal in amblyopia. Vision Research (submitted).

5. **Mansouri, B.,** Hess, R. F., Allen, H. A. & Dakin, S. C. Integration, segregation, and binocular combination. Journal of Optical Society of America A: Optics, Image Sciences, and Vision 22, 38-48 (2005).

6. **Mansouri, B.** & Hess, R. F. The nature of the extra-striate deficit in human amblyopia. Vision Research (submitted).

Contribution of authors

For all these experiment conceptualization, realization and designing the experiment were a joint effort between Dr. Hess and myself. I was the major contributor in screening the subjects, collecting the data and analyzing the results. Their final interpretation and preparation into manuscript was also a joint effort.

The main author of the chapter 1 was Harriet Allen. My contribution was in the experimental design, collection of data and the editing of the manuscript stages. Chapter 2 was an extension to a previous work by Steven Dakin, but in amblyopes. He wrote the original code, which was modified later by Harriet Allen and myself. Oliver Ehrt was involved in screening the amblyopic observers, data collection and discussions in this chapter. For chapters 2 to 6, I was the main author and experimenter.

Preface

Amblyopia or “lazy eye”, which means poor vision in Greek, is a condition of reduced best-corrected visual acuity mostly in one eye (i.e. 20/40 or less). It has been shown that the peripheral visual system in amblyopia, before the visual cortex (i.e. retinal cells and lateral geniculate bodies of the hypothalamus) is similar to that of normals (Cleland, Crewther, Crewther & Mitchell, 1982; Derrington & Hawken, 1981; Hess & Baker, 1984). There is evidence in human (Hess, Baker, Verhoeve, Tulunay, Keesey & France, 1985) and animal (Crewther, Crewther & Cleland, 1985) that the abnormality in amblyopia is due to defective central visual processing. Electrophysiology studies showed that some cells in striate visual cortex (i.e. V1) are affected (Kiorpes, Kiper, O'Keefe, Cavanaugh & Movshon, 1998; Kiorpes & McKee, 1999). Such dysfunction was sufficient to explain the well-documented psychophysical contrast sensitivity deficit in amblyopia. Furthermore, single cell neurophysiological studies of extra-striate function in amblyopia have shown that fewer cells are driven by the deprived eye (Schroder, Fries, Roelfsema, Singer & Engel, 2002; Sireteanu & Best, 1992). Brain imaging studies showed reduced striate and extra-striate visual cortex activity in amblyopia (Barnes, Hess, Dumoulin, Achtman & Pike, 2001; Sireteanu, Tonhausen, Muckli, Lanfermann, Zanella, Singer & Goebel, 1998).

Amblyopia affects up to 5% of the population worldwide and 2%-3% population in North America (Bateman & Caprioli, 2003). Amblyopia is an important public health problem because it is life-long and is the most important cause of uniocular blindness in adults (Blindness, ; Hillis, Flynn & Hawkins, 1983). Although this condition has been known for more than a millennium and initial treatments have been suggested more than a century ago, we do not have sensitive and specific measures to diagnose it, neither do we have an ideal treatment. The clinical diagnosis is exclusion of all other possible causes of poor vision and is based on reduced visual acuity. It has been shown that the poor visual acuity is neither a sensitive measure nor represents the severity of the visual deficits in amblyopia (Simmers, Gray, McGraw & Winn, 1999). Current treatment of amblyopia, aside from the optical correction of the refraction and surgical alignment of the affected eye, is nothing more than temporarily disabling the fellow fixing eye by patching it, which has been applied for more than hundred years. Recently an alternative treatment has been suggested that involves temporarily paralyzing the accommodation of the fellow fixing eyes (atropine eye drop). This treatment is also based on a similar rationale to patching. With current measures of diagnosis many amblyopes are missed and left to eventually develop poor vision. Furthermore, it has been shown that the compliance of children with this current treatment is no more than 25%. The author of this thesis has witnessed the frustration of children and their caregivers during the patching treatment. School age children have to wear a patch on their good eye even during school hours. Many of these children abandon their treatment because of its psychological stress, which costs them their vision in one eye. With current treatment protocols, even after a successful treatment, amblyopes never develop some specific visual functions such as stereovision because of the lack of targeting of such functions in the current treatments. Part of the failure to develop proper diagnostic measures and treatments is due to a lack of scientific knowledge regarding the main reasons for poor vision in amblyopia.

This research aims to help the scientists and clinicians to better understand the different aspects and causes of poor vision in amblyopia with emphasis on global integration function, which is believed to be performed in extra-striate cortex. Certainly, discovering the main causes of poor vision in amblyopia, will help us to establish better measures of early diagnosis and new methods of treatments.

Table of contents

Introduction

Precise orientation and direction perception of static and moving objects are important constituents to survival of many animals (e.g. food search and hunt chase). Local orientation information is a basic element of many textures; therefore, texture recognition would not be possible without accurate local orientation discrimination and precise global integration. Furthermore, the direction of a moving object consists of combined local directions of its elements and direction recognition crucially depends on subsequent integration. Our knowledge of the neurophysiological basis of these functions is still developing.

Cells in primary visual or "striate cortex" are sensitive to changes of the luminance within their receptive field, which is correlated with the contrast of the stimulus. For most V1 cells, the response to luminance changes is selective to the presence of image attributes such as orientation, spatial frequency, and direction (Hubel & Wiesel, 1979). The visual field is precisely represented on the striate cortex, which is called the retinotopic map. For any specific location of the visual field, corresponding V1 cells cover the whole range of the possible orientations (i.e. 0°-180°) and directions (i.e. 0°-360°). The receptive field of a neuron in primary visual cortex is relatively small (~1° and ~5° in simple and complex cells, respectively). Individual V1 cells mainly respond to local information within their receptive fields.

Extra-striate cortex consists of different areas that are represented by separate retinotopic maps (Zeki, 1978). The different areas in extra-striate cortex have been suggested to be functionally different. Originally, a dichotomy has been suggested in primates, which divides the extra-striate cortex into independent and separate ventral and dorsal pathways. The ventral pathway in temporal cortex is believed to perform form processing. The dorsal pathway which was leads to parietal cortex is believed to process motion information (DeYoe & Van Essen, 1988; Ungerleider & Mishkin, 1982; Van Essen, Anderson & Felleman, 1992). However, evidence is emerging that areas of the dorsal pathway can also analyse object shape therefore this dichotomy may not be as absolute as originally was thought (Kourtzi, Bulthoff, Erb & Grodd, 2002).

Different regions within these two processing streams are organized in a hierarchical way although they are not completely separated (Kourtzi et al., 2002). The dorsal stream involves areas V2, V3, V5 (MT) and MST and is thought to mediate motion processing and the localization of objects in space. The ventral pathway, which includes areas V2, V3, V4 and IT is thought to mediate the processing of spatial form and may be associated with perceptual discrimination of shape and contour. It has been shown that more complex processing occurs at areas further along the pathways.

Cells at later stages of the visual system (e.g. V2) have larger receptive fields and so can respond to bigger stimuli. However, in contrast to the responses of the cells at V1, their responses to stimuli is independent of contrast (Morrone, Burr & Vaina, 1995). The fact that the receptive field size of a neuron increases at higher levels of visual processing (e.g. V2), suggests that global integration of spatial information takes place at extra-striate cortex. However, we should bear another possibility in mind that the pattern of activation of V1 cells and their lateral interactions, independent of the activation of the cells at the next visual processing stage, may partially contribute to a more global analysis (e.g. opponency mechanism).

Normal visual system

Integration of first-order orientation spatial information

Initially, it was shown that our visual system responds to the changes of luminance across the visual field. Single cell recordings showed that the neurons in primary visual cortex respond to luminance-modulated information, which was selective for orientation and direction (Campbell & Robson, 1968). Suggested linear models, at the time, could perfectly describe the respond of the visual system to the luminance-modulated or first-order stimuli in local region of the visual field.

Integration of first-order orientation information across space has also been studied (Dakin, 2001; Dakin & Watt, 1994). These results suggest that the normal visual system can integrate orientation information efficiently across the spatial field (3°-12° of visual angle), number of elements (4-256), and densities. Observers had to average the orientation of an array of oriented Gabors and detect whether the mean orientation was tilted to right or left of vertical. The orientation of each element was a sample from a parent distribution with predetermined mean and standard deviation. As the standard deviation of the population (external noise) increased, the performance of the observer decreased. Interestingly, the visual system didn't perform perfectly without any external noise (i.e. all Gabors aligned). This suggested a noisy internal representation of the orientation in the visual system, either at local or global stages. At low external noise values the performance of the visual system was dependent on the internal representation of the external stimuli, which contained noise (i.e. internal noise). Increasing the variance in the stimuli array increased the effect of external noise, which was inversely affected by the number of samples that the visual system took into account, until it eventually overcame the internal noise. At high levels of variances, performance is mainly limited by the external noise. The number of utilized samples defines the steep region of the performance curve. A standard form of an equivalent noise model could describe the behaviour of the visual system well (Dakin, 2001). The internal noise parameter has been shown to be dependent on the density of the array of stimuli and the sampling efficiency to the number of elements in the array. We have applied a similar approach to investigate the integration function in amblyopic visual systems.

Integration of second-order orientation spatial information

It has been shown that, in addition to luminance-modulated information, there is contrast-modulated information in the visual field that contributes to visual perception from our surrounding environment (Derrington & Badcock, 1985). In other words, some stimuli in spite of having the same average luminance across a receptive field can be perceived by the visual system. The linear models could not describe the perception of such stimuli.

To explain the processing of contrast-modulated or second-order information in the visual system, an extra mechanism was needed, which involved a non-linearity such as rectification in between two stages of linear filtering (Chubb & Sperling, 1988; Graham, Beck & Sutter, 1992; Malik & Perona, 1990; Wilson, Ferrera & Yo, 1992). To what extent the first- and second-order information interact in the visual system is not yet clear. Neither do we know how much each type of information contributes to the final perception. We investigated whether first- and second-order orientation information is combined in the visual system. Our results show that they are not. Although the visual system could combine information of each type across space well when they are presented alone, when they are presented together, just one or the other is taken into consideration. The visual system didn't combine first- and second-order orientation information even when it would be of benefit (e.g. when the combination contains more useful information). If the observers didn't know which type contained the useful information, they tended to consider only the first-order information and segregate the second-order information. This suggests separate mechanisms for combining first- and second-order orientation information in the visual system where the first-order processing has dominance. This is discussed in detail in chapter 1.

Integration of motion information

Visual processing of global motion information (i.e. dorsal pathway) has been investigated more than global form processing (i.e. ventral pathway), possibly due to the availability of better-developed stimuli. Most studies concur on the location of motion integration in cortex. Previous studies showed that lateral occipital and posterior inferior parietal lobes in human, which are equivalent locations to MT (V5) and MST in monkey are involved in global motion integration (Mikami, Newsome & Wurtz, 1986a; Mikami, Newsome & Wurtz, 1986b; Movshon, Adelson, Gizzi & Newsome, 1985). The MT and MST cells have much larger receptive fields than the V1 cells, possibly containing many small subunits that represent V1 inputs (Movshon et al., 1985) with extensive centre-surround interactions (Allman, Miezin & McGuinness, 1985). Lesion studies in monkey (Newsome & Pare, 1988) and in human (Baker, Hess & Zihl, 1991) showed that the defect in MT/MST regions selectively impairs motion integration. Furthermore, it has been shown that micro-stimulation within these regions can bias motion direction discrimination (Salzman, Murasugi, Britten & Newsome, 1992). Cells in MT fall into two categories depending on whether they have facilitative or suppressive surrounds (Born & Tootell, 1992). Cells in the former category are hypothesized to be involved in integrative functions, whereas cells in the latter category in segregative functions.

Amblyopia

Integration of first-order orientation spatial information

Poor vision in amblyopia is due to deficits in central visual processing. Initially, it was shown that certain functions such as contrast sensitivity for high spatial frequency (Gstalder, 1971; Hess & Howell, 1977; Lawwill & Burian, 1966; Levi & Harwerth, 1977) are deficient, which it was suggested may be due to an abnormality of the neurons in striate cortex (V1) (Crewther & Crewther, 1990; Eggers & Blakemore, 1978; Movshon, Eggers, Gizzi, Hendrickson, Kiorpes & Boothe, 1987). However, the deficiency in amblyopia is not limited to V1 cells and contrast sensitivity. Amblyopes have been shown to be deficient in discrimination tasks involving orientation (Bradley & Skottun, 1984; Caelli, Brettel, Rentschler & Hilz, 1983; Demanins, Hess, Williams & Keeble, 1999; Vandenbussche, Vogels & Orban, 1986), spatial frequency (Hess, Burr & Campbell, 1980a), contrast (Hess, Bradley & Piotrowski, 1983) and phase (Caelli et al., 1983; Lawden, Hess & Campbell, 1982; Pass & Levi, 1982; Treutwein, Rentschler, Zetzsche, Scheidler & Boergen, 1996), in positional judgments for well separated elements where contrast sensitivity does not play a part (Hess & Holliday, 1992), in detection of contrast-defined stimuli (Wong, Levi & McGraw, 2001) and in tasks involving global vision (Hess, McIlhagga & Field, 1997b; Hess, Wang, Demanins, Wilkinson & Wilson, 1999c; Popple & Levi, 2000; Simmers, Ledgeway & Hess, 2005). Integration of orientation information across space has been shown to be deficient in different forms of amblyopia (Ellemberg, Lewis, Maurer, Brar & Brent, 2002; Simmers, Ledgeway, Hess & McGraw, 2003). Amblyopic deficiencies in performing tasks that especially require combining local information over larger areas is consistent with an abnormality of the neurons beyond V1 (Kiorpes et al., 1998; Schroder et al., 2002) as well as the abnormal interaction of the V1 cells (Schmidt, Galuske & Singer, 1999).

Previous studies showed that the integration of form is abnormal in amblyopia, which was shown to be independent of the V1 contrast sensitivity deficit. We were interested to find out to what extend the global orientation integration is affected in amblyopia, using a task where positions of the local elements were not important for the purpose of the task and where orientation discrimination had been equated in amblyopic and fellow fixing eyes at the local processing level. This would allow us to investigate pure orientation integration in amblyopic eyes. We used a mean orientation task similar to that applied by Dakin (2001), where the observer had to judge the average orientation of an array of oriented Gabors. The orientation of each Gabor was a sample from a parent distribution with predetermined mean and standard deviation. To better understand the integration function in amblyopia, we needed a model, which could describe and quantify our data. We used an equivalent noise model (Dakin, 2001) to derive the best fitting estimates of internal noise and number of samples from the threshold data. Internal noise and number of sample are two independent parameters that each captures one aspect of the overall integrating function in visual system. Internal noise, theoretically, describes internal uncertainty in the visual system when it combines the local elements in absence of external noise (i.e. all Gabors aligned, in this task). Internal noise consists of accumulated noises from different sources at various stages of visual processing from very early stages of local V1 processing to the orientation integration level (e.g. extra-striate cortex). The estimation of the average orientation of the stimulus array is poorer when the orientation standard deviation of the stimulus array increases. Therefore, the integration threshold increases when the stimuli array variance increases and this increases inversely with the number of samples that the visual system averages over. The equivalent noise model has been used in a number of vision studies before, e.g. contrast sensitivity (Ahumada & Watson, 1985; Pardhan, 2004), luminance offset detection (Barlow, 1957), coding of spatial position (Watt & Hess, 1987; Zeevi & Mangoubi, 1984), discrimination of edge blur (Watt & Morgan, 1983), spatial frequency acuity (Heeley, 1987), contour integration (Hess & Dakin, 1999), orientation discrimination (Heeley, Buchanan-Smith, Cromwell & Wright, 1997). In a similar task to ours, Dakin (2001) applied the equivalent noise model in normal observers. The model could nicely describe normal data. He showed that normal observers could integrate local orientation information efficiently over a large range of stimulus sizes, numerosity and density.

In chapter 2 we study whether the integration of orientation information across space in amblyopes is similar to normals.

Integration of second-order orientation spatial information

Studying the second-order global orientation information integration is particularly interesting in amblyopia for three reasons.

1- It has been shown that the amblyopes are deficient in detecting local second-order information (Wong et al., 2001), which is independent of their contrast deficiency. Interestingly, the fellow fixing eyes also show similar deficiencies in processing of second-order information.

2- It has been recently shown that amblyopes are deficient at integrating orientation (Lewis, Ellemberg, Maurer, Wilkinson, Wilson, Dirks & Brent, 2002; Simmers et al., 2005) and motion (Ellemberg et al., 2002; Simmers et al., 2003) information across space and this deficiency is worse for second-order stimuli.

3- There is evidence suggesting that the processing of second-order information takes place in extra-striate cortex (Dumoulin, Baker, Hess & Evans, 2003) and there have been profound functional anomalies found in the extra-striate regions of human amblyopes (Barnes et al., 2001).

In chapter 2 we asked whether amblyopic eyes could integrate first-order orientation information across space. If they cannot, one would presume that they wouldn't be able to integrate second-order orientation information either, because all previous studies showed that processing of second-order information is poorer in amblyopia (Ellemberg et al., 2002; Lewis et al., 2002; Simmers et al., 2005; Simmers et al., 2003). However, if they can, it would be very interesting to know whether normal integration of first-order orientation information extends to second-order stimuli.

In chapter 3 we study whether the integration of second-order orientation information is similar to that of normal eyes. We did a systematic study of second-order information processing at both local and global levels. First we equated the performance of the amblyopic and fellow fixing eyes for the first-order component (i.e. carrier) of the second-order stimuli. Then we equated the amblyopic and fellow fixing eyes for discrimination of second-order orientation at the local level. As a result, we were able to investigate pure second-order integration. If the amblyopic eye is abnormal in integrating second-order orientation, it would not be simply due to its first-order (contrast) deficiency neither would it be because of a deficient local second-order orientation discrimination. We used a similar task to that of our first-order integration experiment (i.e. mean orientation task). The equivalent noise model was fitted to the data, which provided the two parameters, internal noise and number of samples.

Integration of motion information

It has been shown that motion integration is disrupted in amblyopia (Ellemberg et al., 2002; Simmers et al., 2003). These studies have used a random dot kinematogram paradigm where the ratio of signal to noise elements is varied (termed % coherence). Observers discriminate the direction of the signal elements for different levels of coherence noise. It is hypothesized that if observers can integrate local information, they can perform the task. However, the inability of observers to perform such tasks may be due to one of two possibilities. First, abnormal signal integration might lead to abnormal results. Second, abnormal signal from noise segregation might cause a similar deficiency because in order to do the task visual system has to segregate noise from signal and then integrate just the signal elements. An abnormality in either function would cause an inability to perform the task.

We have investigated the extra-striate ventral pathway in amblyopia through studying orientation integration in chapter 2 and 3. It has been suggested that the dorsal pathway is more vulnerable than the ventral pathway to the visual abnormalities during the critical period of visual system development (first decade of life in human) (Braddick, Atkinson & Wattam-Bell, 2003). It is of interest therefore to study whether amblyopes are abnormal in pure integration of motion across space. We answered this question in chapter 4. We used a paradigm where all elements presented are signals and carry useful information. The direction of each moving element is a sample from a parent distribution with mean equal to the cued direction and predetermined variance. In order to perform the task, observers had to combine direction information across space.

The effect of coherence noise

In chapter 1, we show that the presence of pedestal noise elements, which are random samples from a uniform distribution, disrupt the performance of a normal observer in an integration task such as ours. It results in an increase in the internal noise and a decrease in the number of samples parameters. Increasing internal noise might be due to the fact that noise elements do not contain relevant information for the task. Combing this information with the signal information in the model will lead to a noisier internal representation of the stimuli at the global processing stage. Decreased number of samples however is expected because part of the stimuli do not contain relevant information and so do not contribute in the process of decision making. For the number-of-samples parameter of the model, this is as if the noise elements do not exist.

In chapter 5 we ask to what extend does the introduction of noise affect the inter-ocular interaction in normal observers. Different variations of signal and noise oriented elements are presented to the dominant and non-dominant eyes of normal observers under dichoptic condition. In an extra control experiment, the signal and noise are presented in different disparity planes. Comparing the results to that already known about the physiology of cells at different sites in the visual cortex enables us to localize the probable site of where the orientation information is combined related to where the information from two eyes is combined. Our results suggest that the information from two eyes is not linearly combined and the effectiveness of noise depends on the eye of origin (i.e. noise to the dominant eye is dramatically stronger in disrupting the overall performance of the visual system than noise to the non-dominant eyes). Also we suggest a probable site for integration of orientation information.

In mean orientation tasks where all elements carry equally useful information, one possible strategy that the visual system could adopt is to blindly integrate information across as many elements as it can (i.e. averaging). In chapter 5 we describe the performance of an ideal observer, which blindly averages over all the local orientation information of the array elements. Comparing the ideal observer results with those of real observers, we can study whether the visual system applies such an averaging strategy or not. The performance of this ideal observer was always better than the real observers with tasks where all elements contained useful information (i.e. all signal elements). Although the internal noise in ideal observer is close to zero, the results from ideal and real observers are comparable. However, introducing noise disrupts the performance of the ideal observer dramatically more than that of a real observer. While the threshold increases 2-5 times (depending on which eye is presented with noise) in real observers, it increases about 40 times in an ideal observer. Therefore, indiscriminate integration of spatial information cannot explain the performance of the normal visual system in presence of noise. We suggest that there is an extra process of segregation that occurs before integration; in other words, the visual system possesses a mechanism that segregates the noise (i.e. irrelevant information) and then integrates the signal elements.

Previous studies suggest that amblyopes were abnormal in performing global coherence tasks (Huxlin & Pasternak, 2004; Newsome & Pare, 1988; Rudolph & Pasternak, 1999). Although no attempt has been made to disentangle the integration versus the segregation functions, there is evidence that confirms that these two functions may be separable. For example, the motion-blind patient (Baker et al., 1991) could discriminate motion direction of globally moving elements when there was no coherence noise. Adding only 10% noise was enough to reduce the performance of the observer to chance level. Normal observers could easily segregate this amount of noise. This patient had a lesion in her extra-striate cortex (i.e. lateral occipital and inferior posterior parietal lobes).

In chapter 6 we measure the performance of the amblyopic and normal observers with and without pedestal random noise. The standard deviation of the signal population and the percentage of the coherence noise were two sources of noises, which could independently affect the performances of the observers. We studied the interaction between these two sources of noise in amblyopic and normal visual systems. While we can study pure integration in no pedestal noise condition, in conditions with pedestal noise we can investigate integration as well as segregation. To the extent that different combinations of these two noise sources can affect the performance of amblyopic, fellow fixing, and normal eyes, allows us to evaluate integration and/or segregation abnormalities. Our results suggest that the segregation function is selectively impaired in amblyopia and since this is true in all three forms of amblyopia, it may suggest that segregation is of general importance to early visual development.

Chapter 1: Integration of orientation information

Integration of first and second-order orientation

Harriet. A. Allen

School of Psychology, University of Birmingham, Birmingham, B15 2TT, U.K.

Robert. F. Hess, Behzad Mansouri

McGill Vision Research Unit, 687 Pine Avenue West, Rm. H4-14, Montreal,
H3A 1A1, Quebec, Canada

Steven. C. Dakin

Institute of Ophthalmology, University College London, 11-43 Bath St. London
EC1V 9EL, U.K.

The problem of how visual information such as orientation is combined across space bears on key visual abilities, such as texture perception. Orientation signals can be derived from both luminance and contrast, but it is not well understood how such information is pooled or how they interact in the integration process. We measured orientation discrimination thresholds for arrays of equi-visible first-order and second-order Gabors. Thresholds were measured as the orientation variability in the arrays increased, and we estimated the number of samples (or efficiency) and internal noise of the mechanism being used. Observers were able to judge the mean orientation of arrays of either first- or second-order Gabors. For arrays of first-order and arrays of second-order Gabors, estimates of the number of samples used increased as the number of Gabors increased. When judging the orientation of arrays of either order, observers were able to ignore randomly oriented Gabors of the opposite order. If observers did not know which Gabor type carried the more useful orientation information they tended to use the information from first-order Gabors (even when this was poorer information). Observers were unable to combine information from first- and second-order Gabors, though this would have improved their performance. The visual system appears to have separate integrators to combine local orientation across space for luminance- and contrast-defined features.

Introduction

Many patterns in the visual world are primarily defined by modulations in luminance or contrast. The response of cells to luminance-defined patterns is typically described by a model employing linear filters (Campbell & Robson, 1968). The response of the visual system to contrast-defined patterns is typically described by a model in which there is a non-linearity such as rectification sandwiched between two stages of linear filtering (Chubb & Sperling, 1988; Graham et al., 1992; Malik & Perona, 1990; Wilson et al., 1992). Several models of this type have been proposed to account for the ability of observers to see contrast-modulated spatial structure be it static or in motion (Baloch, Grossberg, Mingolla & Nogueira, 1999; Lu & Sperling, 1995; Zhou & Baker, 1996). A model that estimates the spatio-temporal gradients present in an image has been useful in accounting for the perception of moving second-order stimuli (Johnston & Clifford, 1995). A similar model is capable of resolving static second-order structure, however it has not been extensively applied to orientation discrimination performance (McOwan & Johnston, 1996).

If contrast-defined structure is to provide useful information then the visual system must be able to resolve the precise orientation of contrast-modulations. When asked to discriminate the minimum orientation difference from vertical, thresholds for contrast-modulated patterns are higher than those for luminance-modulations (Lin & Wilson, 1996). However, these thresholds depend on the spatial frequency of the contrast modulation and the duration of presentation. When the contrast-modulation is presented at the optimum spatial frequency and for long durations (about 500ms) thresholds for luminance- and contrast-modulations are much closer, or even the same. The orientation of contrast-defined structure is, therefore, processed accurately by the visual system in many circumstances. However in the natural world, to segment texture patterns the visual system must be able to estimate both average orientations and orientation changes. This places conflicting demands on the visual system: it must both be able to both factor out differences in orientation or features, by combining them together, while keeping these differences available e.g. to compute boundaries.

There is conflicting evidence as to whether this is possible. Second-order patterns will induce an illusionary tilt in an adjacent pattern to a similar degree as first-order patterns (Smith, Wenderoth & Van der Zwan, 2001b; Van der Zwan & Wenderoth, 1995). Similarly, Smith et al. (Smith, Clifford & Wenderoth, 2001a) found that there are limited interactions between second-order textures over space. They measured the ability of observers to judge the orientation of either luminance or contrast modulations of binary noise, and found that the perceived orientation of a contrast modulation can be influenced by the presence of a surrounding contrast modulation. They also found that the perceived orientation of a central contrast modulation can be influenced by a surrounding luminance modulation. The illusion induced by the second-order component of a pattern is, however, robust to many of the stimulus manipulations that destroy the first-order illusion, suggesting that it might reflect a different process. Similarly, adapting to the position of a second-order pattern will induce positional adaptation effects, as will adapting to a first-order pattern (McGraw, Levi & Whitaker, 1999). Unlike the effect of adapting to first-order patterns, the effects of adapting to second-order patterns will occur if the pattern is presented inter-ocularly and decays slowly, consistent with a later or higher process than first-order adaptation effects.

This evidence is consistent with the idea that second-order orientation is resolved by a later process than first-order structure. Both first-order and second-order patterns show simple interactions over space. However, such studies have only tested *local interactions,* i.e. between two abutting stimuli. These types of interactions are insufficient to estimate the dominant orientation in a texture or the direction of a contour. In a test of far-reaching interactions, observers were unable to link the orientation of multiple second-order elements into a path or contour (Hess, Ledgeway & Dakin, 2000). This suggested that second-order orientation information can't be used to understand larger more complex image features such as partially obscured contours, or possibly texture boundaries. Observers are also poor at comparing multiple estimates of second-order motion (Allen & Derrington, 2000; Ashida, Seiffert & Osaka, 2001; Hess & Ziegler, 2000) and stereo (Ziegler & Hess, 1999) when they are presented in different spatial locations.

Here we used observers' ability to judge the mean orientation of an array of Gabors to investigate whether information from multiple second-order elements can ever be combined. For first-order, luminance-defined patterns observers' performance for discriminating the mean orientation of arrays of Gabors has been found to be almost as good as their performance judging the orientation of sine wave gratings (Dakin & Watt, 1997). Performance is good when the task is to judge the orientation of a set of Gabors with similar orientation. Performance deteriorates as the orientations of Gabors are drawn from wider distributions of orientations. The rate that sensitivity decreases allows one to estimate the efficiency with which the observer is able to combine such information.

We use an *equivalent noise* (Pelli, 1981) technique to describe the performance of observers when they judge the orientation of arrays of first- and second-order Gabors. This is a well established technique for investigating both detection and orientation of 1-D and 2-D signals of varying complexity (Barlow, 1957) (Ahumada & Watson, 1985) (Heeley et al., 1997) (Lu & Dosher, 1998). Dakin (Dakin, 2001) has shown that such a model describes observers data well when they are performing this task. The equivalent noise model assumes that when observers' performance with noiseless stimuli is not ideal, then this is due to *internal noise*. This internal noise is a combination of all the sources of uncertainty in making the response, including errors encoding the stimulus, errors in the retinal signals, errors initiating a finger press etc. When *external noise* is added to the stimulus, performance will deteriorate when the external noise exceeds the internal noise. In the case of our mean orientation task, where observers are forced to average across many elements, a logical choice for the external noise source is the variability of the individual orientations themselves. At low levels of external noise (i.e. narrow orientation distributions) one need only consider the orientation of a very few elements to successfully perform a judgment of mean orientation. Thus performance is limited by, and therefore may be used to quantify, internal noise (the observers' uncertainty as to the orientation of each element). As the width of the orientation distribution increases the orientation of elements becomes more variable and this external noise swamps the effect of any uncertainty the observer has about the orientation of any one element. Observers are now forced to combine many orientations to estimate the mean, and the degree to which this strategy overcomes the orientation variability in the stimulus allows one to quantify sampling efficiency, or how many samples they are using. Thus, we consider a judgment of mean orientation to be limited by two sources of variance, that of the internal noise and that of the external noise moderated by sampling efficiency. The relationship between internal noise, external noise and efficiency (effective number of samples) can be expressed as:

$$\sigma_{obs} = \sqrt{\sigma_{\text{int}}^2 + \frac{\sigma_{ext}^2}{n}} \qquad (1)$$

Where σ_{obs} is the observer's threshold (standard deviation, see Methods), σ_{int}^2 is the variance of the internal noise, σ_{ext}^2 is the variance of the external noise and n is the number of samples. The equivalent noise model can be used to estimate the internal noise in and the number of samples taken by the visual system when judging mean orientation.

For first-order orientation, observers are able to efficiently combine orientation information over the Gabor array (Dakin, 2001), and specifically, use a sample size that scales with the number of Gabors presented, (suggesting an informational limit on the integration process). In this study we investigated whether this is also true for second-order, contrast-defined orientation information.

If similar performance is found with first- and second-order Gabor arrays, then it is possible that both types of orientation are combined over space by a common integrator. To investigate if combination occurs between these two types of signal, we also measured performance with arrays made of mixtures of first and second-order elements.

Methods

Observers

There were 5 observers. Three of these were the authors; the others were naïve to the purposes of the experiment. All had normal or corrected-to-normal vision.

Equipment

The stimuli were presented on a Sony Trinitron 520GS monitor, driven by an ATI Rage 128 graphics card. The screen had a mean luminance of 33 cd/ m^2. The programs for running the experiments were written on an Apple Macintosh G3 computer using the Matlab environment (MathWorks Ltd) and code from the Psychophysics Tool Box (Brainard, 1997) and the VideoToolbox (Pelli, 1997) packages. The monitor had a resolution of 1152x870 pixels and had a frame refresh rate of 75Hz. One pixel on the screen was $0.32mm^2$. The screen was viewed binocularly at 52cm. Pseudo 12 bit contrast accuracy was achieved by combining the RGB outputs of the graphics card using a video attenuator (Pelli & Zhang, 1991). The non-linear relationship between the voltage sent to the display and the luminance output to the screen was characterized using a Graseby S370 photometer and calibration routines from the VideoToolbox. The output luminance of the screen was corrected to linear using a look-up table. After calibration and correction, the linearity of the screens output luminance was rechecked. An equal input voltage increment sent to the screen led to an equal luminance increment at the screen

Stimuli

The stimuli were arrays of Gabor micro-patterns. The modulation of each Gabor micro-pattern could be either first or second-order. For both types of micro-pattern the peak spatial frequency of the modulator (either luminance or contrast) was 0.7 cycles/degree and the standard deviation of the Gaussian envelope was 0.4°.

The second-order Gabor micro-pattern was a contrast modulation (modulation depth 1) of a 2-D binary noise pattern. This noise pattern was windowed by the Gaussian envelope and had a peak contrast of 75%. The noise elements were 1 pixel in size. The second-order Gabors can be described by the equation:

$$L_{(x,y)} = L_{(mean)} + (1 + \cos(\alpha\theta + \phi)).RC_{(x,y)}.env \qquad (2)$$

Where θ is the spatial frequency of the oriented modulation, α is the orientation, ϕ is the phase (randomized), $L_{(\text{mean})}$ is the mean luminance of the screen, RC is a random distribution of $\pm L_{(\Delta\text{max})}/2$ and *env* is the Gaussian envelope (0-1). Luminance profiles of the stimuli can be seen in Figure 1. With narrow-band carriers, an oriented contrast-modulation can cause a change in the first-order orientation content (Dakin & Mareschal, 2000), however this is only the case when the ratio of the spatial frequencies of the carrier and modulation are within about an octave. Although the carriers used here are binary and therefore spatially broadband, they have a white power spectrum and as such are perceptually dominated by their high spatial frequency structure. Because any first-order artefacts (a.k.a. "side-bands") must be impacting on the low spatial frequency aspects of the carrier they will be very low contrast and are likely to be invisible to observers. Dakin and Mareschal (Dakin & Mareschal, 2000) proposed that the simplest way to confirm that no useful (i.e. oriented) first-order artefacts are introduced is to generate a phase-randomized version of the second-order stimulus. This has an identical power-spectrum, and therefore side-band structure, but no useful contrast structure. We phase scrambled typical stimuli from the experiment and confirmed that no useful orientation information was present. This confirms that it is only second-order structure that carries useful orientation information in our stimulus. Finally, some authors have proposed that contrast modulations should only be presented with dynamic carriers, however for orientation judgments performance is the same for static and dynamic carriers (Ledgeway & Hess, 2002).

The first-order Gabor micro-patterns were presented in the presence of a 75% contrast mask, to match the contrast of the carrier component of the second-order patterns. The first-order Gabors can be described by the equation:

$$L_{(x,y)} = L_{(mean)} + (R_{(x,y)} + C\cos(\alpha\theta + \phi))env \quad (3)$$

Where θ, α, ϕ, $L_{(mean)}$ and *env* have the same meaning as above, R is a random distribution of ±the noise contrast and C is the contrast of the luminance modulation.

In each trial, typically, 16 micro-patterns were randomly positioned in a circular array within the stimulus area. The contrast values of overlapping patches were summed. Grey levels falling outside the permissible range of the screen were clipped at the maximum or minimum grey level appropriately. Since patterns contained a high contrast carrier, high-density textures would have a large number of clipped regions. For this reason we limited the density with which the Gabor patches could be placed. The centre of the distribution was the centre of the screen and the stimulus area was between 6° and 24° wide.

The orientation of the modulation in each Gabor micro-pattern was selected from a Gaussian distribution with a mean equal to the cued orientated (i.e. 90° ±the cue generated by the APE procedure, see below) and a variable bandwidth. The bandwidth standard deviation, σ, was varied from 0 (all elements aligned) to 32° (high orientation variability or 'noise'). Figure 1 shows examples of first- and second-order stimuli with bandwidths $\sigma = 0°$, 8° and 24°.

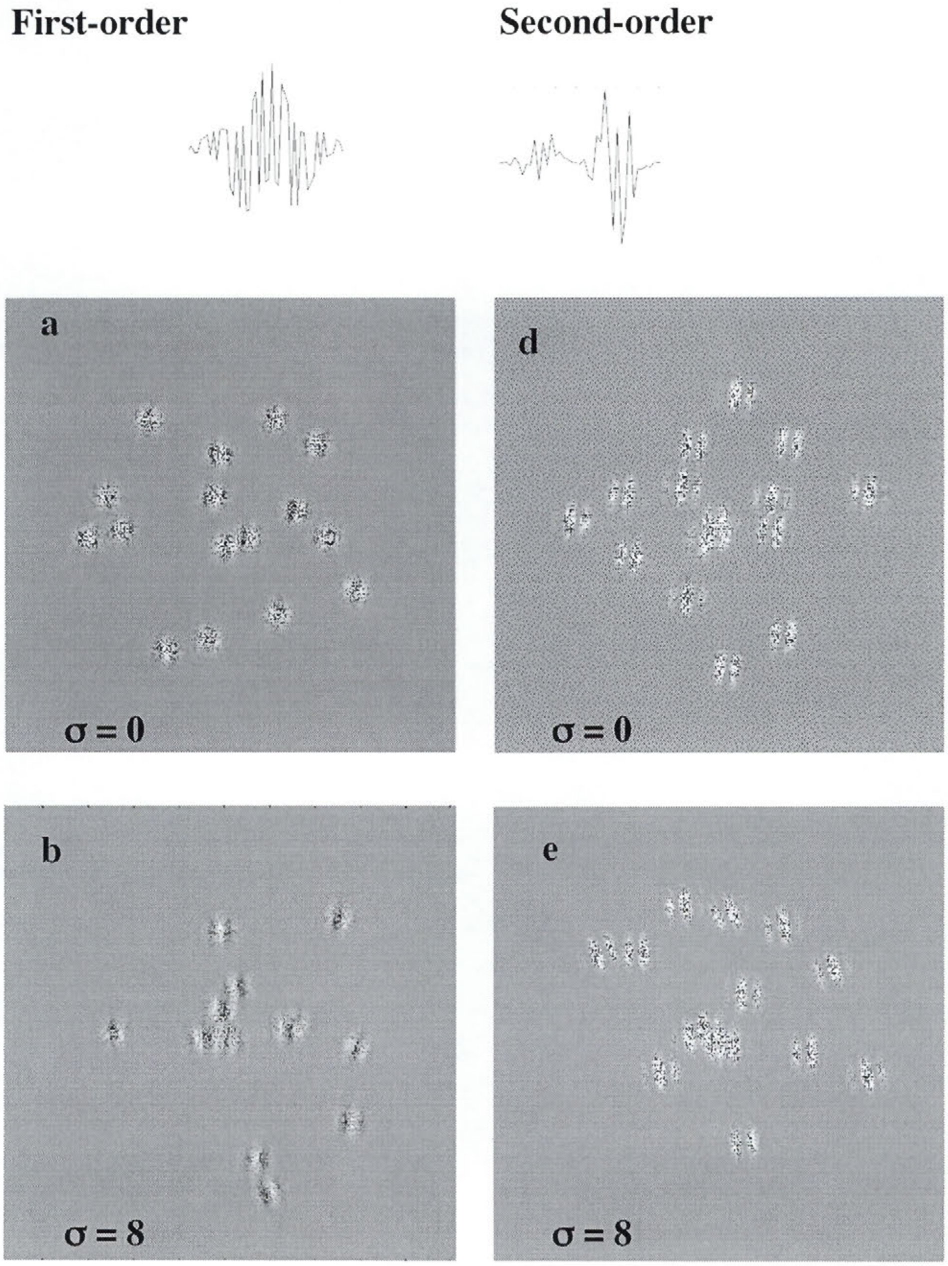
First-order
Second-order
a
σ = 0
d
σ = 0
b
σ = 8
e
σ = 8

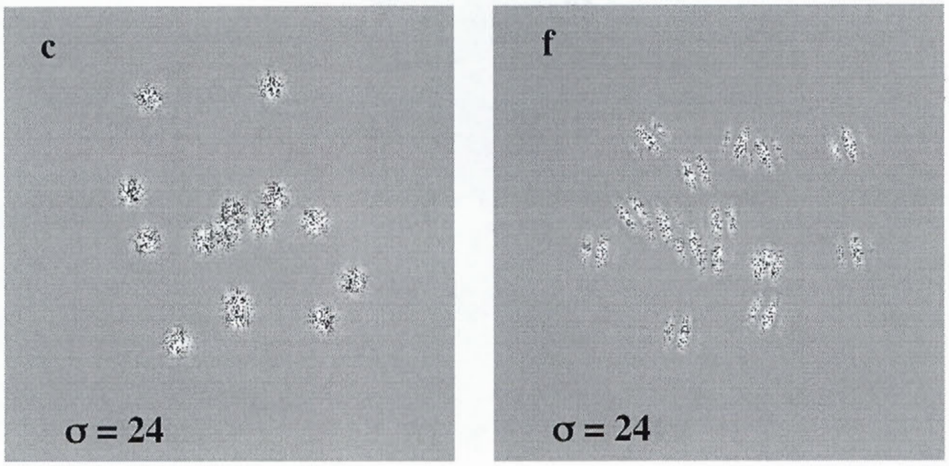

Figure 1: Examples of stimuli: typical arrays of first-order (a-c) and second-order (d-f) Gabors are shown. The orientation of each Gabor is drawn from a Gaussian distribution with standard deviation as shown in the leftmost column. Observers judged whether the mean orientation of all the Gabors in the array was tilted left or right of vertical.

Procedure

The experiments measured the ability of observers to discriminate whether the mean orientation of an array of Gabors was clockwise or anticlockwise of vertical. Prior to commencing the experiment, all observers were trained on the task until their performance reached a stable level (two or three runs).

The observers' task was a single interval binary forced choice. An array of Gabors was presented in the centre of the display for 500 ms and the observer was asked to judge whether the overall orientation of the texture was tilted right or left compared to their internal standard for vertical. Observers signalled their response with a key press. No feedback was given.

Performance was measured as the mean orientation of the generating orientation distribution of the micro-pattern array was varied around vertical. APE, an adaptive method of constant stimuli was used to sample a range of mean orientations appropriate to each observer's performance (Watt & Andrews, 1981). A session consisted of up to 9 interleaved runs of 64 trials, one run for each of the orientation bandwidths tested. At least three runs were undertaken for each data point plotted. Data were pooled across all runs with each stimulus configuration and orientation bandwidth and a bootstrapping procedure was used to fit a cumulative Gaussian function to the data. This procedure yielded estimates of the standard deviation (reciprocal of slope) and bias parameters of the fitting function. The term 'orientation threshold' is used throughout to refer to the standard deviation of the best fitting psychometric function. Estimates of the associated

95% confidence intervals were derived using a bootstrapping procedure that pooled data across separate runs for a given observer (Foster & Bischof, 1997).

Observers showed little systematic bias on the task and the data reported are based on the orientation thresholds with their 95% confidence intervals. The thresholds for each observer with each stimulus were fitted with an equivalent noise model to estimate the observers' internal noise and the number of information samples that they used for each task. Separate estimates of both internal noise and number of samples were made for each condition (radius, density, combination of Gabor type). 95% confidence intervals for the model parameters were estimated from 1000 bootstrap replications. The reported 95% CIs are the range containing 95% of the distribution of the replicated parameters (i.e. we did not assume a Gaussian distribution). Where parameters are described as significantly or not significantly different this reflects a comparison of the appropriate confidence intervals.

Equating the visibility of first- and second-order Gabors

Since we were interested in comparing the integration of local first-order signals with that of local second-order signals we first ensured that performance levels were equivalent for isolated first and second-order elements. We reduced the contrast of the first-order elements until orientation discrimination performance was equal to that found for isolated second-order elements. In so doing we are assuming that any loss of orientation resolution sensitivity that might occur with our isolated Gabors will not disadvantage our main task that exclusively involves integration of orientation. To achieve this, prior to the main experiment, we measured each observer's threshold for discriminating the orientation of an individual Gabor. The first and second-order Gabors were as described above. One Gabor was presented in a random position within the stimulus area. The orientation of the Gabor was rotated clockwise or anticlockwise of vertical and was under control of APE, as in the main experiment. The observers indicated with a key press whether the Gabor was oriented to the left or right of vertical and an orientation threshold was estimated from the best fitting psychometric function from their data.

The orientation discrimination threshold for second-order Gabors was measured at the maximum modulation depth. Orientation discrimination thresholds were measured for a range of luminance modulation contrasts of first-order Gabors. As expected, for first-order Gabors orientation discrimination threshold increased with decreasing contrast. Figure 2 shows example data from one observer, with 95% CIs (vertical bars). In the main experiment, second-order Gabors were always presented at their maximum modulation depth. The contrast of the first-order Gabors was adjusted to match orientation discrimination performance for second-order Gabors (25% contrast or lower).

Figure 3: Summary of parameters derived from fits of equivalent noise model. a), b) results of conditions where the radius remained constant, so that as more Gabor patches are presented there is a corresponding increase in density. c), d) results of conditions where the density remained constant, so that as more Gabor patches are presented, the stimulus area increased. a and c show the estimated Internal noise for the observers, b and d show the estimated number of samples used by the observers. In all four plots the parameter is plotted against the number of Gabor patches. Lines represent the mean estimate (solid – first order, dashed, second order). Points represent the estimated parameters from each observer. Each shape represents a different observer. Solid shapes and ✳ are data from first-order conditions, open symbols and ✕ are data from second-order conditions.

Figure 3 summarizes the estimated parameters from the equivalent noise model. Each plot represents averaged and individual data from 5 observers. Each subplot plots the model parameter against the number of Gabor patches presented. Figure 3 a and b summarize data from the conditions where the radius of the array was constant, so as more Gabors were presented the density increased. For both first-order (solid symbols and line) and second-order (open symbols, dashed line) Gabors, the estimate of internal noise (a) remains approximately constant. The estimated number of samples used by the observers increases with the number of patches presented (b). Although the number of samples used is higher for first-order than for second-order and, as with previous studies there are some inter-observer differences, the difference between estimates for the two types of pattern is not significant.

Figure 3 c and d summarize the results from the conditions where the density was fixed; as more Gabor patches were presented the radius of the array was also increased. The estimated internal noise (c) remained approximately constant for first-order Gabors (solid symbols). For second-order Gabors the internal noise was also approximately constant. For both first-order and second-order Gabors, the estimated number of samples (d) increases with increasing number of Gabor patches presented. The estimated number of samples is lower for second-order Gabors than for first-order Gabors, but, again, this difference is not significant.

For first-order Gabors our results replicate those of previous work except that, we find that when array radius is fixed, only the estimated number of samples increased. This discrepancy could be due to the fact that we used an added noise mask, and as a consequence (to avoid clipping) we were restricted to lower densities than previously investigated. Observers are able to combine information from multiple second-order Gabor patches, furthermore, observers' ability to discriminate the mean orientation of arrays of second-order Gabors is similar to their ability to discriminate the mean orientation of arrays of first-order Gabors.

Experiment 2: Ignoring randomly oriented Gabors

Observers can judge the mean orientation of arrays of exclusively first-order, or exclusively second-order Gabors. It is possible that, the same, common, integrator acts on both first-order and second-order patterns. It may be beneficial to combine estimates from the two types of pattern to achieve a more robust estimate of image properties. The next experiment was conducted to investigate whether this is the case. We compared performance in three different conditions:

1. Signal alone. Arrays (diameter 12.5°) of 32 signal Gabors. The orientation of signal Gabors was drawn from a Gaussian distribution centred on the mean orientation, exactly as described in the methods and used in Experiment 1.
2. Signal + Random, different orders. 32 signal Gabors were presented, as in 1, plus 32 random Gabors. The orientation of every random Gabor was re-selected on each trial. When the signal Gabors were first-order, the random Gabors were second-order and vice versa.
3. Signal + Random, same order. 32 signal Gabors plus 32 random Gabors, as in 2 except that the signal and random Gabors were either first-order or both second-order.

Conditions were not interleaved so observers always knew whether the signal was being carried by first- or second-order Gabors. If the visual system combines the information from 'Signal' and 'Random' Gabors, the estimated number of samples will fall. If some elements are randomly oriented, and are combined to estimate mean orientation, there will be a decrease in the estimated number of samples since only half (on average) the used samples actually contain orientation information. If the visual system is able to segment the pattern on the basis of Gabor type, then the estimated number of samples is expected to be the same with and without randomly oriented Gabors of a different order.

The results for these conditions are shown in Figures 4 and 5. Figure 4 and 5 show the results from when the signal was first-order or second-order, respectively. Each subplot shows orientation discrimination thresholds plotted for each width, σ, of the distribution of orientations in the signal distribution. The error bars are 95% confidence intervals. Also shown on each subplot are the estimated parameters for the equivalent noise model for each case.

Figure 4: First-order Gabors with/without randomly oriented Gabors

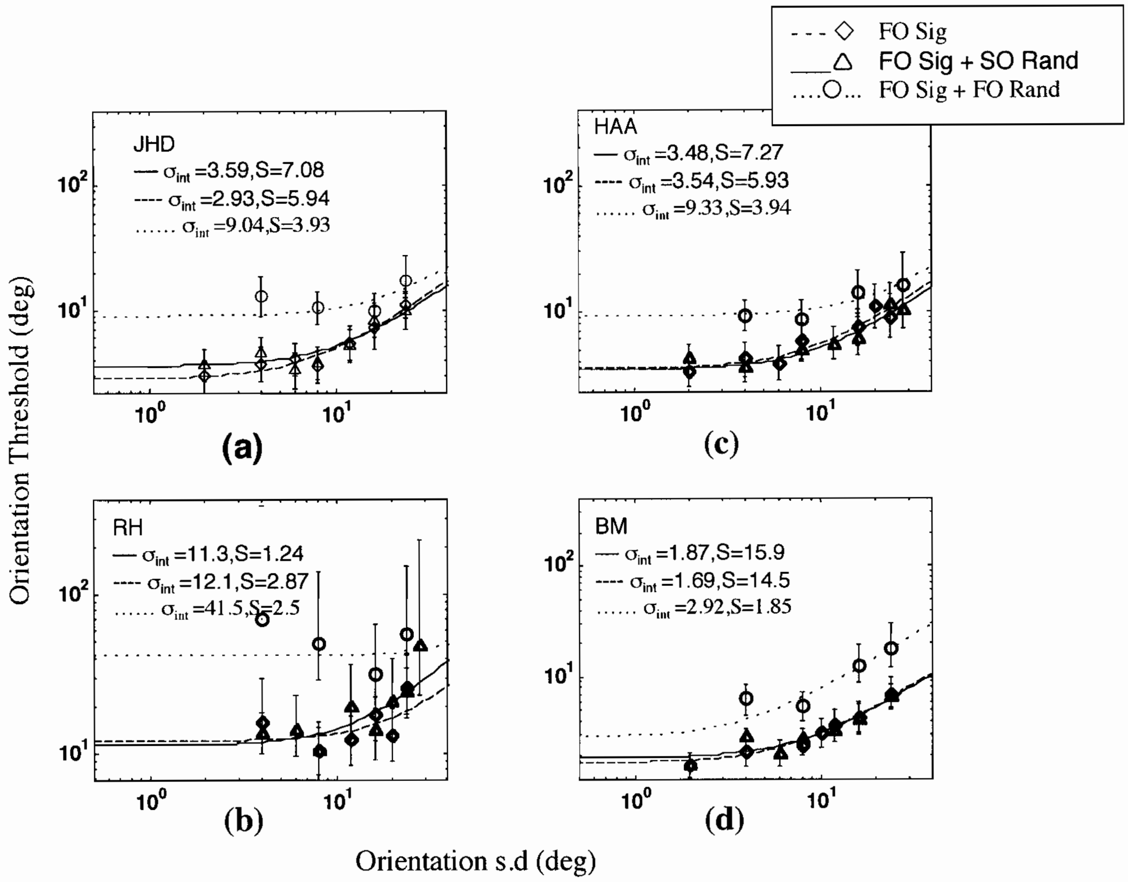

Figure 4: Graphs comparing observers' performance judging the mean orientation of arrays of first-order Gabors with, and without, intermixed randomly oriented Gabors. Orientation thresholds were measured as the standard deviation of the distribution of orientations in the 'signal' population increased. Each plot shows thresholds and the fitted equivalent noise model for performance when there were 32 first-order 'signal' Gabors (dashed line, diamonds) and 32 first-order 'signal' Gabors and 32 second order random Gabors (solid line, triangles). The data from the case with 32 first-order 'signal' plus 32 random first-order is summarized by the fitted function (dotted line, circles).

Figure 5: Second-order Gabors with and without randomly oriented Gabors

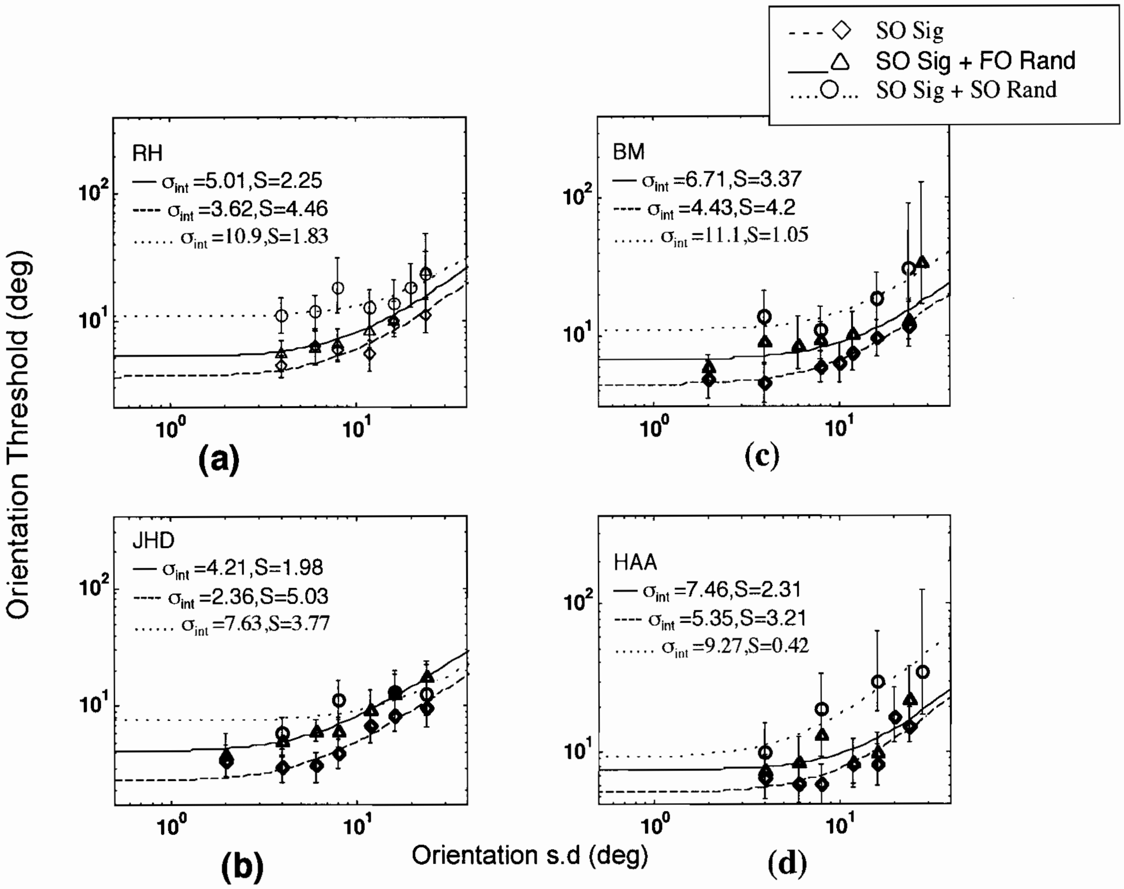

Figure 5: Graphs comparing observers performance judging the mean orientation of arrays of second-order Gabors either with, or without, intermixed randomly oriented Gabors. Orientation thresholds were measured as the standard deviation of the distribution of orientations in the 'signal' population increased. Each plot shows thresholds and the fitted model for performance when there were 32 second-order 'signal' Gabors (dashed line, diamonds) and 32 second-order 'signal' Gabors and 32 first order random Gabors (solid line, triangles). The data from the case with 32 second-order 'signal' plus 32 random second-order is summarized by the fitted function (dotted line, circles).

Adding randomly oriented second-order Gabors to first-order signal Gabors does not affect observers' ability to discriminate the mean orientation of the first-order Gabors (see Figure 4). Performance with first-order signal plus random second-order Gabors (solid line, triangles) is the same as performance with first-order signal Gabors alone (dashed line, diamonds). If the visual system were unable to segment the image based on type of Gabor, or there was some effect of the additional (non-oriented) first-order information in the random second-order Gabors, then we would predict that performance with first-order signal and random second-order Gabors would be similar to performance with both signal and random Gabors being first-order (dotted line, circles) since these also contain the non-oriented first-order noise. This is not the case.

When the signal Gabors were second-order the results are not so clear (see Figure 5). Observers have the lowest estimated internal noise and highest number of samples when they judge the mean orientation of second-order signal Gabors alone (dashed line, diamonds). When randomly oriented first-order Gabors are also presented (solid line, triangles) the estimated number of samples decreases but is still greater than when both the signal and random Gabors are second-order (dotted line, circles).

The visual system seems able to judge the mean orientation of first-order Gabors in the presence of second-order Gabors. Our observers were less able to discriminate the mean orientation of second-order Gabors in the presence of first-order Gabors. This may reflect asymmetric interactions between two mechanisms or an interaction between first-order and second-order stages in one mechanism.

Experiment 3: Signal choice

In the previous experiment, observers knew which type of Gabor contained the 'Signal'. In principal, they were able to use top-down processes to select the useful signal from the array. It is not clear, however, whether the selection was automatic and occurring at a low level or whether top-down processes were needed to segment the image. In this experiment, as in experiment 2, the arrays contained a signal distribution plus randomly oriented Gabors. When the signal Gabors were first-order, the random Gabors were second-order and vice versa. However, conditions with a first-order signal were randomly interleaved with conditions with second-order signal Gabors. All arrays contained the same number of both types of Gabors (32 of each) but which contained the signal was randomly chosen on each trial (each with arrangement with $p=0.5$). The observer did not know which type of Gabor contained the signal and which were randomly oriented however data from the two signal types was separated for analysis. Figure 6 a-c compares performance with 32 first-order signal Gabors (dashed line, triangles) with performance with 32 first-order signal Gabors plus 32 random second-order Gabors (solid line, diamonds). The presence of the random Gabors does slightly change the estimates of internal noise and number of samples but this is not a significant change ($p<0.05$, from comparison of the confidence intervals for the model parameters). Figure 6 d-f compares performance with 32 signal second-order Gabors alone (dashed line, triangles) to performance with 32 second-order Gabors plus 32 random first-order Gabors (solid line, diamonds). When the random Gabors are present, orientation discrimination thresholds are much higher than those for when the signal is presented alone. Estimates of internal noise are also much higher and the estimated number of samples is much lower.

When observers do not know which order of Gabor is signal and which is randomly oriented noise, estimates of first-order mean orientation still seem immune to added second-order orientation (and its carrier). Observers do not seem, in this condition, as able to select only second-order orientation without top-down processes. This suggests that there is either a mismatch in the strength of the two signals or that there is a bias towards one type of signal.

Figure 6

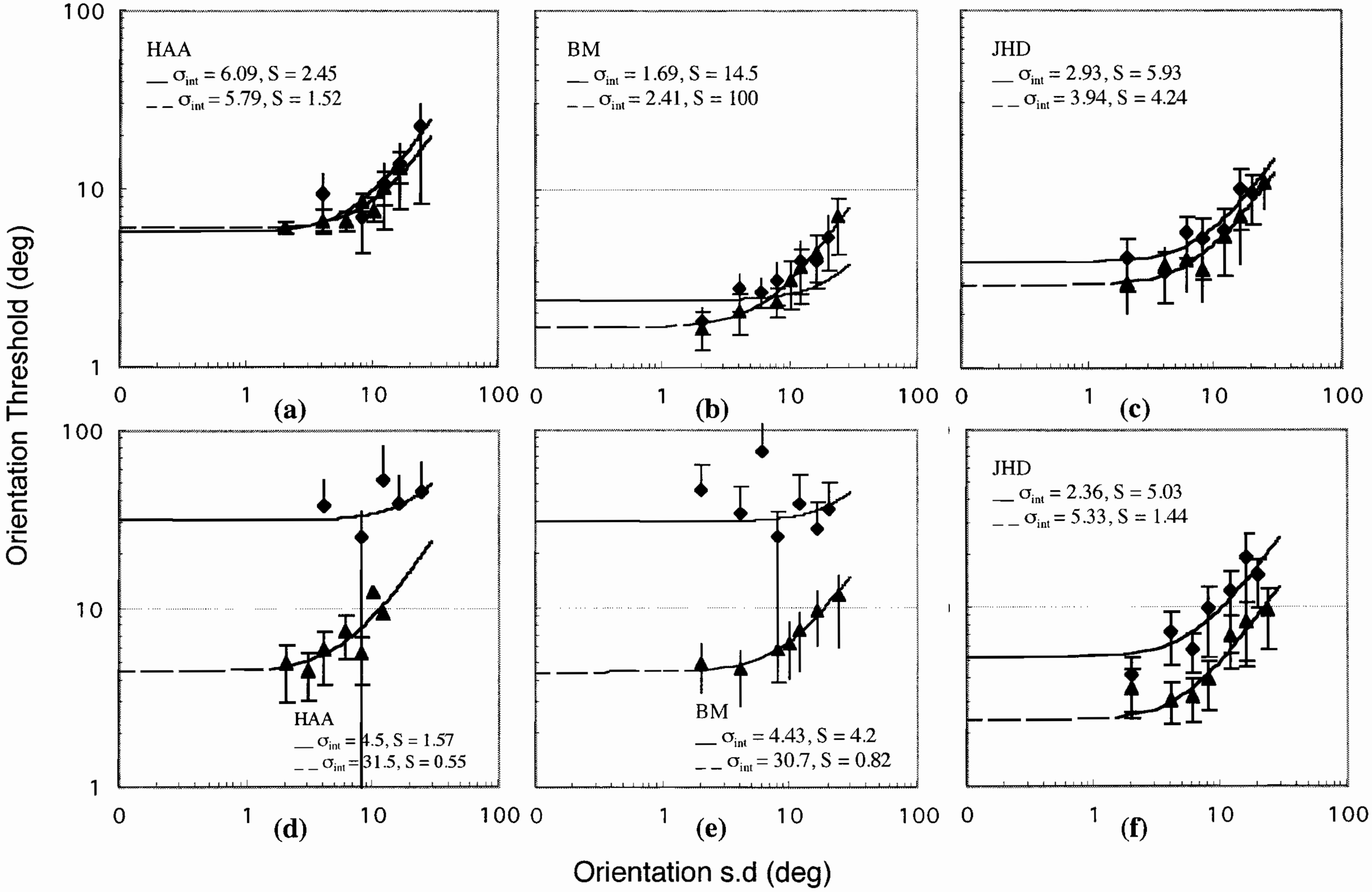
HAA
— σ_{int} = 6.09, S = 2.45
– – σ_{int} = 5.79, S = 1.52
BM
— σ_{int} = 1.69, S = 14.5
– – σ_{int} = 2.41, S = 100
JHD
— σ_{int} = 2.93, S = 5.93
– – σ_{int} = 3.94, S = 4.24
HAA
— σ_{int} = 4.5, S = 1.57
– – σ_{int} = 31.5, S = 0.55
BM
— σ_{int} = 4.43, S = 4.2
– – σ_{int} = 30.7, S = 0.82
JHD
— σ_{int} = 2.36, S = 5.03
– – σ_{int} = 5.33, S = 1.44
(a)
(b)
(c)
(d)
(e)
(f)
100
10
1
0
1
10
100
Orientation Threshold (deg)
Orientation s.d (deg)

Figure 6: Graphs comparing observers' performance judging the mean orientation of arrays of Gabors with, or without, randomly oriented 'noise' Gabors of the opposite order being present. Observers did not know whether the first-order or second-order Gabors were the 'signal' Gabors. Orientation thresholds were measured as the standard deviation of the distribution of orientations in the 'signal' population increased. Each plot shows thresholds and the fitted model for performance when there were 32 'signal' Gabors (dashed line, triangles) compared to 32 'signal' Gabors plus 32 'noise' Gabors (solid line, diamonds). a-c) conditions when the 'signal' was first-order ('noise' was second-order). d-f) conditions where the signal was second-order ('noise' was first-order).

Experiment 4: Mixing First- and Second-order Gabors

The visual system is able to estimate the mean orientation of arrays of both first and second-order Gabors. This experiment was designed to investigate whether information from first and second-order Gabors can ever be combined. In some situations it is to be expected that first and second-order information provide similar information about a surface and combining information from the two sources would be advantageous. Recall that results from Experiment 1 indicated substantial changes in sampling when the number of elements changed from 32 to 64 (see Figure 3b,d) so that we could be confident that if subjects were combining across both first and second-order patches, then this would show up clearly in the parameters derived from the equivalent noise model. Observers judged the mean orientation of arrays containing 32 first-order plus 32 second-order Gabors, the orientations of all the Gabors were drawn from the signal distribution as described in the methods. If the visual system is not able to combine the first- and second-order Gabors then the estimated number of samples from the combined array will be similar to the estimated number of samples from 32 first-order or second-order Gabors alone. Figure 7 shows the mean orientation discrimination thresholds for each σ of the distribution of Gabor orientations. Performance when there were first- and second-order Gabors combined (solid line, diamonds) was close to performance with either the first-order or second-order Gabors alone (dashed line, triangles). It seems that the observers were unable to combine the information from first and second-order Gabors, even though that would have improved their performance.

Figure 7

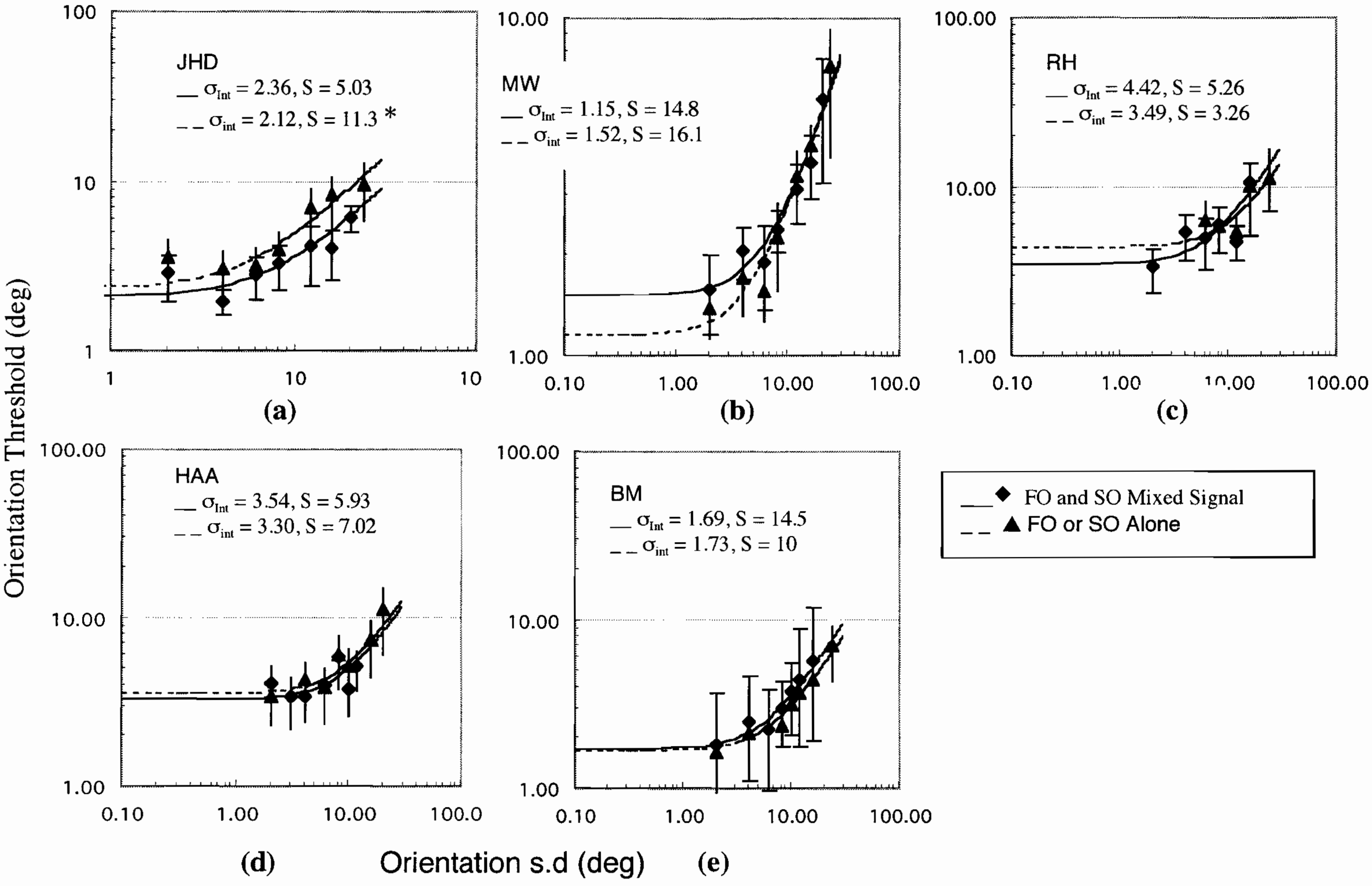
JHD
— σInt = 2.36, S = 5.03
– – σint = 2.12, S = 11.3 *
MW
— σInt = 1.15, S = 14.8
– – σint = 1.52, S = 16.1
RH
— σInt = 4.42, S = 5.26
– – σint = 3.49, S = 3.26
HAA
— σInt = 3.54, S = 5.93
– – σint = 3.30, S = 7.02
BM
— σInt = 1.69, S = 14.5
– – σint = 1.73, S = 10
◆ FO and SO Mixed Signal
▲ FO or SO Alone
Orientation Threshold (deg)
Orientation s.d (deg)
100
10
1
1
10
10
10.00
1.00
0.10
1.00
10.00
100.0
100.00
10.00
1.00
0.10
1.00
10.00
100.00
100.00
10.00
1.00
0.10
1.00
10.00
100.0
100.00
10.00
1.00
0.10
1.00
10.00
100.00
(a)
(b)
(c)
(d)
(e)

Figure 7: Graphs of observers' performance judging the mean orientation of arrays containing <u>either</u> 32 first-order or 32 second-order Gabors (dashed line, triangles) and their performance judging the mean orientation of arrays containing <u>both</u> 32 first- and 32 second-order Gabors (solid line, diamonds). Orientation thresholds were measured as the standard deviation of the distribution of orientations in the 'signal' population increased. Each subplot shows a different observer's data. Performance in the mixed Gabor condition is compared to performance with 32 first-order Gabors for HAA, BM, and MW and to 32 second-order Gabors for JHD and RH (see text).

It is reasonable to ask what would be predicted if first and second-order information was combined. One prediction is that the observer would produce the same performance as when they had 64 Gabors of one order. To make this assumption, one has to assume that there is both perfect combination and that there is an equal quality of information from both types of Gabors. Since we found that individuals had slightly different mean orientation performance for first and second-order arrays of Gabors these did not seem valid assumptions. From experiment 1 we do know, however, that for both first and second-order Gabor arrays, as the number of Gabors increases from 32 to 64, the effective number of samples used by the visual system also increases. So, if the visual system were able to combine the mean orientation of first-order and second-order Gabors we would expect the estimated number of samples to be greater for the mixed arrays than for 32 Gabors alone. We find that only one observer's (JHD) estimated number of samples is significantly greater ($p<0.05$) for the mixed stimulus than for 32 Gabors alone (indicated with a * on Figure 7).

A second, related argument also supports the argument that the visual system is not combining the information from first and second-order Gabors. The estimated internal noise of the observer reflects observers' performance with stimuli in the absence of external noise. Estimated internal noise is different for arrays of first- and second-order Gabors, although which provides a lower estimate depends on the observer. If the visual system uses one type of Gabor then we might expect that, given a combined stimulus, each observer should use the order of Gabors that gives the lower estimate of internal noise. Figure 7 plots thresholds and fitted equivalent noise model for the combined stimulus with data from arrays of either 32 first-order or 32 second-order Gabors whichever had the lower estimated internal noise. The estimated internal noise from the combined array is the same as the estimated internal noise from the array with only one order of Gabors. Furthermore, the estimated number of samples is also the same in these two conditions.

When presented with arrays of both first-order and second-order Gabors, where all the Gabors contain useful information, the visual system is does not use information from both types of Gabor. The visual system may even estimate mean orientation from the order of Gabor that produces the lower internal noise.

Discussion

We investigated whether observers could judge the mean orientation of arrays of Gabors, a task requiring that the visual system combine local estimates of orientation across space. Observers were able to judge the mean orientation of arrays of either first-order or second-order Gabors. When presented with arrays containing both first-order and second-order Gabors, observers were able to estimate the mean orientation of either first-order or, to a lesser extent, second-order, ignoring the other order. Observers seemed unable to effectively combine information from first- and second-order Gabors or to automatically select the Gabor type that contained the signal information.

Figure 8: Summary of possible mechanisms underlying the judgment of mean orientation

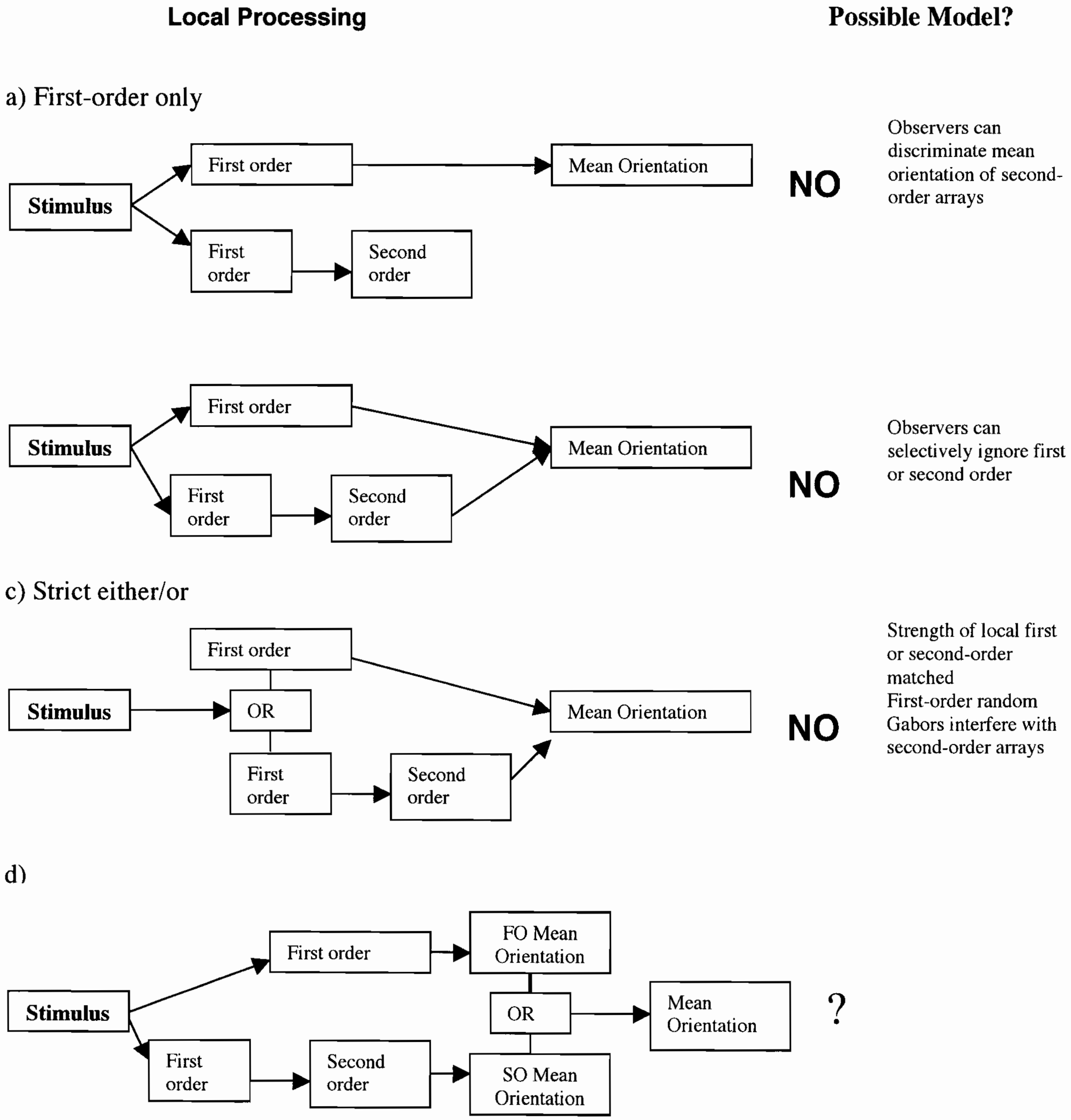

Observers can discriminate mean orientation of second-order arrays

Observers can selectively ignore first or second order

Strength of local first or second-order matched
First-order random Gabors interfere with second-order arrays

Figure 8 shows four possible schema of how first- and second-order mean orientation could be estimated by the visual system. Each possible arrangement begins with filters tuned to the local first-order orientation and the second-order channel also has filters tuned to the local second-order orientation (Local Processing). The last stage of each model is always an estimate of mean orientation. The right column of Figure 8 summarizes whether this model is plausible given our data. First-order only processing, suggested by the non-combination of information from multiple patches of second-order motion (8a) and blind combination (8b) are easily ruled out by our data. Observers can discriminate the mean orientation of arrays of first- and second-order Gabors (8a) and can base their judgments on either order selectively (8b). Observers can use either first- or second-order Gabors but do not perfectly ignore first-order Gabors. This result seems inconsistent with an either/or process (described by 8c) where the mean orientation of either first-order or second-order local information is computed, however the second-order channel does also process first-order information (the carrier), which could explain this result. However, since the strength of the local signal was matched (in terms of the orientation discrimination of individual Gabor elements) for first- and second-order, it is not clear on what basis the visual system would choose to use either first- or second-order local information.

8d shows separate first-order and second-order integrators for mean orientation. This allows the strength of the mean orientation output signal to be different for first- and second-order patterns. The two mean orientation estimates are subject to an OR combination before the final estimate of mean orientation. Which of the two mean orientation signals is used is controlled by the relative strengths of the outputs from first- and second-order integrators and by top-down modulating processes. Normally the output of the first-order integrator is stronger/preferred. This scheme accounts for observers' ability to judge the mean orientation of arrays of either first- or second-order Gabors and to selectively exclude information from one or other type of Gabor. Because the output of the first-order mean orientation unit is stronger/preferred, this accounts for observers tendency to use only first-order Gabors when they did not know which order of Gabor carried the useful information. Furthermore, when asked to ignore the first-order Gabors, this is imperfectly done due to the stronger signal/preference from the first-order mean orientation integrator and the processing of first-order structure by the first stage of the second-order channel. Similarly when both first- and second-order Gabors signal the same mean orientation, performance is based on one type of Gabor, but it is possible that some information from the other type of Gabor can be accessed.

These results are relevant to three questions; each will be discussed in turn. First: Can second-order information be combined over space? Second, is information from first-order and second-order stimuli analyzed separately by the visual system? Third, does the visual system segment the image based on the order of the signal?

Spatial Interactions between second-order stimuli

It is clear from our results that second-order information from multiple patches can be combined over space. Smith and colleagues (Smith et al., 2001a) had previously shown that the mechanism that processes second-order (contrast-defined) stimuli is capable of producing the same repulsion and attraction tilt illusions found for first-order stimuli. They proposed that the mechanism that processes second-order orientation, whilst being slightly higher in the processing stream, is of the same type of mechanism as the mechanism for first-order stimuli.

The tilt illusion is likely to be due to horizontal, inhibitory connections between orientation selective cells (Gilbert, Das, Ito, Kapadia & Westheimer, 1996; Gilbert & Wiesel, 1990; Westheimer, 1990). The estimation of mean orientation may not involve inhibitory connections, but is likely to involve lateral connections between multiple cells. It has been shown that there are considerable excitatory and inhibitory connections between orientation selective cells. Furthermore the nature of the interactions can depend to a large part on the exact properties of the stimulus (Gilbert & Wiesel, 1990). Thus it seems likely that these same connections exist between cells responsive to second- order contrast-defined structure.

One finding seems to conflict with the idea that second-order orientation information is combined over space and that is the failure of observers to identify contours of second-order elements (Hess et al., 2000). It has been proposed that contours are analyzed by "association fields" (Field, Hayes & Hess, 1993). It is possible that association fields represent a different process to the lateral interactions involved in mean orientation estimation or the tilt illusion. Contour integration is sensitive to increasing levels of position uncertainty (Hess & Dakin, 1999), whereas judging mean orientation, almost by definition, discards information about the position of pattern elements. Furthermore, orientation is averaged over pattern elements, irrespective of polarity (Parkes, Lund, Angelucci, Solomon & Morgan, 2001) whereas previous studies found that elements of alternate polarity do not form contours as well as elements of the same polarity (Field, Hayes & Hess, 2000; McIlhagga & Mullen, 1996). It is clear from the present findings that the visual system's failure to link oriented second-order elements into contours represents a special case failure of second-order processing rather than a general failure to undertake global operations on the orientation of spatially distributed elements. From a functional perspective, it may be that contour structure in natural images is largely conveyed by luminance information whereas texture could be conveyed by a variety of cues including, but not limited to, contrast-defined and luminance-defined form

Combination of first- and second-order orientation

We also find that information from first-order and second-order patterns is available separately to the decision processes. Models of the first- and second-order visual mechanisms usually assume that information from the two types of stimuli is combined. For moving patterns, for example, when information from first- and second-order structure is low quality, the two sources can combine to improve spatial frequency discrimination (Smith & Scott-Samuel, 2001). However, in other circumstances, such as when there is global motion of first and second-order structures, the two sources of information do not combine to improve performance (Edwards & Badcock, 1995).

For static patterns, several authors have shown that first-order and second-order orientation information interacts. These studies can be divided into two camps. First, there are those studies that have investigated the interaction between luminance-defined and contrast-defined components of the same object, which might be considered to be interactions between the two stages of a filter-rectify-filter type model. Second, there are investigations of interactions across space between separate first and second-order contours. We will deal with these in turn.

First, the perceived orientation of a second-order envelope in a pattern is influenced by the orientation of its carrier (Dakin, Williams & Hess, 1999; Morgan, Mason & Baldassi, 2000). In these studies observers judged the orientation of the high spatial frequency first-order components or the low spatial frequency second-order component of the same patch. First- and second-order orientation information is not kept separate, indeed it is inextricably connected and it is unsurprising that there are interactions. The experiments reported here, however, addressed the interactions between first- and second-order patterns of the same spatial frequency but at different visual field loci, after the orientation of local second-order structure has been resolved.

When first-order and second-order modulations of the same spatial frequency are presented at the same visual field locus, second-order modulations will mask first-order modulations (Schofield & Georgeson, 1999). Similarly both first-order and second-order modulations will bias the perceived orientation of the other type of modulation (Smith et al., 2001a). To account for the masking data, Schofield and Georgeson (Schofield & Georgeson, 1999) proposed a two-pathway model with energy summation between separate first- and second-order pathways. A two-pathway model followed by a combination process also accounts for the tilt illusion between first and second-order patterns (Smith et al., 2001a); one pathway processes only first-order information and the other pathway processes first- and second-order information. Consistent with this we find that observers are sometimes unable to completely ignore first-order random Gabors when they are judging the orientation of second-order Gabors. Both first-order and second-order Gabors contain binary noise, which may be processed by the early stage of the pathway that processes second-order structure, adding to its internal noise. There are likely to be horizontal connections between cells in each pathway, as described above, but the two mechanisms may not be interconnected. Possible reasons for this are discussed in the next section.

Does 'order' segment the image

Our results show that estimates of mean orientation seem to keep first and second-order information separate. Even when it would be advantageous to do so, the observers do not fully combine the two sets of information.

The tilt illusion is reduced when the inducing and test patterns are clearly segregated (Mareschal, Sceniak & Shapley, 2001). This suggests that the segmentation of the image influences how orientation signals are combined. Taken with our results, this might suggest that the visual system has a tendency to segment first-order from second-order information.

It must also be considered that first and second-order information may be segmented not because of specific processes for these types of patterns. Rather this might arise from other processes. Patterns of different spatial frequencies are easily segmented. In our stimulus, only the first-order stimulus contained a low frequency (luminance-defined) oriented contour. Simple linear filters could easily discriminate between the two stimuli (although not resolve an oriented signal from the second-order stimuli). The output of these early filters could be used to determine whether orientation signals are treated as if they come from one object or assigned to different objects. This would lead to the two types of pattern being treated as if they were separate image objects. The *current experiments cannot distinguish between whether segmentation occurs on the basis of order directly or as a by-product of another stimulus attribute.*

The fact that first and second order orientation signals are not combined across space with a common integrator may, however, follow from the statistics of natural images. It is only if there is a strong correlation between like orientations of luminance and contrast-defined features within the same region of the image that it would be useful to combine such estimates.

Conclusion

We find that observers are able to judge the mean orientation of arrays of contrast-defined, second-order Gabors. It is likely that similar, but separate, processes underlie the estimation of mean orientation for first- and second-order patterns.

Acknowledgements

This work was supported by a Canadian Institute for Health Research grant (MT108-18) to Robert Hess.

Preface to chapter 2

In chapter 1, we studied how the normal visual system integrates local first- and second-order orientation across space. We examined whether the first- and second-order orientation information is combined in the visual system. Furthermore, we tested the effect of randomly oriented noise element on orientation integration performance of normal visual systems.

We showed that the visual system combines local orientation information, being either first-order or second-order. However, it does not integrate them when they are presented simultaneously. Also when they are presented together, the visual system tends to use only first-order information. Our findings supported our suggested model for integration of first- and second-order orientation information (see Conclusion, chapter 1). Integration of first-order orientation information has been studied previously (e.g. Dakin, 2001) and it has been shown that the normal visual system integrates local orientation information robustly (i.e. different size, density and number of elements).

We now go on to address the next interesting question as to whether the amblyopic visual system can integrate orientation information across space. We address this question for first-order orientation in the chapter 2.

Chapter 2: First-order orientation integration in amblyopia

Integration of orientation information in amblyopia

Behzad Mansouri, Robert F. Hess

McGill Vision Research Unit, 687 Pine Avenue West, Rm. H4-14, Montreal,
H3A 1A1 Quebec, Canada

Harriet A. Allen

School of Psychology, University of Birmingham, Birmingham, B15 2TT, U.K.

Steven C. Dakin

Institute of Ophthalmology, University College London, 11-43 Bath St. London
EC1V 9EL, U.K.

Oliver Ehrt

‡ Department of Ophthalmology, Ludwig Maximilians University,
Mathildenstrasse 8, 80336 Muenchen, Germany.

A recent report suggests that amblyopes are deficient in processing local orientation at supra-threshold contrasts. To determine whether amblyopes are also poor at integrating local orientation signals, we assessed performance for an orientation integration task in which the orientations of static signals are integrated across space. Our results show that amblyopic visual systems can integrate local static oriented signals with the same level of efficiency as normal visual systems. Although internal noise was slightly elevated, there was no indication that fewer samples were used to achieve optimal performance. This finding suggests normal integration of local orientation signals in amblyopia.

Introduction

Our emerging understanding of the underlying neural dysfunction in amblyopia has paralleled, to a great extent, our understanding of normal visual function. Initially, amblyopes were found to be poor at detecting spatially simple targets. This deficiency involves the detection of high spatial frequencies (Gstalder, 1971; Hess & Howell, 1977; Lawwill & Burian, 1966; Levi & Harwerth, 1977). Evidence from animal models suggests that the underlying problem lies in the contrast sensitivity and spatial properties of the high spatial frequency responsive neurons in V1 that receive their input from the amblyopic eye (Crewther & Crewther, 1990; Eggers & Blakemore, 1978; Movshon et al., 1987).

There is reason to suspect that the performance loss in amblyopia is not limited to contrast detection of simple high spatial frequency patterns and that, as a consequence, the neural anomaly is not limited to a subset of neurons in V1. Amblyopes have been shown to be deficient in discrimination tasks involving orientation (Bradley & Skottun, 1984; Caelli et al., 1983; Demanins et al., 1999; Vandenbussche et al., 1986), spatial frequency (Hess et al., 1980a), contrast (Hess et al., 1983) and phase (Caelli et al., 1983; Lawden et al., 1982; Pass & Levi, 1982; Treutwein et al., 1996), in positional judgments for well separated elements where contrast sensitivity does not play a part (Hess & Holliday, 1992), in detection of contrast-defined stimuli (Wong et al., 2001) and in tasks involving global vision (Hess et al., 1997b; Hess et al., 1999c; Popple & Levi, 2000; Simmers et al., 2005) and motion detection (Simmers et al., 2003). While the above-mentioned anomalies suggest a more extensive deficit, our incomplete knowledge of processing sites of these tasks precludes any strong conclusion about whether there is a primary deficient locus in the extra-striate cortex. One exception of this is the global motion task as there is detailed neurophysiological evidence in monkeys and psychophysical evidence in humans that this involves the integration of local V1 motion signals within area MT/MST in extra-striate cortex. The evidence for this comes from single cell recording in extra-striate cortex, where cells have large receptive fields, with sub-units thought to be the basis of such integration (Movshon et al., 1985), and firing patterns that are highly correlated with performance in global motion tasks (Britten, Shadlen, Newsome & Movshon, 1992; Salzman et al., 1992). Furthermore, there is behavioural evidence for an extra-striate basis for this task from both monkeys with target lesions to area MT (Newsome & Pare, 1988) and patients with vascular lesions involving this area who exhibit specific deficits involving motion integration (Baker et al., 1991; Rizzo, Nawrot & Zihl, 1995; Vaina, Lemay, Bienfang, Choi & Nakayama, 1990; Zihl, von Cramon & Mai, 1983) but not for detection of local motion (Hess, Baker & Zihl, 1989). Although a number of deficits have been identified in V1 cells driven by the amblyopic eye of deprived animals (e.g. spatial and orientational tuning, contrast sensitivity, etc.) there have been no reports of V1 motion deficits (Kiorpes et al., 1998). Thus the finding of global motion deficits in amblyopes (Simmers et al., 2003) suggests that the amblyopic deficit may involve integrative functions known to occur beyond V1. Simmers et al (2003), relying on an accepted 2-stage model of global motion processing (Morrone et al., 1995) in which the first stage is contrast sensitive and identified with V1 processing and the second stage is purely integrative and identified with extra-striate processing (e.g. area MT/MST), delineate both components of the overall motion deficit for global stimuli. They isolate a significant deficit that involves the integration of local motion signals, implicating the extra-striate cortex. Having ruled out any contribution from the reduced contrast sensitivity exhibited by cells in V1, the only other possible V1 influence could be from positional uncertainty, if its site were to be in V1. Such an influence is unlikely in a task where the element positions are stochastic unless it contributes, in some way, to a deficit to the processing of local motion. Such a proposal has neither psychophysical (Hess & Anderson, 1993) nor neurophysiological (Kiorpes et al., 1998) support. Furthermore, Simmers et al (2003) show that the fellow fixing eye is also deficient at global motion detection and that this is also confined to the integrative aspect of the task, implicating a site in the dorsal pathway where the majority of cells are binocular. Recently, (Simmers et al., 2005) has shown, using an equivalent global form task, that this extra-striate deficit in amblyopia also affects the ventral stream.

In order to ascertain whether this global motion deficit is a reflection of a more general inability to integrate visual information across space, we examined the efficiency with which the amblyopic visual system can integrate visual information of a purely spatial character. We chose orientation not only because of its importance in early visual processing but also because it has recently been suggested that global orientation processing of supra-threshold stimuli is specifically disrupted in amblyopia (Barrett, Pacey, Bradley, Thibos & Morrill, 2003; Popple & Levi, 2000). We chose a paradigm where integrative performance did not depend on the spatial distribution of the elements whose orientation signals were to be integrated. This factored out any contribution from the, already known, elevated positional uncertainty in amblyopia (Hess & Holliday, 1992;

Levi & Klein, 1985) allowing us to measure unambiguously the integrative performance of amblyopic eyes for local, oriented, stimuli of supra-threshold contrast.

The equivalent noise approach has been applied in a number of vision studies before e.g. contrast sensitivity (Ahumada & Watson, 1985; Pardhan, 2004), luminance offset detection (Barlow, 1957), coding of spatial position (Watt & Hess, 1987; Zeevi & Mangoubi, 1984), discrimination of edge blur (Watt & Morgan, 1983), spatial frequency acuity (Heeley, 1987), contour integration (Hess & Dakin, 1999), orientation discrimination (Heeley et al., 1997).

Previously, Dakin (2001) used this task and showed that normal observers can integrate local orientation information efficiently over a large range of stimulus sizes, numerosity and density. His results were well described by the equivalent noise model. Given that thresholds are estimates of response variance, the non-ideal behaviour of observers with noiseless stimuli (zero orientation variance) can be expressed as an additive, internal noise, which means that in no variance condition, the visual system behaves as if it is performing the task in the presence of a certain amount of variability in the stimulus population. The level of internal noise can be simply measured by increasing the amount of external noise in the stimulus and determining the point at which observer's performance begins to deteriorate. The observer's robustness to increasing amounts of external noise will depend decreasingly on internal noise and increasingly on how many samples are averaged over because more samples gives a better average estimate from the stimuli population which decreases the effect of the external noise. The form of the equivalent noise model is:

$$\sigma_{obs} = \sqrt{\sigma_{int}^2 + \frac{\sigma_{ext}^2}{n}}$$

Where σ_{obs} is the observed threshold, σ_{ext} is the external noise, σ_{int} is the estimated equivalent intrinsic or internal noise and n is the estimated number of samples being employed. In terms of the orientation discrimination task, σ_{obs} corresponds to the threshold for orientation discrimination, σ_{ext} to the standard deviation of the distribution from which the samples are derived (see Method), σ_{int} to the noise associated with the measurement of each orientation sample and their combination and n corresponds to the estimated number of orientation samples being combined by the visual system.

Assumptions underlying equivalent noise

1. Orientation integration involves averaging. Efficiency on our tasks indicates that observers invariably employ more than one sample, i.e. they are combining information across space and are not relying on a single element to perform the task. This does not mean observers necessarily use the average (although this would be optimal); other strategies, such as using a peak in the orientation statistics, might also suffice. However, by employing textures composed of orientations drawn from skewed distributions (Dakin & Watt, 1994) were able to show that observers' performance was consistent with their using the average orientation and not the peak.

2. Nature of the noise. Equivalent noise assumes that performance is limited by additive and multiplicative noise. Additive noise is due to noise on the detectors registering local orientation and could, for example, be plausibly linked to the finite orientation bandwidth of cells in V1. Sampling efficiency is equivalent to a global multiplicative noise source; i.e. one that increases with the strength of signal being pooled. Multiplicative noise is a ubiquitous feature of neural systems and has been observed in neurons responsible for integration along other stimulus dimensions, e.g.

motion; MT neurons; (Britten, Shadlen, Newsome & Movshon, 1993).

3. Constant internal noise. The two parameters of internal noise and sampling efficiency in the standard equivalent noise function are fixed across all levels of external noise. This assumption is made on the grounds of parsimony; we do not need to change noise levels as a function of stimulus variance to account for our data.

In the main experiment, observers viewed an array of 16 randomly positioned, oriented Gabors that were samples from an orientation distribution whose standard deviation was varied. The task was to determine whether the mean orientation of the array was clockwise or counter-clockwise (see figure 1) from vertical. The results were fitted by the equivalent noise model, described above, to derive the measures of internal noise and number of samples. To ensure that any differences between these measures for normal and amblyopic observers were due solely to integrative function, we equated performance for a single Gabor element for a similar orientation task. This ensured that performance was equated for this task for an individual element and that therefore any difference in the derived measures must be the results of integration per se.

Methods

Observers

Ten normal and twelve amblyopic observers were recruited for this experiment. Two of the normal observers were the authors. The others were naïve to the purpose of experiment. All observers were optically corrected if necessary. Clinical details of amblyopic observers are presented in table 1. Eye dominance in normal observers was assessed for each subject using a sighting test (Rosenbach, 1903).

Table 1

Obs.	Age	Type	Refraction	Acuity	Strabismus	History, stereo
AM	31y	RE strab	–3.75 DS –3.25 DS	20 / 50 20 / 25	ET + 3°	Detected age 3y, patching for 3 y
LN	49y	RE strab	+3.75 –3.75 120° +3.00 –2.00 80°	20 / 30 20 / 20	ET + 10°	Detected age 3y, glasses since, patching 6w,strabismus surgery RE age 20 y
MA	22y	LE aniso	–0.25 DS +3.50 –0.50 0°	20 / 15 20 / 200	Ortho	Detected age 3y, patching for 4 y, glasses for 8 y
MG	28y	RE strab	–0.50 DS +0.50 DS	20 / 100 20 / 15	ET +1°	Detected age 4y, patching for 6m, no surgery
MM	27y	LE aniso	+0.25 –1.75 135° +0.75 –3.50 55°	20 / 20 20 / 30	Ortho	Detected age 6y, 6 mo patching basic stereovision present
NG	30y	RE mixed	+5.00 –2.00 120° +3.50 –1.00 75°	20 / 70 20 / 20	ET +8°	Detected age 5y, patching for 3m, no glasses tolerated, 2 strabismus surgery RE age 10-12y
RB	49y	LE aniso	+3.25 DS +4.75 –0.75 45°	20 / 15 20 / 40	XT –5°	Detected age 6y, glasses since 6y, no other therapy, near normal local stereo vision
VL	35y	LE aniso	+0.50 DS +3.50 –3.00 50°	20 / 20 20 / 50	Ortho	Detected age 6y, ϕ
YC	31y	LE strab	+2.00 DS +2.00 DS	20 / 15 20 / 40	ET +10°	Detected age 2y, patching for 4y, glasses for 16y
BB	58y	LE strab	+0.50 – 0.50 +1.25 – 0.25	20 / 15 20 / 600	ET +5°	Detected age 8y, surgery to correct angle of large eso, patching for 6 mo.
AT	21y	LE aniso	+0.50 DS +0.50 –2.0 200°	20 / 15 20 / 30	Ortho	Detected age 3y, glasses since 8y. no other therapy.
PH	33y	LE strab	-2.0 +0.50 DS +0.50 DS	20 / 25 20 /63	ET +5°	Detected age 4y, patching for 6m, Surgery when he was 5y.

Table 1: Clinical details of the amblyopic observers participating in the experiment. The following abbreviations have been used; strab for strabismus, aniso for anisometropic, RE for right eye, LE for left eye, ET for esotropia, XT for exotropia, ortho for orthotropic alignment, sph for dioptre sphere.

Stimuli

The stimuli were arrays of Gabor micro-patterns presented on a mid-gray background. The envelope of the Gabor had a standard deviation of 0.4°. The spatial frequency of sinusoidal modulation within the Gabor was varied between 0.52 cycles per degree (cpd) and 4.16 (cpd) depending on the experiment. Gray levels of patches were added when they overlapped and clipped appropriately at the maximum or minimum gray level when they were outside the range of the screen, although this only happened rarely. The Gabors were randomly distributed in a circular area, which varied between 3° and 12° wide. The centre of the distribution was the centre of the screen. The orientation in each Gabor micro-pattern was selected from a Gaussian distribution with a mean equal to the cued orientation (i.e. 90° ± the cue generated by APE, an adaptive method of constant stimuli (Watt & Andrews, 1981) and a variable bandwidth. The distribution's standard deviation, σ, was varied from 0° (all elements aligned) to 28° (high orientation variability) as shown in figure 1. The dotted lines and arrows in figure 1 represents the notional vertical and mean orientation of the array.

Figure 1

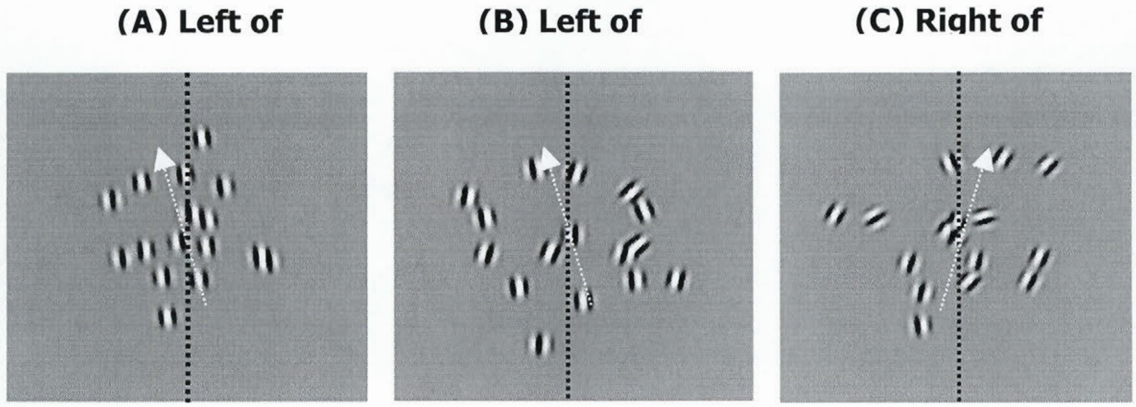
(A) Left of

(B) Left of

(C) Right of

Figure 1: Arrays of 16 randomly placed, oriented Gabor elements with mean orientation (indicated by the arrow for illustrative purposes only, not present during testing) relative to the vertical (indicated by the dashed lines for illustrative purposes only, not present during testing). Each Gabor is a sample from a Gaussian distribution of orientations with a mean equal to the cued orientation and a variable bandwidth. In this figure we show example stimuli for three different standard deviations of the parent orientation distribution; a standard deviation of 0° (A), 16° (B), and 28° (C).

Apparatus

An Apple Macintosh G3 computer was utilized in the experiment. The Matlab environment (MathWorks Ltd) and Psychophysics ToolBox (Brainard, 1997) were used for programming. All stimuli were displayed on a 20 inch Sony monitor (Trinitron 520GS), which was calibrated and linearized using Graseby S370 photometer and the Video Toolbox (Pelli, 1997) package. Pseudo 12 bit contrast accuracy was achieved by using a video attenuator (Pelli & Zhang, 1991), which combined the RBG outputs of the graphic card (ATI Rage 128) into the G gun. The monitor had a refresh rate of 75 Hz. The mean luminance of the screen was 33 cd/m^2 and the resolution was 1152 x 870 pixels. One pixel on the screen was 0.32 mm, which was 2.12 Arc min of the observers' visual angle from the viewing distance of 52 cm. The observers performed the task monocularly beginning with the fellow fixing eye (in amblyopes) and dominant eye (in normals), with the other eye patched.

Psychophysics

(A) Equating orientation discrimination performance for isolated stimuli: In order to equate the performance levels for this task for an individual Gabor stimulus for fixing and amblyopic eyes, we measured the orientation discrimination threshold for a single Gabor, of the exact type used in the later integration experiment, as a function of the contrast of the Gabor. This single Gabor was presented in a random position within the 6° stimulus area and was tilted clockwise or counter-clockwise from vertical. The magnitude of the tilt was determined by the APE procedure. A single temporal interval two

Figure 2

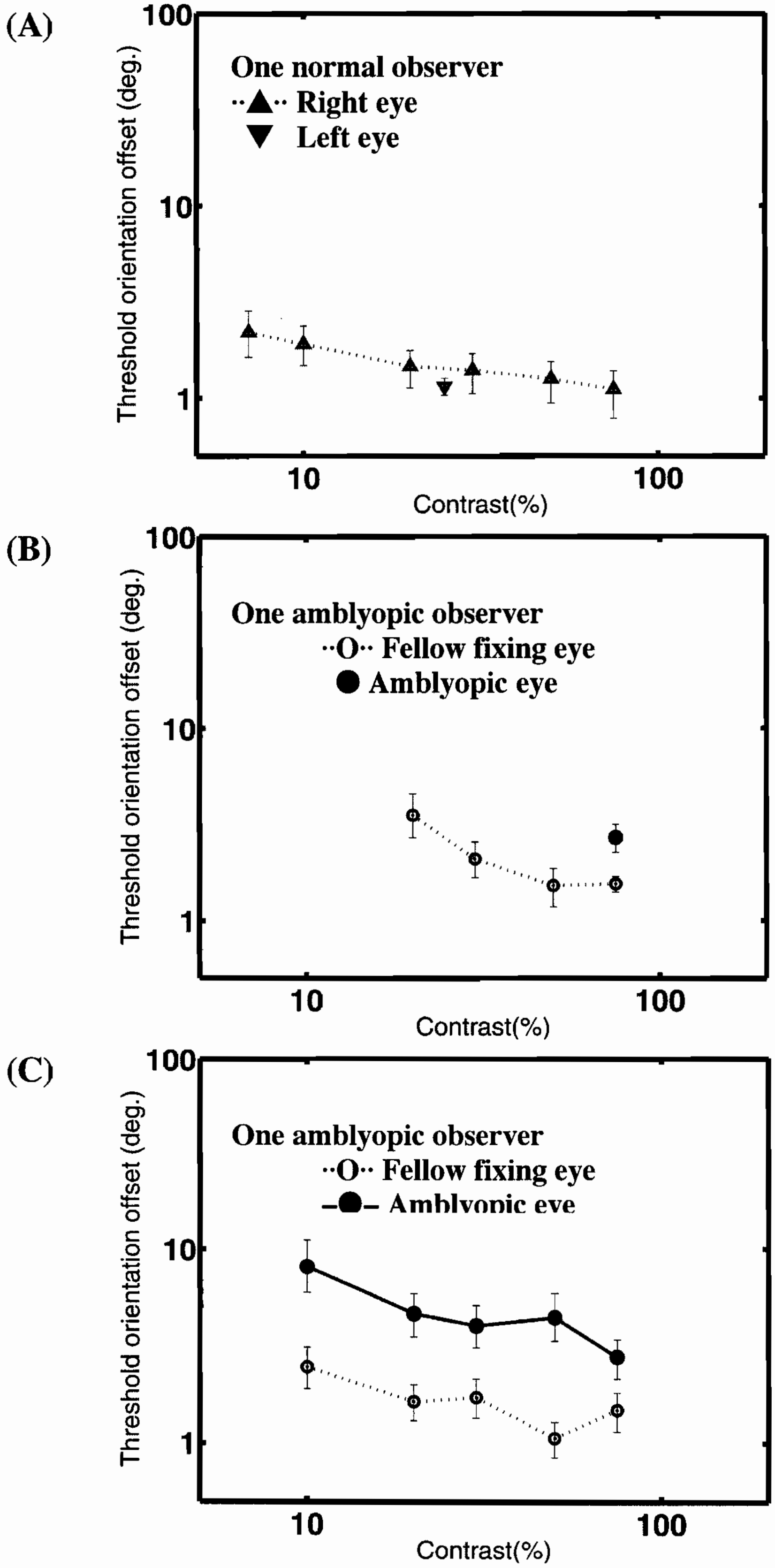
(A)
One normal observer
··▲·· Right eye
▼ Left eye
Threshold orientation offset (deg.)
100
10
1
10
100
Contrast(%)
(B)
One amblyopic observer
··O·· Fellow fixing eye
● Amblyopic eye
Threshold orientation offset (deg.)
100
10
1
10
100
Contrast(%)
(C)
One amblyopic observer
··O·· Fellow fixing eye
–●– Amblyopic eye
Threshold orientation offset (deg.)
100
10
1
10
100
Contrast(%)

Figure 2: Equating performance for single elements. Orientation discrimination thresholds measured as a function of contrast for a single Gabor element. In (A), results are shown for a normal observer. In (B), results are shown for an amblyope (AM) in which the performance of the amblyopic eye is fixed at a high contrast (75%) and the performance of the fellow fixing eye is measured as a function of contrast. In this case to equate performance for the amblyopic eye viewing a 75% contrast stimulus, we would need to use a 25% contrast stimulus viewed by the fellow fixing eye. In (C), results are shown for the amblyopic and fellow fixing eyes of an amblyope (BB) as a function of contrast. With lower contrast, there is worse orientation discrimination performance. Error bars: 95% Confidence intervals (CIs).

(B) Orientation integration: Arrays of randomly positioned, oriented Gabors were presented. The orientation of an individual array element was chosen from a Gaussian distribution. A single temporal interval two alternative forced choice paradigm was used. The observers' task was to judge whether the mean orientation of the array of Gabors was rotated clockwise or counter clockwise (tilted to right or left of vertical) (see figure 1). In the main experiment, the stimuli were shown for 500 ms although this was varied (13-500 ms) in a later experiment. Orientation discrimination thresholds were obtained from between 192-340 presentations for each of a number of standard deviations of the parent distribution i.e. external noise (10 levels typically between 0-28°). The orientation threshold for each level of variability of the parent distribution was estimated as the slope of the best fitting cumulative Gaussian function using a maximum likelihood procedure. The model described in the introduction was fitted to the thresholds separately for each eye of each observer in each condition.

Statistics

We tested the parameters from our equivalent noise model, internal noise and number of samples separately. In order to compare the differences between the groups, we used a 2 (between) x 2 (within) x 3 (within) analysis of variance (ANOVA) for the variables of observer (normal and amblyopic), eye (amblyopic and fellow fixing in amblyopic observers and dominant and non-dominant in normal observers) and spatial frequency (low, medium and high). We also calculated 95% confidence intervals for the thresholds from each individual psychometric function and used it to compare individual sets of data within the groups.

Experimental manipulations

Integration within different spatial frequency bands

In the first experiment low spatial frequency stimuli (0.52 cpd), which were well within the acuity limit of all observers, were tested in 10 amblyopic and 10 normal observers. In each trial, 16 micro-patterns were presented within the stimulus area (see figure 1). The stimulus area was 6° of visual angle. The exposure duration time was 500 ms.

Since contrast sensitivity is similar to normal in the majority of amblyopes for low spatial frequencies (Hess & Howell, 1977), these stimuli are useful to compare the integration function of the amblyopic and normal eyes with a stimulus for which contrast thresholds are normal or only minimally affected.

In order to better understand the influences of different spatial frequencies on orientation integration for the amblyopic visual system, 6 amblyopic (AM, LN, MA, MG, MM and RB see table 1.) and 6 normal observers were tested with medium and high spatial frequency Gabor arrays. The spatial frequency of the high frequency stimulus was a factor of 2 below the highest spatial frequency that the observers reported that they could see – except in the (MA) case where this led to a very high orientation discrimination threshold (87°), so the spatial frequency was reduced by a further factor of 2. The average high spatial frequency stimuli were about a factor of 6-8 (3.12 - 4.16 cpd) above the low frequency stimuli (0.52 cpd). These were stimuli for which contrast thresholds were elevated in amblyopic eyes. The medium frequency stimuli typically were between the high and low spatial frequencies (e.g. 2 cpd).

Exposure duration

While some studies have argued that amblyopic visual system is more detrimentally affected by decreasing the exposure duration than the normal visual system (Rentschler & Hilz, 1985; Weiss, Rentschler & Caelli, 1985), others have shown very little effect of decreasing exposure duration (Demanins & Hess, 1996a; Loshin & Jones, 1982). The discrepancy may be due to the different tasks studied, in the former case it was vernier acuity and phase discrimination, whereas in the latter it was contrast thresholds and positional sensitivity for well separated stimuli. To ascertain whether exposure duration is important for local orientation integration in amblyopia, we measured integration performance for a range of exposure durations, between 13 ms and 500 ms. This was done in one normal and five amblyopic observers (MA, PH, RB, MM and BB).

Numerosity, density and stimulus extent

It has been previously shown in normal observers (Dakin, 2001) that the number of presented elements relates strongly to the sampling efficiency of an observer and the internal noise can be affected by the density of the element array. To better understand the mechanisms involved in integration by the amblyopic visual system, we varied these parameters in one normal and five amblyopic observers (MA, AT, PH, RB and MM).

Three parameters were varied in this experiment; number, density of elements and radius of stimulus area. Since these parameters are inter-related, changing one without changing the others is not possible. Therefore to study the effects of these parameters individually, one variable was kept fixed at a time, whilst allowing the other two to co-vary. In the first condition, radius of stimulus area was held constant (6°) and the number of elements (16, 64 and 256) and the density (0.176, 0.705 and 2.820 element/cm^2) co-varied. In the second condition, the number of elements was held constant (64) and the radius of stimulus area (3°, 6° and 12°) and the density (2.820, 0.705 and 0.176 element/cm^2) co-varied. In the third condition, the density was held constant (0.705 element/cm^2) and the radius of stimulus area (3°, 6° and 12°) and the number of elements (16, 64 and 256) co-varied. In all conditions, the presentation time was 500 ms.

Results

Equating orientation performance levels. Figure 2A shows the relationship between the orientation discrimination threshold for a single Gabor and contrast for a normal observer. Performance is relatively constant at high contrasts but deteriorates as the contrast is reduced (Hess et al., 2000). Similar threshold performance at one contrast level is seen for the non-dominant eye (inverted triangle) of this normal observer. In figure 2B an example is shown of data equating the performance levels between fellow fixing and amblyopic eyes of our amblyopic observers. The filled symbol represents the orientation discrimination performance of the amblyopic eye for a fixed 75% contrast stimulus. The open symbols and dotted curve represent the performance of the fellow fixing eye as a function of stimulus contrast. In this case, to equate performance levels for the single element, the contrast of the stimuli for the fellow fixing eye needs to be reduced to a third (i.e. 25%) of that seen by the amblyopic eye. We repeated these measurements for all amblyopic observers and used the appropriate contrast for the fellow fixing eye that equated orientation discrimination performance for 75% contrast stimuli seen by the amblyopic eye. In figure 2C, we show how the amblyopic eye's performance (filled symbols and solid curve) changes with reducing the contrast below 75%. It exhibits a stronger dependence on contrast than that seen for the fellow fixing eye (unfilled symbols and dotted curve), which was expected due to the known poor performance for orientation discrimination for amblyopic observers when using low contrast stimuli (Demanins et al., 1999).

Averaged results for the orientation discrimination of an isolated Gabor are shown in figure 3A for fellow fixing eyes at two contrast levels and amblyopic eyes for the three spatial frequencies tested. At the same physical contrast, the amblyopic eye exhibits poorer orientation discrimination compared with the fellow fixing eye ($p<0.05$) although the magnitude of this effect is only large at high spatial frequencies. When the contrast of the fellow fixing eye is reduced to around 20% there was no statistically significant difference between the performance of the fellow fixing and amblyopic eyes.

Figure 3

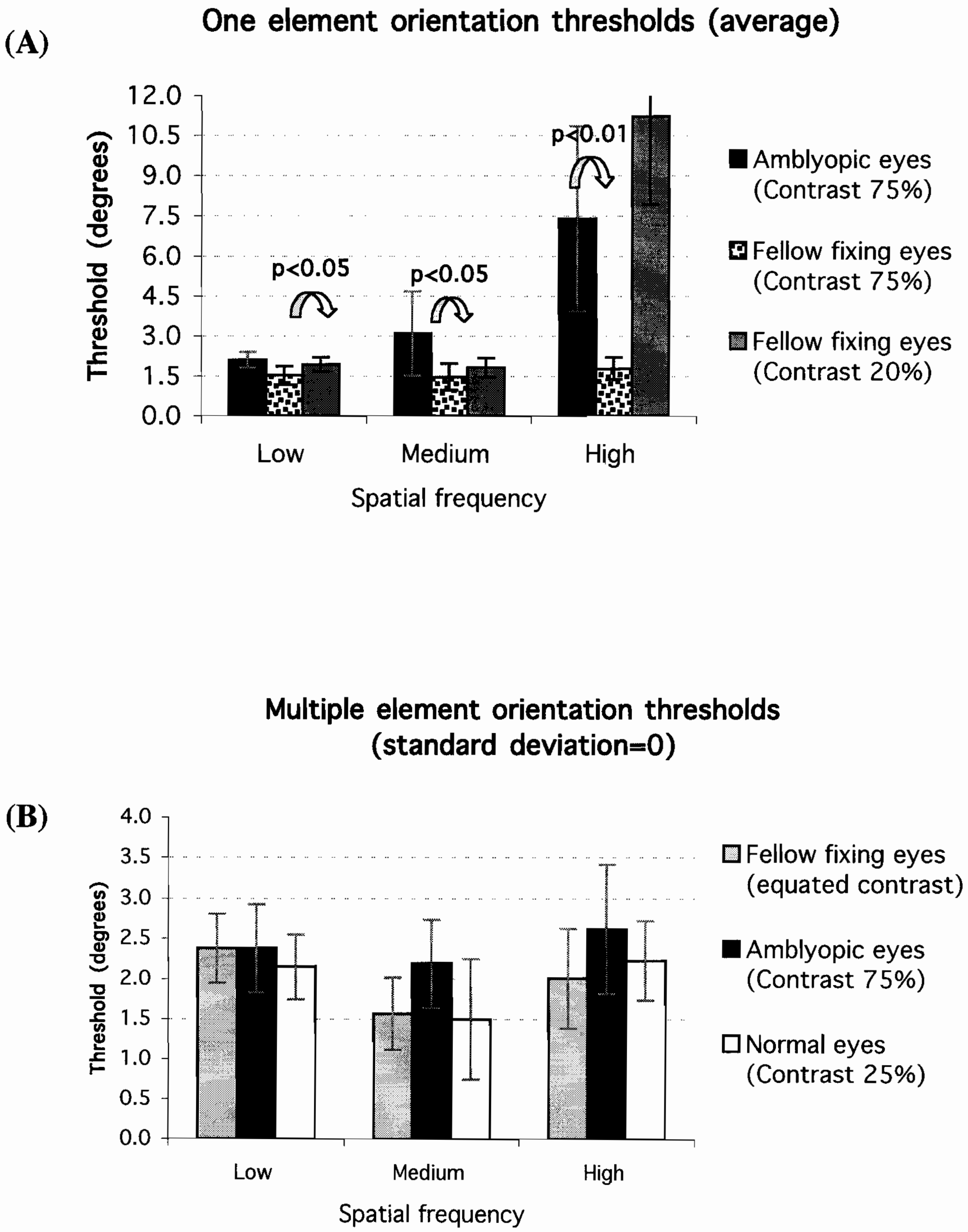
(A)
One element orientation thresholds (average)
Threshold (degrees)
12.0
10.5
9.0
7.5
6.0
4.5
3.0
1.5
0.0
p<0.05
p<0.05
p<0.01
Low
Medium
High
Spatial frequency
■ Amblyopic eyes (Contrast 75%)
▨ Fellow fixing eyes (Contrast 75%)
▨ Fellow fixing eyes (Contrast 20%)
(B)
Multiple element orientation thresholds
(standard deviation=0)
Threshold (degrees)
4.0
3.5
3.0
2.5
2.0
1.5
1.0
0.5
0.0
Low
Medium
High
Spatial frequency
▨ Fellow fixing eyes (equated contrast)
■ Amblyopic eyes (Contrast 75%)
☐ Normal eyes (Contrast 25%)

Figure 3: Equating performance for single elements. Orientation discrimination thresholds measured as a function of contrast for a single Gabor element. In (A), results are shown for a normal observer. In (B), results are shown for an amblyope (AM) in which the performance of the amblyopic eye is fixed at a high contrast (75%) and the performance of the fellow fixing eye is measured as a function of contrast. In this case to equate performance for the amblyopic eye viewing a 75% contrast stimulus, we would need to use a 25% contrast stimulus viewed by the fellow fixing eye. In (C), results are shown for the amblyopic and fellow fixing eyes of an amblyope (BB) as a function of contrast. With lower contrast, there is worse orientation discrimination performance. Error bars: 95% Confidence intervals (CIs).

Integrating local oriented signals

The results shown in figure 3B represent a similar comparison to that in 3A for an array of identically oriented Gabors. Here we compared mean orientation performance for the amblyopic (75% contrast) and fellow fixing eye (adjusted contrast) and the normal eye of non-amblyopic observers (25% contrast). There is no statistically significant difference between the means of these three conditions indicating that our method of equating performance between the amblyopic eyes, fellow fixing, and normal eyes was successful. Notice that the orientation thresholds for the high spatial frequency Gabors are much reduced in the multiple elements, compared with the isolated element, condition. It would seem that the reduced orientation discrimination performance for isolated high spatial frequency Gabors (figure 3A) may be due to either an inability to detect some stimuli when their position is uncertain or to the benefit of being able to integrate a number of identical individual signals.

Our next step was to compare performance for the mean orientation task when the individual Gabor elements within the array did not have identical orientations. As illustrated in figure 1 we introduced orientational variability into the display by having the orientation of each Gabor element be a sample from a parent Gaussian orientation distribution whose mean was at the vertical ±the cued orientation. We measured the threshold orientation offset required to reach criterion performance on this mean orientation task as a function of the standard deviation of the distribution from which the individual orientation samples were drawn. Example results of a normal observer (A) and an amblyopic observer (B) are displayed in figure 4. The discrimination threshold for judging the mean orientation of an array of 16 randomly positioned Gabors is plotted against the standard deviation of the orientation distribution. The error bars represent 95% confidence intervals obtained from our bootstrapping procedure. The curves represent the equivalent noise model described in the introduction fitted to the orientation thresholds with the best fit estimates for internal noise (I.N.) and number of samples (N.S.) values shown in the inset. In the case of the normal observer (figure 4A), performance of the right (dominant - open symbols and dotted curve) and left (non-dominant - filled symbols and solid curve) eyes are consistent with approximately 6.2 and 5.0 out of the 16 available samples being used to estimate the mean orientation of the Gabor array, respectively. The estimate of internal noise was 1.1° and 1.6°. The results in figure 4B compare performance for the fellow fixing (open symbols and dotted curve) and amblyopic eyes (filled symbols and solid curve) of one of our amblyopic observers (RA). This is a typical result showing similar performance with the fellow fixing and amblyopic eyes of this individual. The internal noise and number of samples in amblyopic eye (2.0° and 6.3) were not significantly different from those of the fellow fixing eye (2.3° compared with 5.2).

Figure 4

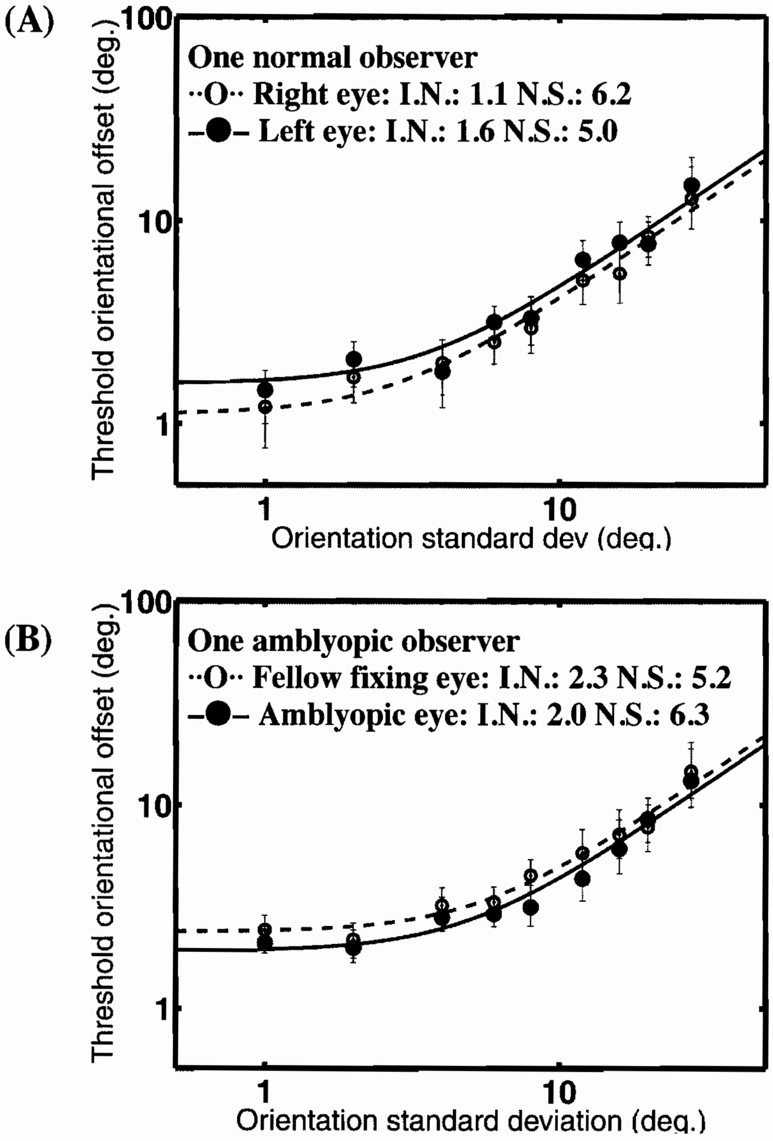
(A)
One normal observer
··O·· Right eye: I.N.: 1.1 N.S.: 6.2
–●– Left eye: I.N.: 1.6 N.S.: 5.0
Threshold orientational offset (deg.)
100
10
1
1
10
Orientation standard dev (deg.)
(B)
One amblyopic observer
··O·· Fellow fixing eye: I.N.: 2.3 N.S.: 5.2
–●– Amblyopic eye: I.N.: 2.0 N.S.: 6.3
Threshold orientational offset (deg.)
100
10
1
1
10
Orientation standard deviation (deg.)

Figure 4: Mean orientation thresholds. Orientation discrimination thresholds are plotted against the standard deviation of the orientation distribution from which the samples were taken. In this case, 16 Gabors comprised the stimulus array. The curve is the best fit for the equivalent noise model. The error bars represent 95% confidence intervals. The parameters of this fit, internal noise (I.N.) and number of samples (N.S.) are shown in the inset. In (A), results are shown for dominant (open symbols and dotted curve) and non-dominant (filled symbols and solid curve) eyes of a normal observer (HA) whereas in (B), results are shown for the amblyopic (filled symbols and solid curve) and fellow fixing (open symbols and dotted curve) eyes of a strabismic amblyope (MA).

Integration for different spatial frequencies

In figure 5 we show results in a similar form to that described above but averaged over the eyes of our normal and amblyopic observers. In each case, we plot the averaged thresholds for each eye of our normal observers (dominant and non-dominant eyes) and for each eye of our amblyopes (fellow fixing and amblyopic). The error bars represent ±0.5 standard deviation (SD) of the population. We did not find any significant differences between the thresholds from normal and amblyopic eyes. This was true for all low (figure 5A), medium (figure 5B) and high (figure 5C) spatial frequencies.

Figure 5

Low spatial frequency (mean threshold)

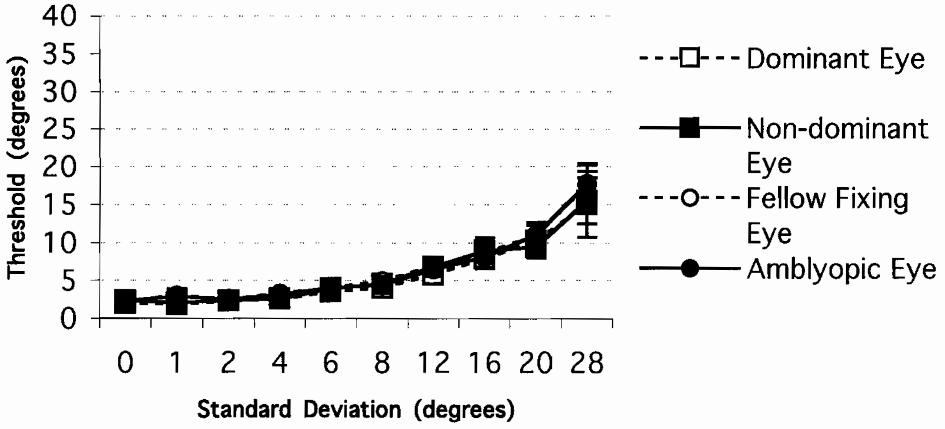

Medium spatial frequency (mean threshold)

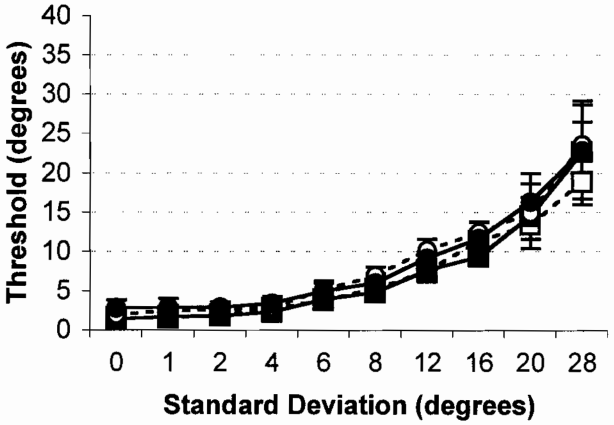

High spatial frequency (mean threshold)

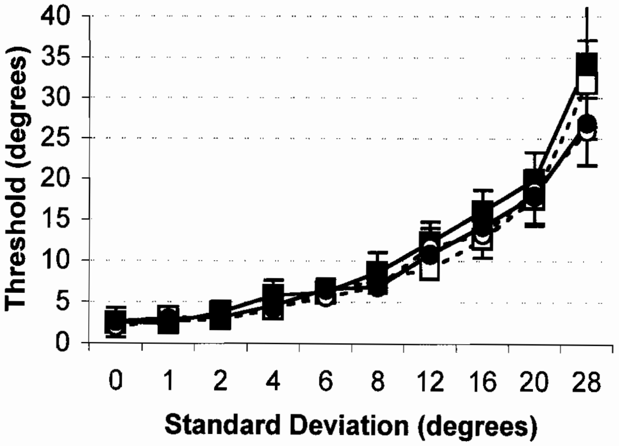

Figure 5: Average mean orientation thresholds. Averaged thresholds are displayed for the amblyopic (filled circles and solid lines) eyes, the fellow fixing eyes (open circles and dotted curve) and eyes of normal observers (open and filled square symbols correspond to dominant and non dominant eyes, respectively) for stimuli of low (A), medium (B) and high (C) spatial frequency. The error bars represent ±0.5 SD.

From each individual result we derived the best fits for the parameters of internal noise and number of samples and averaged these individually derived measures across our observer populations. These measures are shown for the three populations, normals (average threshold of both eyes of normal observers) and fellow fixing eyes and amblyopic eyes (of amblyopic observers) in figure 6. For the purpose of clarity, the error bars represent ±0.5 SD. The internal noise parameter was significantly higher at high spatial frequencies (fellow fixing vs. amblyopic eye only, $p<0.05$), however at low and medium spatial frequencies, internal noise was not significantly different for amblyopic eyes ($p>0.05$). In terms of the number of samples parameter (figure 6B), as the spatial frequency increased, the number of samples taken by the visual systems decreased, regardless of being amblyopic or non-amblyopic ($p<0.05$ for medium vs. high spatial frequency and $p<0.01$ for low vs. high spatial frequency). There was no significant difference between the number of samples taken by the amblyopic and non-amblyopic eyes ($p>0.05$).

For the purpose of clarity, the internal noise and number of samples values in each individual amblyopic (table 2(A, B), respectively) and normal observer (table 2(C, D), respectively) are presented.

Figure 6

(A)

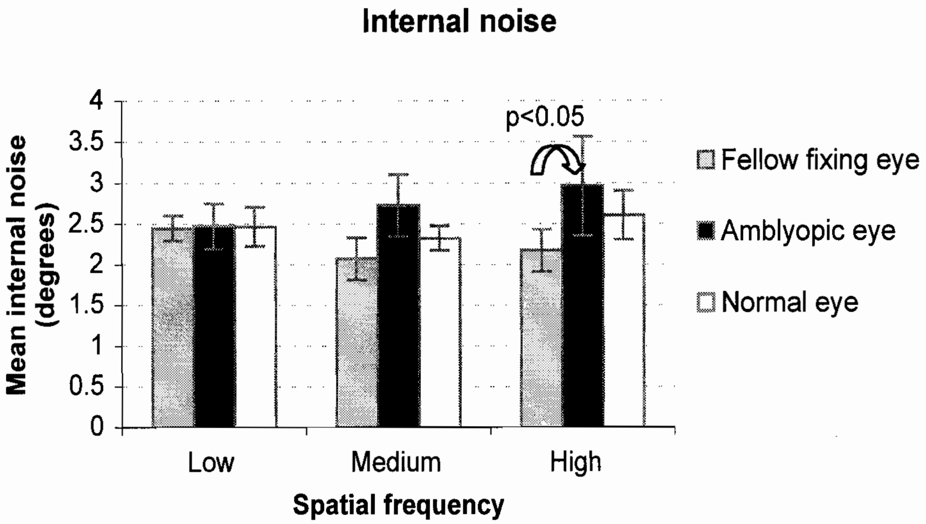
Internal noise
Mean internal noise (degrees)
4
3.5
3
2.5
2
1.5
1
0.5
0
p<0.05
Low
Medium
High
Spatial frequency
▨ Fellow fixing eye
■ Amblyopic eye
□ Normal eye

(B)

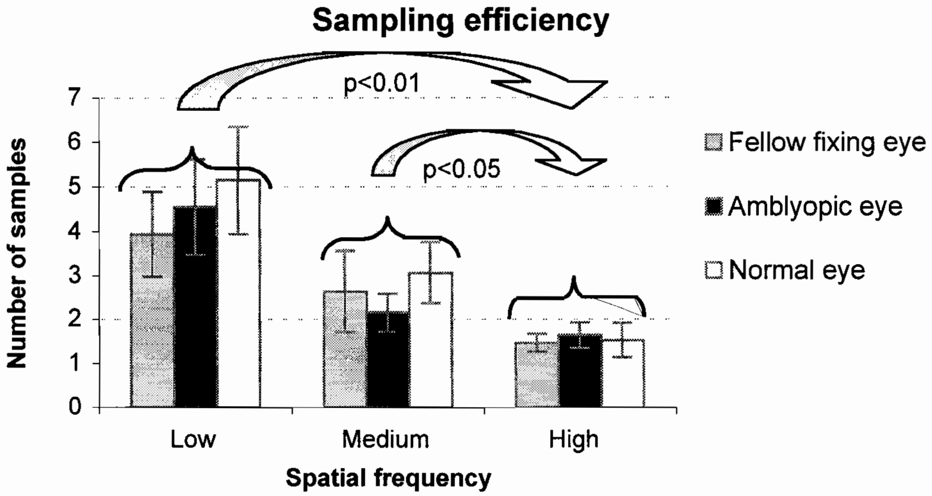
Sampling efficiency
Number of samples
7
6
5
4
3
2
1
0
p<0.01
p<0.05
Low
Medium
High
Spatial frequency
▨ Fellow fixing eye
■ Amblyopic eye
□ Normal eye

Figure 6: Internal noise and number of samples. Comparison of the average of the individual estimates of internal noise (A) and number of samples (B) from our model fits for the three variables of, fellow fixing eyes (gray bars), amblyopic eyes (filled bars), and eyes of normal observers (open bars). The error bars represent ±0.5 SD. In (A), there is significantly higher internal noise for amblyopic eyes compared with either normal eyes or fellow fixing eyes only at high spatial frequency condition ($p<0.05$). For the number of samples measured in (B), we found no significant different between amblyopic and either normal eyes or fellow fixing eyes, although the number of samples, unlike the internal noise, did show a significant overall reduction with increasing spatial frequency ($p<0.05$).

Table 2

(A)

Observers	LSF FFE	LSF AME	MSF FFE	MSF AME	HSF FFE	HSF AME
AM	1.43	1.54	0.27	0.87	0.56	0.98
LN	2.35	1.51	0.96	1.14	1.36	2.24
MA	2.39	1.58	1.38	2.37	3.61	3.78
MG	4.43	5.24	3.75	4.83	4.18	6.78
MM	1.51	1.50	1.16	1.34	1.41	2.07
NG	2.76	2.41	N/A	N/A	N/A	N/A
RB	2.49	2.96	2.35	2.67	1.92	1.93
VL	2.51	2.29	N/A	N/A	N/A	N/A
YC	1.78	1.33	N/A	N/A	N/A	N/A
BB	4.08	5.87	N/A	N/A	N/A	N/A
AT	3.79	5.58	N/A	N/A	N/A	N/A
PH	1.82	2.36	N/A	N/A	N/A	N/A

(B)

Observers	LSF FFE	LSF AME	MSF FFE	MSF AME	HSF FFE	HSF AME
AM	5.44	6.58	6.55	2.84	1.16	2.14
LN	3.89	3.07	2.00	2.81	1.20	2.06
MA	5.21	6.24	1.87	3.03	2.01	0.79
MG	2.46	3.49	1.89	1.74	1.87	2.17
MM	2.89	3.47	1.60	2.47	1.12	1.43
NG	2.54	4.52	N/A	N/A	N/A	N/A
RB	1.79	2.26	1.25	1.36	1.36	1.24
VL	4.10	8.69	N/A	N/A	N/A	N/A
YC	8.15	5.08	N/A	N/A	N/A	N/A
BB	1.50	0.75	N/A	N/A	N/A	N/A
AT	3.41	4.26	N/A	N/A	N/A	N/A
PH	5.43	5.61	N/A	N/A	N/A	N/A

Table 2.

(C)

Observers	LSF FFE	LSF AME	MSF FFE	MSF AME	HSF FFE	HSF AME
BM	1.1	1.57	0.72	0.96	1.34	2.09
HA	2.32	2.68	2.07	1.74	3.69	2.00
LA	1.63	1.77	1.25	0.99	1.17	1.80
EK	1.65	1.57	1.03	0.98	1.76	1.82
SD	2.32	2.24	2.39	2.12	3.38	6.77
MA	1.43	1.51	1.31	1.21	2.78	2.66
OE	2.27	1.83	N/A	N/A	N/A	N/A
MM	2.04	1.87	N/A	N/A	N/A	N/A
CH	3.12	3.54	N/A	N/A	N/A	N/A
PA	1.42	1.83	N/A	N/A	N/A	N/A

(D)

Observers	LSF FFE	LSF AME	MSF FFE	MSF AME	HSF FFE	HSF AME
BM	6.24	4.96	3.82	5.24	1.92	1.65
HA	4.77	5.24	2.42	2.92	0.77	1.24
LA	2.95	1.60	1.42	1.58	1.28	1.83
EK	5.25	5.60	3.10	2.88	2.75	2.75
SD	1.80	1.97	1.68	1.71	1.01	0.49
MA	4.91	4.95	4.95	5.05	2.17	0.55
OE	5.18	4.27	N/A	N/A	N/A	N/A
MM	6.67	10.37	N/A	N/A	N/A	N/A
CH	3.18	4.73	N/A	N/A	N/A	N/A
PA	10.74	7.49	N/A	N/A	N/A	N/A

Table 2: Internal noise and number of samples in the amblyopic and normal observers. (A) Internal noise in amblyopic observers. (B) Number of samples in amblyopic observers. (C) Internal noise in normal observers. (D) Number of samples in amblyopic observers. The following abbreviations have been used; LSF: Low spatial frequency, MSF: Medium spatial frequency, HSF: High spatial frequency, FFE: Fellow fixing eye, AME: Amblyopic eye.

Exposure duration

The previous results were obtained at an exposure duration of 500 ms. In figure 7A we show the effect of two presentation durations, 500 ms versus 100 ms on orientation discrimination performance on our single element task for one of our amblyopic observers (BB). Short stimulus durations disadvantage the performance of the amblyopic eye relative to its fellow fixing eye and therefore a lower contrast is required for the fellow fixing eye to equate the orientation performance of the fellow fixing and amblyopic eyes. However, once performance for the single element has been equated, the subsequent integration of oriented signals is not significantly different ($p>0.05$) for fellow fixing and amblyopic eyes (figure 7B). Internal noise and number of samples for five amblyopic observers are presented in Table 3.

For completeness we found that integration of orientation information was quite similar across a wide range (500-13 ms) of exposure durations in normal vision (figure 7C).

Figure 7

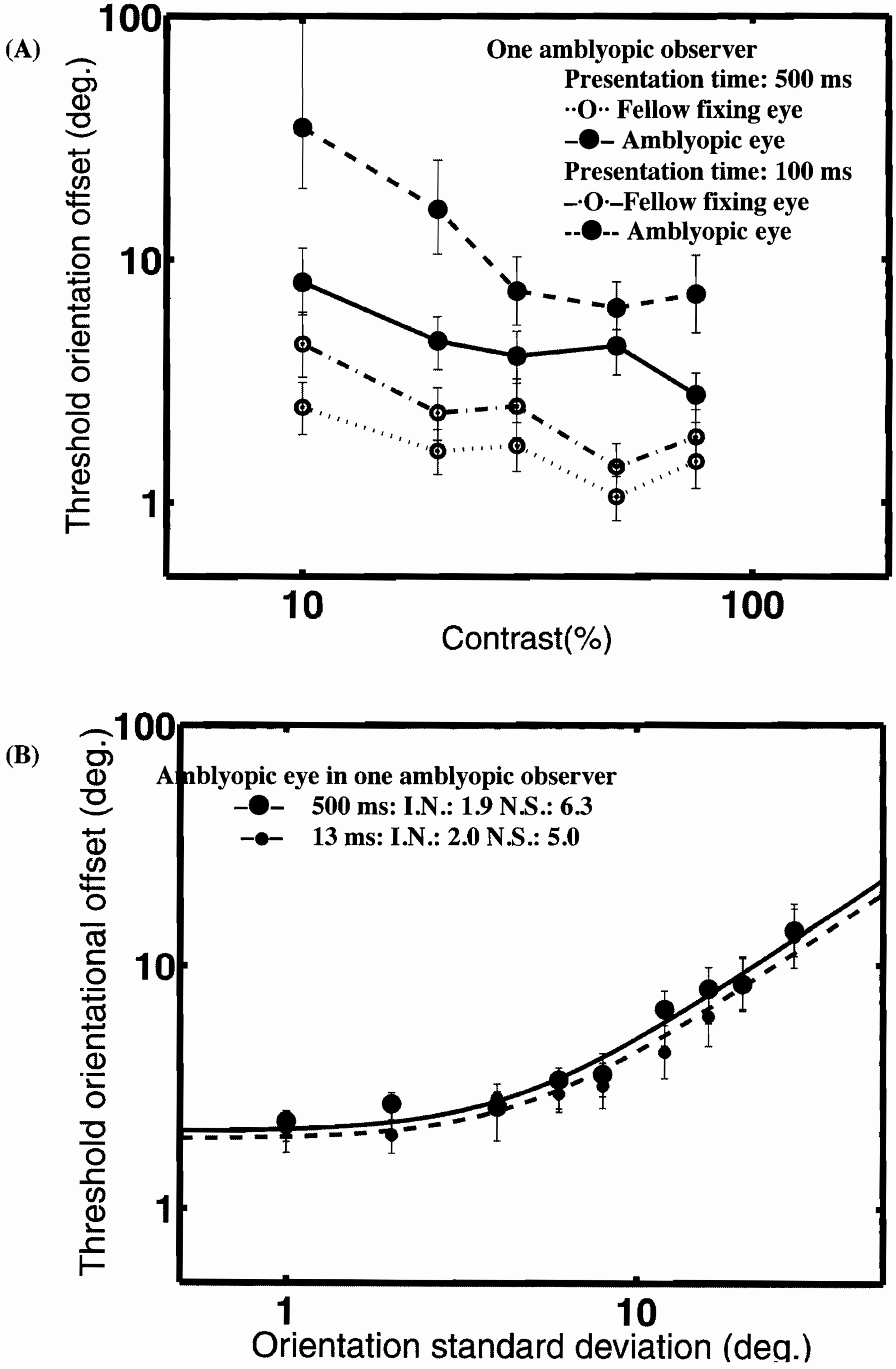
(A)
One amblyopic observer
Presentation time: 500 ms
··O·· Fellow fixing eye
–●– Amblyopic eye
Presentation time: 100 ms
–·O·–Fellow fixing eye
--●-- Amblyopic eye
Threshold orientation offset (deg.)
100
10
1
10
100
Contrast(%)
(B)
Amblyopic eye in one amblyopic observer
–●– 500 ms: I.N.: 1.9 N.S.: 6.3
–•– 13 ms: I.N.: 2.0 N.S.: 5.0
Threshold orientational offset (deg.)
100
10
1
1
10
Orientation standard deviation (deg.)

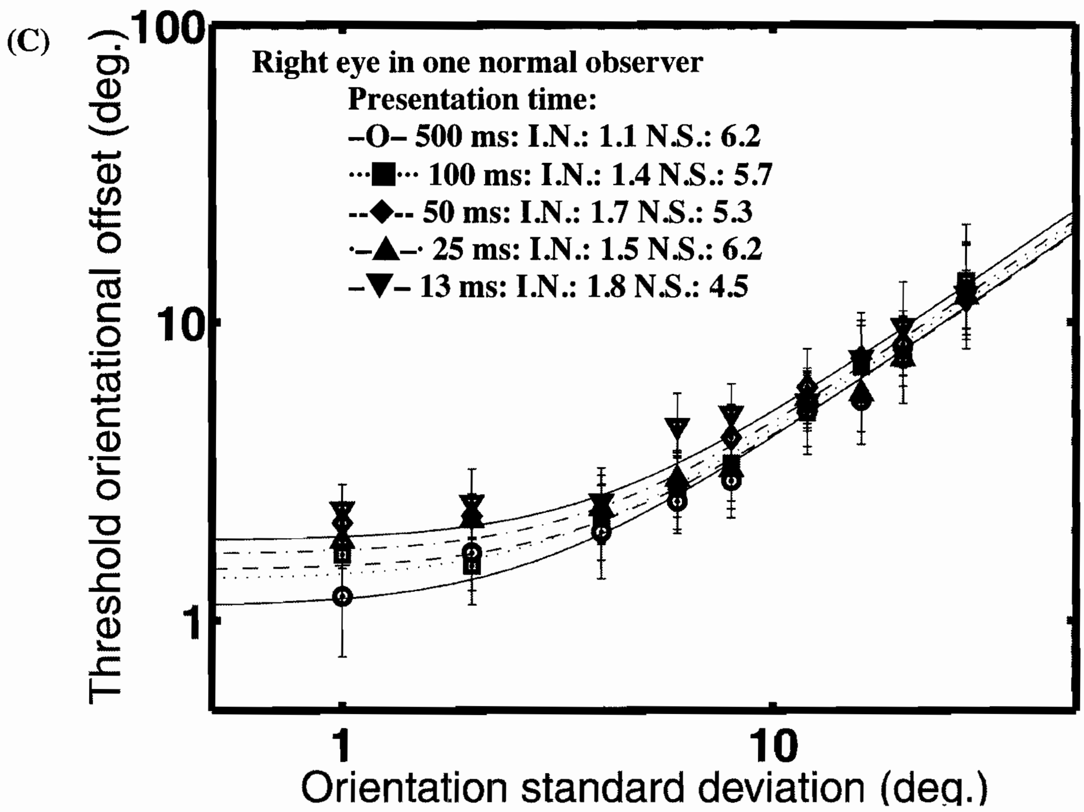

***Figure** 7: Mean orientation thresholds for different exposure durations. In (A), orientation discrimination thresholds are plotted for a single Gabor element for the amblyopic and fellow fixing eyes of a strabismic amblyope (BB) for two exposure durations (100 ms & 500 ms). The amblyopic eye is disadvantaged when the exposure duration is short and this necessitates a different correction factor to bring the performance of amblyopic and fellow fixing eyes together for the single element case. In (B), mean orientation thresholds are plotted against orientation discrimination standard deviation for an amblyopic observer (MA). Orientation integration is not significantly different for two exposure durations (500 ms & 13 ms). In (C), orientation integration is seen to be invariant with exposure duration for the dominant eye of a normal observer*

(BM). The parameters of this fit, internal noise (I.N.) and number of samples (N.S.) are shown in the inset. The error bars represent 95% confidence intervals.

Table 3

Observers	Internal noise FFE	Internal noise AME	Number of samples FFE	Number of samples AMB
MA	5.00	2.5	2.28	4.85
PH	2.60	2.91	6.92	9.24
RB	3.56	3.26	1.75	2.55
MM	2.79	4.60	2.00	2.40
BB	5.01	5.95	1.30	0.95
BM (normal)	DE 1.47	NDE 1.75	DE 5.42	NDE 4.54

***Table 3:** Internal noise and number of samples in one normal and four amblyopic observers in 13 ms presentation time condition. The following abbreviations have been used; FFE: Fellow fixing eye, AME: Amblyopic eye, DE: dominant eye, NDE: non-dominant eye.*

Numerosity, density and stimulus extent

In our main experiment we used arrays of 16 Gabors, randomly distributed within an area with radius of 6°, giving a density of 0.705 element / cm2. We wondered to what extent this initial choice of parameters affected our conclusions. To test this, we varied the numerosity, density and stimulus extent of the oriented Gabors for our integration task with stimuli of the low spatial frequency and compared results for the eyes of one normal (BM) and five amblyopic observers (MA and AT, RA, PH and MM), which are displayed in figure 8 (the error bars represent 95% confidence intervals). The results from all of these conditions showed similar patterns of increasing or decreasing internal noise and number of samples for all dominant fellow fixing eyes (open symbols and dashed lines) and non-dominant and amblyopic eyes (filled symbols and solid lines). Furthermore, in almost all of the variable levels, there were no significant differences between the values of internal noise and number of samples found for amblyopic and fellow fixing eyes. In the constant radius condition, our data showed that increasing the number of elements and the density of the texture has little effect on the magnitude of the internal noise (figure 8A), but it did increase the number of samples (figure 8D). In the constant numerosity condition, as the radius increased and the density decreased, the internal noise decreased (figure 8B) but the number of samples did not show a consistent pattern (figure 8E). In the constant density condition, as the number of elements and the radius increased, the internal noise decreased (figure 8C) and the number of samples increased (figure 8F).

These results highlight the importance of numerosity for this task. Unlike density or stimulus extent, the numerosity appears to determine how many samples are taken, a result consistent with the previous work of Dakin (Dakin, 2001) and Allen (Allen, Hess, Mansouri & Dakin, 2003). We find this also to be the case for amblyopic and fellow fixing eyes. An interesting difference between results for amblyopic and fellow fixing eyes of the amblyopic observers in our experiment and normal eyes of normal observers in the previous work (Dakin, 2001) concerns the internal noise. Dakin showed that in normals, internal noise varied with density. We found in our amblyopic observers that it varied inversely with the stimulus extent, although the results are not definite.

Figure 8

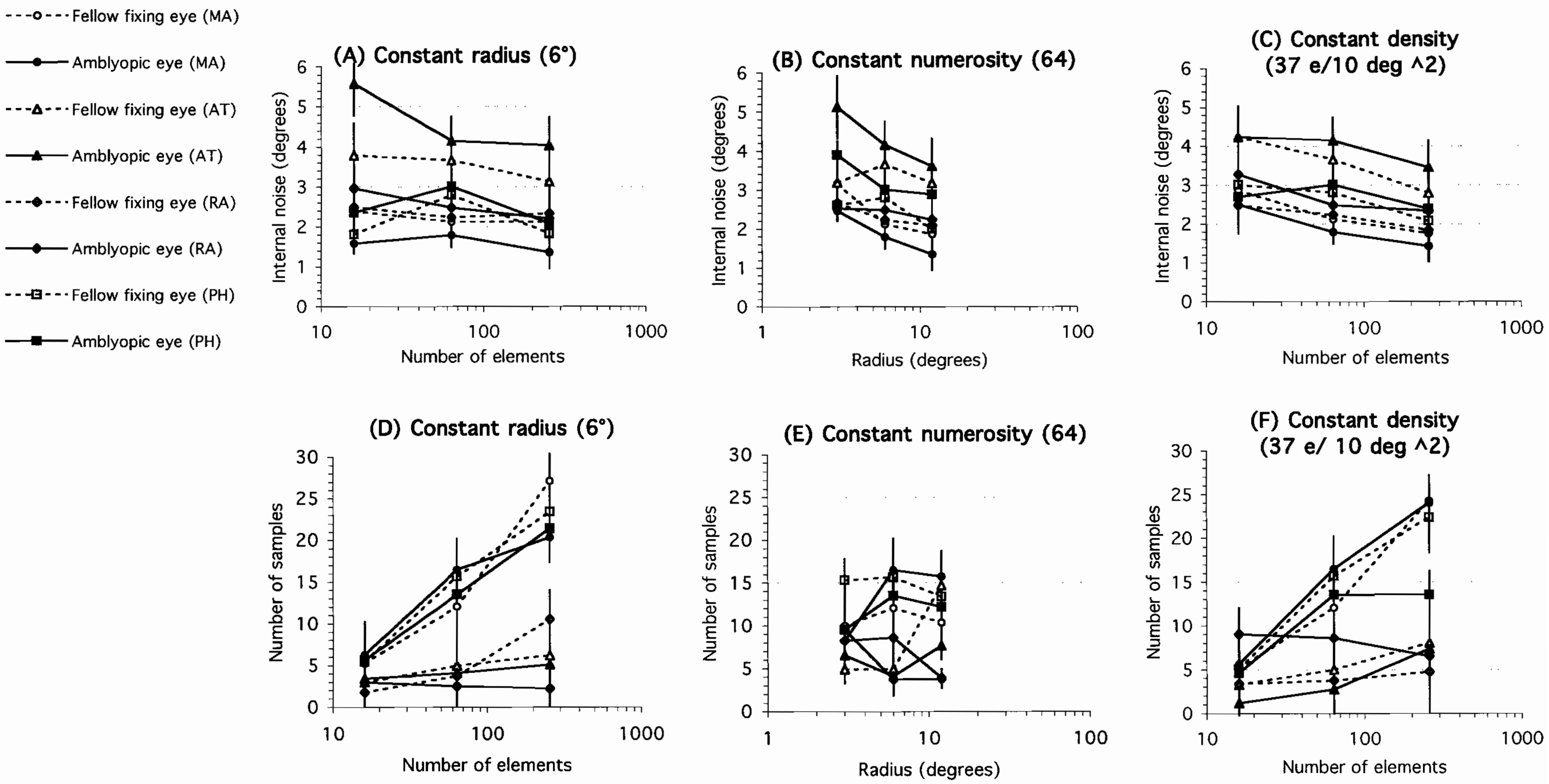
Fellow fixing eye (MA)
Amblyopic eye (MA)
Fellow fixing eye (AT)
Amblyopic eye (AT)
Fellow fixing eye (RA)
Amblyopic eye (RA)
Fellow fixing eye (PH)
Amblyopic eye (PH)
(A) Constant radius (6°)
Internal noise (degrees)
0
1
2
3
4
5
6
10
100
1000
Number of elements
(B) Constant numerosity (64)
Internal noise (degrees)
0
1
2
3
4
5
6
1
10
100
Radius (degrees)
(C) Constant density (37 e/10 deg ^2)
Internal noise (degrees)
0
1
2
3
4
5
6
10
100
1000
Number of elements
(D) Constant radius (6°)
Number of samples
0
5
10
15
20
25
30
10
100
1000
Number of elements
(E) Constant numerosity (64)
Number of samples
0
5
10
15
20
25
30
1
10
100
Radius (degrees)
(F) Constant density (37 e/ 10 deg ^2)
Number of samples
0
5
10
15
20
25
30
10
100
1000
Number of elements

Figure 8: Effects of various number of elements, presentation area and density on the internal noise and sampling efficiency. In (A) & (D), internal noise and number of samples estimates are compared for the amblyopic and fellow fixing eyes for the fixed radius condition (density and numerosity co-vary). In (B) & (E), internal noise and number of samples estimates are compared for the amblyopic and fellow fixing eyes for the fixed numerosity condition (density and numerosity co-vary). In (C) & (F), internal noise and number of samples estimates are compared for the amblyopic and fellow fixing eyes for the fixed density condition (radius and numerosity co-vary). The error bars represent 95% confidence intervals.

Discussion

The main finding of our study is that amblyopic observers can integrate local orientation information that occurs within different regions of their visual field just as efficiently as normals. This finding is robust across a number of stimulus parameters including exposure duration, numerosity, density and stimulus extent. At the level at which this integration takes place, we find no evidence of either a grossly elevated internal noise or a reduced number of samples. The amblyopic cortex processes these stimuli with the same efficiency as that of the normal cortex or indeed the cortex driven by the fellow fixing eye.

Previous research has highlighted a number of processing deficits in amblyopia, these include, contrast sensitivity, positional uncertainty (Hess & Holliday, 1992; Levi & Klein, 1985), global motion (Simmers et al., 2003), global form (Simmers et al, 2005) and orientation (Barrett et al., 2003; Popple & Levi, 2000). How do the present results relate to these deficits? Our method of equating performance in terms of the discrimination of a single Gabor element by manipulating the contrast of the stimuli presented to the fellow fixing eye had the effect of factoring out any downstream influence due to differences in contrast sensitivity or local orientation processing between the parts of the visual system driven by fellow fixing and amblyopic eyes. Furthermore, the fact that the local position of the Gabor elements within the array was irrelevant to the task meant that any positional uncertainty that might be present at the level of the integration process studied here would not influence performance. Thus, the present results are not inconsistent with what we already know about the amblyopic deficit. They are relevant to the findings with a similar task requiring integration of motion (Simmers et al., 2003) and orientation (Simmers et al., 2005) where deficits were revealed for amblyopic observers Our finding that local static signals can be integrated with normal efficiency in amblyopia argues that the deficit in amblyopia does not involve integration in general but certain types of integration in particular. It is unlikely however that a common mechanism would determine both the integration of static oriented signals and the direction of moving signals. From the little we know of the physiology, the former would take place within the ventral stream and the latter within the dorsal stream (Mishkin & Ungerleider, 1982). Thus in terms of global integration of visual information, the dorsal stream may be more disadvantaged in amblyopia when it comes to processes involving global integration. Although it should be kept in mind that such deficits might be highly task specific.

Special forms of orientation integration

The present findings may be relevant to why amblyopes have similar performance to normals when detecting textures based on orientational contrast (Mussap & Levi, 1999). Such texture discriminations however, in principle, can be accomplished by local processes involving orientation discrimination at the edge of the texture-defined region. The present findings are consistent with the conclusions of two earlier studies concerning special forms of orientation integration, in which the encoding of spatial position is a key factor, namely contour integration (Hess et al., 1997b) and global shape discrimination (Hess et al., 1999c). Amblyopes may be anomalous at these special forms of orientation integration not because their integration of orientation signals per se is necessarily anomalous but because of poor positional encoding (Demanins & Hess, 1996b; Hess & Holliday, 1992; Levi & Klein, 1985).

Explanations for amblyopia

There are three competing explanations for the neural nature of the underlying anomaly in amblyopia; loss of cells (Levi & Klein, 1986), disarray of cells (Hess, Campbell & Greenhalgh, 1978) or anomalous interaction between cells (Hess, Campbell & Zimmern, 1980b; Polat, Sagi & Norcia, 1997). Although there is no reason to expect that these explanations are mutually exclusive, let us for simplicity consider that they are. The above explanations are sufficiently vague that it is difficult to know to what extent the present results support or refute them. Some general comments can be made but it should be kept in mind that they relate specifically to the type of model used here to fit the data.

Loss of cell

Our measure of the number of samples comes from the statistical nature of the task. It does not, therefore, relate simply to the number of neural samples taken by the amblyopic visual system. It is really a general measure of efficiency. If there were fewer samples taken by the amblyopic visual system at any point up to the site where orientation integration takes place, one would expect to see a reduction in our "number of samples" measure.

Disarray of cells

Since the individual Gabors within our arrays were randomly positioned, any purely positional disarray involving cells with orientation tuning would not be expected to affect the type of integration we report here. If the positional disarray were at the input stage (i.e. involving the lay-out of the non-oriented sub-units) to cells with orientation tuning, one might expect an anomaly to local orientation processing which in our case is corrected for in our initial equating experiment. If the disarray occurs within the orientation domain, one would expect to see an elevated level of internal noise, which we did observe, but it was of small magnitude and restricted to high spatial frequencies.

Anomalous interactions between cells

We found that the efficiency of integration in amblyopia did not depend on the spatial arrangement of the local oriented signals (numerosity, density or spatial extent). A particularly revealing case is where multiple elements are used but integration is not required (i.e. where the distribution SD=0; see figure 3B). In this case, at high spatial frequencies where we show the integration of orientation is defective in amblyopic eyes, performance in the case where the standard deviation was zero, is the not significantly different between normal and amblyopic eyes. This suggests that there were no detrimental effects in the multi-element case per se due to lateral interactions. We can therefore rule out anomalous lateral interactions of the most general form occurring before the site of integration for the type of integration measured here. However, our results do not bear on some more specific types of anomaly between neighbouring elements that does not affect their later integration.

Acknowledgements

This work was supported by a Canadian Institute for Health Research (CIHR) grant (MOP 108-18) to Robert F. Hess.

Preface to chapter 3

In chapter 2 we showed that the amblyopes can integrate first-order orientation information across space similar to normal. We found that our model of "equivalent noise" could describe the amblyopic eyes' data well. The parameter of internal noise was higher in amblyopic eyes but only for high spatial frequencies. We didn't find any evidence for less sampling efficiency in amblyopic eyes compared with normal eyes.

Previous studies showed that amblyopes are specifically deficient in processing second-order information (Wong et al., 2003). Also it is shown that cells at early and late stages of the visual system respond to second-order information. There is evidence for deficiencies in striate and extra-striate cortex of amblyopes. Having said that, it is interesting to know whether amblyopes can integrate second-order orientation information similar to normal. We address this question in chapter 3 using the techniques already described in the two preceding chapters.

Chapter 3: Second-order orientation integration in amblyopia

Detection, discrimination and integration of second-order orientation information in strabismic and anisometropic amblyopia

Behzad Mansouri and **Robert F. Hess**

McGill Vision Research Unit, 687 Pine Avenue West, Rm. H4-14, Montreal,
H3A1A1 Quebec, Canada

Harriet A. Allen

School of Psychology, University of Birmingham, Birmingham, B15 2TT, UK

To better understand the nature of the cortical deficit in amblyopia we undertook a systematic investigation of second-order processing in 8 amblyopic and 8 normal observers. We investigated local detection, discrimination and global integration. Our local stimulus consisted of a Gaussian patch of fractal noise multiplied by a 1-d sinusoidal modulator. Our global stimulus consisted of an array of such elements.

We revealed second-order detection deficits for stimuli with equi-visible carriers. Orientation discrimination for an isolated second-order patch was comparable in normal and amblyopic eyes. We showed that pure integration of second-order patterns can be normal in amblyopia.

Introduction

Amblyopia involves more than just a deficit to the detection of high spatial frequencies (Gstalder, 1971; Hess & Howell, 1977; Lawwill & Burian, 1966; Levi & Harwerth, 1977). It involves deficits to the processing of supra-threshold stimuli as well (Bedell & Flom, 1981; Bradley & Skottun, 1984; Caelli et al., 1983; Demanins et al., 1999; Fronius & Sireteanu, 1989; Hess et al., 1980a; Hess & Holliday, 1992; Lawden et al., 1982; Pass & Levi, 1982; Treutwein et al., 1996; Vandenbussche et al., 1986). A large number of such deficits have been highlighted, involving the processing of orientation, spatial frequency, phase, position and contrast and this has modified the once held view that the neural substrate of amblyopia could be found in the properties of single cortical neurons in V1 (Crewther & Crewther, 1990; Eggers & Blakemore, 1978; Movshon et al., 1987). It is now accepted that there are not only anomalous interactions between cells, that is network abnormalities (Schmidt et al., 1999) but also processing beyond area V1 is likely to be affected (Kiorpes et al., 1998; Schroder et al., 2002).

Two important additions to this emerging picture have occurred recently. First, it has been shown that global processing of both motion and form are disturbed in amblyopia and that the basis for this is unlikely to be in V1 (Simmers et al., 2003). Second, this deficit to global processing involves both luminance- modulated stimuli (first-order) and contrast-modulated stimuli (second-order) processing mechanisms, although the latter is more severely affected (Simmers et al., 2003) also see (Wong et al., 2001). Most visual patterns are defined by a change in luminance over space. Second-order stimuli, on the other hand, are defined by a modulation in some other feature, for example contrast. It is likely that the mechanism that processes second-order texture or motion is at a higher level than the mechanism that processes luminance-defined patterns (Dumoulin et al., 2003). The global processing deficit in amblyopia for both first- and second-order stimuli does not appear to be a consequence of the V1 loss; it is not due to a loss in visibility of the individual elements, the accuracy with which their positions are encoded or to anomalies at a more local level of processing (i.e. directional or orientational bandwidths). Since the main anomaly involves the stage of global processing (in particular second-order) and this type of processing is thought to occur in specific regions of extra-striate cortex (Dumoulin et al., 2003; Smith, Greenlee, Singh, Kraemer & Hennig, 1998), it has been suggested that the extra-striate cortex may be primarily affected in amblyopia. This suggestion receives support from brain imaging studies using both PET (Imamura, Richter, Fischer, Lennerstrand, Franzen, Rydberg, Andersson, Schneider, Onoe, Watanabe & Langstrom, 1997) and fMRI (Barnes et al., 2001; Sireteanu et al., 1998). Since both motion and form global processing have been shown to be disrupted in amblyopia (Simmers et al., 2003) it is assumed that both dorsal and ventral streams are affected. These psychophysical conclusions are consistent with animal neurophysiology where it has been recognized for some time now that the local processing deficits in V1 are not sufficient to explain the full extent of the behavioural loss (Chino, Shansky, Jankowski & Banser, 1983; Crewther & Crewther, 1990; Kiorpes et al., 1998).

The two tasks that have been used to identify the deficit to global processing in amblyopia have both involved signals embedded in noise. In such a task, it is optimal for the visual system to integrate as much signal as possible but as little noise as possible:

involving both integration and segregation. Our hypothesis is that it is the segregation aspect of these global tasks, rather than signal integration per se, that is particularly deficient in amblyopia. We have two reasons for thinking this. There is a large literature on the role of areas MT and MST in the primate in motion processing and in particular global motion processing (Baker et al., 1991; Britten et al., 1992; Movshon et al., 1985; Newsome & Pare, 1988; Rizzo et al., 1995; Salzman et al., 1992; Vaina et al., 1990; Zihl et al., 1983). It is known that lesions to this region of the dorsal stream result in specific deficits for global motion processing in both monkeys (Newsome & Pare, 1988) and human (Rizzo et al., 1995; Vaina et al., 1990; Zihl et al., 1983). Furthermore, a study on a "motion-blind" patient (Baker et al., 1991) showed that the patient exhibited a severe deficit for motion perception, only being able to perform well for very high values of coherence. The reason for this is probably deficient segregation processes rather than deficient signal integration per se because less than 10% of the total elements, if stationary, were sufficient to disrupt performance. Such stationary elements are easily segregated by the normal visual system.

The second piece of evidence is that in a recent study Mansouri and co-workers (Mansouri, Allen, Hess, Dakin & Ehrt, 2004b) found that amblyopes performed normally on a global orientation task that relied solely on integration (i.e. devoid of any noise). This task involved estimation of the mean orientation of an array of 1-D Gabor patches, each of which was a sample of a distribution whose mean orientation was to be judged. In such a task, ideally one should integrate all the local orientation information, as all elements are signal and all contain relevant information for the task (Dakin, 2001). No performance deficits were found at low and medium spatial frequencies and only modest ones were found at high spatial frequencies. The finding that global integration was normal for low to mid spatial frequencies is surprising in view of the large deficits reported for a similar task involving global orientation integration using moderate-sized elements (e.g. 0.47° diameter elements) (Simmers et al., 2003). The main difference between the task used by Simmers and co-workers which revealed global motion and orientation deficits in amblyopia and the task used by Mansouri and co-workers which did not, involves the role of noise. The former involved signal as well as noise and therefore integration as well as segregation. The latter, on the other hand, involved only signal and hence purely integration.

The fact that tasks involving solely integration do not reveal a deficit in amblyopia whereas tasks that require both integration and segregation, do, suggests that the problem lies with the segregation side of the task. So far this distinction in the results between tasks requiring integration as well as segregation and those requiring integration alone has been shown only for luminance-defined (i.e. first-order) stimuli (Mansouri et al., 2004b) for which the global deficit for integration/segregation tasks is known to be modest (less than a factor of 2); (Simmers et al., 2005; Simmers et al., 2003). Global processing for contrast-defined (i.e. second-order) stimuli has been shown to be much more affected (factor of 3.5) than its first-order counterpart in both motion and equivalent form tasks in amblyopia (Simmers et al., 2005) but see (Wong et al., 2001). Therefore, a stronger test of the hypothesis that pure signal integration does not lie at the heart of the reported deficit on tasks involving signal and noise would be to investigate the ability of amblyopes to integrate second-order form information. In this study we undertake an evaluation of the purely integrative capacity of amblyopic eyes using second-order stimuli. The task is one where all elements are signal and it is in the best interests of observers to integrate all the available information. We used an equivalent noise model to derive the equivalent internal noise (Barlow, 1957; Pelli & Farell, 1999) and sampling associated with threshold performance (Dakin, 2001), after first ensuring that the performance of the amblyopic and fellow normal eye are equated, at the local element level, for this particular task. This latter step is important because only if performance is equated locally can one be sure that any deficit observed involves purely global processing. Additionally, since deficient first-order processing can result in loss of performance for second-order stimuli, we also ensure that our second-order stimuli have been equated at the first-order (i.e. carrier) level of processing. This next step is important because only if performance is equated at the level of the carrier is it possible to conclude whether there is a deficit for second-order processing. The results show deficient detection of second-order stimuli by the fellow fixing and amblyopic eyes but normal orientation discrimination both locally and globally by amblyopic eyes.

Methods

Observers

Eight amblyopic and eight normal observers were tested. In the amblyopic group there were four strabismic, two anisometropic and two mixed amblyopic observer (for details see table 1). The average ages in normal and amblyopic groups were 31.5 and 33.25, respectively. All observers wore appropriate refractive corrections during the testing period. Informed consent was obtained from all observers before data collection.

Table 1.

Observers	Age	Type	Refraction	Acuity	Squint	History, stereo
AG	41 y	RE strab	+0.50 DS +0.50 + 0.05 90^{c}	20 / 400 20 / 16	ET 15°	Detected age 3 y, 6 mo patching, strabismus surgery RE age 5 y, glasses from 13 y
GN	30 y	RE strab	+5.00 –2.00 120^{c} +3.50 –1.00 75^{c}	20 / 70 20 / 20	ET 8°	Detected age 5y, 3m patching no glasses tolerated, 2 strabismic surgery RE age 10-12y
MA	22 y	LE aniso	–0.25 DS +3.50 – 0.50 0^{c}	20 / 15 20 / 200	Ortho	Detected age 3 y, patching for 4 y, glasses for 8 y
ML	20 y	RE mixed	+1.0 - 0.75 90^{c} –3.25 DS	20 / 80 20 / 25	ET 6°	Detected age 5y, patching for 2 y
PH	33 y	LE mixed	-2.00 + 0.50 +0.50 90^{c}	20 / 20 20 / 65	ET 5°	Detected age 4 y, 6 mo patching, strabismus surgery on LE age 5 y
RB	49 y	LE strab	+3.25 DS +4.75 – 0.75 45^{c}	20 / 15 20 / 40	XT 5°	Detected age 6y, glasses since 6y, no other therapy, near normal local stereo vision
SV	48 y	LE strab	+1.5 DS +3.00 – 0.5 150^{c}	20 / 25 20 / 50	ET 2°	Detected age 7y, no therapy
SW	23 y	LE aniso	-0.75 DS +3.25 – 1.75 68^{c}	20 / 16 20 / 63	Ortho	Detected age 5 y, patching for 3 m, no glasses tolerated, 2 strabismus surgery RE age 10-12y

Table 1: This table shows the clinical details of the amblyopic observers participating in the experiment. The following abbreviations have been used; strab for strabismus, aniso for anisometropic, RE for right eye, LE for left eye, ET for esotropia, XT for exotropia, ortho for orthotropic alignment, DS for dioptre sphere.

Apparatus

We used an Apple Macintosh G3 computer to create and present the stimuli, run the experiment, collect the data and analyze the results. For programming, we used Matlab environment (MathWorks Ltd) and Psychophysics ToolBox (Brainard, 1997). All stimuli were displayed on a 20 inch Sony monitor (Trinitron 520GS), which was calibrated and linearized using a Graseby S370 photometer and the Video Toolbox (Pelli, 1997) package. In order to have high contrast accuracy, we used a video attenuator (Pelli & Zhang, 1991). The attenuator combined the RGB outputs of the graphics card (ATI Rage 128) into the green (G) gun. The monitor had a refresh rate of 75 Hz. The mean luminance of the screen was 33 cd/m^2 and the resolution was 1152 x 870 pixels. One pixel on the screen was 0.32 mm, which was 1.94 Arc min of the observers' visual angle from the viewing distance of 57 cm. The observers performed the task monocularly beginning with the fellow fixing eye (in amblyopes) and dominant eye (in normals), with the other eye patched.

Figure 1

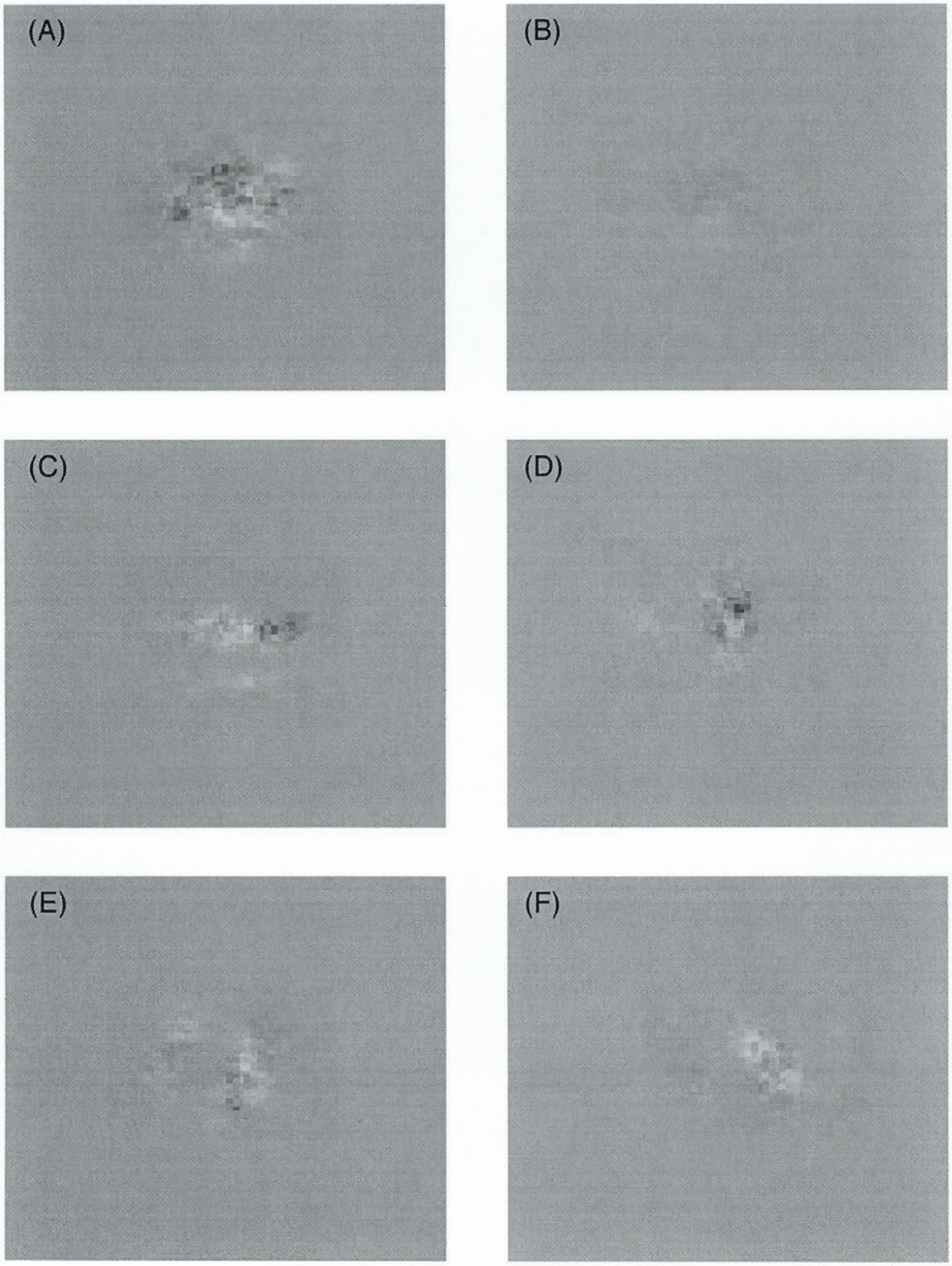

Figure 1: Stimuli for exp. 1 to 3: Fig. 1A and 1B are the fractal noise carrier tested in exp. 1. Contrasts of these examples are 0.98 (fig. 1A) and 0.02 (fig. 1B). In fig. 1C and 1D, the stimuli for exp. 2 are shown; these were second-order horizontal or vertical patches with modulation of 1 cycle per degree and fractal noise carriers with contrast determined by exp. 1 (see method). The carrier was modulated by the oriented envelope. This figure shows stimuli with maximum modulation depth (98%). In fig. 1E and 1F, the stimuli for exp. 3 are presented. These stimuli are similar to the stimuli from exp. 2, except that the orientations of the patches are around the vertical and tilted to right (fig. 1E) and left (fig. 1F) of vertical.

Stimuli and procedure

In overview, we undertook a systematic study of second-order function, both local and global, in amblyopia. The sequential nature of the experimental design is diagrammatically illustrated in table 2 and is an important part of this study. First, we determined the detectability of our carriers (exp. 1) and then using a second-order element with an equi-detectable carrier, we determined the detectability of local second-order stimuli (exp. 2). Third, we assessed the accuracy with which the orientation of a local, equi-detectable second-order element could be discriminated (exp. 3). Finally, we evaluated the efficacy with which an array of equi-detectable and discriminable, local second-order stimuli could be integrated globally (exp. 4).

In exp. 1, the observers' task was to detect the presence of the stimulus in a 2 alternative forced-choice task. The stimulus was a Gaussian windowed fractal noise patch, which was presented on a mid-gray background. We used the following formula to generate the patch:

$$L_{xy=}L_{mean}+L_{mean}(CN\times \exp(x^2/\sigma_x^2)\times \exp(y^2/\sigma_y^2)) \qquad (1)$$

Where L represents luminance, C is the noise contrast, and N is the 1/f noise pattern. The standard deviation of the patch (σ) was 0.4° in both x and y directions. The stimulus was presented at the centre of the screen for 500 ms. A fixation point was provided for the observers before and after the stimulus was presented. We used the method of constant stimuli to select the contrasts of the stimuli presented to the observers on each trial. The data in each eye was derived from at least 300 trials for 5 different contrasts from 0.05 to 0.50. Contrast detection threshold was estimated as the contrast that gave 75% correct on a Weibull function fitted to the data (see fig. 1A and 1B and in table 2A).

In exp. 2 observers were asked to discriminate horizontal from vertical second-order stimuli in a 2 alternative forced-choice task. To create the second-order stimuli we took the contrast detection threshold (from exp. 1) for the carrier in each individual observer separately and multiplied it by 3. Then we modulated the carrier with a 1-d modulator that could be oriented vertically or horizontally. The spatial frequency of the envelope was 1 cpd (cycles per degree). We applied the following equation to generate the stimuli:

$$L_{xy} = L_{mean}\,(N(1+m_{cos}\,(2\pi f x+\phi))C/2 \times exp\,(x/\sigma_x^{\,2}) \times exp\,(y/\sigma_y^{\,2}) \qquad (2)$$

Where L represents luminance, C is the noise contrast, N is the 1/f noise pattern, m is the modulation depth, f represents the spatial frequency of the pattern and ø is the phase. The standard deviation of the patch (σ) was 0.4° in both x and y directions. The range of tested modulation depths varied from 0.25 to 0.75 in normal observers. This range was broader in amblyopic observers (up to 98%) because they had higher discrimination thresholds than the normal observers. Similar to exp. 1, the stimulus was presented at the centre of the screen and a fixation point was provided to the observers. The threshold was the modulation depth required to achieve 75% correct on the fitted Weibull function to the data that was derived from at least 300 trials for 5 modulation depths (see fig. 1C and 1D and table 2C).

In exp. 3 we used a similar stimulus as in exp. 2; however the orientation of the patch was varied around the vertical and the stimulus was presented in a random position in a 6° circle from the observers' fixation point, which was centred at the centre of the screen. The Observers' task was to judge whether the stimulus patch was tilted to right or left of vertical (clockwise- or counter-clockwise) (see fig. 1E and 1F and table 2E). The carrier contrast of the stimulus patch was the same as in exp. 2 for each individual observer (3 times the threshold measured in exp. 1). The modulation depths were 1, 1.25, 1.5 and 2 times modulation threshold obtained from exp. 2. Varying the modulation depth, we measured the orientation threshold offset for discrimination of a single second-order oriented element. Through this process we could find modulation depths with which the amblyopic (AME) and fellow fixing eyes (FFE) produces similar performance in discriminating the orientation of a single local stimulus, in other words, the stimulus was equi-visible to both fellow fixing and amblyopic eyes.

Figure 2

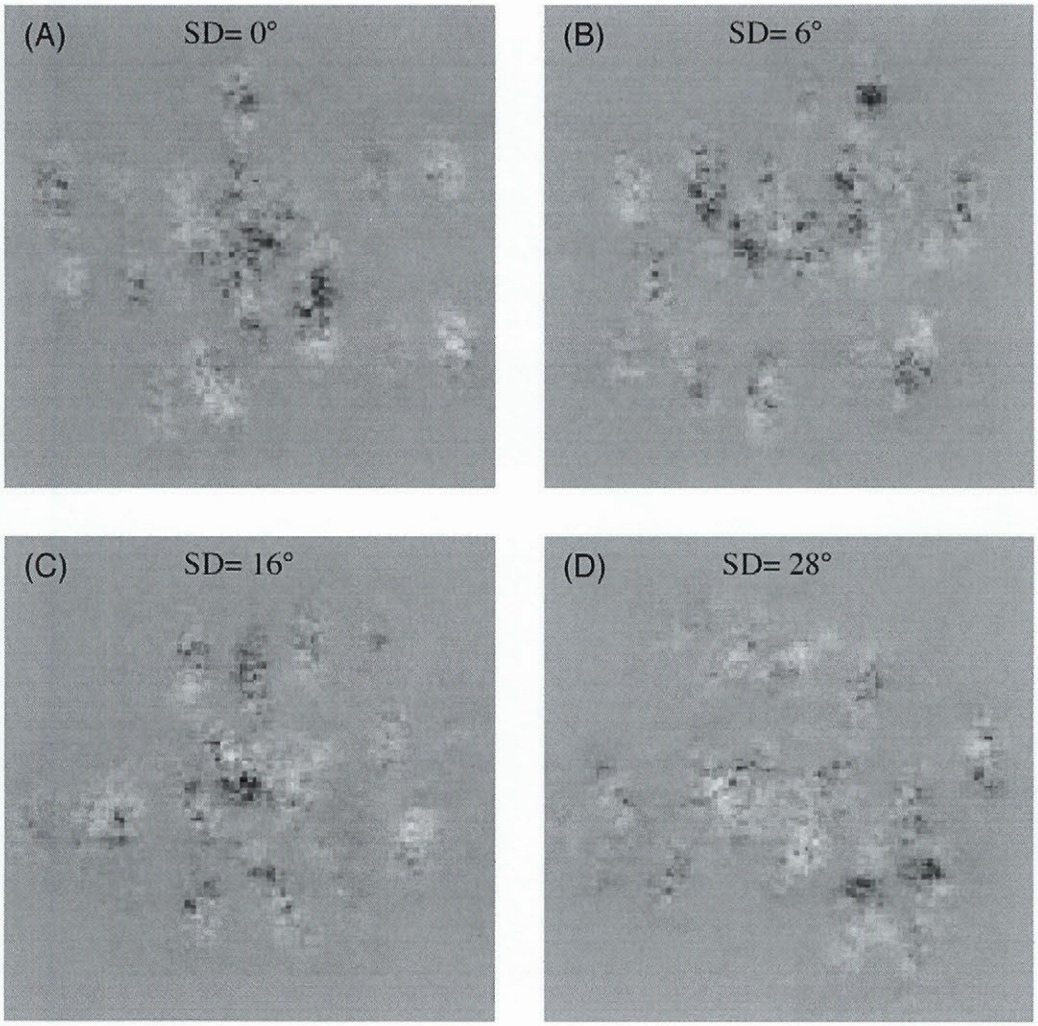

Figure 2: Stimuli for exp. 4: In each trial 16 second-order micro-patterns were presented to the observers. The orientations of the Gabors were randomly selected from parent distributions with specific means and predetermined standard deviations (SD). 4 populations with standard deviations of 0, 6, 16 and 28 are shown are shown in fig. 2A, 2B, 2C, and 2D, respectively.

In exp. 4, we used sixteen oriented patches of the type described for exp. 3. The orientation of each patch was randomly selected from a parent distribution. The observers' task was to judge whether the mean orientation of the patches was tilted to right or left of vertical (clockwise- or counter-clockwise) (see fig. 2 and table 2G). Parent distributions, with the standard deviation determined by the experimenter, were generated on each trial. 10 standard deviations of 0, 1, 2, 4, 6, 8, 12, 16, 20 and 28 were tested in each eye for each observer. Observers' performance was typically measured for 4 different distribution standard deviations in a session. Performance with each distribution standard deviation was measured at least three times over the experiment (producing a total of 192-320 trials per condition). Performance from multiple runs was averaged to estimate performance.

For each standard deviation, the method for measuring the ability of observers to judge mean orientation was the same. The mean orientation of the distribution was varied from vertical (which produced chance performance) to some degrees off vertical. The mean orientations to be tested within a particular run were chosen by an adaptive method of constant stimuli (Watt & Andrews, 1981). The range of mean orientations, however, never exceeded ±20°. Using these ranges of standard deviations and averages, we could avoid the problem of circularity in our oriented stimuli (e.g. one 181° stimulus looks the same as a 1° stimulus). We used a standard equivalent noise model (described below) to derive the parameters of internal noise and number of samples that best describe performance on this global orientation integration task.

Given that our orientation integration thresholds are estimates of response variance, the non-ideal behaviour of observers with noiseless stimuli (i.e. all having the same orientation) can be expressed as additive internal noise. The level of internal noise is measured by increasing the amount of external noise (i.e. standard deviation of the parent distribution from which the samples are taken) in the stimulus and determining the point at which observers' performance begins to deteriorate. As this task requires integration, then observers' robustness to further increasing amounts of external noise depends decreasingly on internal noise and increasingly on how many samples are averaged. Thus the form of the equivalent noise model is:

$$\sigma_{obs}^2 = (\sigma_{int}^2 + \sigma_{ext}^2) / n \qquad (3)$$

Where σ_{obs} is the observed threshold, σ_{ext} is the external noise; σ_{int} is the estimated equivalent intrinsic or internal noise and (n) is the estimated number of samples being employed. In terms of the orientation discrimination task, σ_{obs} corresponds to the threshold for orientation discrimination, σ_{ext} to the standard deviation of the distribution from which the samples are derived; σ_{int} to the noise associated with the measurement of each orientation sample and their combination and (n) corresponds to the estimated number of orientation samples being combined by the visual system. The parameters of internal noise and number of samples for each individual observer were obtained from fitting the model equation to individual data sets (for examples of stimuli we used for all 4 experiments see http://ego.psych.mcgill.ca/labs/mvr/Behzad/Second-order.html).

Statistics: 95% confidence intervals were estimated from 1000 bootstrap replications of the fit (Foster & Bischof, 1987) in all four experiments. We used the 95% confidence intervals to compare the results of the two eyes of each individual observer with one another. However, for comparing the differences across all observers we used ANOVA and t-tests.

In exp. 1 and 2, first-order stimuli contrast detection and second-order stimuli horizontal and vertical discrimination thresholds were compared, respectively. In both experiments we had 2 variables. The first variable was "observer" with two levels of "normal" and "amblyopic". The second variable was "eye" with two levels of "dominant eyes" (DE) and "non-dominant eyes" (NDE) in normal and "fellow fixing eyes" (FFE) and "amblyopic eyes" (AME) in amblyopic observers. Since we measured the same eyes of the same observers all through the experiment, both variables were considered correlated.

In exp. 3 the results from the one element orientation discrimination task were compared. For this experiment we designed a 2 by 2 by 3 ANOVA test. The first 2 variables were similar to those of exp. 1 and 2. The third variable was modulation depths with three levels of 1, 1.25 and 1.5 times thresholds.

In exp. 4, we compared the two parameters of internal noise and number of samples separately as well as the threshold orientation offset for the mean orientation discrimination task. For the two parameters of internal noise and number of samples, we designed same ANOVAs as for the exp. 1 and 2. For the latter, we designed a three way ANOVA, 2 by 2 by 10. The first two variables are similar to the previous designs. The last variable is the standard deviation of the stimuli population with 10 levels of 0, 1, 2, 4, 6, 8, 12, 16, 20 and 28 (degrees).

In all experiments, if the interactions were significant, we followed the testing with a Tukey's post-hoc. The alpha was adjusted for repeated measurements when necessary. We applied t-tests when we needed to compare two individual groups and were unable to do so with the ANOVA.

Results

As a first step we compared the contrast thresholds for detection of a Gaussian patch of fractal noise that was to be the carrier for later second-order stimuli. The average contrast detection thresholds from exp. 1 for amblyopic and normal observers are shown in fig. 3. The difference between DE and NDE was insignificant ($p>0.1$). In AME, contrast detection threshold was significantly higher than those of the FFE (df adjusted=14, F=14.47, $p=0.0019$) and normal eyes (e.g. non-dominant eye, df adjusted=14, F=6.35, $p=0.048$). Interestingly, the threshold in the FFE was significantly lower than the thresholds in normal eyes (e.g. FFE versus NDE (df=7, t=2.72, t-critical=1.89, $p=0.029$). In other experiments not shown here we found that there was no difference between FFE and normal observers' eyes (DE and NDE) for binary noise. Why fractal noise shows up such a difference is presently unknown.

Figure 3

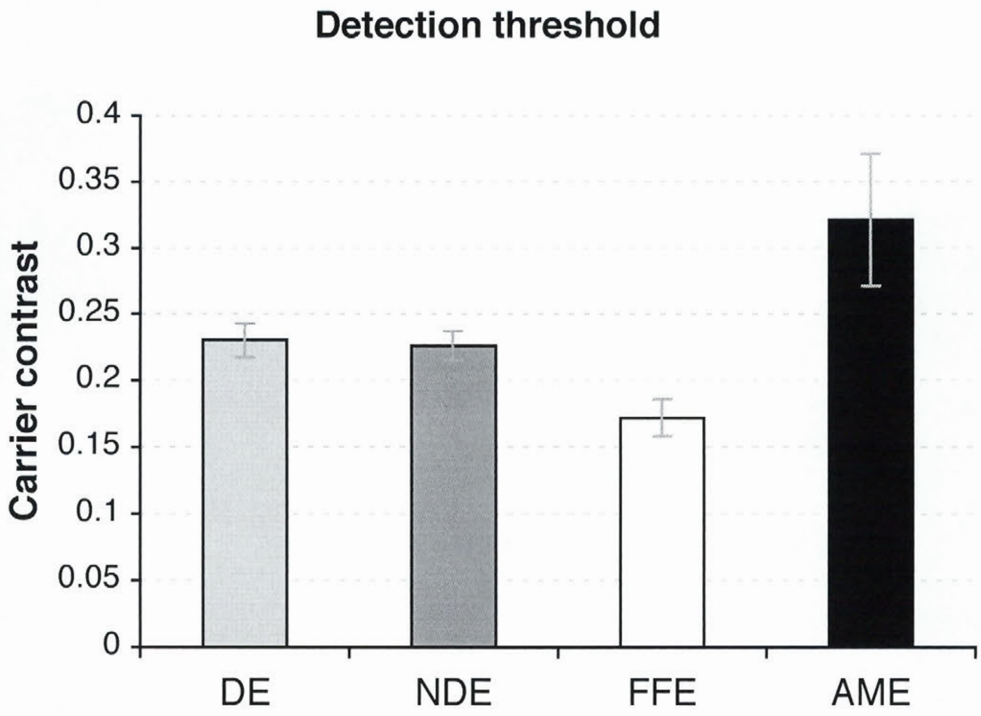

Figure 3: The averaged contrast detection thresholds (exp. 1) for DE - light gray bar, and NDE - dark gray bar of the normal and FFE - white bar, and AME - black bar of the amblyopic observers are shown in this figure. The average thresholds for contrast detections are equal in DE and NDE of the normal observers. The average contrast detection threshold in AME is significantly higher than those of the FFE, DE and NDE. However, the average contrast threshold in FFE is significantly less than the average detection threshold in DE and NDE of the normal eyes. The error bars represent ±1 standard error.

Knowing that the first-order carrier was less detectable by the amblyopic eye allowed us to create second-order stimuli whose carriers were equi-detectable by increasing the contrast of the carrier by an amount that compensated for this difference in detectability (i.e. the use of carriers of equal supra-threshold contrast). This was done on an individual basis for each amblyope. This enabled us to address the next question, namely do amblyopes exhibit anomalies for the detection of second-order stimuli not due to deficient first-order (i.e. carrier) processing? If so, an abnormality at the level of second-order processing must exist. We measured modulation thresholds for the detection of a second-order micro-pattern based on a horizontal/vertical discrimination of the 1-d modulator. This procedure ensured that performance depended on the envelope (i.e. second-order component) and not the carrier (i.e. first-order component). The contrast of the fractal noise carrier was set to 3 times its individual contrast threshold, obtained from the preliminary experiment described above.

Figure 4

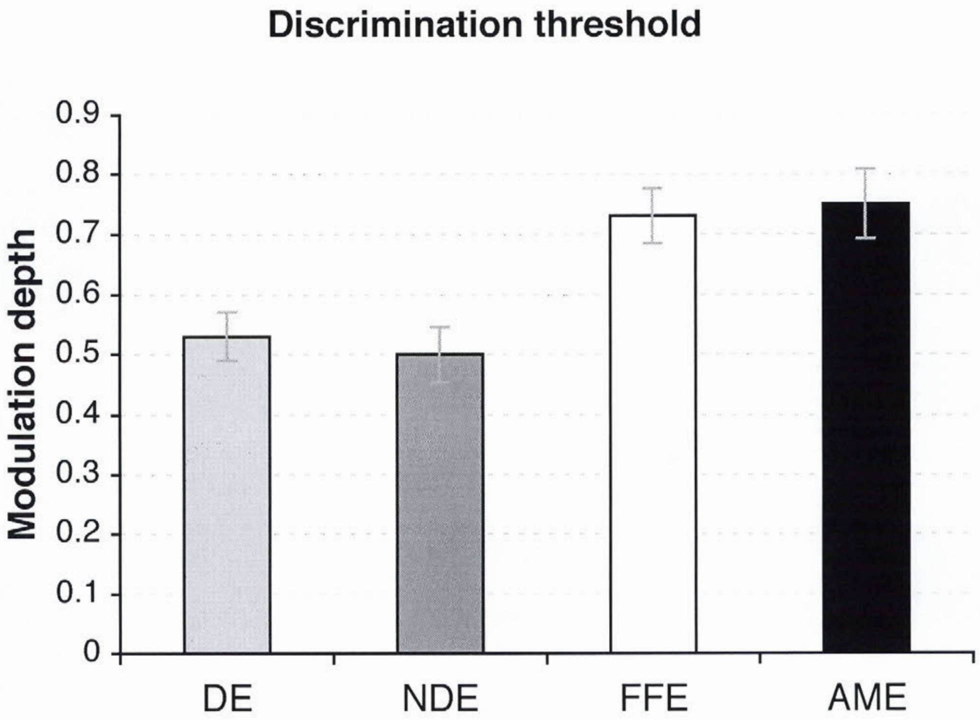

Figure 4: The average horizontal/vertical discrimination threshold (exp. 2) for DE - light gray bar, and NDE - dark gray bar of the normal and FFE - white bar, and AME - black bar of the amblyopic observers are shown in this figure. The average thresholds are equal in normal eyes as well as the amblyopic observers' eyes. However, the amblyopic observers' eyes (AME and FFE) average thresholds are significantly different from those of the normal eyes' (DE and NDE). The error bars represent ±1 standard error.

In fig. 4 average horizontal/vertical discrimination thresholds for second-order stimuli are shown. The discrimination thresholds are not significantly different in DE and NDE of normal observers ($p>0.1$). The thresholds in FFE and AME are not significantly different either ($p>0.1$). However, comparing both eyes in amblyopic observers with both eyes in normal observers, thresholds are significantly higher in amblyopic observers' eyes (df total 31, $F=9.11$, $p=0.0194$). This suggests that the amblyopic and FFE of amblyopes exhibit second-order detection deficits that can not be simply attributed to the known deficiency in first-order processing (Gstalder & Green, 1972; Hess & Howell, 1978; Levi & Harwerth, 1978; Wong et al., 2001).

Knowing the detectability of an individual second-order micro-pattern in normal and amblyopic observers' eyes (including FFE of amblyopes) allows us to create an equi-detectable second-order micro-pattern by adjusting the relative modulation depth for such stimuli seen by normals and amblyopes (i.e. present them at equal supra-threshold modulation depths). This in turn allows us to address the next question, namely do amblyopes exhibit local orientation discrimination deficits for equi-detectable second-order stimuli? In our case we were interested in local orientation discrimination and therefore use a single second-order micro-pattern.

Figure 5

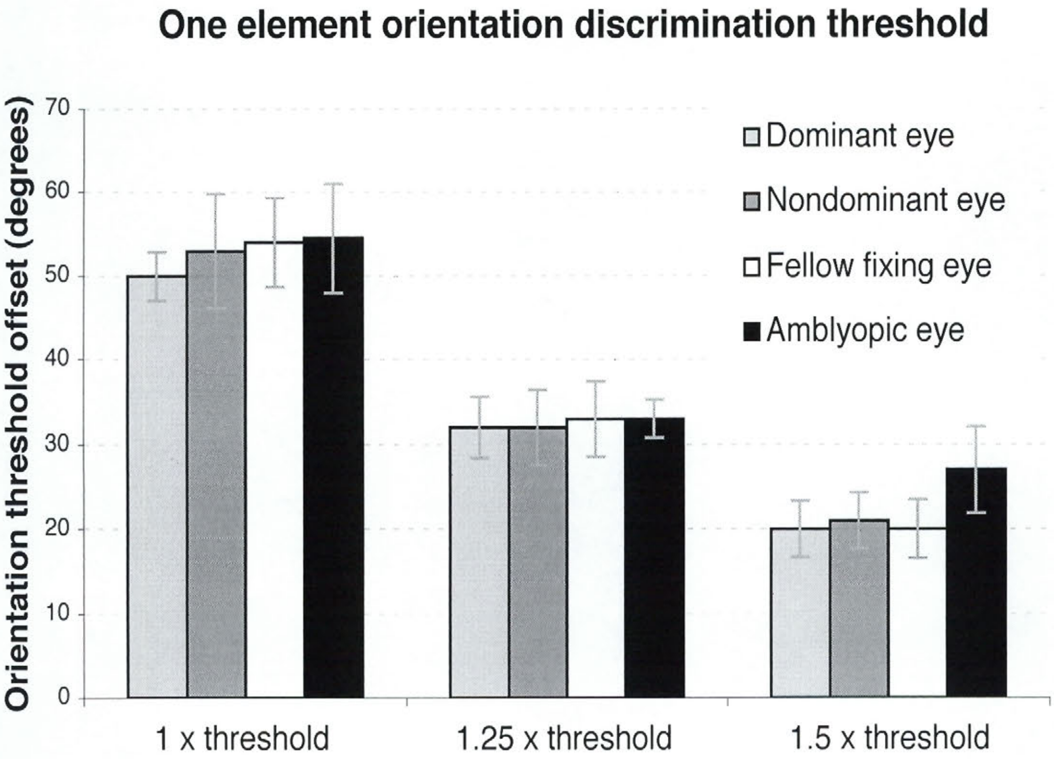

Figure 5: The average orientations offset thresholds for one oriented element (exp. 3) in DE - light gray bars, NDE - dark gray bars, FFE - white bars, and AME - black bars, and for 3 conditions (1, 1.25 and 1.5 times the threshold modulation depths) are presented in this figure. In 1 times threshold condition the thresholds in all eyes are high and statistically equal. Increasing the modulation depth to 1.25 and 1.5 times thresholds decreases the thresholds significantly. The thresholds for DE, NDE and FFE keeps improving with increasing the modulation depth from 1.25 to 1.5 condition, although this effect was not statistically significant. The threshold in AME, however, didn't show this effect. The error bars represent ±1 standard error.

The results from exp. 3 (one element orientation discrimination task) are shown in fig. 5. In this figure, the average threshold orientation offsets (in degrees) are presented for three different conditions (multiples of thresholds) (see fig. 4). Generally, the modulation depth thresholds (exp. 2) were multiplied by 1, 1.25, 1.5 and 2. These multiples were used in exp. 3 to ensure that all second-order micro-patterns were equally detectable for normals and amblyopes. However, in amblyopic observers, due to their elevated modulation depth thresholds (exp. 2) and the fact that we couldn't increase the modulation depth beyond 100%, we could not use contrast modulation depths more than 1.5 times thresholds. Therefore we used the collected data from all normal and amblyopic observers up to 1.5 times their thresholds. In fig. 5, the average thresholds in DE and NDE groups were similar ($p>0.1$). The results for FFE and AME show that as modulation depth increases the orientation discrimination threshold for a single element decreases. The improvement in the amblyopic eyes' performance stops at 1.25 x modulation threshold (i.e. the average threshold for 1.25 times threshold is similar to that for 1.5) (see the black bars in fig. 5). However, increasing the modulation depth of beyond 1.25 times threshold consistently improves the performance in FFE, DE and NDE eyes, although this improvement wasn't statistically significant (3 variables interaction: df =2, F= 0.19, $p>0.1$). This data shows that for the equi-detectable second-order stimuli that we used (with their carriers also equated for first-order detectability), orientation discrimination was comparable in normal and amblyopic eyes at the suprathreshold levels tested. Knowing this allows us to take the final step in this investigation and ask whether amblyopes are normal at globally integrating local second-order orientation information.

Since performance has been equated at the local level not only for the detectability of the carrier and envelope but also for the orientation discrimination of the envelope, we are now in a position to assess whether second-order global processing in amblyopia is normal. To accomplish this we use an array of such second-order micro-patterns, each of which has an orientation that is a sample of a parent distribution whose mean is to be judged (see fig. 2). This task has been extensively studied in normals for both first (Dakin, 2001) and second-order stimuli (Allen et al., 2003). In amblyopes only first-order micro-patterns have been studied so far (Mansouri et al., 2004b) and integrative function has been found to be normal.

Figure 6

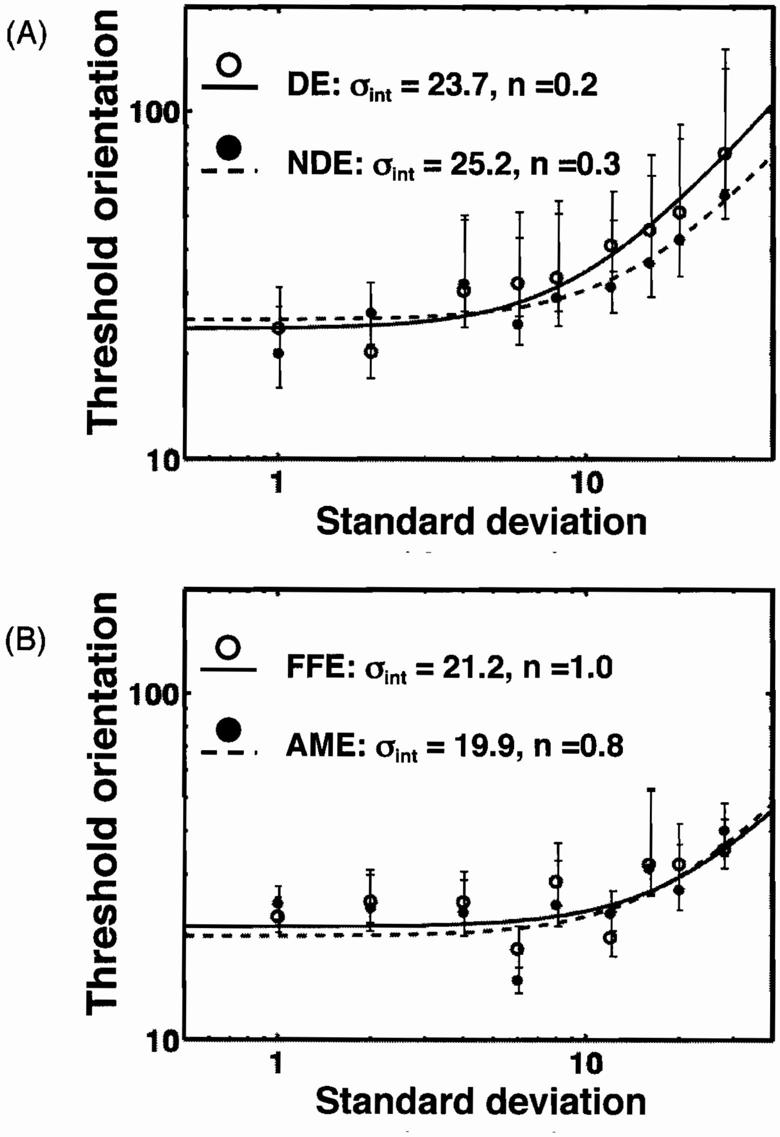
(A)
Threshold orientation
100
10
1
10
Standard deviation
DE: σ_{int} = 23.7, n =0.2
NDE: σ_{int} = 25.2, n =0.3
(B)
Threshold orientation
100
10
1
10
Standard deviation
FFE: σ_{int} = 21.2, n =1.0
AME: σ_{int} = 19.9, n =0.8

Figure 6: Mean orientation threshold for the multi element array, plotted against the standard deviation of the orientation distribution from which the orientations of the elements were taken, for two observers (one normal and one amblyopic). Sixteen second-order Gabors comprised the stimulus array. The curve is the best fit for the equivalent noise model. The error bars represent 95% confidence intervals. The parameters of this fit, internal noise (σ_{int}*) and number of samples (n) are shown in the inset. In (A), results are shown for DE - open symbols and solid line, and NDE - filled symbols and dashed line, of a normal observer whereas in (B), results are shown for the FFE - open symbols and solid line, and AME - filled symbols and dashed line, of an anisometropic amblyope (MA).*

Two sample results from exp. 4 are shown in fig. 6. The data in fig. 6 were obtained from one normal observer (fig. 6A) and one amblyopic observer (fig. 6B). The threshold orientation offset (degrees) is plotted for each standard deviation (degrees) of the parent population. In fig. 6A, the lines are fits to the data from the equivalent noise model (see methods). In fig. 6B, the open circles represent data from the FFE and filled circles from AME of an amblyopic observer. Solid and dashed lines are the model fits to the data from FFE and AME, respectively. The figures show that the thresholds for DE and NDE are very similar as well as the thresholds for FFE and AME in these individual normal and amblyopic observers. The parameters of internal noise (σ_{int}) and number of samples (n), which were obtained from the equivalent noise model (see method) are shown in the figures. These parameters are very similar in both eyes of the amblyopic and the normal observers.

Figure 7

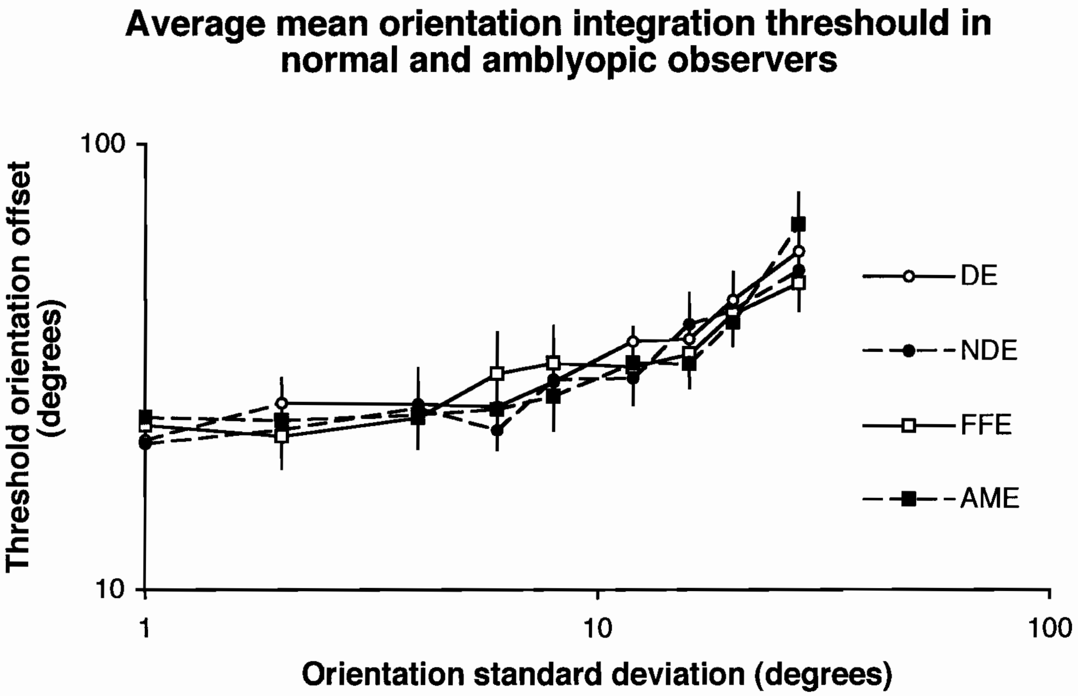

Figure 7: This figure shows the average mean orientation threshold offsets in exp. 4 for DE - open circle and solid line, NDE - closed circle and dashed line, FFE - open square and solid line, and AME - close square and dashed line. The thresholds are similar and increase equally in all eyes when the standard deviation of the stimuli population is increased. The error bars represent ±1 standard error.

Fig. 7 shows the average thresholds over 8 normal and 7 amblyopic observers for whom a complete data set was obtained for the DE - open circles and solid lines, NDE - filled circles and dashed line, FFE - open squares and solid lines, and AME - filled squares and dashed line. The average thresholds are plotted against the standard deviation of the parent populations. The average thresholds were not significantly different between all 4 types of visual system ($p>0.1$).

Fig. 8 summarizes the average values of the two model parameters, namely internal noise (fig. 8A) and number of samples (fig. 8B). The internal noise is statistically similar (interaction of the variables $df=1$, $F=0.47$, $p>0.1$) across all eyes (fig. 8A). The number of samples (fig. 8B) in the DE of normal observers is statistically lower than all other groups (e.g. comparing the number of samples in DE and NDE; $df=7$, $t=2.61$, $p=0.045$). The number of samples is similar in NDE, FFE, and AME (e.g. comparing the number of samples in FFE and AME; $df=7$, $t=0.05$, $p>0.1$).

Figure 8

(A) Average internal noise in normal and amblyopic observers

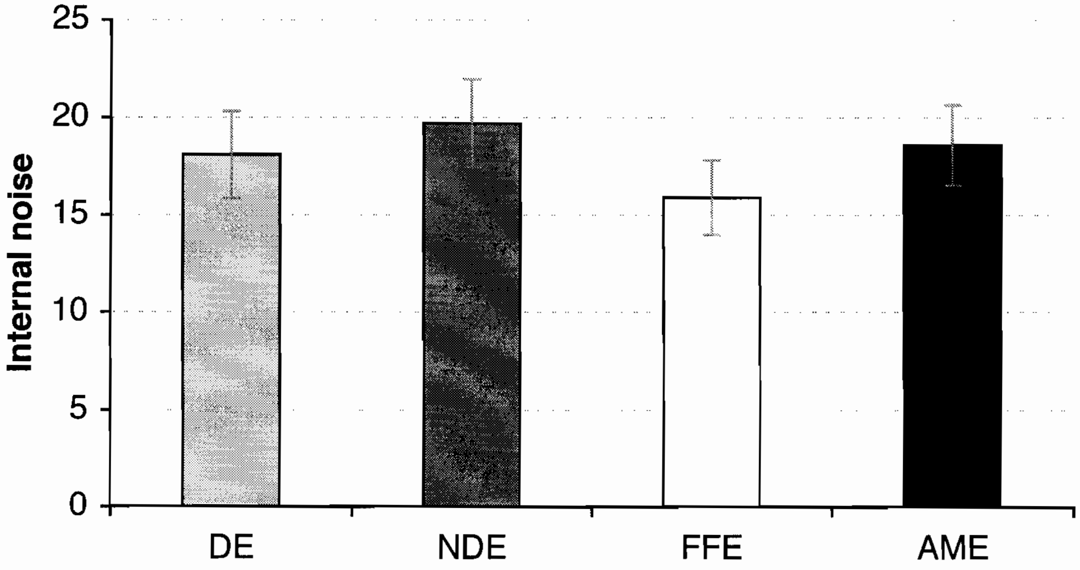

(B) Average number of samples in normal and amblyopic observers

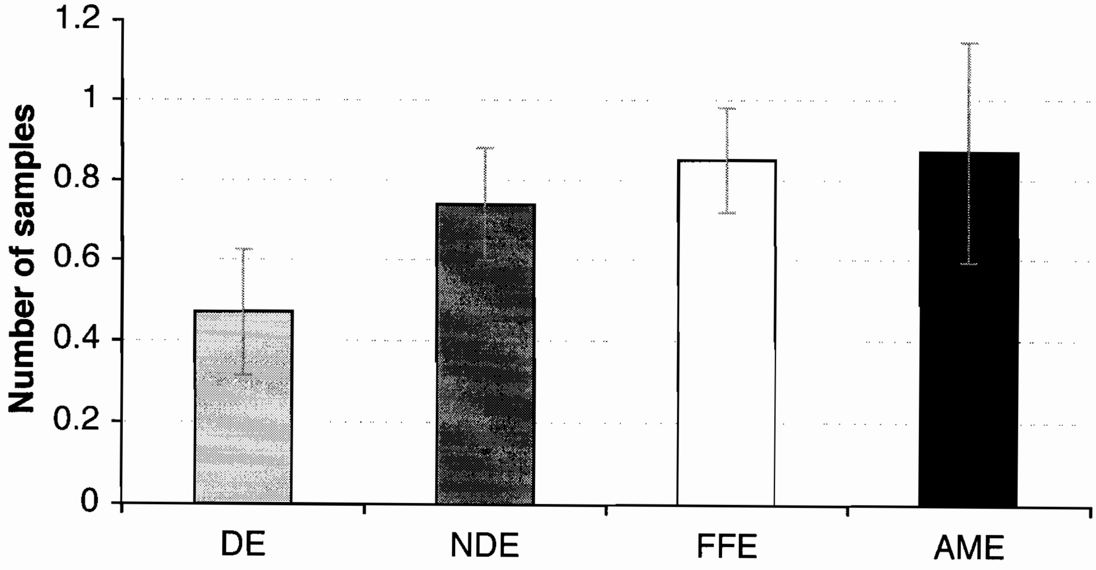

Figure 8: Comparison of the average of the individual estimates of internal noise (A) and number of samples (B) from our model fits in DE - light gray bars, NDE - dark gray bars, FFE - white bars, and AME - black bars. In (A), the averages internal noises in all groups are statistically equal. For the number of samples measured in (B), we found lower number of samples in DE than the NDE, FFE and AME. There were no significant differences between NDE and either FFE or AME. The error bars represent ±1 standard error.

Discussion

In this study we investigated, in a systematic way, the processing of second-order stimuli by the amblyopic visual system. We began by assessing the detection of second-order stimuli with equated carriers. Using these first-order equated stimuli, we show that there are small but significant second-order detection deficits in both amblyopic and fellow fixing eyes that are not a consequence of the known first-order loss. Then, using second-order stimuli of equated modulation depth, we show that the orientation discrimination of a single second-order micro-pattern, while being worse than its first-order counterpart by factor of 10 (for comparison see (Mansouri et al., 2004b), is comparable in normal and amblyopic eyes. Finally, having equated for both second-order detection and orientation discrimination at the local micro-pattern level, we address the final issue of whether the global integration of second-order orientation information is normal in amblyopia. The answer is yes, though with one reservation. Using an equivalent noise model we show that both the internal noise and number of samples are comparable between amblyopic eyes, fellow fixing eyes and non-dominant eyes of normal observers, though a significant difference does exist between the sampling efficiency of the dominant eye of normals compared with either that of the amblyopic or fellow fixing eyes of amblyopes.

The finding that there are detection deficits at the level of second-order processing for both eyes of amblyopes agrees with a previous report that second-order deficits that occur in amblyopia can not be explained by the known first-order loss (Wong et al., 2001). Three things should be borne in mind: first, the detection deficits shown here for second-order stimuli were small. Second, our use of a broadband carrier leaves us open to the criticism that at some scale (i.e. the highest) relevant to second-order detection our method of equating detectability may not have been perfect. However, the fractal noise attenuates high more than low spatial frequencies and this might actually have improved the equivalency of stimuli between amblyopic and normal observers. The performance of normal observers in our study is much worse than previously found (Allen et al., 2003) with a non-fractal broadband carrier suggesting that it may be the high spatial frequency components of the carrier that are most useful for normal observers. Since amblyopic observers are poor at tasks involving high spatial frequencies (Hess & Howell, 1977; Levi & Harwerth, 1977; Mansouri et al., 2004b) it is likely that fractal noise carrier in amblyopes should not be as detrimental on their performance as it is for normals. Third, the fellow fixing eye exhibits similar second-order detection deficits although it is not thought to show obvious first-order detection anomalies (Mansouri et al., 2004b). All things considered, it would appear that there are detection deficits in amblyopia at the second-order processing stage. The finding that the fellow fixing eyes of amblyopes are just as anomalous for the detection of second-order stimuli can best be explained by this detection occurring at a binocular site in cortex (see also Wong et al, 2001)

This study for second-order stimuli and its predecessor for first-order stimuli (Mansouri et al., 2004b) demonstrate that the integration of local orientation, be it luminance- or contrast-defined is at best only minimally disrupted in amblyopia. This result appears at first sight to be in conflict with other recent studies using global motion (Simmers et al., 2003) and orientation (Simmers et al., 2005) where substantial global integration deficits have been shown that are selective for second-order stimuli. However, on a closer look, the task used here and that used previously by Simmers and colleagues has one fundamental difference. In the present task, it is in the amblyopes' interest to integrate all available local orientation because all micro-patterns contain equally relevant information about the shape of the distribution to be estimated. In the task used by Simmers and colleagues, the task involves signal and noise where the optimal strategy is to integrate as much of the signal and as little of the noise as possible. Thus the task used by Simmers and co-workers could be said to involve segregation as well as integration. The importance of the current study and that of its predecessor (Mansouri et al., 2004b) is to show that amblyopes can integrate spatial information (in this case, orientation) normally. The problem that has been highlighted in percent coherence tasks involving global motion and orientation (Simmers et al., 2005; Simmers et al., 2003) must involve the segregation aspect of the task.

Little is known about how or where the visual system accomplishes the important but competing processes of integration and segregation (Braddick, 1993; Simmers et al., 2005) except that it does not occur early in the pathway, being after binocular combination but before relative disparity encoding (Mansouri, Hess, Allen & Dakin, 2005). In the case of the coherence task used by Simmers and co-workers where signal and noise are not spatially segmented, it presumably involves an opponent process of some type. The present conclusion that amblyopes experience particular difficulty in doing global tasks in which there is signal to integrate and noise to segregate is reminiscent of an earlier finding on a patient who lacked motion perception (Zihl et al., 1983). This observer also had problems with percent coherence motion tasks and could only perceive left/right motion when the percent coherence was close to 100% (i.e. all signals, no noise). The addition of 10% stationary elements was sufficient to reduce performance to chance levels. Her problem was a large bilateral lesion in the dorsal part of the extra-striate cortex corresponding to where the human analogue of monkey MT and MST are located. In the light of the profound functional anomalies that have been demonstrated in the extra-striate regions of human amblyopes (Barnes et al., 2001) the binocular nature of the second-order detection loss and its selectivity for signal/noise tasks, it is tempting to speculate that the site of this segregation problem in amblyopia is in the extra-striate cortex. Since the segregation problem is more acute for second-order stimuli (Simmers & Bex, 2004; Simmers et al., 2003) on the basis of the functional MRI results of Dumoulin et al, (2003) in normals, the chief candidates are the anterior superior parietal lobe and the lateral occipital cortex.

Acknowledgment

This study has been supported by a Canadian Institute of Health Research grant (CIHR MOP-10818) to Robert F. Hess.

Preface to chapter 4

In chapter 2 and 3 we showed that the amblyopic visual system could integrate orientation information, either being first- or second-order, well across space. However, we found some deficiencies in amblyopic eyes in processing first-order at high spatial frequency and detection of second order information. Since it is known that the ventral pathway specializes in form processing, we conclude that, if we equate the amblyopic eyes for their early striate cortex deficiency, its integrative mechanisms are normal in amblyopia.

It is known that the dorsal pathway, which is more specialized for processing motion information, is more susceptible to the visual developmental disorders such as amblyopia. In order to study the dorsal pathway in amblyopes we used motion stimuli and tested amblyopes as well as normals in chapter 4 using techniques that we had previously developed for form vision and discussed in previous chapters.

Chapter 4: Integration of motion information in amblyopia

Integration of local motion is normal in amblyopia

Robert F. Hess and Behzad Mansouri

McGill Vision Research Unit, 687 Pine Avenue West, Rm. H4-14, Montreal, H3A 1A1
Quebec, Canada

Steven C. Dakin

Institute of Ophthalmology, University College London, 11-43 Bath St. London EC1V
9EL, United Kingdom

Harriet A. Allen

School of Psychology, University of Birmingham, Birmingham, B15 2TT, United
Kingdom

We investigate the global integration of local motion direction signals in amblyopia, in a task where performance is equated between normal and amblyopic eyes at the single element level. We use an equivalent noise model to derive the parameters of internal noise and number of samples, both of which we show are normal in amblyopia for this task. This result is in apparent conflict with a previous study in amblyopes showing that global motion processing is defective (Simmers et al., 2003). A similar discrepancy between the normalcy of signal integration (Mansouri et al., 2004b) and anomalous global form processing has also been reported (Simmers et al., 2005). We suggest that these discrepancies for form and motion processing in amblyopia point to a selective deficit in segregating signal from noise.

Introduction

Motion processing is a fundamental aspect of vision, being involved in early detection, eye-movement control, visual stabilization and scene segmentation. It is not at all surprising therefore that a substantial proportion of visual cortex is devoted to it. Although our understanding of the intricacies of cortical motion processing is still in its infancy, there appears to be initially a two stage process; the detection of local motion in different parts of the field through cells with localized receptive fields with directional selective properties in V1 (Hubel & Weisel, 1968) and a more global processing of these local motions over larger regions of the field in areas of the dorsal, extra-striate pathway including areas MT (V5) and MST (Mikami et al., 1986a; Mikami et al., 1986b). Neurons in MT and MST have much larger receptive fields, possibly containing many small subunits that represent V1 inputs (Movshon et al., 1985) with extensive centre-surround interactions (Allman et al., 1985). The receptive fields of MT neurons are large and fall into two classes with either antagonistic or facilitative surrounds producing sensitivity to local motion boundaries, or to global motion direction over a large area, respectively (Born & Tootell, 1992).

The task of choice for investigating MT and other associated areas in the dorsal extra-striate pathway has involved directional judgments for global motion. The stimulus used for these tasks contains localized signal elements moving in a coherent direction combined with a variable proportion of other similar elements moving in random directions (termed noise elements). Sensitivity on such a task is determined by the signal/noise ratio at which the signal direction can be accurately gauged. Sensitivity to global motion is disrupted if area MT/MST is lesioned. This has been shown in monkey (Lauwers, Sounders, Vogels, Vandenbussche & Orban, 2000; Newsome & Pare, 1988; Rudolph & Pasternak, 1999; Schiller & Lee, 1994) and in human (Baker et al., 1991). Abnormalities have been reported in human global motion sensitivity in a large variety of conditions including amblyopia (Ellemberg et al., 2002; Simmers et al., 2003), Williams syndrome (Atkinson, Anker, Curran, Andrews & Braddick, 2003), autism (Spencer, O'Brien, Riggs, Braddick, Atkinson & Wattam-Bell, 2000), developmental dyslexia (Cornelissen, Richardson, Mason, Fowler & Stein, 1995) and hemiplegia (Gunn, Cory, Atkinson, Braddick, Wattam-Bell, Guzzetta & Cioni, 2002). It has been suggested that the underlying processes exhibit an early maturation, which could account for its greater developmental vulnerability (Braddick et al., 2003).

Amblyopia is a good example. Although originally thought to involve purely spatial dysfunction (Hess & Howell, 1977; Levi & Harwerth, 1977), recent evidence suggests that humans with amblyopia have defective motion processing (Hess, Demanins & Bex, 1997a; Simmers et al., 2003). There are different forms of amblyopia (i.e. strabismic, anisometropic and form-deprivation) and there is good evidence for different spatial deficits in each (Hess, France & Tulunay-Keesey, 1981), however one thing that all three subtypes have in common is that they all exhibit deficits for global motion processing (Ellemberg et al., 2002; Simmers et al., 2003). Furthermore, in a recent study by Simmers, Ledgeway et al. (2003), it was argued that the deficit for global motion processing is not due to deficient local motion processing in, say, V1 but to impaired global motion processing in MT/MST. This paper aims to clarify just what such a deficit might involve. It has often been loosely assumed that global motion processing refers to integration of local motion direction in different parts of the visual field; thus, by inference the reduced global motion processing in amblyopia must be due to anomalous global integration of local motion signals. What has been overlooked is that the typical global motion task involves not only integration of local motion but also the segregation of the local motion signal from the spatially coextensive noise. It is not in the best interests of the visual system to blindly integrate all local motion signals especially when, at threshold conditions, 80% of them are noise. Some degree of segregation of signal from noise is required prior to signal integration. We feel that this latter aspect of the task may be the more important one when it comes to the reduced performance of amblyopic eyes. To test this we measure the purely integrative capacity of amblyopes representing all three sub-categories (i.e. strabismic, anisometropic and form-deprived) for which global motion deficits have been reported using a similar global motion task. In our task all local motion signals carry relevant information to solve the task and in this case blind integration of all local motion signals is the optimum strategy. We show, in this case, that performance is normal in amblyopia. We conclude that the defective global motion processing previously reported in amblyopia is a consequence of abnormal noise segregation not abnormal signal integration.

Methods

Observers

Twelve naïve observers (six amblyopic and six normal) were tested. The visual acuity in amblyopic eyes ranged from 20/40 to 20/400 (for details see table 1). Refraction was examined in all observers and appropriately corrected prior to the testing period. Informed consent was obtained from all observers before data collections.

Apparatus

A Macintosh G3 computer was used to generate and present the stimuli and collect the data. For programming we used the Matlab environment (MathWorks Ltd) and the Psychophysics ToolBox (Brainard, 1997). All stimuli were presented on a 20-inch Sony monitor (Trinitron 520GS). The monitor was calibrated and linearized using Graseby S370 photometer and the Video Toolbox (Pelli, 1997) package. Pseudo 12 bit contrast accuracy was achieved by using a video attenuator (Pelli & Zhang, 1991), which combined the RBG outputs of the graphic card (ATI Rage 128) into the G gun. The refresh rate, mean luminance, and the resolution of the screen were 75 Hz, 33 cd/m2, and 1152 x 870 pixels, respectively. The viewing distance was 57 cm from the screen in all experiments. One pixel on the screen was 0.32 mm, which subtended 2.12 Arc min at the viewing distance used. The observers performed the task monocularly with one eye patched at a time.

Table 1

Observers	Age	Type	Refraction		Acuity	Squint	History, stereo
ML	20 y	RE mixed	+1.0-0.75 –3.25 DS	90°	20/80 20/25	ET 6°	Detected age 5y, patching for 2y
MA	22 y	LE aniso	–0.25 DS +3.50 –0.50	0°	20/15 20/200	Ortho	Detected age 3y, patching for 4y, and glasses for 8y.
LS	22 y	BE depriv	-2.00 +0.50 +0.50	90°	20/20 20/125	Ortho	Detected age 6y, bilateral cataract surgery age 6y. Patching at 8y for 4m
ED	43 y	LE strab	+0.75 +0.75		20/16 20/63	ET 5°	Detected age 6y, patching for 1y
RB	49 y	LE strab	+3.25 DS +4.75 –0.75	45°	20/15 20/40	XT 5°	Detected age 6y, glasses since 6y, no other therapy, near normal local stereo vision
XL	31 y	LE strab	-2.50 -2.75+0.75	110°	20/20 20/400	ET 15°	Detected age 13y, no treatment

Table 1: This table shows the clinical details of the amblyopic observers participating in the experiment. The following abbreviations have been used; strab for strabismic, aniso for anisometropic, depriv for deprived amblyopia, RE for right eye, LE for left eye, ET for esotropia, XT for exotropia, ortho for orthotropic alignment, DS for dioptre sphere.

Stimuli

We studied motion integration using stimuli comprising arrays of spatially band-pass micro-patterns, which were presented on a mid-grey background. The stimuli were randomly distributed within a 6° wide circle, centred on the screen. The presentation time was 500 ms. 128 moving Laplacian-of-Gaussian (∇^2G) blobs (see fig. 1) were used which were defined as:

$$\nabla^2 G(x,y) = \frac{x^2 + y^2 - 2\sigma^2}{2\pi\sigma^6} \exp\left(-\frac{x^2 + y^2}{2\sigma^2}\right)$$

Where σ represents the space constant. The peak spatial frequency of the blobs was defined as:

$$f_{peak} = \frac{1}{\pi\sigma\sqrt{2}}$$

For this experiment σ was equal to 6.75 arc minute and the peak spatial frequency was 2 c/deg. Each blob was moving upward and to left or right of vertical for the whole presentation time. If one blob passed the border of the presentation window, it was regenerated at the opposite side simultaneously.

Direction of each moving blob was selected from a Gaussian parent distribution with a mean equal to the overall mean direction (i.e. 90°± the cue generated by APE (Watt & Andrews, 1981)) and a variable bandwidth. The direction distributions' standard deviation was varied from 0° (all elements moving to one direction) to 50° (see fig. 1). Since the motion direction of all elements was selected from the Gaussian parent distribution, all signals contained useful information about the mean of this distribution.

Thus, the best strategy for the visual system to employ to perform the task involving estimating the mean direction of the array motion would be to integrate motion direction across all elements (see fig. 1 b-d).

In the rare cases when the patches overlapped, their gray levels were added and clipped appropriately at the maximum or minimum gray level when they were outside the range of the screen (to see an example of stimuli we used see http://ego.psych.mcgill.ca/labs/mvr/Behzad/Motion.html).

Figure 1

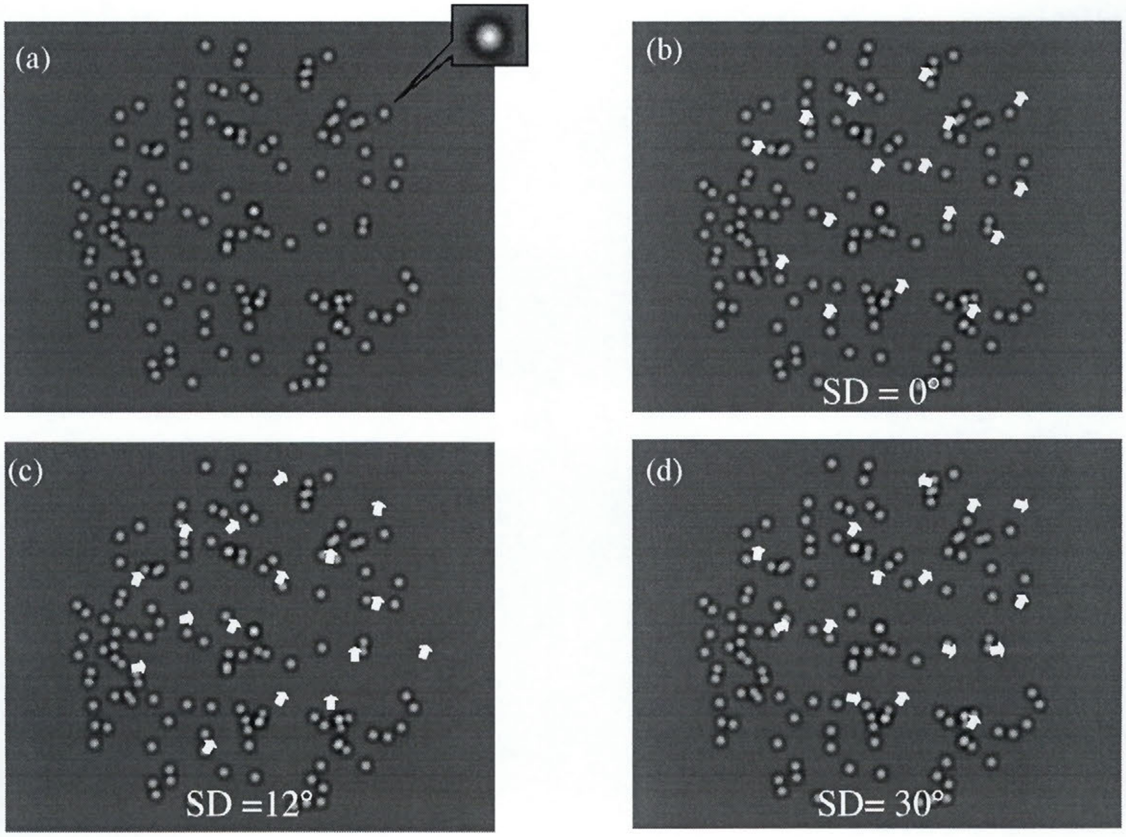

Figure 1: Illustrations of stimuli used in the experiment. Arrays of 128 randomly positioned, moving blobs were presented in a 6° circle at the centre of the screen. The size of one single blob is magnified (a) for illustration only. The blobs were moving upward and to left or right of vertical. The direction of each element is a sample from a Gaussian distribution of directions with average equal to the cue direction (i.e. 90° ± the cue generated by APE) and a variable bandwidth. The white arrows (in b-d), schematically represent the directions of the blobs. In fig. 1b, 1c and 1d the average directions are tilted to right of vertical and standard deviations of the stimuli arrays are 0°, 12° and 30°, respectively.

Statistics

We measured thresholds for the discrimination the mean direction of motion in the array and derived the parameters, internal noise and number of samples, from our equivalent noise model, for four groups, namely the fellow fixing eyes (FFE) and amblyopic eyes (AME) of amblyopic observers, and the dominant eyes (DE) and non-dominant eyes (NDE) of normal observers. There was one factor namely, the standard deviation of the signal population (SD) having 10 levels (0,1, 2, 4, 6, 8, 12, 16, 20, and 28). We used t-test to analyze the data. Each group was separately compared with the others. We used paired t-test (repeated measure t-test) when we compared amblyopic with fellow fixing eyes in amblyopic observers and dominant with non-dominant eyes in normals. We also calculated 95% confidence intervals for the thresholds from each individual psychometric function using a bootstrapping technique and used it to compare individual sets of data within the groups.

selected. In the subsequent integration experiment the stimuli were presented with contrasts for the fellow fixing and amblyopic eyes that gave comparable thresholds for the single element task.

For our group of normal controls we used stimuli of 25% contrast in the integration experiments. This contrast represents the average contrast level used for the fellow fixing eyes of amblyopes.

Motion integration

Arrays of 128 randomly positioned, moving blobs were presented. The direction of an individual blob was chosen from a Gaussian distribution with a variable bandwidth and a mean equal to the cue (i.e. 90° ± the cue generated by APE). A single temporal interval, two-alternative forced choice paradigm was used. The observers' task was to judge whether the mean direction of the array of blobs was to right or left of vertical. Direction discrimination thresholds were obtained from between 256-512 presentations for each standard deviation (10 levels typically between 0°-50°) of the parent distribution. The motion direction threshold for each level of variability of the parent distribution was estimated from the slope of the best fitting cumulative Gaussian function using a maximum likelihood procedure. An equivalent noise model (Dakin, 2001) was fitted to the thresholds separately for each eye of each observer in each condition.

Results

In fig. 2 results are shown for direction discrimination of a single element for a normal and three of our amblyopic subjects, a strabismic, an anisometropic and a form-deprived amblyope. The threshold for direction discrimination is plotted against the contrast of the element. For amblyopic observers, performance was measured for the amblyopic eye with a high (50%) contrast element. The contrast used for the fellow fixing eye was that which gave equivalent performance (indicated by the vertical arrow). The subsequent integration experiments were carried out with element contrasts for which performance was equated at the single element level.

Figure 2: This figure represents the matching local direction discrimination in one normal (a) and three amblyopic observers (b-d). The amblyopic observers include deprived amblyopia (b), strabismic amblyopia (c), and anisometropic amblyopia (d). The X-axis is the contrast of the stimuli and the Y-axis is the threshold direction offset for one single moving element. In (a), the open circles and the solid line represent data for dominant eye at various contrasts (10% to 50%) and the filled circle for non-dominant eye at 25% contrast for one normal observer. As the contrast of the stimuli decreases, the discrimination threshold increases for the dominant eye. At 25% contrast the thresholds on both eyes are statistically the same (CI 95%, $p>0.05$). In (b-d), the open circles and the solid lines represent the data for fellow fixing eyes. The filled circles represent the thresholds for amblyopic eyes at a fixed high contrast of 50%. The arrows show the contrast chosen for elements to be presented to the fellow fixing eye in the rest of the experiment. This contrast produces equivalent performance to the amblyopic eye when presented with a 50% contrast element. The error bars represent 95% confidence intervals.

Fig. 3 shows sample data sets of thresholds for a normal and for each of the three representative amblyopic observers (i.e. strabismic, anisometropic and form-deprived amblyope) for motion direction integration. The task involved determining the mean direction of the array of element motions with respect to the vertical. The X-axis is the standard deviation of the signal population which was varied from 0° to 50° (0, 1, 2, 4, 8, 12, 20, 30, 40, and 50). The Y-axis is the motion direction threshold offset (deg). The data is fit by an equivalent noise model (Mansouri, Allen, Hess & Dakin, 2004a; Mansouri et al., 2004b). The parameters of internal noise (i.n.) and number of samples (n.s.) are shown in the inset. Increasing the standard deviation beyond a point (at around a standard deviation of 6°) leads to a rise in thresholds. The circles and dashed lines represent the data for the fellow fixing eye (FFE) and the square and solid line represent the amblyopic eye (AME). The AME and FFE show similar thresholds (95% CI, $p>0.05$). Furthermore, comparing AME with FFE, the parameters of internal noise and number of samples are not statistically different ($p>0.05$).

Figure 3

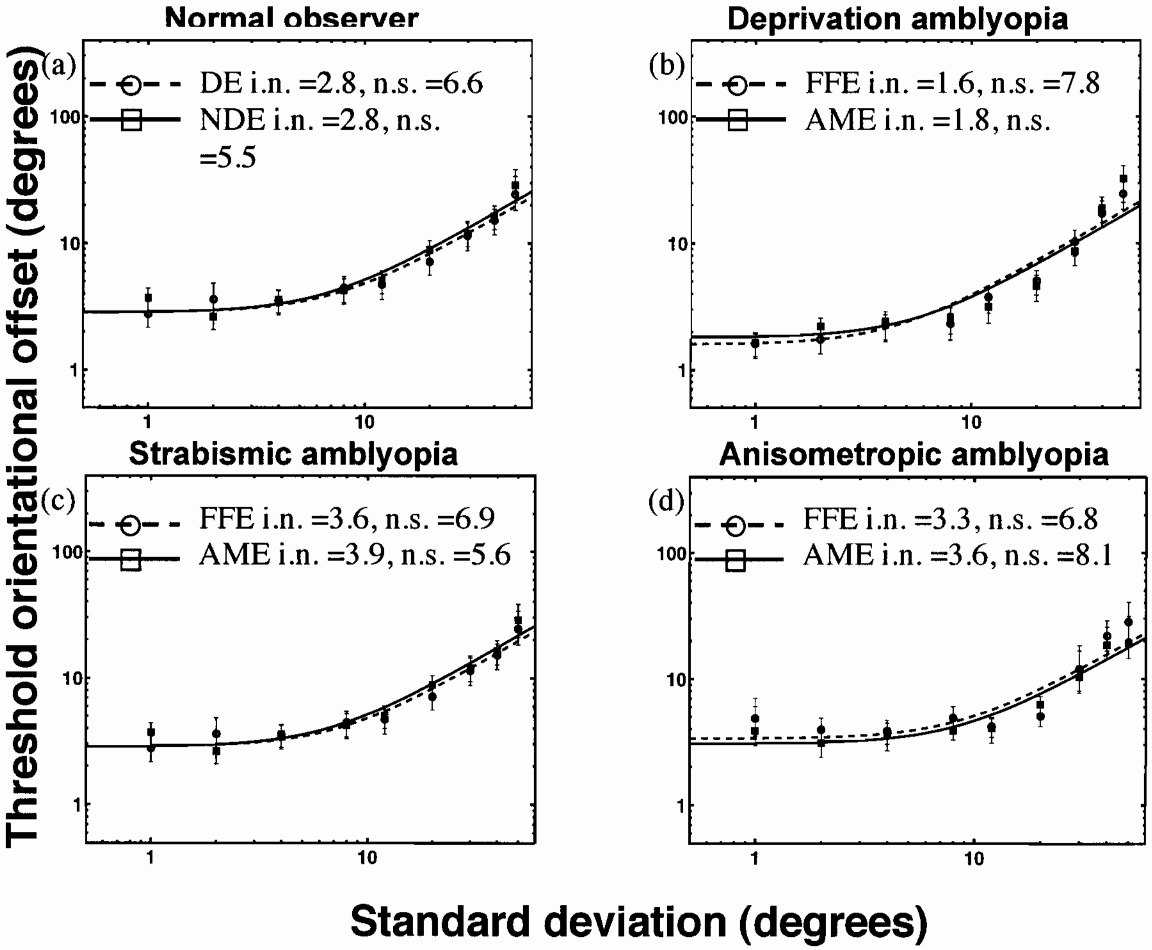

Figure 3: The motion direction integration threshold is measured as a function of the standard deviation (0° to 50°) of parent motion direction populations. Circles and dashed lines show the thresholds for dominant eye of one normal observer (a) and the fellow fixing eyes of three amblyopic observers (b-d). Squares and solid lines represent the thresholds for non-dominant eye of one normal observer (a) and amblyopic eyes of three amblyopic observers. The parameters of internal noise (i.n.) and number of samples (n.s.) from the equivalent noise model are shown in inset. The error bars represent 95% confidence intervals.

Similar results to these were collected for all normal and amblyopic observers. In all cases, the normal observers' dominant (DE) and non-dominant (NDE) eyes showed similar performances to the fellow fixing (FFE) and amblyopic (AME) eyes of the amblyopic observers.

In Fig. 4 the average values for the parameter of internal noise (X-axis) are compared for DE (light grey bar) and NDE (dark grey bar) of 6 normal and the AME (black bar) and FFE (white bar) of 6 amblyopic observers. The internal noise is comparable and not statistically different ($p>0.05$) among all four groups.

In Fig. 5, the Y-axis represents the number of samples parameter. The number of samples parameter was not statistically different in DE, NDE, FFE and AME either.

Figure 4

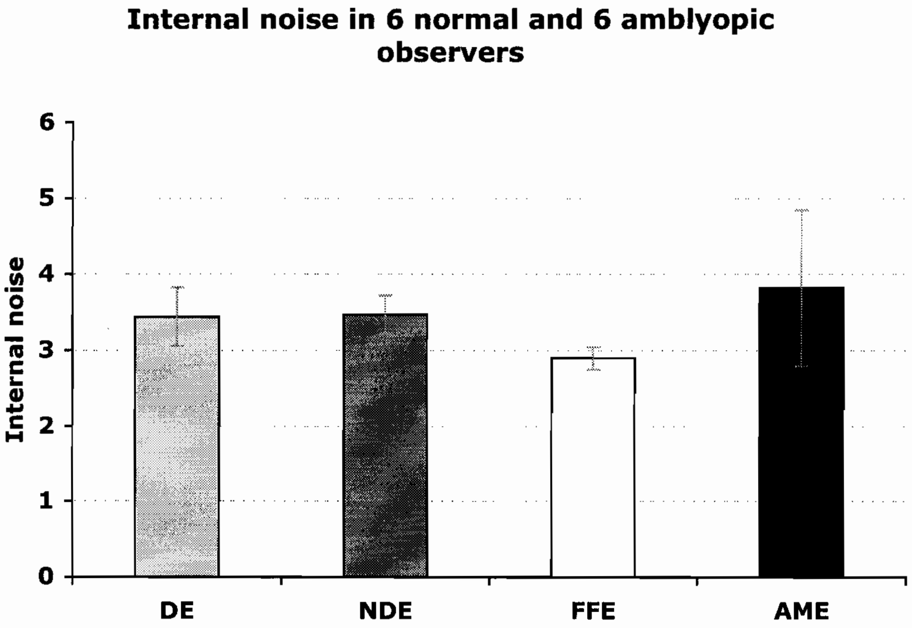

Figure 4: The average internal noise in 6 normal and 6 amblyopic observers are plotted for dominant (light gray), non-dominant (dark gray), fellow fixing (white) and amblyopic eyes (black) bars. The error bars represent ±0.5 standard deviations. The internal noise is statistically similar in all amblyopic and normal observers' eyes (p>0.05).

Figure 5

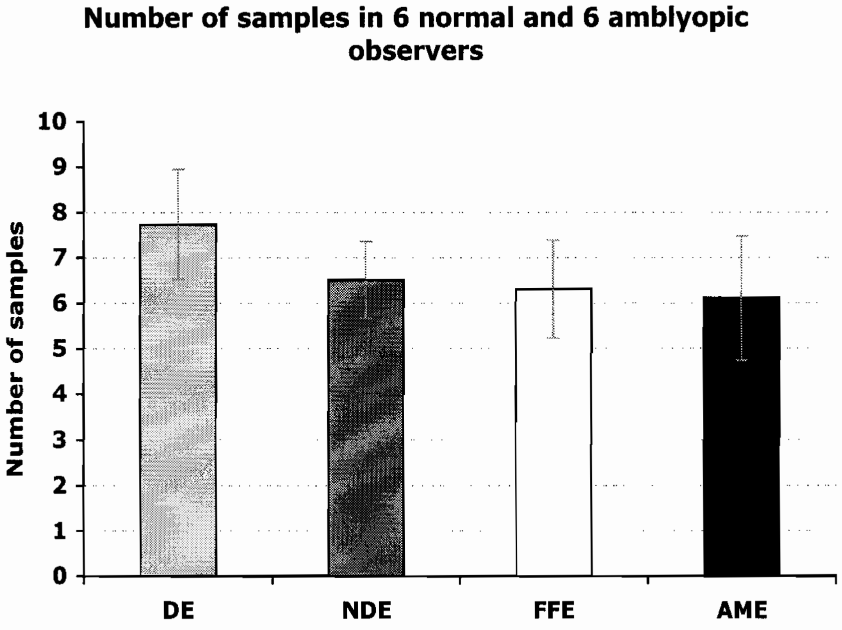

Figure 5: The average number of samples in 6 normal and 6 amblyopic observers are plotted for dominant (light gray), non-dominant (dark gray), fellow fixing (white) and amblyopic (black) eyes. The error bars represent ±0.5 standard deviations. The number of samples is statistically similar in all amblyopic and normal observers' eyes ($p>0.05$).

Discussion

We used a global motion direction task in a group of amblyopes in which direction detection performance was equated at the single element level. This ensured that any deficit for estimating the mean direction of the array of element motions was due to deficient global integration rather than any deficit at the level of local motion transduction. Performance was measured as a function of the standard deviation of the parent distribution from which the motion direction of individual element represented samples. We used an equivalent noise model to derive two parameters, one additive (i.e. internal noise) and one multiplicative (i.e. number of samples). Our results show that amblyopes, be they strabismic, anisometropic or form-deprived, exhibit normal integration of motion direction. The internal noise and number of samples were comparable between the normals and amblyopes and between the normal fellow eye and the amblyopic eye of amblyopes. This result is in stark contrast to the abnormal performance of amblyopic observers reported by (Simmers et al., 2003) for strabismic and anisometropic amblyopes and (Ellemberg et al., 2002) for form-deprived amblyopes in a similar task involving global motion. Since this previous study (Simmers et al., 2003) also ensured, as we did, that any performance deficit was not due to the encoding of motion at the single element level, any discrepancy between this previous study and ours must pertains to the level at which global motion is analysed.

A similar discrepancy is present for global form processing. In a subsequent paper, (Simmers et al., 2005), using a comparable global form task showed that amblyopes exhibit anomalies at the stage of global rather than local form processing.

Furthermore, the anomaly for global form processing is greater for second order (i.e. contrast-defined) than for first order (i.e. luminance-defined) stimuli. We have subsequently shown, using a global form task, similar to that described here for motion, that global spatial integration of first (Mansouri et al., 2004b) and second order (Mansouri, Allen & Hess, in press) stimuli is normal in amblyopia. The discrepancy between our finding and those of Simmers and co-workers (2003, 2005) that involve both form and motion processing point to where the problem is in amblyopia and possibly why global processing is often found to be abnormal in developmental brain disorders (Braddick, O'Brien, Wattam-Bell, Atkinson & Turner, 2000a). In our task where all the elements contain relevant information about the mean of the distribution to be estimated, an ideal observer would blindly integrate all the available information. Amblyopes can do this normally as we have shown this for form tasks (Mansouri et al., 2004b) and, in the present study, for motion tasks. In the more typical global motion or form task where there are signal and noise elements, an ideal observer would first segregate signal from noise and then integrate the signal. It appears, therefore, that amblyopes can't do this. The obvious conclusion is that although amblyopes can integrate normally, they cannot segregate signal from noise as well as normal observers.

This conclusion that amblyopes may exhibit a selective deficit for signal/noise segregation is further strengthened by the finding that normals exhibit much better sensitivity than expected on the basis of blind integration for integration tasks of the form described here when additional noise elements are introduced, suggesting a role for a noise segregating process (Mansouri et al., 2005). Also, deficits to the dorsal stream in the extra-striate cortex that lead to global motion deficits (Newsome & Pare, 1988) are characterized by profound anomalies to the signal segregation aspect of the task (Baker et al., 1991). It will be interesting to know to which of the two complimentary extra-striate processes other developmental anomalies (i.e. Williams syndrome, developmental dyslexia, autism) are more vulnerable during development (Braddick et al., 2003), integration or segregation?

Acknowledgements

This work was supported by a CIHR grant (#108-18) to RFH. We are grateful to all our amblyopic subjects who so unselfishly gave up their time for research.

Preface to chapter 5

In chapter 1 we showed that randomly oriented elements, to some extent, could disrupt the performance of the normal visual system in integrating orientation information across space. We used this paradigm to study how and where information from two eyes is combined. Here we are interested to know whether information from dominant eye or non-dominant eye are treated differently in the visual system. These issues are discussed in chapter 5.

Chapter 5: The site of orientation integration and the effect of noise

Integration, Segregation and Binocular Combination

Behzad Mansouri and Robert F. Hess

McGill Vision Research, 687 Pine Ave W, H4-14, Montreal, H3A 1A1, Quebec, Canada

Harriet A. Allen

School of Psychology, University of Birmingham, Birmingham, B15 2TT, U.K.

Steven C. Dakin

Institute of Ophthalmology, University College, 11-43 Bath St. London EC1V 9EL, U.K.

The human visual system can accurately judge the mean of a distribution of different orientation samples. In this study we ask whether the site of this integration is before or after the sites of binocular combination and disparity processing. Furthermore, we are interested in whether the efficiency with which local orientation information is integrated depends on the eye of origin.

Our results suggest that orientation integration occurs after binocular integration but before disparity coding. We show that the effectiveness of added orientation noise is not only less than expected on signal/noise grounds but also it depends on the dominance of the eye to which it is presented, suggesting an inter-ocular opponent interaction where the dominant eye input has higher gain.

Introduction

Early visual processing consists of a patch-wise local decomposition of the retinal image into its spatial, orientational, contrast, motion and chromatic components (Robson, 1975). These local operations are represented in the firing patterns of individual cells in V1 of the cortex (DeValois & DeValois, 1988). Subsequent non-linear operations reveal and consolidate global patterns of activation that allow the extraction of ecologically relevant global image features. We know more about the initial quasi-linear local processing than we do about the later non-linear global processes of integration and segregation.

In terms of orientation processing there have been a number of psychophysical studies that bear upon these later global operations, particularly with reference to shape discrimination (Achtman, Hess & Wang, 2003; Braddick, O'Brien, Wattam-Bell, Atkinson & Turner, 2000b; Hess, Wang & Dakin, 1999b; Wilkinson, Wilson & Habak, 1998; Wilson & Wilkinson, 1998). A simpler form of integration is one where subjects are asked to report on the mean value (e.g. orientation) of a group of local, randomly positioned spatial samples where global shape is irrelevant. Such a task involves integration in its purest form. Using such an integration task, Dakin (Dakin, 2001) has shown that normal observers can integrate local orientation information efficiently over a large range of stimulus size, numerosity and density. His results were well described by the equivalent noise model used to estimate the visual system's internal noise and sampling efficiency. He showed that such integration is robust to changes in stimulus size, element numerosity and density. More recently, it was shown that a similar type of integration occurred for second-order stimuli (i.e. where orientation is defined by a contrast variation), thereby extending its generality, although the underlying mechanisms may be different (Allen et al., 2003).

It is of interest to know where in the visual processing hierarchy such a basic type of integration takes place. For example, is it before or after binocular combination? If it is after binocular combination, is it before or after the site of disparity processing? The site of visual integration of local orientation is of interest for a number of different reasons. First, being one of the simplest forms of integration it may occur early in the pathway. Second, a comparable integration for motion direction is thought to occur in extra-striate area MT (Movshon et al., 1985; Newsome & Pare, 1988; Salzman et al., 1992) and it would be of interest to know if there is also an extra-striate locus for orientation information. Third, by introducing a noise distribution into this integration task one might be able to assess whether the processes of integration and segregation occur at the same or different sites along the pathway.

At present there have been no studies on the site of this specific form of orientation integration involving estimation of the mean. However, some work has been done on the site of other types of global orientation processing relevant to shape processing. For example, the integration of orientation information for the extraction of global contours (Field et al., 1993) is thought to involve disparity-tuned (i.e. V2) as well as binocular (i.e. superficial layers of V1) mechanisms because not only can dichoptic versions of the stimulus be detected (Huang, Hess & Dakin, 2004) but also contours that oscillate between different depth planes can be easily detected (Hess & Field, 1995). The integration of local orientation information to define object shape and in particular circularity has been shown, in an imaging study (fMRI), to involve area V4 of the ventral pathway (Hess & Field, 1995; Wilkinson, James, Wilson, Gati, Menon & Goodale, 2000). On the other hand, texture boundaries based on local orientation can only be discriminated at a monocular site (e.g. layer 4B of V1) in the pathway (Solomon & Morgan, 1999).

To determine the site of this form of orientation integration (i.e. involving mean estimation) we measured the ability of normal subjects to estimate the mean orientation of an array of oriented Gabor patches. The orientations of the Gabors were sampled from a signal population, which had different variances under monocular, dichoptic and stereoscopic viewing conditions. In some conditions, these 'signal' stimuli were accompanied by a set of randomly oriented Gabors (our 'noise' stimuli). If the visual system averages over all the available stimuli, then introducing this orientation noise will enormously disrupt the visual system's performance. However, if the visual system applies extra mechanisms, such as segregation, it might be, to some extent, robust to the effect of the added randomly oriented noise Gabors.

We used an equivalent noise model to derive the best fitting estimates of internal noise and number of samples from the threshold data. Our results suggest that the site of orientation integration is after the site of binocular integration but before the site of disparity encoding. In a separate manipulation we introduce noise (i.e. samples unrelated to the orientation distribution whose mean is to be estimated) to our stimulus to assess the role of segregation under our stimulus conditions. We find that the effectiveness of noise depends on the eye to which it is presented, suggesting that the eye of origin influences inter-ocular segregation processes.

Methods

Observers

Three observers who were naïve to the purposes of the experiments and the first author were tested. All observers wore their usual optical correction.

Eye dominance

Eye dominance was assessed for each subject using a sighting test (Rosenbach, 1903). Three subjects were right eye dominant, one was left eye dominant.

Apparatus

A Power Macintosh 6600/800 computer was used to generate and display the stimuli. Stimulus presentation was controlled by the Matlab environment (MathWorks Ltd) and Psychophysics ToolBox (Brainard, 1997). In the main experiment all stimuli were displayed on a 20-inch NANAO FlexScan 6600 monitor, however we used a 20-inch Sony Trinitron GDM-F520 monitor for the disparity and control experiments. Both monitors were calibrated and linearized using a Graseby S370 photometer and the Video Toolbox (Pelli, 1997) package. Pseudo 12 bit contrast accuracy was achieved by using a video attenuator (Pelli & Zhang, 1991), which combined the RBG outputs of the graphic card (ATI Rage 128) into the green (G) gun. Both monitors had refresh rates of 75 Hz. The mean luminance of the screens was 28 cd/m^2. The resolution was 1152 x 870 pixels for both. One pixel on the screen was 0.32 mm, which was 2.12-arc min of the observers' visual angle from the viewing distance of 52 cm.

Stimuli

Separate stimuli were presented to the left and right eyes, using a mirror stereoscope. Each eye viewed an independent image. These images were 6° x 6° wide and arranged on the screen centrally and adjacent to each other. The left and right eye images were fused into one cyclopean image by the observer.

Stimuli were arrays of Gabor micro-patterns presented on a 30° (height) x 38° (width) (from the observers distance) mean luminance background. The envelope of each Gabor had a standard deviation of 0.4 degree of visual angle. The spatial frequency of sinusoidal modulation within the Gabors was 0.52 cycles per degree (cpd). Typically, 8 Gabors were presented to each eye. These were positioned randomly within a circular area inside the box outline, centred on the centre of the box. When the patches overlapped (as could occasionally occur), their gray levels were added, if this led to brightness levels outside the possible luminance range, they were clipped appropriately at the maximum or minimum contrast values.

The orientation of each Gabor was controlled by its parent distribution. Two types of parent distribution were used, producing two different Gabor populations: 'noise' and 'signal'. The orientation of each Gabor micro-pattern in the signal population was selected from a Gaussian distribution with a mean equal to the orientation cue (i.e. 90° ± the cue generated by APE, an adaptive method of constant stimuli (Watt & Andrews, 1981)) and a variable bandwidth. The distribution's standard deviation, σ_{ext}, was varied from 0° (all elements aligned) to 28° (high orientation variability). The orientations of Gabors in the noise population were selected from a Gaussian distribution with a standard deviation of 90°. We used the same method to generate the parent distribution of the noise Gabors as we used to generate the parent distribution of the signal array. This meant that the noise population distributions had a randomly selected (on each trial) mean orientation, however, given the breadth of the distribution this was not discernable. Note also that since orientation is a circular variable (i.e. any orientation beyond 180° or below 0° is equivalent to its equilibrium in the 0° to 180° range), our noise populations were equivalent to uniform distributions between 0 and 180 degrees. Different combinations of signal and noise were tested. Depending on which condition was tested, each eye's image could contain a signal population, a noise population, both, or just a fixation point. A stereoscope was used to show the left image to the left eye and the right image to the right eye (see figure 1A and 1B). To prevent any bias, the observers were not informed which population (e.g. signal or noise) was being presented at any time and if different Gabor populations were presented to different eyes, the process was randomized within a run so that observers were unaware of which stimulus was presented to which eye. Observers did not receive feedback.

Figure 1

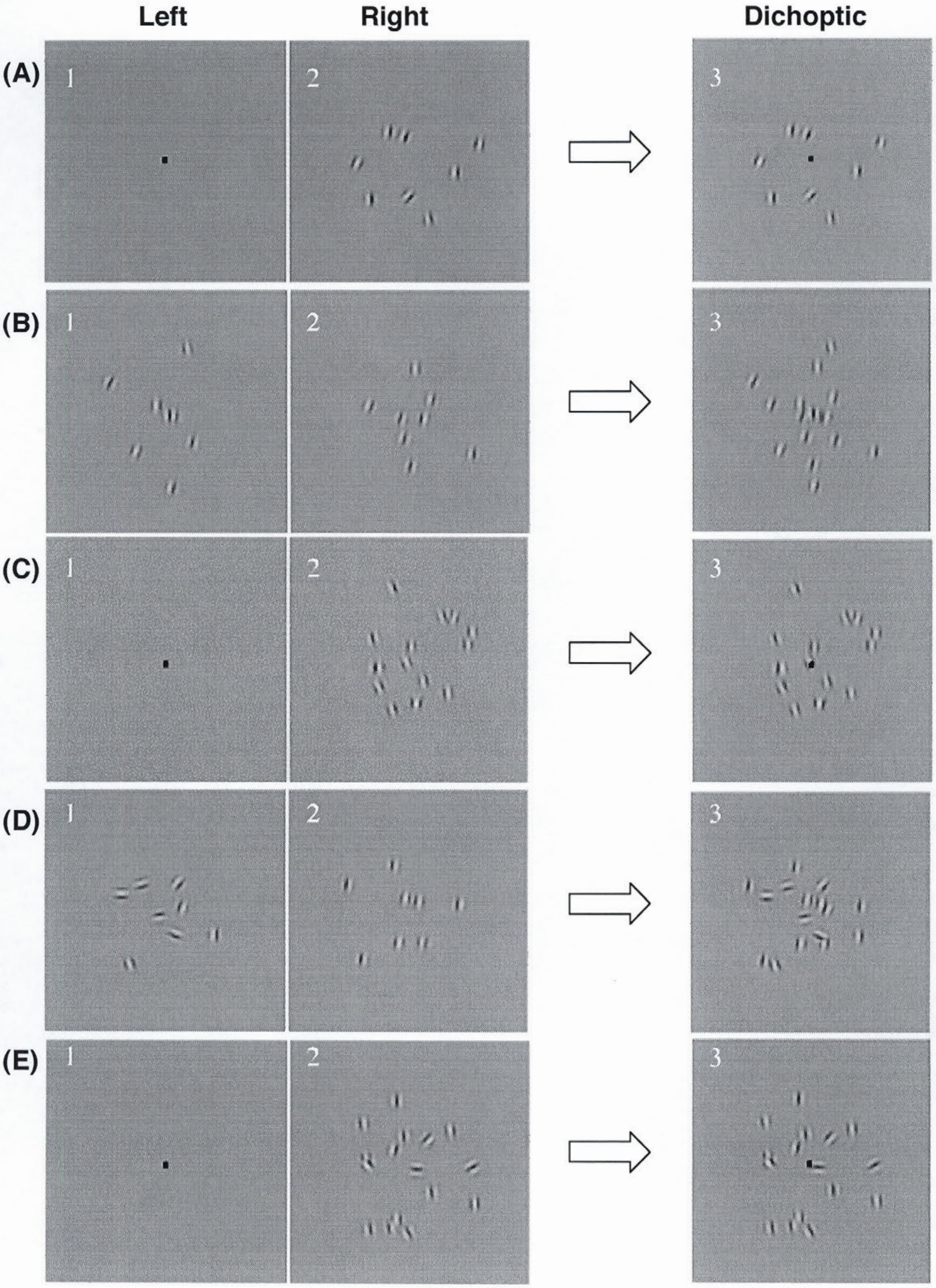

Figure 1: Two adjacent boxes (1, 2) each holding either stimuli or a fixation point were located at the centre of the screen. Looking through a stereoscope, observers could see one box (3), which contained a fused image. However, the left eye could only see the left box and the right eye could see the right box. The stimuli could be signal, noise or both (see Method section).

(A) 8 signal Gabors are presented to one eye and fixation point to the other eye. (B) 8 signal Gabors are presented to each eye. (C) 16 signal Gabors are presented to one eye and fixation point to the other eye. (D) 8 signal Gabors are presented to one eye and 8 noise Gabors are presented to the other eye. (E) 8 signal Gabors and 8 noise Gabors are presented to one eye and fixation point to the other eye.

Six combinations of signal and noise were tested (see Figure 1):

In the first five conditions (A–E) the signal population, the noise population and the fixation point were presented in the same disparity plane.

(A) Signal population presented to the dominant eye (DE) and fixation point to the non-dominant eye (NDE), and vice versa.

(B) Signal populations presented simultaneously to DE and NDE eyes.

(C) 16 signal Gabors (two times the typical 8 Gabors) presented to DE and fixation point to the NDE, and vice versa.

(D) Signal population presented to DE and noise population to the NDE, and vice versa.

(E) Signal and noise populations presented to DE and fixation point to the NDE, and vice versa.

Procedure

A single temporal interval two alternative forced choice paradigm was used. The observers' task was to judge whether the mean orientation of the array of Gabors was rotated clockwise or counter-clockwise (tilted to right or left of vertical) (see figure 1). The stimulus presentation time was 500 ms in the main experiment. In a later control experiment this was reduced to 100 ms. On each trial, observers indicated their decision with a button press. The mean orientation of the signal population was controlled by APE, an adaptive method of constant stimuli (Watt & Andrews, 1981), which sampled a range of orientations around vertical.

Given that thresholds are estimates of response variance, the non-ideal behaviour of observers with noiseless stimuli can be expressed as an additive internal noise. The level of internal noise is measured by increasing the amount of external noise in the stimulus and determining the point at which observers' performance begins to deteriorate. If the task requires integration, then observers' robustness to increasing amounts of external noise will depend decreasingly on internal noise and increasingly on how many samples are averaged. Thus the form of the equivalent noise model is:

$$\sigma_{obs}^2 = (\sigma_{int}^2 + \sigma_{ext}^2) / n \qquad (1)$$

Where σ_{obs} is the observed threshold, σ_{ext} is the external noise, σ_{int} is the estimated equivalent intrinsic or internal noise and n is the estimated number of samples being employed. In terms of the orientation discrimination task, σ_{obs} corresponds to the threshold for orientation discrimination, σ_{ext} to the standard deviation of the distribution from which the samples are derived, σ_{int} to the noise associated with the measurement of

Figure 2: The data from observers (BM, SS, PC and HA) are presented in four columns (1, 2, 3 and 4), respectively. Five conditions of (A, B, C, D and E) are tested as described in Method section. The orientation threshold offset is plotted for each standard deviation of the signal population (external noise). The circles represent the data from the signal to dominant eye (StoD) and the stars show the data from the signal to non-dominant eye presentation (StoND). In condition B both eyes are presented with signal (StoB). The best fits for (StoD) and (StoND) data are shown respectively as dotted and solid lines. The parameters of internal noise (σ_{int}) and number of samples (n) from the fitting model (see Method section) are shown for each observer and for each condition (StoD and StoND). Error bars represent 95% confidence intervals.

Results

Orientation discrimination thresholds are shown in Figure 2. In each figure threshold orientation offset (T.O.O.) is plotted against the standard deviation of the population from which the local orientation samples were derived. The solid and dotted lines are the fits of the model from which the parameters of internal noise (σ_{int}) and number of samples (n) are derived (inset in figure). The internal noise parameter is determined by the asymptotic thresholds at low variances whereas the sampling rate determines how rapidly thresholds rise with increasing variance. Results for 4 subjects' dominant (dotted line) and non-dominant eyes (solid line) are shown for the stimulus conditions (A-E) previously outlined in figure 1.

Parameters from the fitted equivalent noise model are summarized in Figure 3.

Figure 3A shows the internal noise parameter for each condition, averaged over the observers. We compared conditions when the signal was presented to the dominant eye (StoD - open bars) with the case when the signal was presented to the non-dominant eye (StoND - filled black bars). Depending on the condition (for key to column titles see figure 1) noise Gabors might have accompanied the signal Gabors. In terms of the internal noise, the interaction of the two variables was significant (F(4,12)=14.55, p=0.0001). Therefore, the following analyses have been extracted from simple effect and post-hoc tests.

Figure 3

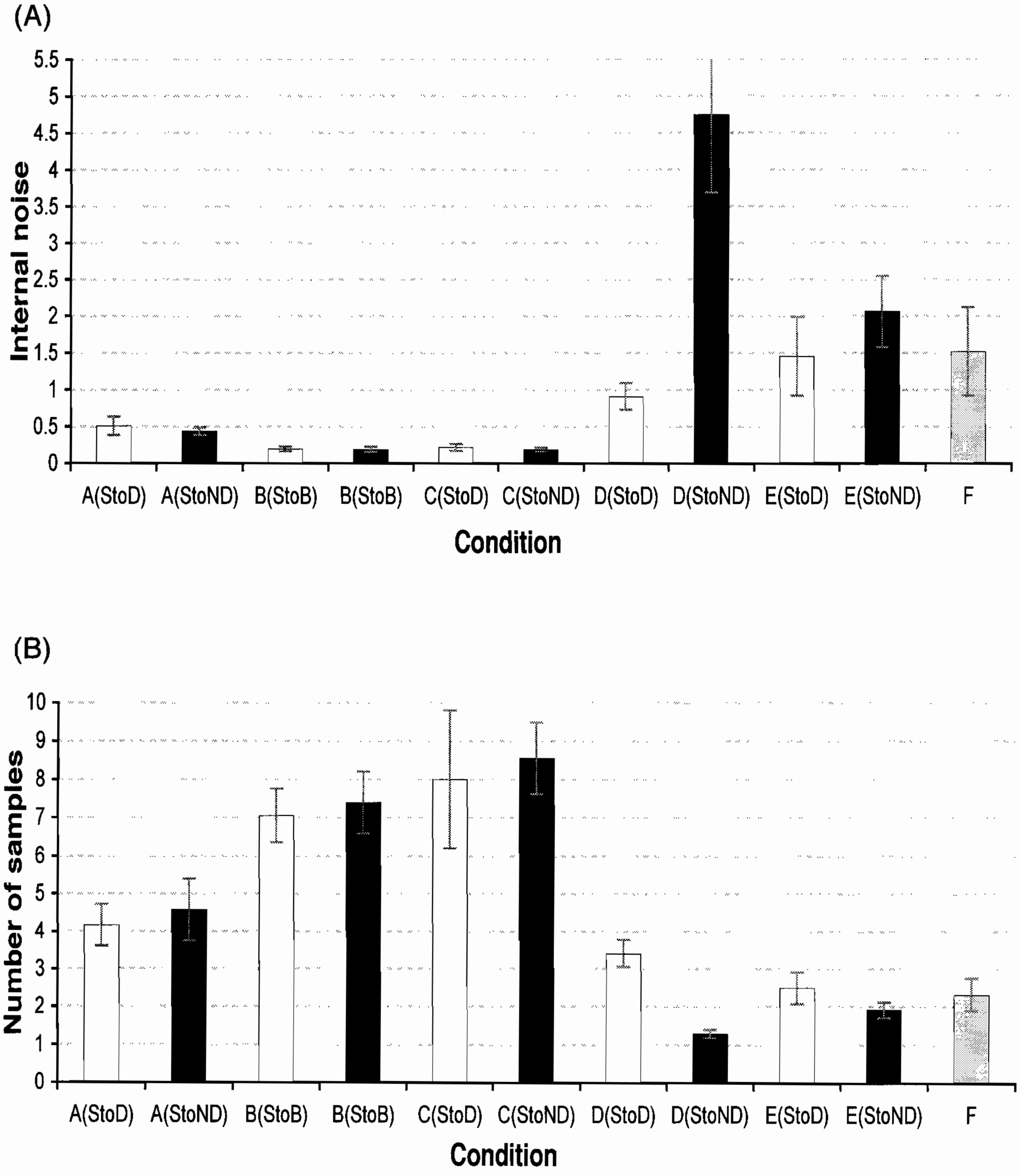

Figure 3: Internal noise (a) and number of samples (b) parameters are shown from the different conditions (see Method section). Open and filled black bars represent

StoD and StoND, respectively. In condition B both eyes are presented with signal (StoB). Filled gray bars (F) represent the condition in which signal and noise are presented in different disparity planes. Error bars represent ±0.5 standard deviations.

(1) Comparing StoD (compare open bars in figure 3A) across all observers, there is no statistically significant difference between these five conditions (A(StoD)-E(StoD)) ($F(4,20)=2.17$, $p>0.05$). However, the results from individual subjects showed a trend of increasing internal noise when noise Gabors were added to the signal. The fact that dichoptically (to non-dominant eye) and monocularly presented noise Gabors have the same effect on performance with signal Gabors presented to the dominant eye (compare D(StoD) versus E(StoD)) suggests that signal and noise are linearly combined in the dominant eyes visual stream when they are presented dichoptically.

(2) When the signal is presented to the non-dominant eye (StoND) and the noise is presented to the dominant eye (condition D(StoND)) or non-dominant eye (condition E(StoND)), (compare filled black bars in figure 3A), internal noise is significantly higher than when only the signal is presented to the non-dominant eye either monocularly or binocularly (conditions A(StoND), B(StoB) and C(StoND)) ($q(5,19.49)=9.2$ (in average), $p<0.01$). These differences were more prominent when the noise Gabors were dichoptically presented to the dominant eye (D(StoND)) ($q(5,19.49)=12.6$ (on average), $p<0.01$), which was also significantly higher than the internal noise in noise to the non-dominant eye (E(StoND)) condition ($q(5,19.49)=7.82$, $p<0.01$).

(3) Comparing dominant eyes with non-dominant eyes (compare open and filled black bars of figure 3A), internal noise is only significantly different in condition D

where signal Gabors were presented to the dominant eye and randomly oriented noise Gabors were presented to the other eye. The internal noise in StoND (D(StoND)) is significantly higher (F(1,13.67), $p<0.0001$) than the internal noise in condition D(StoD).

Figure 3B. The differences in "condition" variable were significant (F(4,12)=25.09, $p<0.0001$) when we tested the number of samples parameter. Figure 3B summarizes the number of samples parameter for each condition, averaged over all observers. The number of samples is significantly higher when signal populations are presented to both eyes (B), rather than to just one eye (A) (q(5,12)=5.09, $p<0.05$), suggesting an improvement with binocular viewing. The number of samples is significantly greater when a population of twice the size is presented monocularly (C) than when the regular sized population is presented to the dominant eye (A) (q(5,12)=6.98, $p<0.05$). When the signal population is evenly distributed between the 2 eyes in binocular viewing, however, the number of samples is equal to the case when a signal population of twice the size is presented to just one eye (compare conditions B with C) (q(5,12)=1.9, $p>0.05$). This suggests binocular linear combination. Adding a noise population decreases the estimates from sampling efficiency of both eyes. Conditions D and E have lower number of samples estimates than any of the conditions without noise Gabors (A, B, C) (q(5,12)=7.87, $p<0.01$). However, this decrease did not reflect a decrease in the visual system's sampling efficiency because the randomly oriented noise Gabors, which the visual system integrates, are not useful in estimating the mean and must automatically be registered as lower estimates of number of samples by the model.

Figure 4

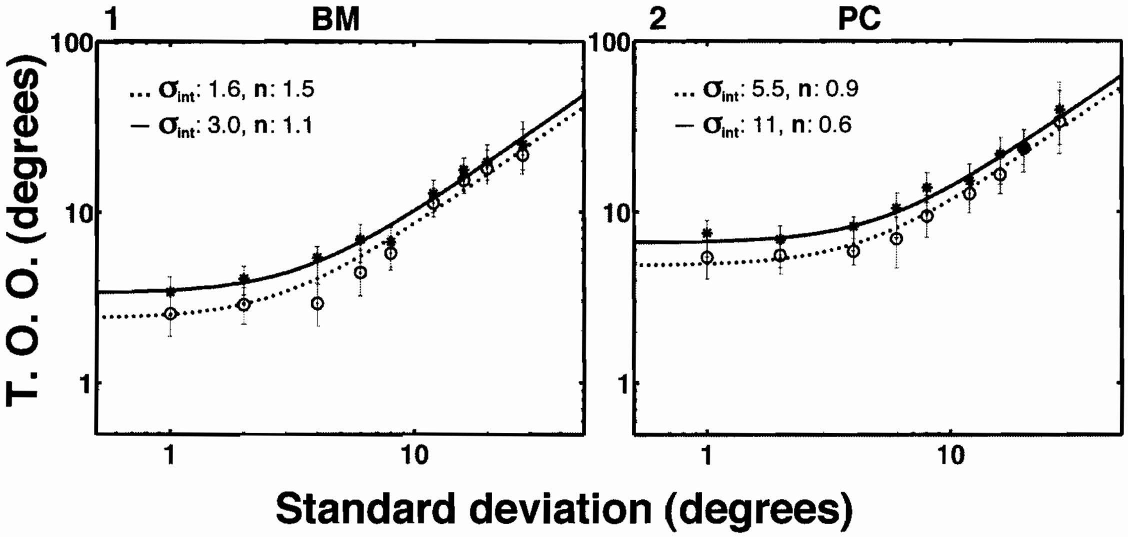

Figure 4: The orientation discrimination thresholds and the parameters from the equivalent noise model are presented for condition F(StoD) and F(StoND). The disparities are 33.92 arc min and zero, respectively. The orientation discrimination thresholds, internal noise and number of samples in condition F(StoD) are not significantly different (CI 95%, p>0.05) from those of the control condition F(StoND). Error bars represent 95% confidence intervals. T.O.O.: threshold orientation offset.

In a separate experiment we tested whether noise presented in a different disparity plane was effective in raising the internal noise and lowering the number of samples as illustrated above for stimuli in the same depth plane. Two disparity planes were used, one was in the fixation plane and contained the 8 signal elements, and the other was at a crossed disparity of 33.92 min of arc and contained 8 noise elements. Observers were not aware of which population (e.g. signal or noise) was presented to which plane. The results are shown in figure 4 and the parameter summaries are given in figure 3A (F) for internal noise and figure 3B (F) for number of samples. The internal noise and the number of samples found when noise is added in a different depth plane in condition (F(StoND)) are more similar to when the noise is added in a same plane as the signal (D & E) than they are when there is no noise (A). This suggests that noise presented in a different depth plane is equivalent to noise presented in the same depth plane.

Figure 5

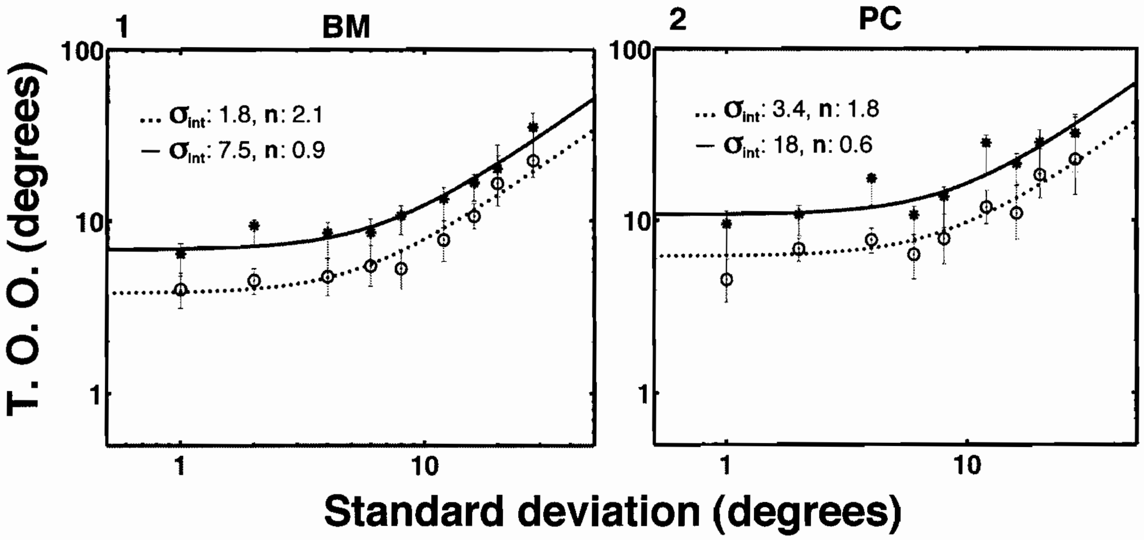

Figure 5: Data from a control experiment that reduced presentation duration for condition D(StoD) and D(StoND). Presentation time was 100 ms for two observers. The differences in thresholds, internal noise and number of samples are significant (CI 95%, p<0.05). Error bars represent 95% confidence intervals. T.O.O.: threshold orientation offset.

In the main experiment when signal or noise elements were presented to separate eyes we did not prevent the few cases where left and right eye elements overlapped. Consequently, we wondered whether rivalry could have played a part in our initial finding that noise presented to the dominant eye is more effective. Since rivalry takes some time to build up and can be disrupted by brief presentations(Wolf, 1986) we undertook a control experiment where the stimulus was presented for 100 ms rather than the 500 ms that we had used previously. These results are shown in figure 5 for the dichoptic condition when signal is presented to one eye and noise to the other (as in figure 1D). Circles are for StoD (and noise to the non-dominant eye) and stars are for StoND (and noise to the dominant eye). There is a significant increase in internal noise (CI 95%, $p<0.05$) and a significant decrease in the number of samples (CI 95%, $p<0.05$) when noise is presented to the dominant eye and signal to the non-dominant eye compared to the other way round. This confirms that the asymmetry observed in our main experiment is also present when the exposure duration is shortened to 100 ms, making it unlikely that binocular rivalry played a major role.

Finally, we show in figure 6 the results for one subject (SS) for populations of Gabors ranging from 2-32 elements, displayed in the same manner to that already described for figure 2.

Figure 6

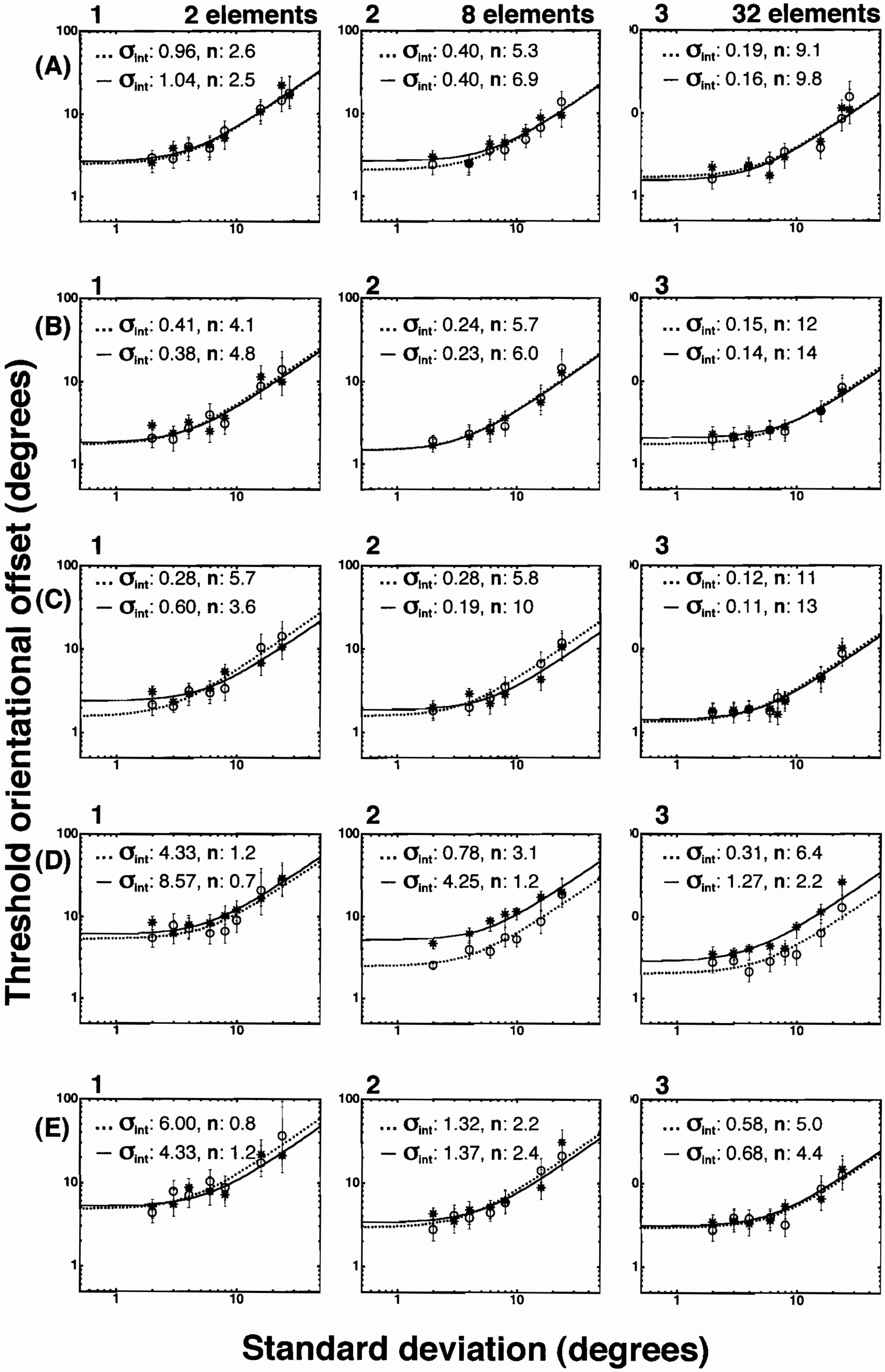
1 2 elements
2 8 elements
3 32 elements
(A)
... σ_{int}: 0.96, n: 2.6
— σ_{int}: 1.04, n: 2.5
... σ_{int}: 0.40, n: 5.3
— σ_{int}: 0.40, n: 6.9
... σ_{int}: 0.19, n: 9.1
— σ_{int}: 0.16, n: 9.8
(B)
... σ_{int}: 0.41, n: 4.1
— σ_{int}: 0.38, n: 4.8
... σ_{int}: 0.24, n: 5.7
— σ_{int}: 0.23, n: 6.0
... σ_{int}: 0.15, n: 12
— σ_{int}: 0.14, n: 14
(C)
... σ_{int}: 0.28, n: 5.7
— σ_{int}: 0.60, n: 3.6
... σ_{int}: 0.28, n: 5.8
— σ_{int}: 0.19, n: 10
... σ_{int}: 0.12, n: 11
— σ_{int}: 0.11, n: 13
(D)
... σ_{int}: 4.33, n: 1.2
— σ_{int}: 8.57, n: 0.7
... σ_{int}: 0.78, n: 3.1
— σ_{int}: 4.25, n: 1.2
... σ_{int}: 0.31, n: 6.4
— σ_{int}: 1.27, n: 2.2
(E)
... σ_{int}: 6.00, n: 0.8
— σ_{int}: 4.33, n: 1.2
... σ_{int}: 1.32, n: 2.2
— σ_{int}: 1.37, n: 2.4
... σ_{int}: 0.58, n: 5.0
— σ_{int}: 0.68, n: 4.4
100
10
1
1
10
Threshold orientational offset (degrees)
Standard deviation (degrees)

Figure 6: Beside the 8 Gabors in the main experiment, two different numbers of Gabors (2, 32) were tested with one observer (SS). Five conditions are presented in the same configuration as used in figure 1. Internal noise is generally decreased and number of samples increased when the number of Gabors is increased. The significant differences in condition D is replicated within 2 and 32 Gabors condition. Error bars represent 95% confidence intervals.

Figure 7

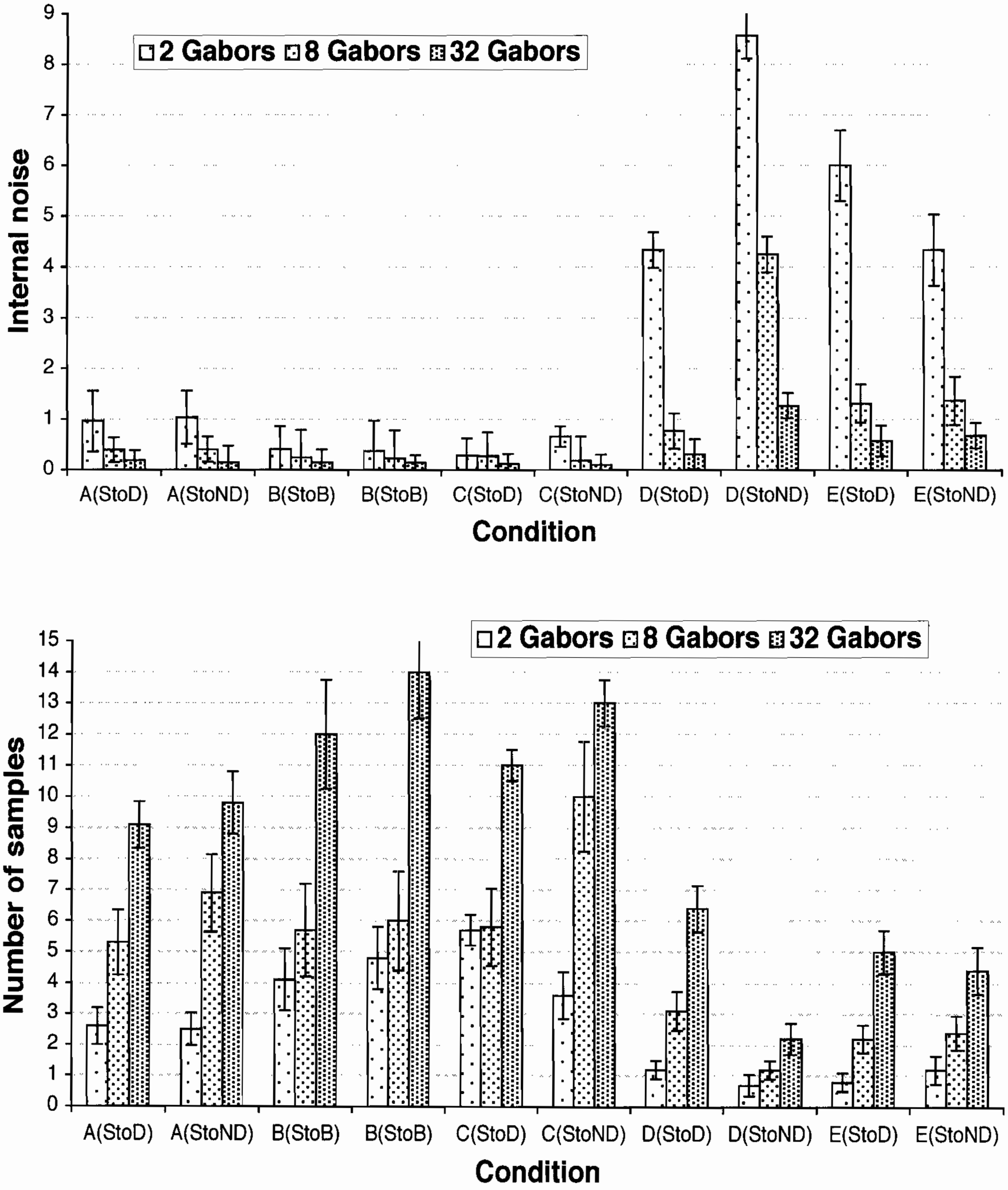
□2 Gabors ▨8 Gabors ▦32 Gabors
Internal noise
0
1
2
3
4
5
6
7
8
9
A(StoD)
A(StoND)
B(StoB)
B(StoB)
C(StoD)
C(StoND)
D(StoD)
D(StoND)
E(StoD)
E(StoND)
Condition
□2 Gabors ▨8 Gabors ▦32 Gabors
Number of samples
0
1
2
3
4
5
6
7
8
9
10
11
12
13
14
15
A(StoD)
A(StoND)
B(StoB)
B(StoB)
C(StoD)
C(StoND)
D(StoD)
D(StoND)
E(StoD)
E(StoND)
Condition

Figure 7: Internal noise and number of samples parameters are shown for 3 different number of Gabors (2, 8, and 32) and all conditions displayed in figure 6 (see Method section). Dotted and solid lines represent StoD and StoND, respectively. In condition B both eyes are presented with signal (StoB). Error bars represent 95% confidence intervals.

Model parameters (internal noise and number of samples) derived from the continuous (solid & dotted) curve fits to this data are summarized in figure 7 in a manner comparable to that already described for figure 3. The results show that our conclusions derived from a population of 8 Gabors (figures 2 & 3) can be generalized to populations from 4 to 32 elements. In particular, signal summation is comparable within eyes (A(StoD) & A(StoND)) and between eyes (B(StoB) & B(StoB)), even in the presence of added noise (E(StoD) & E(StoND)). However, noise to the dominant eye D(StoD) is statistically more effective in raising the internal noise and lowering the number of samples than noise to the non-dominant eye (D(StoND)).

Discussion

We have used a task which involves the integration of local orientation information and which is processed in an efficient and pre-attentive fashion by the visual system (Dakin, 2001). What appears to limit performance on this task is more the informational capacity of the stimulus rather than the visual processing per se (Dakin, 2001). By varying the standard deviation of a Gaussian distribution from which the samples are drawn, integrative performance can be quantified in terms of a two-parameter model (equivalent noise model) where the parameters are: internal noise and number of samples.

Integration site

Our first issue concerned the site of this integration relative to binocular and disparity processing. Since we find that our two model parameters (internal noise and number of samples) are similar under monocular (figure 2C) and dichoptic (figure 2B) conditions, we conclude that this form of orientation integration is likely to occur after binocular combination. This is strengthened by the finding that dichoptically presented noise (figure 2D) can be, in some situations, more detrimental than the same noise presented monocularly (figure 2E) and that the addition of signal or noise dichoptically and monocularly are equivalent. Furthermore we found that the effects of such noise cannot be reduced when it is presented in a different depth plane (figure 2F). This suggests that the site of this form of integration is prior to the site of disparity processing. This indicates that the integration of arrays of Gabors occurs after the processing of simple texture boundaries (Solomon & Morgan, 1999) but at a similar stage to contour integration (Hess & Field, 1995; Huang et al., 2004). Since the earliest site of binocular combination is in layer 4 of V1 (Hubel & Wiesel, 1977) and the earliest site where relative disparities are processed is V2 (Cumming & Parker, 2000), it would seem that this form of orientation integration occurs somewhere between the input cells in layer 4C of V1 and the input layer 4 in V2 (Thomas, Cumming & Parker, 2002). The finding that orientational opponency is present in V1 (Knierim & van Essen, 1992) is suggestive that the site of integration may be in the more superficial layers of V1.

Segregation

Adding randomly oriented Gabor patches, our 'noise' never reduced performance as much as would be predicted if the visual system was blindly sampling from the orientation elements and integrating these samples. We devised an ideal observer model that blindly integrated signal and noise Gabors. We used the model to estimate the internal noise that would arise if observers took the observed number of samples but blindly selected either signal or noise. For example, when signal and noise Gabors were presented to one eye, the mean estimate of number of samples was 2.21 and the average estimated internal noise was 2.82. Blindly integrating signal and noise elements by an ideal observer model, predicts an internal noise estimate of approximately 19.49. If the model takes the samples from a more restrictive range of orientations around the mean, instead of averaging every element, the ideal observer is more robust to the effect of added noise. Our simulations show that comparable internal noise to that found experimentally is found when our ideal observer model takes the samples over a range of 50 degrees (mean ±25 degrees). Although this assumes that the more restrictive region over which signal and noise integration takes place is fixed, an assumption that has, as yet, no experimental support. It should be stressed that the signal and noise Gabor populations were identical in every way except orientation distribution. Some segregation of signal and noise elements must have taken place. This suggests that there are monocularly based segregation processes at work to reduce the effectiveness of the noise and, by analogy to luminance adaptation in the retina; this may involve an opponent interaction. An opponent mechanism that estimated the magnitude of orientation noise present by, for example the response of a population of non-oriented neurons, could regulate sensitivity.

Eye dominance

We also investigated the effect of noise on signal integration. We show that the two key model parameters for signal integration are statistically identical between dominant and non-dominant eyes of our observers. This is also the case when a population of noise elements is introduced. When this population of noise elements is introduced through one eye and the signal through the other eye, the effectiveness of that noise depends on the eye of origin. At the binocular site where we suggest integration takes place, segregation (i.e. involving signal and noise), but not integration (involving just signal), is less effective when the noise comes from the dominant eye rather than vice versa. This segregation can only take place after binocular combination for these dichoptic stimuli. These results suggest that the monocular input-weights at the site of binocular combination are different for integration compared with segregation.

Of particular interest is the finding that the effect of the so-called dominant eye, defined by sighting tests (Rosenbach, 1903) is shown to be selective for segregation. We found no eye-based differences for pure signal integration under either monocular (figure 2A, 2C) or dichoptic (figure 2B) conditions. When the task had a segregation component there was a clear eye-based difference, but only in the dichoptic condition (figure 2D), not in the monocular condition (figure 2E). It is unlikely that this can be explained by other than low-level processes since the eye through which the noise entered was randomly interleaved across trials. It is not that the monocular performance of one eye is superior to that of the other (figure 2E) but rather that, under dichoptic conditions, noise through one eye can be better segregated from signal through the other eye when that noise comes from the non-dominant eye. A similar mechanism to that proposed above for monocular segregation, but having inter-ocular inputs may also underlie the benefit of non-dominant eye noise on the integration of dominant eye signal, if one assumes that the input gain varies between eyes.

Acknowledgments

This research has been supported by a Canadian Institute for Health Research (CIHR) grant (MOP-53346) to Robert F. Hess. We thank Sarah Sebbag for her contribution to data collection.

Preface to chapter 6

So far we showed that the amblyopes can integrate orientation and motion information across space similar to normals. This is in contradiction to the results reported by Simmers and co-workers where they showed that amblyopes are deficient in combining form and motion information across space. In both studies, the amblyopic eyes were equated for any deficiencies at the early stages of the visual system.

One essential difference between the two paradigms used in two studies was that Simmers utilized coherence noise paradigm where random elements (i.e. noise) play a critical role in determining performance of an observer. So the best strategy for the visual system would be rejecting the noise elements and integrating the signals. However, in the tasks that I have discussed in preceding chapters, all elements contained useful information (i.e. only signal) and averaging over all elements would be an efficient strategy to integration information across space. In the last experimental chapter, I examine the effect of adding a noise population to the previously purely signal-integration task that I have used.

Chapter 6: Detrimental effect of noise in amblyopia

The global processing deficit in amblyopia involves noise segregation?

Behzad Mansouri and Robert F. Hess

McGill Vision Research, 687 Pine Ave W, H4-14, Montreal, H3A 1A1, Quebec, Canada

Some previous studies have reported deficits in amblyopia for global form and motion processing, whereas other studies have shown that global integration of form and motion information to be normal in amblyopia. We resolve this apparent conflict by showing that amblyopes only exhibit selective performance deficits on global tasks that contain noise as well as signal elements. This suggests that while signal integration is normal, noise segregation is not. We show this conclusion is valid, using both form and motion global tasks in which controlled amounts of pedestal noise are introduced. We model performance using an equivalent noise model, and show that as pedestal noise is added, the internal noise in the amblyopic visual system becomes abnormally elevated.

Introduction

Our understanding of the cortical processing deficit in humans with amblyopia is still at an early stage. Animal models suggest that some cells in area V1 are affected and the nature of this dysfunction may be sufficient to explain the well documented psychophysical contrast sensitivity deficit in amblyopia (i.e. contrast and spatial sensitivity of neurons with small receptive fields are abnormal in a proportional of cells) (Kiorpes et al., 1998; Kiorpes & McKee, 1999). However, this alone cannot encompass the array of psychophysical deficits that have been reported, amblyopia, and therefore the deficit is likely to involve extra-striate as well as striate function (Kiorpes et al., 1998). Single cell neurophysiological studies of extra-striate function in amblyopia have shown that fewer cells are driven by the deprived eye (Schroder et al., 2002; Sireteanu & Best, 1992). Furthermore, brain imaging in humans has demonstrated a reduced striate and extra-striate function that is uncorrelated with the psychophysical contrast sensitivity deficit (Barnes et al., 2001).

It has become clear that the contrast sensitivity loss in amblyopia does not adequately represent the visual loss. There are numerous examples of reduced performance by the amblyopic visual system on tasks comprising stimuli that are equi-detectable for the normal and amblyopic eye. These tasks include, position (Hess & Holliday, 1992), space (Demanins et al., 1999; Hess, Wang, Demanins, Wilkinson & Wilson, 1999a; Hong, Levi & McGraw, 2001), and motion (Hess et al., 1997a). This suggests a deficit involving more than detection, yet it does not necessitate an explanation involving more than V1. The tasks that amblyopes perform poorly, and argue for extra-striate involvement concern global processing, are believed to occur exclusively in extra-striate cortex. Strabismic and anisometropic amblyopes exhibit defective global motion (Simmers et al., 2003) and global form (Simmers et al., 2005) detection that cannot be ascribed to the visibility deficit thought to reside in V1. The nature of the global processing deficit suggests that areas of both the dorsal and ventral extra-striate pathways that are known to be involved in global motion and form processing respectively are affected. The processing of contrast-defined or 'second-order' information is particularly affected (Simmers et al., 2005; Simmers et al., 2003), and there is evidence to suggest extra-striate specialization for this function in the lateral occipital cortex and the anterior superior parietal lobe (Dumoulin et al., 2003). Complimentary evidence for a luminance defined or 'first-order' global motion (Ellemberg et al., 2002) and form (Lewis et al., 2002) processing deficit has been shown also for the rarer, deprivation form of amblyopia (although in this case the effects are greater for bilateral as compared with unilateral deprivation). The fact that global processing of both form and motion are compromised in all the different forms of amblyopia suggests it is a fundamental consequence of disrupting vision in early development.

The next step is concerned with understanding the nature of this global processing deficit in amblyopia. It has been generally concluded from the above studies that the global integration of local visual information, be it spatial or motion, is abnormal in amblyopia (Ellemberg et al., 2002; Lewis et al., 2002; Simmers et al., 2005; Simmers et al., 2003). We question this conclusion on the basis that our previous results have demonstrated normal global orientation integration for contours (Hess, McIlhagga & Field, 1997c), normal integration of local orientation in a mean orientation task

(Mansouri et al., 2004b), and normal integration for motion in a motion direction task (Mansouri et al., 2004a). In the first case, we measured contour integration performance in amblyopia and showed that once the positional uncertainty of amblyopic visual system had been taken into account, the integration of local oriented signals was normal. In the latter two cases, using an equivalent noise paradigm, we showed that the amblyopic visual system can judge the mean of an array of oriented signals and the mean of an array of motion directions with normal accuracy, quantified in terms of internal noise and number of sample. Taken together, this suggests that contrary to what is currently thought, spatial and motion signals can be indeed integrated with normal efficiency by the amblyopic visual system.

A fundamental difference between the integration task that we have used recently for orientation and motion, which shows normal performance in amblyopia (Hess, Mansouri, Dakin & Allen, in submission; Mansouri et al., 2004b) that of (Simmers et al., 2005), which shows abnormal performance in amblyopia *involves the use of visual noise*. In our task, all the local elements are samples of a distribution whose mean is to be judged, represent signal. Therefore, an ideal observer would integrate blindly each and every stimulus element. The situation in the standard global motion or global form tasks of the type used by Simmers and co-workers (Simmers et al., 2005; Simmers et al., 2003) is very different. In those tasks only some of the elements are signal, while the rest are noise. An ideal observer would certainly not integrate blindly all elements. An ideal observer would first segregate, based on its best estimate of what constituted signal as opposed to noise, and then integrate only the signal. Indeed we have recently shown (Mansouri et al., 2005), using a dichoptic paradigm, that the normal visual system does better than would be expected if it blindly integrated signal and noise in this paradigm, suggesting that it possesses a mechanism to enable it to reject (i.e. segregate) some of the noise prior to signal integration. We recently hypothesized that the problem amblyopes of all kinds have in performing global tasks might not be to do with signal integration, but may have to do with noise segregation (Hess et al., in submission). Here we provide a direct test of this explanation.

We investigate the role noise plays in both spatial and motion tasks that have previously provided evidence for anomalies of global processing in amblyopia (Ellemberg et al., 2002; Simmers et al., 2005; Simmers et al., 2003). We use an equivalent noise model to quantify the extent of the disruption that noise has on the amblyopic as compared with the normal visual system and provide support for the idea that the defect in the extra-striate cortex of amblyopes involves segregation more than integration.

Methods

Observers

Twelve naïve observers (six amblyopic and six normal) were tested. The visual acuity in amblyopic eyes ranged from 20/40 to 20/400 (for details see table 1). Refraction was examined in all observers and appropriately corrected prior to the testing period. Informed consents were obtained from all observers before data collections.

Apparatus

A Macintosh G3 computer was used to generate and present the stimuli and collect the data. For programming we used Matlab environment (MathWorks Ltd.) and Psychophysics ToolBox (Brainard, 1997). All stimuli were presented on a 20-inch Sony monitor (Trinitron 520GS). The monitor was calibrated and linearized using a Graseby S370 photometer and the Video Toolbox (Pelli, 1997) package. Pseudo 12-bit contrast accuracy was achieved by using a video attenuator (Pelli & Zhang, 1991), which combined the RBG outputs of the graphic card (ATI Rage 128) into the G gun. The refresh rate, mean luminance, and the resolution of the screen were 75 Hz, 33 cd/m^2, and 1152 x 870 pixels, respectively. The viewing distance was 57 cm from the screen in all experiments. Therefore one pixel on the screen was 0.32 mm, which subtended 2.12 Arc min at the viewing distance used. The observers performed the task monocularly with one eye patched at a time.

Table 1

Observers	Age	Type	Refraction		Acuity	Squint	History, stereo
ML	20 y	RE	+1.0-0.75	90°	20/80	ET 6°	Detected age 5y, patching for 2y
		mixed	-3.25 DS		20/25		
MA	22 y	LE	-0.25 DS		20/15	Ortho	Detected age 3y, patching for 4y, and glasses for 8y.
		aniso	+3.50 -0.50	0°	20/200		
LS	22 y	BE	-2.00 +0.50		20/20	Ortho	Detected age 6y, bilateral cataract surgery age 6y. Patching at 8y for 4m
		depriv	+0.50	90°	20/125		
ED	43 y	LE	+0.75		20/16	ET 5°	Detected age 6y, patching for 1y
		strab	+0.75		20/63		
RB	49 y	LE	+3.25 DS		20/15	XT 5°	Detected age 6y, glasses since 6y, no other therapy, near normal
		strab	+4.75 -0.75	45°	20/40		
XL	31 y	LE	-2.50		20/20	ET 15°	Detected age 13y, no treatment
		strab	-2.75+0.75	110°	20/400		

Table 1: Clinical details of the amblyopic observers participating in the experiment. The following abbreviations are used; strab for strabismic, aniso for anisometropic, depriv for deprived amblyopia, RE for right eye, LE for left eye, ET for esotropia, XT for exotropia, ortho for orthotropic alignment, DS for dioptre sphere.

Stimuli

We studied 'Motion' and 'Orientation' integration in two experiments using two separate but similar stimuli. In both experiments, the stimuli were arrays of spatially band-pass micro-patterns that were presented on a mid-luminance background. The stimuli were randomly distributed within a 6° wide circle, centred on the screen. The presentation time was 500 ms.

In exp. 1, 128 moving Laplacian-of-Gaussian ($\nabla^2 G$) blobs (see fig. 1a) were used which were defined as:

$$\nabla^2 G(x,y) = \frac{x^2 + y^2 - 2\sigma^2}{2\pi\sigma^6} \exp\left(-\frac{x^2 + y^2}{2\sigma^2}\right)$$

Where σ represents the space constant. The peak spatial frequency of the blobs was defined as:

$$f_{peak} = \frac{1}{\pi\sigma\sqrt{2}}$$

For this experiment σ was equal to 6.75 arc minute and the peak spatial frequency was 2 c/deg. Each blob was moving upward and to left or right of vertical for the whole presentation time. If one blob passed the border of the presentation window, it was regenerated at the opposite side simultaneously.

In exp. 2 we used arrays of 64 1-D Gabor micro-patterns (G) (Mansouri et al., 2004b), which were defined as:

$$G(x,y) = \exp\left(-\frac{(x-m)^2}{\sigma^2}\right) \cos\left(\frac{2\pi(x-m)}{T}\right)$$

Where σ is the standard deviation of the envelope, which was 0.4° for this experiment. The spatial frequency of the sinusoidal modulation within the Gabor was 0.52 cpd, *m* is the Gabor axis, and *T* is the phase.

Direction of each moving blob in exp. 1 and orientation of each Gabor in exp. 2 was selected from a parent Gaussian distribution with a mean equal to the cue (i.e. 90° ± the cue generated by APE (Watt & Andrews, 1981)) and a variable bandwidth. The direction and orientation distributions' standard deviation was varied from 0° (all elements moving to one direction or being aligned, see fig. 1a and 1d) to 50° and 30° (high variability, see fig. 1b and 1 e) in exp. 1 and exp. 2, respectively. Both experiments consisted of two conditions.

In condition (A) all stimuli were selected from the parent Gaussian distribution. Therefore in this case all elements were signals, which contained useful information. Thus, the best strategy for the visual system to employ to perform the task would be to integrate information across all elements (see fig. 1a-b and 1d-e).

In condition (B) the stimuli array comprised signal and pedestal noise elements (noise varied from 25% to 90%). The pedestal noise elements were moving in random directions (exp. 1, see fig. 1c) or were randomly oriented (exp. 2, see fig.1f). Random pedestal elements resembled the signal elements in all aspects but their direction (exp. 1) or orientation (exp. 2) distributions, which were uniform. In this condition, the best strategy for the visual system to adopt would be to integrate information from the <u>segregated</u> signal elements. Fig. 1a-c show static figures of the moving stimuli that were used in exp. 1 (to see an example of stimuli we used see http://ego.psych.mcgill.ca/labs/mvr/Behzad/Motion.html). Fig. 1d-f show the stimuli for exp. 2 (to see an example of stimuli we used see http://ego.psych.mcgill.ca/labs/mvr/Behzad/First-order.html). Fig 1a-b and 1d-e have no pedestal noise Fig. 1c and 1f show the stimuli with 50% pedestal noise.

Figure 1

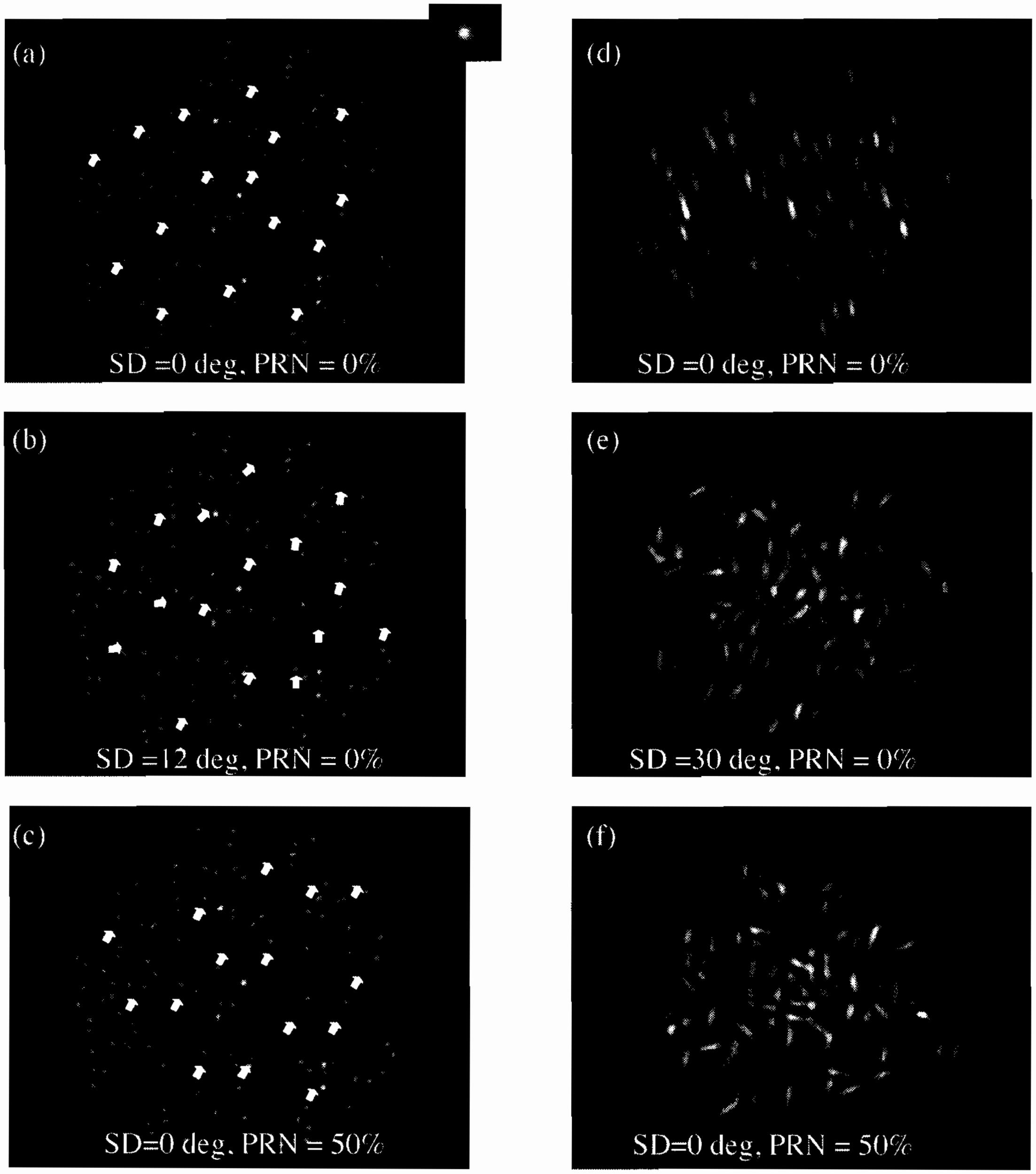
(a)
SD =0 deg, PRN = 0%
(d)
SD =0 deg, PRN = 0%
(b)
SD =12 deg, PRN = 0%
(e)
SD =30 deg, PRN = 0%
(c)
SD=0 deg, PRN = 50%
(f)
SD=0 deg, PRN = 50%

Figure 1: The stimuli for motion and orientation experiments are presented in (a-c) and (d-f), respectively. Arrays of 128 randomly positioned, moving blobs in motion experiment and 64 oriented Gabor elements in orientation experiment, were presented in a 6° circle at the centre of the screen. The motion direction and orientation of each signal element represents a sample from a Gaussian distribution of direction/orientation with average equal to the cue direction/orientation and a variable bandwidth. White and black arrows in a-c show schematically the directions of the signal and noise elements, respectively. Fig. 1a shows the stimuli in 0° standard deviation and no pedestal noise condition and average direction is tilted to the right of vertical. In (b), the orientation standard deviation is 12 degrees, there is no pedestal noise and average direction is tilted to the right of vertical. In (c), the direction standard deviation is 0° but the pedestal noise is 50% (i.e. 50% of the elements are randomly oriented) and average orientation is tilted to the left of vertical. Fig 1. Fig. (d) shows the stimuli in no variance and no pedestal noise condition in exp. 2. Average orientation is tilted to the left of vertical. In (e), the orientation standard deviation is 12°, there is no pedestal noise and average orientation is tilted to the left of vertical. In (f), the orientation standard deviation is 0° but the pedestal noise is 50% (i.e. 50% of the elements are randomly oriented) and the average orientation is tilted to the right of vertical.

Statistic analysis

We measured thresholds for orientation/direction discrimination and derived the parameters, internal noise and number of samples, from the equivalent noise model, for four groups, namely the fellow fixing eyes (FFE) and amblyopic eyes (AME) of amblyopic observers, and the dominant eyes (DE) and non-dominant eyes (NDE) of normal observers. There were two factors namely, the standard deviation of the signal population (SD) with 10 levels (0, 1, 2, 4, 8, 12, 20, 30, 40, and 50 in exp. 1 and 0, 1, 2, 4, 6, 8, 12, 16, 20, and 28 in exp. 2) and the pedestal random noise (PRN) having 6 levels in exp. 1 (0%, 30%, 50%, 70% 80%, and 90%) and 4 levels in exp. 2 (0%, 25%, 50%, and 75%). We used t-test to analyze the data. Each group at any condition was separately compared with the other groups. We used paired t-test (repeated measure t-test) when we compared amblyopic with fellow fixing eyes in amblyopic observers and dominant with non-dominant eyes in normals. We also calculated 95% confidence intervals for the thresholds from each individual psychometric function using a bootstrapping technique and used it to compare individual sets of data within the groups.

Procedure

Equating performance at the single element level

In order to equate the performance levels for this task at the individual element level for fellow fixing and amblyopic eyes, we measured the motion direction (in exp. 1) and orientation (in exp. 2) discrimination threshold for a single element, of the exact type used in the later integration experiment, as a function of the contrast of the stimulus. This single stimulus element was presented in a random position within the 6° presentation area, the same area as for the following integration experiments. The direction of a single blob (in exp. 1) and the orientation of a single Gabor (in exp. 2) with respect to the notional vertical was measured. The magnitude of the tilt was determined by the APE procedure. A single temporal interval, two-alternative forced choice (2-AFC) paradigm was used. Observers had to judge whether the element's motion direction or orientation was clockwise or counter-clockwise (tilted to right or left of vertical). We used a method of constant stimuli in exp. 1, and an adaptive method of constant stimuli in exp. 2. The observers' direction and orientation threshold was estimated from the slope of the best fitting cumulative Gaussian psychometric function derived from between 256-512 presentations. 95% confidence intervals were estimated from 1000 bootstrap replications of the fit (Wichmann & Hill, 2001a; Wichmann & Hill, 2001b)

In amblyopic observers, the single element was presented to the amblyopic eye with a fixed, high contrast (50% in exp. 1 and 75% in exp. 2) and to the fellow fixing eye with a range of contrasts. The threshold for the fellow fixing eye increased with decreasing contrast. Therefore the contrast with which the fellow fixing eye gave an equal threshold for direction or orientation discrimination to that of the amblyopic eye with the fixed high contrast stimulus, was selected. In the subsequent integration experiment, the stimuli were presented with contrasts for the fellow fixing and amblyopic eyes that gave comparable thresholds for the single element task.

For our group of normal controls we used stimuli of 25% contrast in the integration experiments. This contrast represents the average contrast level used for the fellow fixing eyes of amblyopes.

Motion integration (exp. 1)

Arrays of 128 randomly positioned, moving blobs were presented. The direction of an individual blob was chosen from a Gaussian distribution with a variable bandwidth and a mean equal to the cue (i.e. 90°±the cue generated by APE). A single temporal interval, two-alternative forced choice (2-AFC) paradigm was used. The observers' task was to judge whether the mean direction of the array of blobs was to right or left of vertical (see fig. 1a-b). Direction discrimination thresholds were obtained from between 256-512 presentations for each standard deviation (10 levels typically between 0°-50°) of the parent distribution. The motion direction threshold for each level of variability of the parent distribution was estimated from the slope of the best fitting cumulative Gaussian function using a maximum likelihood procedure. An equivalent noise model (Mansouri et al., 2004b) was fitted to the thresholds separately for each eye of each observer in each condition.

Orientation integration (exp. 2)

In the orientation integration experiment (exp. 2), a similar procedure was followed to that for motion integration (exp. 1). Arrays of 64 randomly positioned, oriented Gabors were presented. The orientation of an individual Gabor was chosen from a Gaussian distribution with a variable bandwidth and a mean equal to the cue (i.e. 90°±the cue generated by APE). A single temporal interval, two-alternative forced choice (2-AFC) paradigm was used. The observers' task was to judge whether the mean orientation of the array of Gabors was rotated clockwise or counter-clockwise (tilted to right or left of vertical) (see fig. 1d-e). Orientation discrimination thresholds were obtained from between 192-340 presentations for each of a number of standard deviations (10 levels typically between 0°-30°) of the parent distribution. The orientation threshold for each level of variability of the parent distribution was estimated from the slope of the best fitting cumulative Gaussian function using a maximum likelihood procedure. An equivalent noise model (Mansouri et al., 2004b) was fitted to the thresholds separately for each eye of each observer in each condition.

Pedestal random noise (exp. 1 and 2)

In additional sets of experiments for both the motion and orientation integration tasks, some of the elements contained a pedestal random noise (25%-90%). The direction or orientation of the pedestal random elements was chosen from a uniform distribution (0°-360° in exp. 1, see fig. 1c; and 0°-180° in exp. 2, see fig. 1f). Different percentages of the elements were random in different conditions (30%-90% in motion and 25%-75% in orientation experiment). There were two sources of noise, one resulting from the standard deviation of the parent distribution from which the individual motion or orientation samples were derived and another from the uniform distribution of the pedestal noise. Increasing either the standard deviation of the signal population (i.e. external noise) or the pedestal random noise (i.e. coherence noise) could independently increase the threshold of the observer. To study the interactive effect of these two separate noise sources on performance, we assessed motion and orientation integration (see fig. 3 and fig. 6).

Results

Motion integration

Fig. 2 shows sample data sets of thresholds in one amblyopic observer (ED) in four different pedestal noise conditions for motion direction integration. The X-axis is the standard deviation of the signal population which was varied from 0° to 50° (0, 1, 2, 4, 8, 12, 20, 30, 40, and 50). The Y-axis is the motion direction threshold offset (degrees). The data is fit by an equivalent noise model (Mansouri et al., 2004b). The parameters of internal noise (i.n.) and number of samples (n.s.) are shown in the inset. Increasing the standard deviation of the signal population beyond about 6° leads the thresholds to rise.

In fig. 2a, no pedestal noise condition, the circles and dashed lines represent the data for the fellow fixing eye (FFE) and the square and solid line represent the amblyopic eye (AME). The AME and FFE show similar thresholds (95% CI, $p>0.05$). Furthermore, comparing AME with FFE, the parameters of internal noise (1.8 versus 1.6) and number of samples (9.0 versus 7.8) are not statistically different. In Fig. 2a-d, the pedestal noise is increasing from 0% to 80%. As the pedestal noise gradually increases, the thresholds in the AME rise faster than those of the FFE. In 80% pedestal noise condition, the thresholds of the two eyes are significantly different (95% CI, $p<0.05$) at low parent standard deviations (up to the 10°). This difference is reflected in the internal noise parameter, which is higher in the amblyopic eye, by the factor of 3 (17.6 versus 6.2, 95% CI, $p<0.05$). The numbers of samples are comparable in AME and EEF across all conditions.

Figure 2

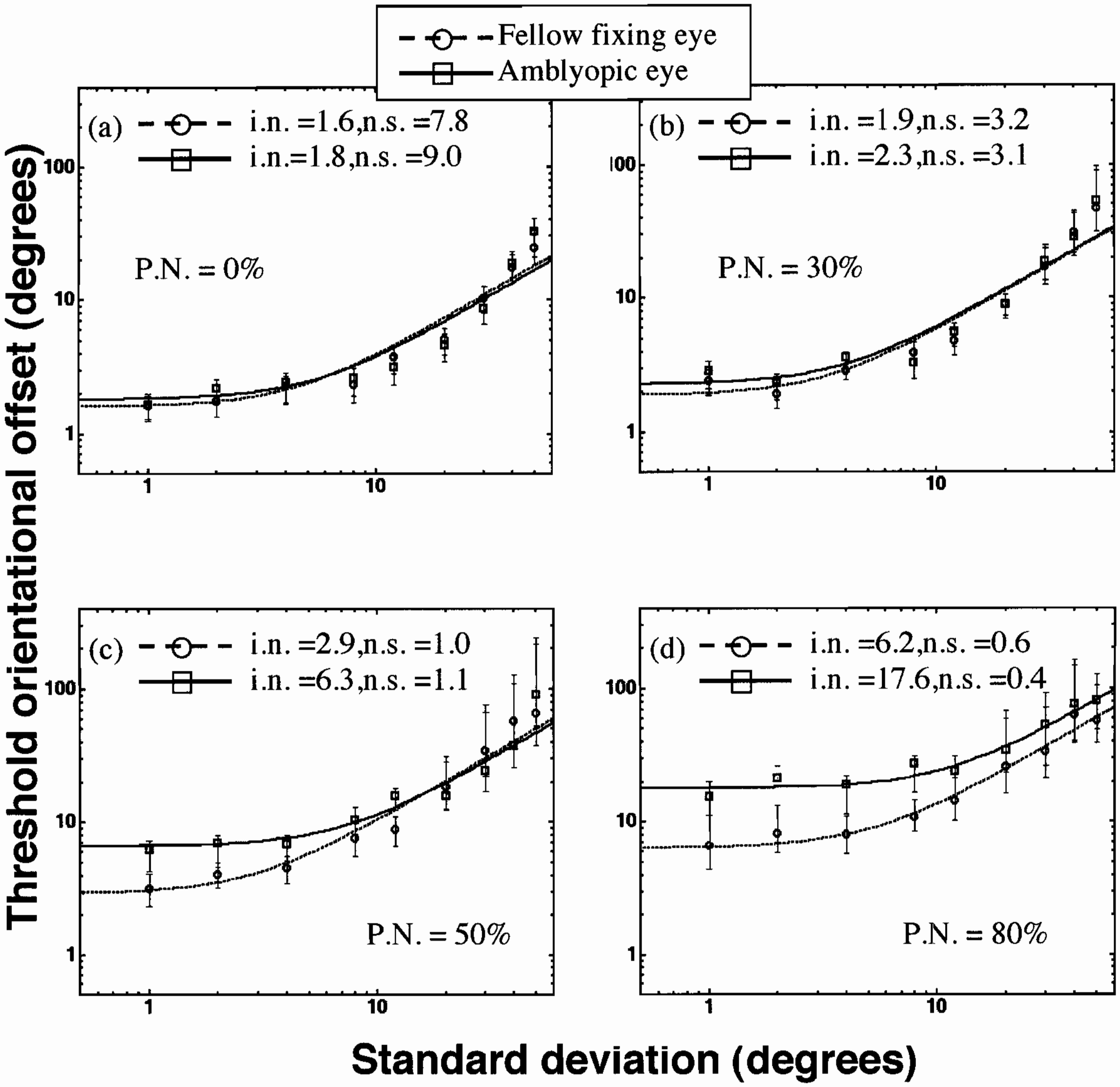

Fellow fixing eye
Amblyopic eye
(a) i.n. =1.6,n.s. =7.8
i.n.=1.8,n.s. =9.0
P.N. = 0%
(b) i.n. =1.9,n.s. =3.2
i.n. =2.3,n.s. =3.1
P.N. = 30%
(c) i.n. =2.9,n.s. =1.0
i.n. =6.3,n.s. =1.1
P.N. = 50%
(d) i.n. =6.2,n.s. =0.6
i.n. =17.6,n.s. =0.4
P.N. = 80%
Threshold orientational offset (degrees)
Standard deviation (degrees)
1
10
100

Figure 2: The motion direction integration threshold is measured as a function of standard deviation of the parent distribution. Sample data is shown for one representative strabismic amblyope (ED). Circles and dotted lines show the fellow fixing eye (FFE) thresholds. Squares and solid line represent amblyopic eye (AME) thresholds. In (a), there is no pedestal noise. The AME perform the task similar to FFE and the internal noise and numbers of samples parameters are not different. Fig 1b, 1c and 1d show the conditions where the pedestal noise increases to 30%, 50% and 80%, respectively. As the pedestal noise increase, the difference between the performances of the FFE and the AME, as reflected by the internal noise parameter, dramatically increases. However, the number of sample parameter stays similar in two eyes as pedestal noise increases.

Similar results to those of this subject were collected for all amblyopic observers. The normal observers' eyes (DE and NDE) showed similar performances to the FFE of the amblyopic observers.

In Fig. 3, the average direction thresholds are shown for the dominant eye (DE) of the 6 normal observers (a) and the amblyopic eye (AME) of the 6 amblyopic observers (b). The statistical differences of the two groups are shown in fig. 3c. The X-axis represents the standard deviations of the signal population (degrees). The Y-axis represents the percent pedestal random noise. The Z-axis in 3a and 3b represent the threshold direction offset (degrees).

At low pedestal noise conditions (e.g. 0%-30%) the threshold in both eye are similar except at high standard deviations of the parent population (e.g. 50°) where the threshold in the AME is higher than that in DE, although it is not significant ($p>0.01$, see Fig. 3c). The thresholds in DEs begin to rise along the pedestal noise axis (knee point) after 50% pedestal noise. However, the thresholds in the AME start to rise at lower pedestal noise values (30%). Furthermore, this difference in thresholds of the DEs and AMEs increases as the pedestal noise increases. The differences are statically significant in a combination of high pedestal noise (more than 50%) and high standard deviation (more than 30°) conditions. However, in very high pedestal noise conditions (e.g. 80% to 90%) the differences are significant even for parent standard deviations as low as 8° and are highly significant for parent standard deviations exceeding 12°. At very high pedestal noise and standard deviation conditions the statistical tests failed to show any significant differences.

Figure 3

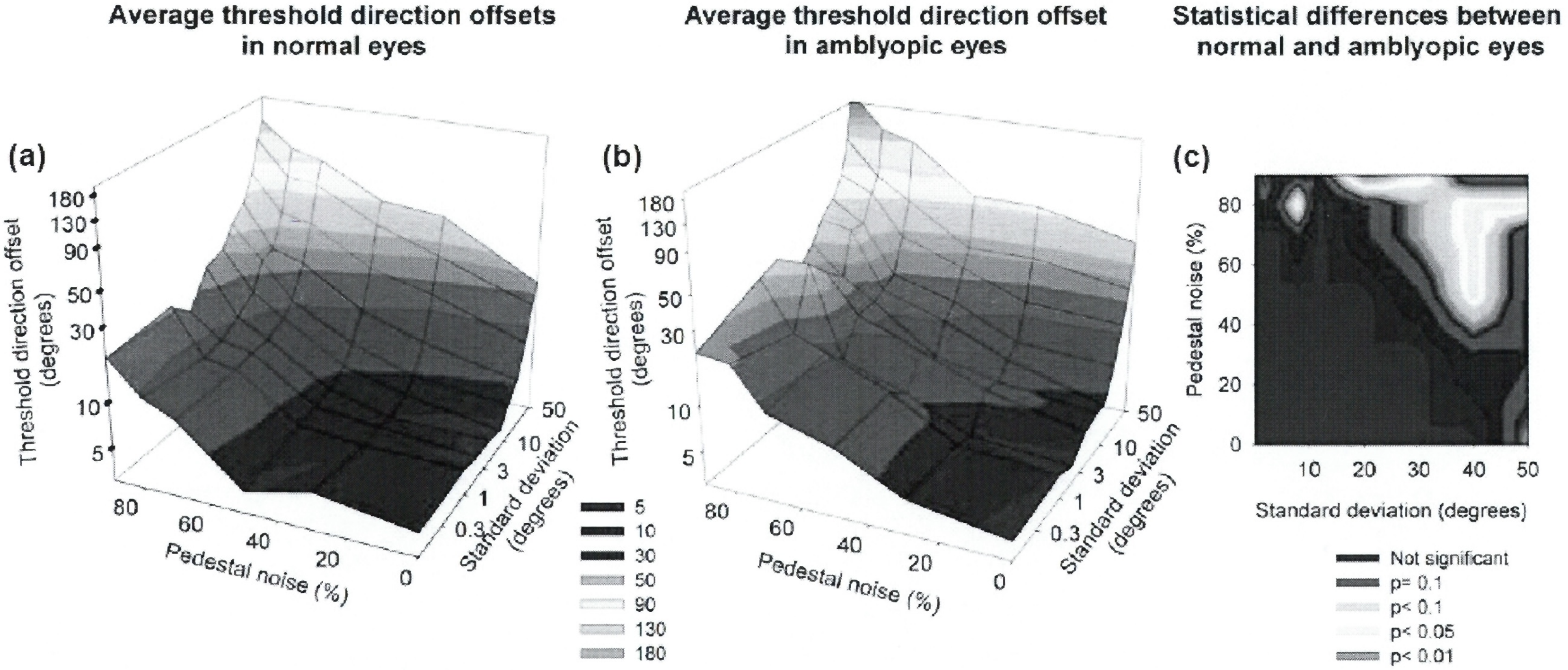
Average threshold direction offsets in normal eyes
Average threshold direction offset in amblyopic eyes
Statistical differences between normal and amblyopic eyes
(a)
(b)
(c)
Threshold direction offset (degrees)
180
130
90
50
30
10
5
80
60
40
20
0
Pedestal noise (%)
50
10
3
1
0.3
Standard deviation (degrees)
5
10
30
50
90
130
180
Pedestal noise (%)
Standard deviation (degrees)
Not significant
p= 0.1
p< 0.1
p< 0.05
p< 0.01

Figure 3: The mesh average threshold data from amblyopic eyes of amblyopic subjects and dominant eyes of normal subjects (a and b, respectively) and their statistical differences (c) are presented in this figure. In (a) and (b) the motion direction integration threshold offset (Z-axis) is plotted as a function of standard deviation of the signal population (X–axis) and pedestal random noise (Y-axis) in amblyopic and dominant eyes respectively.

In Fig. 4 the average values for the parameters of internal noise (a) and number of samples (b) are compared for DEs of 6 normal (open bars) and AMEs of 6 amblyopic (closed bars) observers.

In fig. 4a, the X-axis represents the pedestal noise with 6 levels and the Y-axis represents the equivalent internal noise. The internal noise is comparable and not statistically different in DEs and AMEs at low pedestal noise conditions (e.g. pedestal noise less than 50%). As the pedestal noise increases the differences between the internal noise in DE and AME increases. In 80% to 90% pedestal noise conditions the differences are statistically significant ($p<0.05$). The internal noise was statistically the same in DE, NDE, and FFE at all different pedestal nose levels.

In Fig. 4b, the X-axis represents the pedestal noise with 6 levels and the Y-axis represents the number of samples parameter. The number of samples parameter is only statistically different in DEs and AMEs in 30% pedestal noise condition ($p<0.05$). Otherwise the number of samples parameter was comparable in DEs and AMEs ($p>0.05$). The number of samples parameter was not statistically different in DE, NDE, and FFE.

Figure 4

(a)

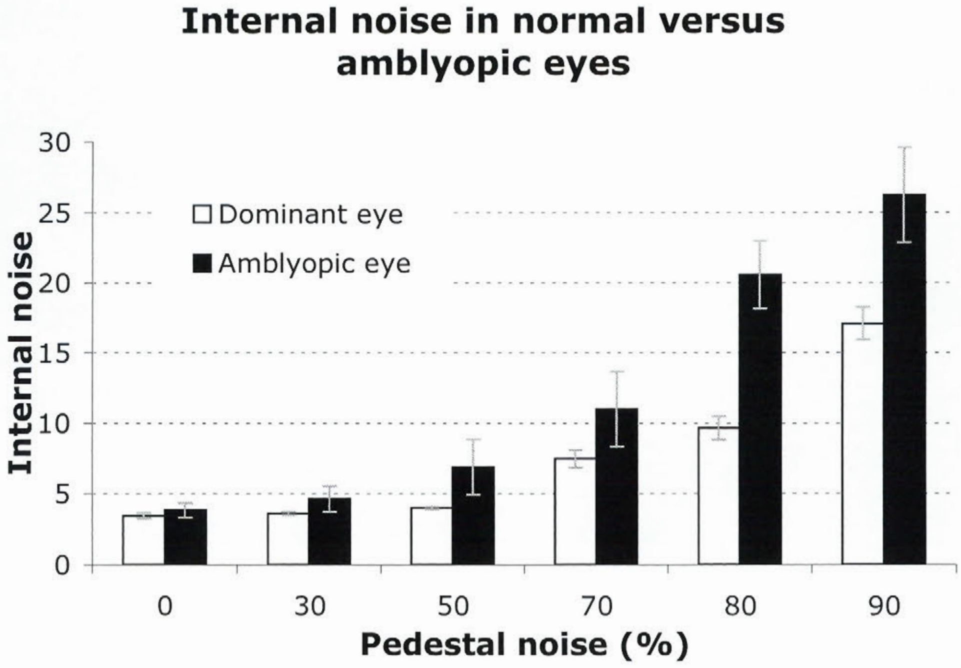
Internal noise in normal versus amblyopic eyes
☐ Dominant eye
■ Amblyopic eye
Internal noise
30
25
20
15
10
5
0
0
30
50
70
80
90
Pedestal noise (%)

(b)

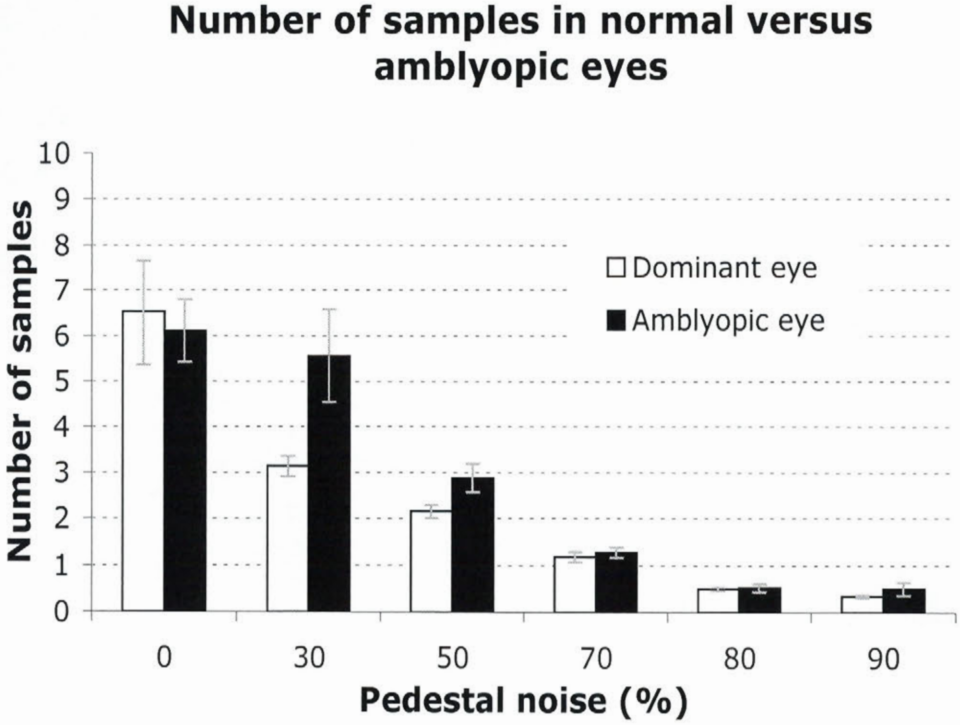
Number of samples in normal versus amblyopic eyes
☐ Dominant eye
■ Amblyopic eye
Number of samples
10
9
8
7
6
5
4
3
2
1
0
0
30
50
70
80
90
Pedestal noise (%)

Figure 4: The averages of the two independent parameters of internal noise (a) and number of samples (b) are plotted for different pedestal random noise (from 0 to 90%) conditions and for amblyopic eyes of amblyopic subjects (closed bars) and dominant eyes of normal subjects (open bars). The error bars represent ±0.5 SD. In 0% pedestal noise condition, the internal noise is similar in two eyes, showing normal integrative function. The internal noise rises faster in amblyopic eyes compared to the normal eyes, when the pedestal noise increases. The internal noise is significantly higher in amblyopic eyes when pedestal noise is beyond 70%. The numbers of samples are also similar in both conditions when there is no pedestal noise. The number of samples decreases faster in the normal eyes comparing to the amblyopic eyes, however, at high pedestal noises (> 50%), the number of samples is similar in amblyopic and normal eyes.

Orientation integration

Fig. 5 shows sample data sets of thresholds in one amblyopic observer for four different pedestal noise conditions for orientation integration. The X-axis is the standard deviation of the signal population which was varied from 0° to 28° (0, 1, 2, 4, 6, 8, 12, 16, 20, and 28). The Y-axis is the orientation threshold offset (degrees). The data is fit to the equivalent noise model (Mansouri et al., 2004b). The parameters of internal noise (i.n.) and number of samples (n.s.) are shown in the inset.

In fig. 5, the circles and dashed lines represent the data for fellow fixing eye (FFE) and the square and solid line represent the amblyopic eye (AME). Fig. 5a, the no pedestal noise condition, shows that the AME and FFE have similar thresholds (95% CI, $p>0.05$). Furthermore, in AME versus FFE the parameters of internal noise (1.9 versus 2.3) and number of samples (8.9 versus 8.9) are not statistically different. In Fig. 5a-d, the pedestal noise is increasing from 0% to 75%. As the pedestal noise gradually increases, the thresholds in the AME rises faster than those of the FFE. In 75% pedestal noise condition, the internal noise is significantly higher in the amblyopic eye (38 versus 26.4, 95% CI, $p<0.05$). Also, there was a trend of higher thresholds in high pedestal noise condition across all amblyopic observers. The numbers of samples are comparable in AME and EEF across all conditions.

Figure 5

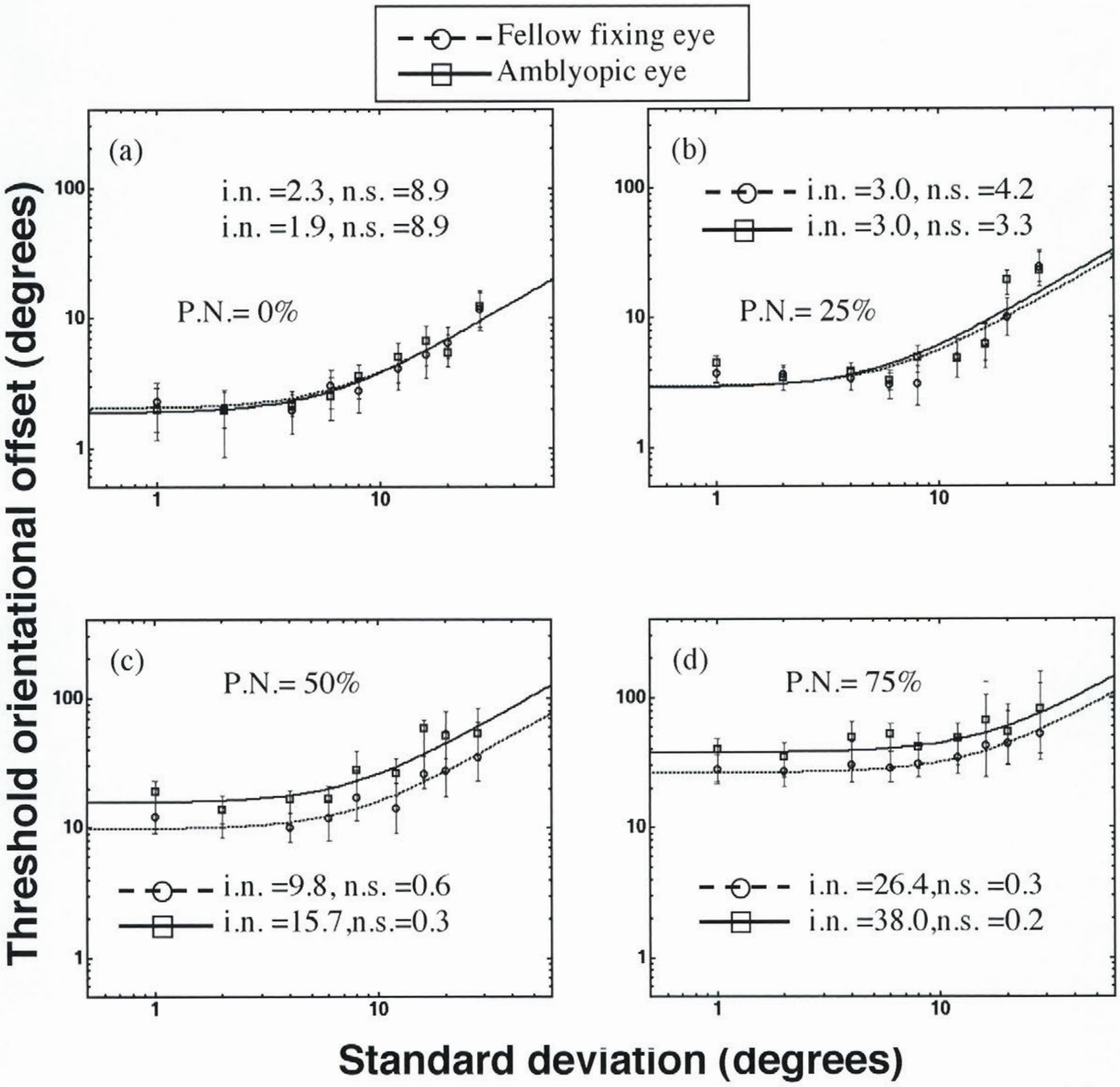

Figure 5: The orientation integration threshold is measured as a function of orientation distribution standard deviation. Sample data is shown for one representative strabismic amblyope (ED). Circles and dotted lines show the fellow fixing eye (FFE) thresholds. Squares and solid line represent amblyopic eye (AME) thresholds. In (a), there is no pedestal noise. The AME performs the task similar to FFE and the internal

noise and numbers of samples parameters are not significantly different. Figure 4b, 4c and 4d show the conditions where the pedestal noise increases to 25%, 50% and 75%, respectively. As the pedestal noise increases, the difference between the performances of the FFE and the AME and the internal noise parameter dramatically increases. However, the number of sample parameter stays similar in two eyes as pedestal noise increases.

Similar results to those of this subject have been collected from all amblyopic observers. The normal observers' eyes (DE and NDE) show similar performances to the FFE of the amblyopic observers.

In Fig. 6, the average orientation thresholds are shown for the DEs of the 6 normal observers (a) and AMEs of the 6 amblyopic observers (b). The statistical differences of the two groups are shown in fig. 3c. The X-axis represents the standard deviations of the signal population (degrees). The Y-axis represents the percent pedestal random noise. The Z-axis in 3a and 3b represent the threshold direction offset (degrees).

At low pedestal noise (e.g. 0%) the threshold in both eyes are similar. The thresholds in DE begin to rise along the pedestal noise axis (knee point) after 25% pedestal noise. However, the thresholds in the AME begin to rise at lower pedestal noise (0%). The differences in thresholds of the DEs and AMEs increases as the pedestal noise increases. The differences are statically significant at high levels of pedestal noise (more than 25%) and standard deviation (more than 20°). At very high pedestal noise (e.g. 75%) the differences are significant even for parent standard deviations of 2° and highly significant when the parent standard exceeds 20°.

Figure 6

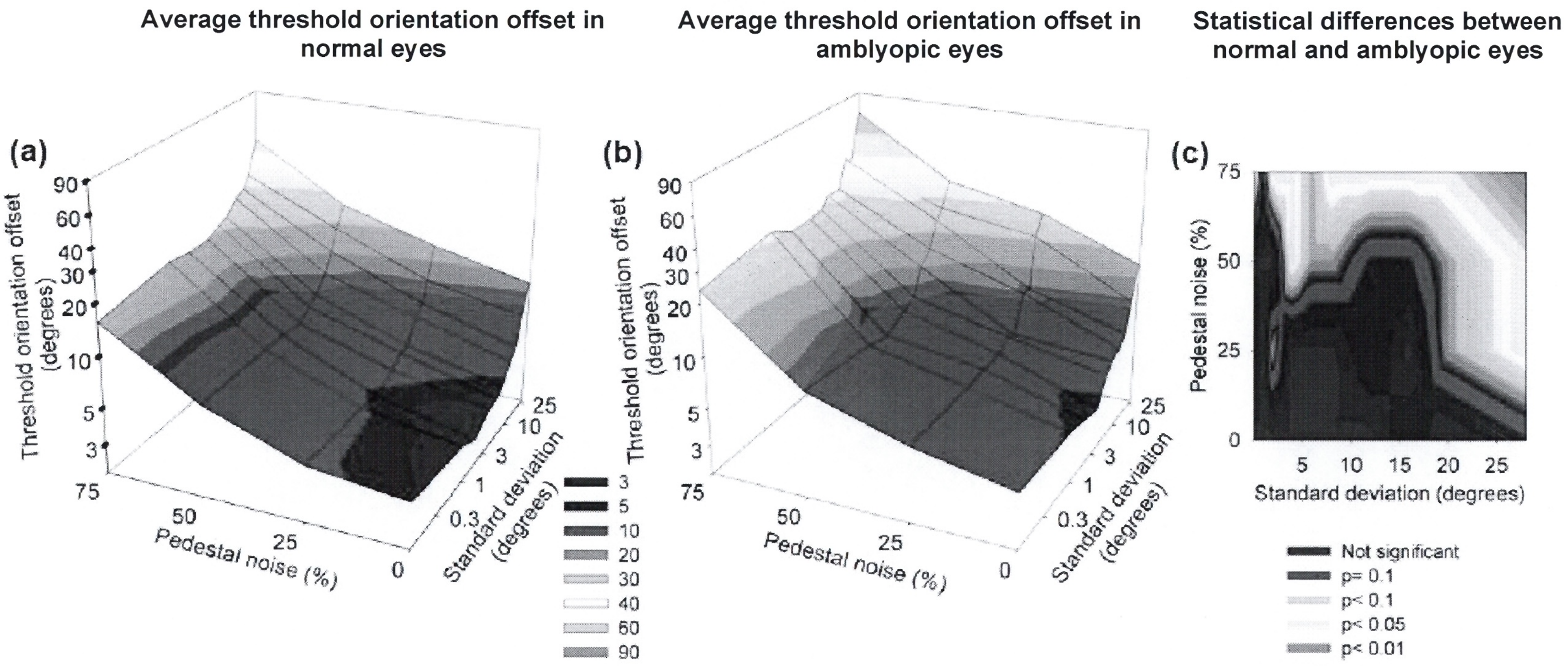

Average threshold orientation offset in normal eyes

Average threshold orientation offset in amblyopic eyes

Statistical differences between normal and amblyopic eyes

Figure 6: The mesh average threshold data from amblyopic eyes of amblyopic subjects and dominant eyes of normal subjects (a and b, respectively) and their statistical differences (c) are presented in this figure. In (a) and (b) the orientation integration threshold offset (Z-axis) is plotted as function of variance of the signal population (X–axis) and pedestal random noise (Y-axis) in amblyopic and dominant eyes respectively.

In fig. 7 the average values for the parameters of internal noise (a) and number of samples (b) are compared for DEs of 6 normal (open bars) and AMEs of 6 amblyopic (closed bars) observers.

In fig. 7a, the X-axis represents the pedestal noise with 4 levels and the Y-axis represents the equivalent internal noise. The internal noise is statistically comparable in DEs and AMEs in low pedestal noise conditions (e.g. 0%). As the pedestal noise increases the differences between the internal noise in DE and AME increases. At high levels of pedestal noise these differences are statistically significant ($p<0.05$). The internal noise was statistically the same in DEs, NDEs, and FFEs across all the conditions.

In fig. 7b, the X-axis represents the pedestal noise with 4 levels and the Y-axis represents the number of samples parameter. The number of samples parameter was comparable in DEs and AMEs ($p>0.05$). The number of samples parameter was not statistically different in DEs, NDEs, and FFEs.

Figure 7

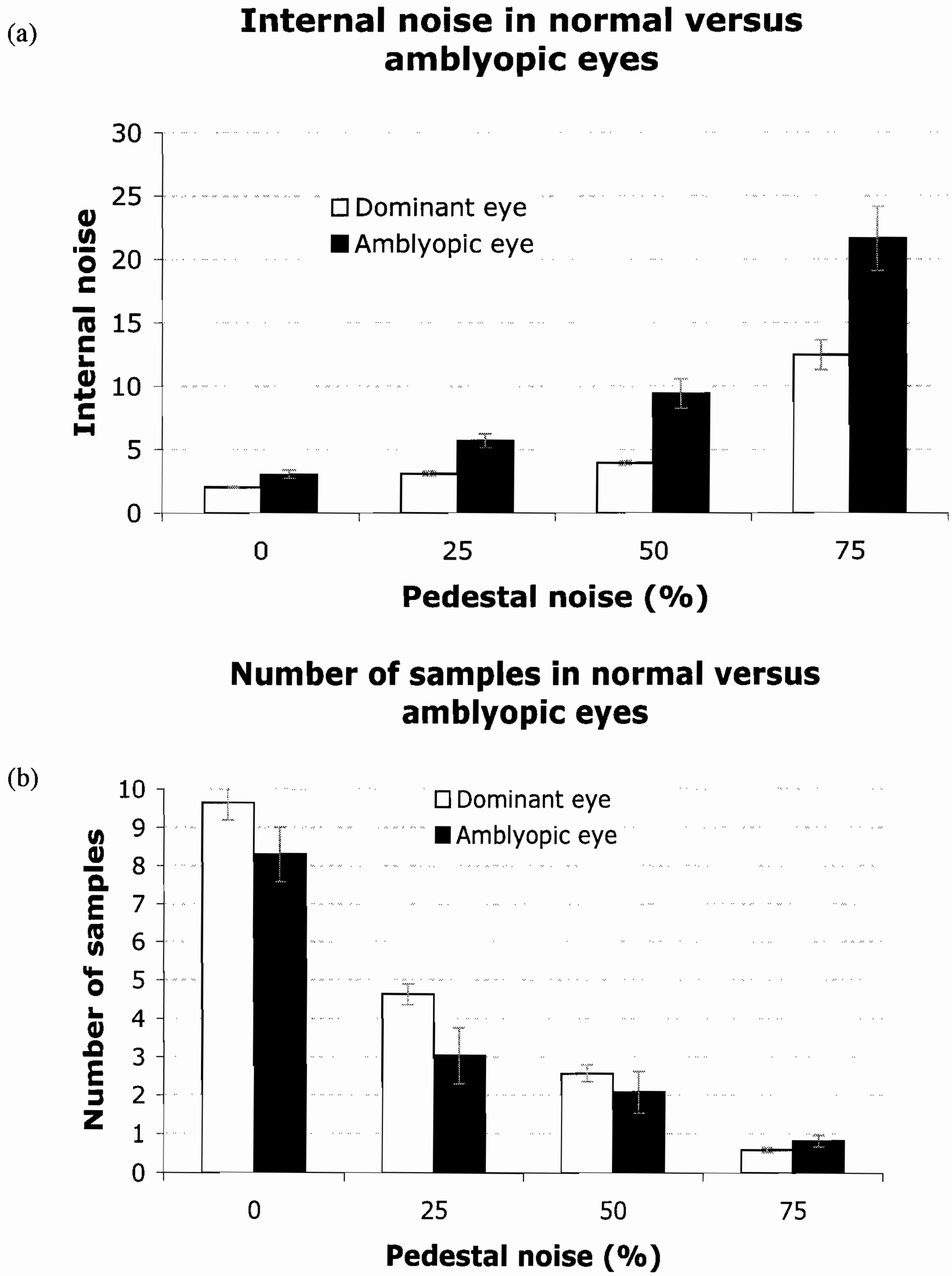
(a)
Internal noise in normal versus amblyopic eyes
Internal noise
30
25
20
15
10
5
0
☐ Dominant eye
■ Amblyopic eye
0
25
50
75
Pedestal noise (%)
Number of samples in normal versus amblyopic eyes
(b)
Number of samples
10
9
8
7
6
5
4
3
2
1
0
☐ Dominant eye
■ Amblyopic eye
0
25
50
75
Pedestal noise (%)

Figure 7: The averages of the two independent parameters of internal noise (a) and number of samples (b) are plotted for different pedestal random noise (from 0 to 75%) conditions and for amblyopic eyes of amblyopic subjects (closed bars) and dominant eyes of normal subjects (open bars). The error bars represent ±0.5 SD. In 0% pedestal noise condition, the internal noise is similar in two eyes. The internal noise rises faster in amblyopic eyes compared to the normal eyes, when the pedestal noise increases. The internal noise is significantly higher in amblyopic eyes when pedestal noise exceeds 50%. The numbers of samples are comparable in AME and DE across all conditions.

Integration of signal and noise with different contrasts

In fig. 8 the threshold orientation offsets are presented for DE of the 2 normal (a and b) and AME of 2 amblyopic (RB c and e; ML d and f) observers. The X-axis is the standard deviation of the signal population which was varied from 0° to 28° (0, 1, 2, 4, 6, 8, 12, 16, 20, and 28). The Y-axis is the orientation threshold offset (degrees). The data is fit to the equivalent noise model (Mansouri et al., 2004b). The parameters of internal noise (i.n.) and number of samples (n.s.) are shown in the inset.

In each graph, three conditions of similar and different contrasts for signal and noise elements are shown. Squares and solid lines represent the case where the element array contained only 16 signal elements. Thresholds, internal noise, and number of samples are comparable in DEs and AMEs. Circles and dashed lines represent conditions when 16 signal elements are accompanied by 48 noise elements (i.e. 75% pedestal noise) with the same contrasts. Although the addition of pedestal noise elements increases the thresholds in all observers, the increase in AMEs is dramatically higher than that in DEs (factor of 3). The star, dotted and dashed lines represent the conditions when noise elements are presented with less contrast than the signal elements. In fig. 8a-d, they represent the condition when the contrast of the noise elements is a factor of 2 lower than that of the signal elements (12.5% versus 25% in DEs and 37.5% versus 75% in AMEs). However, in fig. 8e-f, they represent the conditions only for AME and when the contrast of the noise elements is almost a factor of three (2.93) lower than that of the signal elements (37.5% versus 100% (maximum contrast)). Fig. 8a-b show that a factor of 2 reduction in the contrasts of the noise elements is enough for the normal eyes to perform as if the pedestal noise elements were not present. In other words, when the contrast of the signal and noise is sufficiently different, normal visual system can segregate noise from signal. Fig. 8c-d show that a factor of 2 reduction in the contrast is not enough for the amblyopic eye to segregate signal from noise and the performance of the amblyopic eye is comparable to that when the contrast of the signal and noise elements were the same (i.e. circle and dashed lines).

Figure 8:

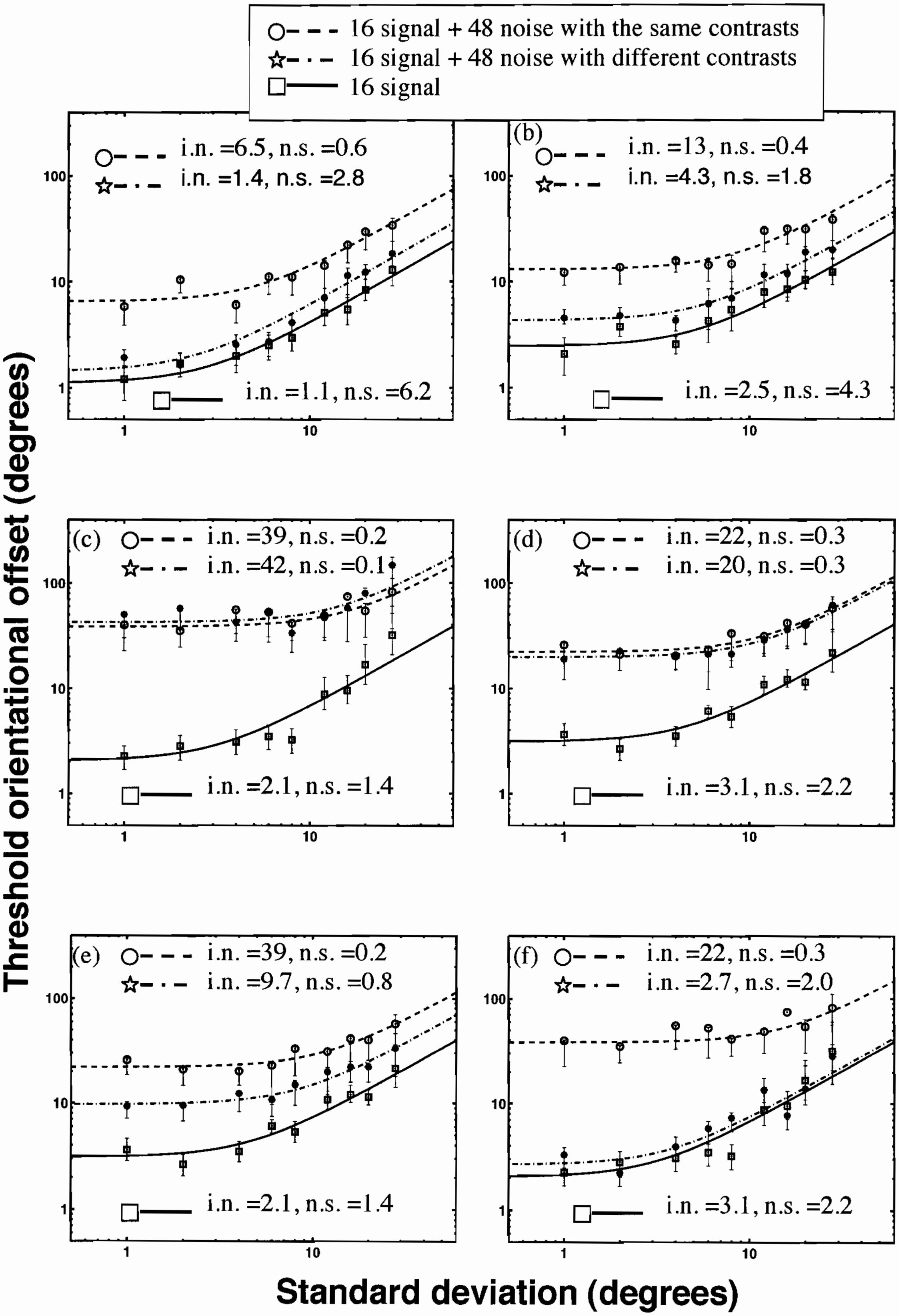
○- - - 16 signal + 48 noise with the same contrasts
☆- · - 16 signal + 48 noise with different contrasts
□—— 16 signal
○- - - i.n. =6.5, n.s. =0.6
☆- · - i.n. =1.4, n.s. =2.8
□—— i.n. =1.1, n.s. =6.2
(b)
○- - - i.n. =13, n.s. =0.4
☆- · - i.n. =4.3, n.s. =1.8
□—— i.n. =2.5, n.s. =4.3
(c)
○- - - i.n. =39, n.s. =0.2
☆- · - i.n. =42, n.s. =0.1
□—— i.n. =2.1, n.s. =1.4
(d)
○- - - i.n. =22, n.s. =0.3
☆- · - i.n. =20, n.s. =0.3
□—— i.n. =3.1, n.s. =2.2
(e)
○- - - i.n. =39, n.s. =0.2
☆- · - i.n. =9.7, n.s. =0.8
□—— i.n. =2.1, n.s. =1.4
(f)
○- - - i.n. =22, n.s. =0.3
☆- · - i.n. =2.7, n.s. =2.0
□—— i.n. =3.1, n.s. =2.2
100
10
1
1
10
Threshold orientational offset (degrees)
Standard deviation (degrees)

Figure 8: Three conditions for orientation experiment where the signal elements were presented with or without pedestal random noise are shown. When the pedestal noise accompanied the signal elements, which could be either with the same or different contrasts. The figure shows the orientation threshold offset (degrees) as a function of the orientation standard deviation of the signal elements in two normal (fig. 8a-b) and two amblyopic (fig. 8c-f) observers. Squares and solid lines are representing the conditions where only 16 signal elements are presented to the observers. The thresholds are comparable in amblyopic and normal eyes. Circles and dashed lines represent the conditions where the contrasts of the 16 signal and 48 random noise elements are the same. Although introducing 75% random pedestal noise elements increased the thresholds in both amblyopic and normal eyes significantly, it was increased 2-4 times more in the amblyopic eyes. The stars and dot-dash lines represent the conditions were the contrasts of the signal and noise elements are different. In 8a-d and 8e-f the contrasts of the signal are two and three times the contrast of the noise elements, respectively. Two times higher contrast was enough for the normal observers to segregate the noise elements and factor out their detrimental effect as the threshold reaches to the condition where there is no noise element (8a-b). However, two times difference in contrast was not enough for the amblyopic observers to segregate the noise and the threshold was still similar to when the noise and signal have similar contrasts (8c-d). Increasing the differences in contrasts to three times helped the amblyopic eyes improve the performance (fig. 8e-f) although, in one amblyopic observer, performance never reached the no-noise condition (fig. 8e).

Discussion

Motion and orientation integration

Previous work has shown that amblyopes exhibit anomalous performance on both global form (Lewis et al., 2002; Simmers et al., 2005) and global motion (Ellemberg et al., 2002; Simmers et al., 2003) tasks. Since it was shown that in each case the loss of performance could not be explained by the low-level visibility deficit thought to reside in V1 (Ellemberg et al., 2002; Simmers et al., 2005; Simmers et al., 2003), it was natural to conclude that global integration was selectively defective in amblyopia. However, subsequent work showed that global integration in form tasks (Mansouri et al., 2004b) and in motion tasks (Mansouri et al., 2004a) was normal in amblyopia, and so another explanation is needed. The present experiments provide such an explanation in terms of deficient segregation of signal from noise in global tasks involving both form and motion.

The typical global form or motion task involves signal and noise and an ideal observer would first segregate the signal from noise before integrating the signal. Amblyopes are unable to perform such a task. In the global form and motion integration tasks we used here, an ideal observer would integrate all information because all elements contain relevant information about the variation and mean of the parent distribution from which the signal represents samples. Amblyopes are normal at this. By introducing pedestal noise into the integration task we were able to show that amblyopes went from normal performance at low pedestal noise (i.e. pure integration) to abnormal performance at high pedestal noise (i.e. segregation and integration). This latter condition is representative of the typical global motion/form task for which previous reports suggests amblyopes are abnormal. Since there is evidence that the normal visual system does better in such tasks than predicted on blind integration of all information (i.e. signal and noise), it must possess mechanisms with which signal can be to some extent segregated from the coextensive noise. Such mechanisms appear to be defective in amblyopia.

For historical reasons we know more about dorsal extra-striate function than we do about its ventral counterpart. Global motion processing appears to involve a number of regions including areas MT (V5) and MST (Mikami et al., 1986a; Mikami et al., 1986b). Neurons in MT and MST have much larger receptive fields, possibly containing many small subunits that represent V1 inputs (Movshon et al., 1985) with extensive centre-surround interactions (Allman et al., 1985). Cells in MT fall into two categories depending on whether they have facilitative or suppressive surrounds (Born & Tootell, 1992). Interestingly, cells in the former category are hypothesized to be involved in integrative functions, whereas cells in the latter category in segregative functions. We suggest the latter cells are selectively affected in amblyopia. Lesions to this region in monkey (Huxlin & Pasternak, 2004; Newsome & Pare, 1988; Rudolph & Pasternak, 1999) and humans (Baker et al., 1991) result in deficits that are selective for global motion. Although no attempt has been made to disentangle the integration versus the segregation components of this loss, there is strong evidence that segregation is anomalous (Baker et al., 1991; Huxlin & Pasternak, 2004; Newsome & Pare, 1988; Rudolph & Pasternak, 1999). A similar deficit occurs in amblyopia, but affects regions of ventral as well as dorsal streams in extra-striate cortex.

Integration of signal and noise with different contrasts

The difference in the performance of normal and amblyopic eyes when signal and noise have different contrasts (fig8 a-d) is open to three different interpretations. First, the amblyopic visual system may not be able to segregate noise from signal for any contrast difference for signal and noise elements so long as both are detectable. Second, this contrast difference may not be sufficient for amblyopes to discriminate and they may not perceive the noise to be of a reduced contrast. Third, the perceived contrast level that is required for amblyopic eyes to segregate based on contrast may be higher than normal. Fig 8e-f shows that the first was not the case. Fig. 8e shows that the 3 times reduction in contrast improves the performance of the amblyopic eyes in segregating the noise, although, interestingly, performance never reaches the no noise condition. Fig. 8f shows that the performance of the amblyopic eye reaches the no noise condition with **60%** difference in contrast of noise and signal elements. We feel that the second explanation based on simply a deficit in contrast discrimination is not sufficient to explain the results. First, the contrast discrimination deficit in human amblyopes is small, rarely greater than a factor of 2 and in many cases absent (Hess et al., 1983) especially at these low spatial frequencies (i.e. 2c/deg). Secondly, it can be accounted for by the threshold difference (Bradley & Freeman, 1985) and performance was equated at the single element level in this experiment. The third explanation is, in our opinions, more likely, namely that since the mechanism for segregating signals from noise is anomalous in amblyopia, more contrast is needed to provide the same improvement found in normals.

Acknowledgements

This work was supported by a Canadian Institute of Health Research grant (CIHR 108-18) to RFH.

Discussion

The nature of the neural deficit in amblyopia

For decades, many scientists have investigated the visual deficiency in amblyopia from different perspectives. A variety of tasks have been used that probed functioning at different stages along the visual systems' processing stream. There is a general concord among the amblyopia researchers about the functional deficiency of the primary visual cortex (V1 cells). The abnormality at the level of V1 could explain most of the deficiencies found involving contrast detection in amblyopia (Bedell & Flom, 1981; Bradley & Skottun, 1984; Caelli et al., 1983; Demanins et al., 1999; Fronius & Sireteanu, 1989; Gstalder, 1971; Hess et al., 1980a; Hess & Holliday, 1992; Hess & Howell, 1977; Lawden et al., 1982; Lawwill & Burian, 1966; Levi & Harwerth, 1977; Pass & Levi, 1982; Treutwein et al., 1996; Vandenbussche et al., 1986). However, there are abnormalities exhibited by the amblyopic visual system that were shown to be independent of the V1 cells deficiencies. A large number of such deficits have been highlighted, involving the processing of orientation, spatial frequency, phase, position and contrast. This has modified the once held view that the neural substrate of amblyopia could be found solely in the properties of single cortical neurons in V1 (Crewther & Crewther, 1990; Eggers & Blakemore, 1978; Movshon et al., 1987). It is now accepted that there may be not only anomalous interactions between cells, that is network abnormalities (Schmidt et al., 1999) but also anomalous processing of cells beyond area V1 (Kiorpes et al., 1998; Schroder et al., 2002). The best examples of studies of global functioning in amblyopia were those of Simmers, et al. Lewis et al. and Ellemberg et al (Ellemberg et al., 2002; Lewis et al., 2002; Simmers et al., 2005; Simmers et al., 2003). Simmers (2003, 2005) showed that the global motion and form integration function was disrupted in amblyopia. They found that these deficiencies were independent of the known contrast sensitivity abnormality residing in primary visual cortex (V1) in amblyopia. Furthermore, since it is unlikely that V1 cells can accomplish such global tasks, Simmers and co-workers suggested that the extra-striate cortex may be selectively impaired in amblyopia. There was support both from the animal (e.g. single cell recording) and human (e.g. patient with lesions) literature that supported a role for extra-striate cortex in such a task. In addition, the studies of Simmers and co-workers showed that the integration function in amblyopia is worse with second-order or contrast-modulated stimuli. On the other hand there have been other studies recently that showed that amblyopes could integrate global information. Hess et al. (Hess et al., 1997c) showed that if the amblyopic visual system is compensated for its positional uncertainty, its performance in contour detection is similar to normal.

Experiment 1

In order to study integration of global information in the amblyopic visual system we must first know how the normal visual system integrates information across space. Integration of first-order orientation information in normals has been studied before (Dakin, 2001). Dakin found that normal observers could combine orientation information across various visual field sizes and different number of elements. However, combining first- and second-order orientation information was not studied before. We found that the normal visual system can integration first- or second-order global orientation information when they are presented alone. However, it does not combine first- and second order information. This suggests that first- and second-order orientation information is processed separately in the normal visual system. Also we showed that the first-order information has priority over the second-order information because if observers are not aware whether first- or second-order stimuli contained the useful information, they tend to only use the first-order information.

Experiment 2

This seeming contradiction in the results of the previous studies, motivated us to investigate the global integration in amblyopia in detail. We have systematically studied the integration of global information in amblyopia. For luminance-modulated information, we have measured the performance of amblyopic and normal eyes at the local processing level. Amblyopic eyes were found to be worse in comparison to the fellow fixing and normal observers' eyes in discriminating the local orientation and local motion directions at comparable contrasts. However, increasing the contrast of the stimuli, which was presented to the amblyopic eye, allowed us to equate the performance of the amblyopic and fellow fixing eyes at the local processing level. We used contrasts that the amblyopic and fellow fixing eyes were performing the local tasks similarly; to explore how local information is integrated. Thus any abnormality found for our subsequent integration experiment could not simply be due to a deficiency of the cells at the local level (i.e. V1). It must be the consequence of either abnormal interaction of the V1 cells or to a deficiency at a later global level.

The global integration task that we employed had a very important characteristic. Since the observers made their judgments based on mean orientation or mean motion direction of the elements, the position of the elements was irrelevant to the purpose of the task. Therefore, we could randomly position our elements and any integration abnormality found cannot be due to the known positional uncertainty in amblyopia (Hess & Holliday, 1992).

Our first experiment showed that the performance of the amblyopic eye in integrating first-order orientation information across space was similar to normal. There was no evidence for higher internal noise at low to mid spatial frequencies. The number of samples was also similar to normals. This contradicts the notion that amblyopia is simply due to a reduction of cells driven by the amblyopic eye. If there were reduced cells, one could expect decreased sampling efficiency as reflected by our number of samples measure.

Experiment 3

In a subsequent experiment, we tested the detection, local discrimination and global integration of the amblyopic visual system with second-order stimuli. Again we equated the performance of the amblyopic and fellow fixing eyes at the local processing level. We showed that although amblyopic and fellow fixing eyes are deficient in detecting and discriminating local second-order orientation information, the performance of the amblyopic eyes in integrating second-order orientation information across space, is similar to normal.

Experiment 4

The results from our previous experiments encouraged us to think that form integration (i.e. ventral pathway) is spared in amblyopia and that the problem might only affect the dorsal pathway which is known to be specialized in motion processing (Simmers et al., 2003). To test this idea we applied a similar approach and assessed the motion direction integration in amblyopia. Subsequently we showed that the integration of motion direction in amblyopia is also similar to normal. No evidence of raised internal noise or decreased number of samples was found.

One of the main differences between our integration paradigm where performance was found to be normal in amblyopia and those previously used where performance was found to be anomalous in amblyopia was the absence of pedestal noise in our experiments. In all previous reports that showed disrupted integration function in amblyopia, a random-dot kinematogram and a coherence noise paradigm was used. In a coherence noise paradigm the signal is embedded in noise. In other words, the signal to noise ratio is varied. In such tasks, the performance of the visual system is close to chance when all stimuli are noise (0% signal and 100% noise). As the ratio of the signal to noise elements increases the correct responses increase. At a certain ratio of signal to noise (i.e. coherence threshold) the visual system can perform the task. The visual system should have access to local signal elements and must efficiently integrate them to perform the task. It has been assumed that such a paradigm measures the integration function of the visual system. However, there are two possible strategies that the visual system could adopt to perform such tasks. First the visual system could average over all elements. When the average contains more signals, a threshold is reached. The second possibility is that the visual system with some, as yet unknown mechanism, might first segregate the noise from signal and only then integrate the signal elements.

Experiment 5

In chapter 5 we designed a paradigm in which an ideal observer blindly averaged over all elements (strategy 1 alone). We ran the ideal observer with our integration experiment. The results showed that the performance of such an ideal observer is much worse than the performance of the real observer when it is confronted by signal and noise elements. It would seem that there is a role for prior segregation in tasks where there is noise as well as signal distributed over space. Although it is accepted that the extra-striate cortex plays some role in the complimentary processes of integration and segregation, there is no information presently available from either human imaging or animal neurophysiology to locate exactly where these separate processes occur. In chapter 5 we showed that the site of orientation integration is after the point where the information from two eyes come together (layer 4 V1) and before the point where the disparity information is processed (layer 4 V2). This supports the view that the integration happens late in striate cortex or early in extra-striate cortex. In terms of motion it would seem that MT and MST are possibly involved in both integration and segregation operations. The motion blind patient offers some support for this because the functions of segregation and integration were profoundly anomalous and the lesion affected both MT and MST. Based on this we would speculate that a lesion occurs in the MT and MST region in human amblyopes and at an equivalent location in the ventral pathway.

In chapter 5 we also showed that even in a normal observer, the noise has different effects on overall performance when it comes from dominant or non-dominant eyes. The noise is significantly more effective in disrupting the performance of the observer when it is presented to the dominant eyes.

Experiment 6

In chapter 6 we specifically investigated the effect the pedestal noise on normal and amblyopic observers. We tested the interactions of two independent and separate sources of noises in the visual system for both motion (dorsal pathway) and orientation (ventral pathway) stimuli. The first noise originated from the bandwidth of the distribution of the local orientations or directions of the elements whose mean was to be judged. The observer had to integrate information across space. All elements contained relevant information for the purpose of this task. The second noise source (i.e. random pedestal noise) came from the ratio of randomly oriented or directed elements and these did not carry any useful information to the purpose of the task. Therefore, in order to perform the task, the visual system ideally should segregate these noise elements prior to integrating the signal elements.

Our results show that for both motion and orientation domains, amblyopes are selectively abnormal at segregating noise elements, although they could integrate signal elements across space similar to normal.

Suggested future experiments

1. We studied integration of global information as well as noise segregation in amblyopes in a series of experiments, which were discussed in this thesis. Although imaging and neurophysiology studies targeted global integration before, delineation between integration and segregation never has been addressed. Human imaging (e.g. fMRI) and animal neurophysiology studies (e.g. single cell recording) with appropriate stimuli for separating segregation of pedestal noise from global signal integration, would be very interesting. Furthermore, since we showed that the segregation is abnormal in amblyopia, fMRI studies with amblyopes would greatly add to our knowledge concerning the extent integration and segregation functions are separated and where such functions locates in human visual cortex.

2. We showed that the normal observers could segregate pedestal noise from signal elements and amblyopes could not. In our task, noise and signal were the same except for the orientation or motion direction distributions. The signal elements were from a parent distribution with predetermined mean and variance. The orientations or motion directions of the noise elements were randomly selected. It was shown that the normal visual system can segregate noise from signal in different attributes of images, for instance, first-order from second-order orientation (Allen et al., 2003) and low from high spatial frequencies (Nothdurft, 1991). It would be interesting to investigate segregation of noise from signal in amblyopia within different attributes of images such as spatial frequency.

3. We showed that if the visual system uses only an averaging strategy, it could perform the mean orientation task. However, averaging alone would not help the visual system segregate the noise. In chapter 5 we show that an ideal observer can avoid the effect of noise elements if it uses a filter with a specific bandwidth around the mean. In our case the bandwidth that produces similar results in the ideal observer to those of a real observer was 50°. This suggests that the amblyopic eye may use wider bandwidth orientation and motion direction filters to average over orientation and motion direction elements across space. However, to segregate the widely distributed noise elements from narrowly distributed signal elements, one possibility is that a normal visual system also has access to fine-tuned filters, which the amblyopic visual system lacks. To investigate directly the bandwidth of the filters that the visual system uses to combine local spatial information, it would be interesting to study the variance discrimination function in amblyopes as well as normal. It has been shown that the normal visual system has good access to local orientation variance information (Dakin, 1999). If the segregation abnormality is due to a lack of fine-tuned filters, one would expect that the amblyopic visual system to be worse compared with the normal visual systems in discriminating variances, specifically for the narrowly distributed populations.

Acknowledgment

Hereby, I have to greatly thank my supervisor Robert Hess, who has always impressed me with his energy, novel ideas and easy solutions. He taught me how to be patient and do good research and science. No question was ever naïve to him. He encouraged me with most of my new ideas, some of which were certainly very simple to him. He is the one who brings relief to his students and colleagues with his extreme knowledge and humorous attitudes. He always made me confident that I have access to the first hand knowledge in my field of research.

I have to thank the faculty members at the McGill Vision Research lab who always were open to my endless questions. I also have to thank my co-workers, Harriet Allen and Steven Dakin who helped to catch up in psychophysics. I am grateful to Aaron Johnson and Richard Watson who edited my manuscripts for many times. I thank Mostafa Modirrousta, Sébastien Cote, and Liza Azeff, who helped me with translating the abstract to French. At last but not the least, I am grateful to Elizabeth Wong who helped me through my PhD pathway and always provided me with useful information. The researches in this thesis were supported by Canadian Institute of Health Research (CIHR) grants (MOP 10818 and 53346) to Robert F. Hess.

References

Achtman, R.L., Hess, R.F., & Wang, Y.Z. (2003). Sensitivity for global shape detection. *Journal of Vision, 3* (10), 616-624.

Ahumada, A.J., Jr., & Watson, A.B. (1985). Equivalent-noise model for contrast detection and discrimination. *Journal of Optical Society of America A: Optics, Image Sciences, and Vision, 2* (7), 1133-1139.

Allen, H.A., & Derrington, A.M. (2000). Slow discrimination of contrast-defined expansion patterns. *Vision Research, 40* (7), 735-744.

Allen, H.A., Hess, R.F., Mansouri, B., & Dakin, S.C. (2003). Integration of first- and second-order orientation. *Journal of Optical Society of America A: Optics, Image Sciences, and Vision, 20* (6), 974-986.

Allman, J., Miezin, F., & McGuinness, E. (1985). Direction and velocity specific responses from beyond the classical receptive field in middle temporal visual atea (MT). *Perception, 14*, 105-126.

Ashida, H., Seiffert, A.E., & Osaka, N. (2001). Inefficient visual search for second-order motion. *journal of optical Society of America A: Optics, Image Sciences, and Vision, 18* (9), 2255-2266.

Atkinson, J., Braddick, O.J., Anker, S., Curran, W., Andrews, R., & Braddick, J. (2003). Neurobiological models of visuo-spatial cignition in young William syndrome children: measures of dorsal stream and frontal function. *Developmental Neuropsychology, 23*, 139-172.

Baker, C.L., Jr., Hess, R.F., & Zihl, J. (1991). Residual motion perception in a "motion-blind" patient, assessed with limited-lifetime random dot stimuli. *Journal of Neuroscience, 11* (2), 454-461.

Baloch, A.A., Grossberg, S., Mingolla, E., & Nogueira, C.A. (1999). Neural model of first-order and second-order motion perception and magnocellular dynamics. *Journal of Optical Society of America, 16* (5), 953-978.

Barlow, H.B. (1957). Increment thresholds at low intensities considered as signal/noise discriminations. *Journal of Physiology, 136* (3), 469-488.

Barnes, G.R., Hess, R.F., Dumoulin, S.O., Achtman, R.L., & Pike, G.B. (2001). The cortical deficit in humans with strabismic amblyopia. *Journal of Physiology, 533* (Pt 1), 281-297.

Barrett, B.T., Pacey, I.E., Bradley, A., Thibos, L.N., & Morrill, P. (2003). Nonveridical visual perception in human amblyopia. *Investigative Ophthalmology & Visual Sciences, 44* (4), 1555-1567.

Bateman, J.B., & Caprioli, J. (2003). Amblyopia. *Preferred Practice Pattern* (American Academy of Ophthalmology.

Bedell, H.D., & Flom, M.C. (1981). Monocular spatial distortion in strabismic amblyopia. *Investigative Ophthalmology & Visual Science, 20* (2), 263-268.

Blindness, N.S.t.P. (1980). Vision problem in the U.S. Data analysis. Publication P-10 (New York: National Society to Prevent Blindness).

Born, R.T., & Tootell, R.B. (1992). Segregation of global and local motion processing in primate middle temporal visual area. *Nature, 357* (6378), 497-499.

Braddick, O. (1993). Segmentation versus integration in visual motion processing. *Trends Neuroscience, 16* (7), 263-268.

Braddick, O.J., Atkinson, J., & Wattam-Bell, J. (2003). Normal and anomalous development of visual motion processing: motion coherence and 'dorsal-stream vulnerability'. *Neuropsychologia, 41*, 1769-1784.

Braddick, O.J., O'Brien, J.M., Wattam-Bell, J., Atkinson, J., & Turner, R. (2000a). Form and motion coherence activate independent but not dorsal/ventral segregated, networks in human brain. *Current Biology, 10*, 731-734.

Braddick, O.J., O'Brien, J.M., Wattam-Bell, J., Atkinson, J., & Turner, R. (2000b). Form and motion coherence activate independent, but not dorsal/ventral segregated, networks in the human brain. *Current Biology, 10* (12), 731-734.

Bradley, A., & Freeman, R. (1985). Is reduced vernier acuity in amblyopia due to position, contrast or fixation deficits? *Vision Research, 25*, 55-66.

Bradley, A., & Skottun, B.C. (1984). The effects of large orientation and spatial frequency differences on spatial discriminations. *Vision Research, 24* (12), 1889-1896.

Brainard, D.H. (1997). The Psychophysics Toolbox. *Spatial Vision, 10* (4), 433-436.

Britten, K.H., Shadlen, M.N., Newsome, W.T., & Movshon, J.A. (1992). The analysis of visual motion: a comparison of neuronal and psychophysical performance. *Journal of Neuroscience, 12* (12), 4745-4765.

Britten, K.H., Shadlen, M.N., Newsome, W.T., & Movshon, J.A. (1993). Responses of neurons in macaque MT to stochastic motion signals. *Visual Neuroscience, 10* (6), 1157-1169.

Caelli, T., Brettel, H., Rentschler, I., & Hilz, R. (1983). Discrimination thresholds in the two-dimensional spatial frequency domain. *Vision Research, 23* (2), 129-133.

Campbell, F.W., & Robson, J.G. (1968). Application of Fourier analysis to the visibility of gratings. *Journal of Physiology, 197* (3), 551-566.

Chino, Y.M., Shansky, M.S., Jankowski, W.L., & Banser, F.A. (1983). Effects of rearing kittens with convergent strabismus on development of receptive-field properties in striate cortex neurons. *Journal of Neurophysiology, 50* (1), 265-286.

Chubb, C., & Sperling, G. (1988). Drift-balanced random stimuli: a general basis for studying non-Fourier motion perception. *Journal of Optical Society of America, 5* (11), 1986-2007.

Cleland, B.G., Crewther, D.P., Crewther, S.G., & Mitchell, D.E. (1982). Normality of spatial resolution of retinal ganglion cells in cats with strabismic amblyopia. *Journal of Physiology, 326*, 235-249.

Cornelissen, P., Richardson, A., Mason, A., Fowler, S., & Stein, J. (1995). Contrast sensitivity and coherent motion detection measured at photopic luminance levels in dyslexics and controls. *Vision Research, 35*, 1483-1494.

Crewther, D.P., & Crewther, S.G. (1990). Neural site of strabismic amblyopia in cats: spatial frequency deficit in primary cortical neurons. *Experimental Brain Research, 79* (3), 615-622.

Crewther, D.P., Crewther, S.G., & Cleland, B.G. (1985). Is the retina sensitive to the effects of prolonged blur? *Experimental Brain Research, 58*, 427-434.

Cumming, B.G., & Parker, A.J. (2000). Local disparity not perceived depth is signaled by binocular neurons in cortical area V1 of the Macaque. *Journal of Neuroscience, 20* (12), 4758-4767.

Dakin, S.C. (1999). Orientation variance as a quantifier of structure in texture. *Spatial Vision, 12* (1), 1-30.

Dakin, S.C. (2001). Information limit on the spatial integration of local orientation signals. *Journal of Optical Society of America A: Optics, Image Sciences, and Vision, 18* (5), 1016-1026.

Dakin, S.C., & Mareschal, I. (2000). Sensitivity to contrast modulation depends on carrier spatial frequency and orientation. *Vision Research, 40*, 311-329.

Dakin, S.C., & Watt, R.J. (1994). Detection of bilateral symmetry using spatial filters. *Spatial Vision, 8* (4), 393-413.

Dakin, S.C., & Watt, R.J. (1997). The computation of orientation statistics from visual texture. *Vision Research, 37* (22), 3181-3192.

Dakin, S.C., Williams, C.B., & Hess, R.F. (1999). The interaction of first- and second-order cues to orientation. *Vision Research, 39* (17), 2867-2884.

Demanins, R., & Hess, R.F. (1996a). Effect of exposure duration on spatial uncertainty in normal and amblyopic eyes. *Vision Research, 36* (8), 1189-1193.

Demanins, R., & Hess, R.F. (1996b). Positional loss in strabismic amblyopia: inter-relationship of alignment threshold, bias, spatial scale and eccentricity. *Vision Research, 36* (17), 2771-2794.

Demanins, R., Hess, R.F., Williams, C.B., & Keeble, D.R. (1999). The orientation discrimination deficit in strabismic amblyopia depends upon stimulus bandwidth. *Vision Research, 39* (24), 4018-4031.

Derrington, A.M., & Badcock, D.R. (1985). Separate detectors for simple and complex grating patterns. *Vision Research, 25*, 1869-1878.

Derrington, A.M., & Hawken, M.J. (1981). Spatial and temporal properties of cat geniculate neurones after prolonged deprivation. *Journal of Physiology (London), 314*, 107-120.

DeValois, R.L., & DeValois, K.K. (1988). Spatial Vision. (New York: Oxford University Press).

DeYoe, E.A., & Van Essen, D.C. (1988). Concurrent processing streams in monkey visual cortex. *Trends in Neuroscience, 11* (5), 219-226.

Dumoulin, S.O., Baker, C.L., Jr., Hess, R.F., & Evans, A.C. (2003). Cortical specialization for processing first- and second-order motion. *Cerebral Cortex, 13* (12), 1375-1385.

Edwards, M., & Badcock, D.R. (1995). Global motion perception: No interaction between the first- and second-order pathways. *Vision Research, 35* (18), 2589-2602.

Eggers, H.M., & Blakemore, C. (1978). Physiological basis of anisometropic amblyopia. *Science, 201* (4352), 264-267.

Ellemberg, D., Lewis, T.L., Maurer, D., Brar, S., & Brent, H.P. (2002). Better perception of global motion after monocular than after binocular deprivation. *Vision Research, 42* (2), 169-179.

Field, D.J., Hayes, A., & Hess, R.F. (1993). Contour integration by the human visual system: evidence for a local "association field". *Vision Research, 33* (2), 173-193.

Field, D.J., Hayes, A., & Hess, R.F. (2000). The roles of polarity and symmetry in the perceptual grouping of contour fragments. *Spatial Vision, 13*, 51-66.

Foster, D.H., & Bischof, W.F. (1987). Bootstrap variance estimators for the parameters of small-sample sensory-performance functions. *Biological Cybernetics, 57* (4-5), 341-347.

Foster, D.H., & Bischof, W.F. (1997). Bootstrap estimates of the statistical accuracy of thresholds obtained from psychometric functions. *Spatial Vision, 11*, 135-139.

Fronius, M., & Sireteanu, R. (1989). Monocular geometry is selectively distorted in the central visual field of strabismic amblyopes. *Investigative Ophthalmology & Visual Science, 30* (9), 2034-2044.

Gilbert, C.D., Das, A., Ito, M., Kapadia, M., & Westheimer, G. (1996). Spatial integration and cortical dynamics. *Proceedings of the National Academy of Sciences U S A, 93* (2), 615-622.

Gilbert, C.D., & Wiesel, T.N. (1990). The influence of contextual stimuli on the orientation selectivity of cells in primary visual cortex of the cat. *Vision Research, 30* (11), 1689-1701.

Graham, N., Beck, J., & Sutter, A. (1992). Nonlinear processes in spatial-frequency channel models of perceived texture segregation: effects of sign and amount of contrast. *Vision Research, 32* (4), 719-743.

Gstalder, R.J. (1971). Laser inferometric acuity in amblyopia. *Journal of Paediatric Ophthalmology, 8*, 251-256.

Gstalder, R.J., & Green, D.G. (1972). Laser interferometry in corneal opacification. Preoperative visual potential estimation. *Archives of Ophthalmology, 87* (3), 269-274.

Gunn, A., Cory, E., Atkinson, J., Braddick, O.J., Wattam-Bell, J., Guzzetta, A., & Cioni, G. (2002). Dorsal and ventral stream sensitivity in normal development and hemiplegia. *NeuroReport, 13*, 843-847.

Heeley, D.W. (1987). Spatial frequency discrimination for sinewave gratings with random, bandpass frequency modulation: evidence for averaging in spatial acuity. *Spatial Vision, 2* (4), 317-335.

Heeley, D.W., Buchanan-Smith, H.M., Cromwell, J.A., & Wright, J.S. (1997). The oblique effect in orientation acuity. *Vision Research, 37* (2), 235-242.

Hess, R.E., Mansouri, B., Dakin, S., & Allen, H. (in submission). Integration of local motion is normal in amblyopia. *Vision Research.*

Hess, R.F., & Anderson, S.J. (1993). Motion sensitivity and spatial undersampling in amblyopia. *Vision Research, 33* (7), 881-896.

Hess, R.F., & Baker, C.L., Jr. (1984). Assessment of retinal function in severely amblyopic individuals. *Vision Research, 24* (10), 1367-1376.

Hess, R.F., Baker, C.L., Verhoeve, J.N., Tulunay Keesey, U., & France, T.D. (1985). The pattern evoked electroretinogram: Its variability in normals and its relationship to amblyopia. *Investigative Ophthalmology & Visual Science, 26*, 1610-1623.

Hess, R.F., Bradley, A., & Piotrowski, L. (1983). Contrast-coding in amblyopia. I. Differences in the neural basis of human amblyopia. *Proceeding of the Royal Society of London, Series B Biological Sciences, 217* (1208), 309-330.

Hess, R.F., Burr, D.C., & Campbell, F.W. (1980a). A preliminary investigation of neural function and dysfunction in amblyopia--III. Co-operative activity of amblyopic channels. *Vision Research, 20* (9), 757-760.

Hess, R.F., Campbell, F.W., & Greenhalgh, T. (1978). On the nature of the neural abnormality in human amblyopia; neural aberrations and neural sensitivity loss. *Pflugers Archiv - Europian Journal of Physiology, 377* (3), 201-207.

Hess, R.F., Campbell, F.W., & Zimmern, R. (1980b). Differences in the neural basis of human amblyopias: the effect of mean luminance. *Vision Research, 20* (4), 295-305.

Hess, R.F., & Dakin, S.C. (1999). Contour integration in the peripheral field. *Vision Research, 39* (5), 947-959.

Hess, R.F., Demanins, R., & Bex, P.J. (1997a). A reduced motion after-effect in strabismic amblyopia. *Vision Research, 37* (10), 1303-1311.

Hess, R.F., & Field, D.J. (1995). Contour integration across depth. *Vision Research, 35* (12), 1699-1711.

Hess, R.F., France, T.D., & Tulunay-Keesey, U. (1981). Residual vision in humans who have been monocularly deprived of pattern stimulation in early life. *Experimental Brain Research, 44* (3), 295-311.

Hess, R.F., & Holliday, I.E. (1992). The spatial localization deficit in amblyopia. *Vision Research, 32* (7), 1319-1339.

Hess, R.F., & Howell, E.R. (1977). The threshold contrast sensitivity function in strabismic amblyopia: evidence for a two type classification. *Vision Research, 17* (9), 1049-1055.

Hess, R.F., & Howell, E.R. (1978). The luminance-dependent nature of the visual abnormality in strabismic amblyopia. *Vision Research, 18* (8), 931-936.

Hess, R.F., Ledgeway, T., & Dakin, S. (2000). Impoverished second-order input to global linking in human vision. *Vision Research, 40* (24), 3309-3318.

Hess, R.F., McIlhagga, W., & Field, D.J. (1997b). Contour integration in strabismic amblyopia: the sufficiency of an explanation based on positional uncertainty. *Vision Research, 37* (22), 3145-3161.

Hess, R.F., McIlhagga, W., & Field, D.J. (1997c). Contour integration in strabismic amblyopia: the sufficiency of an explanation based on positional uncertainty. *Vision Research, 37* (22), 3145-3161.

Hess, R.F., Wang, Y.-Z., Demanins, R., Wilkinson, F., & Wilson, H.R. (1999a). A deficit in strabismic amblyopia for global shape detection. *Vision Research, 39*, 901-914.

Hess, R.F., Wang, Y.Z., & Dakin, S.C. (1999b). Are judgements of circularity local or global? *Vision Research, 39* (26), 4354-4360.

Hess, R.F., Wang, Y.Z., Demanins, R., Wilkinson, F., & Wilson, H.R. (1999c). A deficit in strabismic amblyopia for global shape detection. *Vision Research, 39* (5), 901-914.

Hess, R.F., & Ziegler, L.R. (2000). What limits the contribution of second-order motion to the perception of surface shape? *Vision Research, 40* (16), 2125-2133.

Hess, R.H., Baker, C.L., Jr., & Zihl, J. (1989). The "motion-blind" patient: low-level spatial and temporal filters. *Journal of Neuroscience, 9* (5), 1628-1640.

Hillis, A., Flynn, J.T., & Hawkins, B.S. (1983). The evolving concept of amblyopia: a challenge to epidemiologists. *American Journal of Epidemiology, 118* (2), 192-205.

Hong, E.H., Levi, D.M., & McGraw, P.V. (2001). Abnormal second-order spatial interactions in amblyopia. *Investigative Ophthalmology & Visual Science (suppl), 42* (4), S735.

Huang, P.C., Hess, R.F., & Dakin, S.C. (2004). Different sites for lateral facilitation and contour integration. *Program and Abstracts VSS*, 210.

Hubel, D.H., & Weisel, T.N. (1968). Receptive fields and functional architecture of monkey striate cortex. *Journal of Physiology (London), 195*, 215-243.

Hubel, D.H., & Wiesel, T.N. (1977). Ferrier lecture. Functional architecture of macaque monkey visual cortex. *Proceedings: Biological Sciences, The Royal Society, London, 198* (1130), 1-59.

Hubel, D.H., & Wiesel, T.N. (1979). Brain mechanisms of vision. *Scientific American, 241* (3), 150-162.

Huxlin, K.R., & Pasternak, T. (2004). Training-induced recovery of visual motion perception after extra-striate cortical damage in the adult cat. *Cerebral Cortex, 14*, 81-91.

Imamura, K., Richter, H., Fischer, H., Lennerstrand, G., Franzen, O., Rydberg, A., Andersson, J., Schneider, H., Onoe, H., Watanabe, Y., & Langstrom, B. (1997). Reduced activity in the extrastriate visual cortex of individuals with strabismic amblyopia. *Neuroscience Letters, 225* (3), 173-176.

Johnston, A., & Clifford, C.W. (1995). Perceived motion of contrast-modulated gratings: predictions of the multi-channel gradient model and the role of full-wave rectification. *Vision Research, 35* (12), 1771-1783.

King-Smith, P.E., & Rose, D. (1997). Principles of an adaptive method for measuring the slope of the psychometric function. *Vision Research, 37* (12), 1595-1604.

Kiorpes, L., Kiper, D.C., O'Keefe, L.P., Cavanaugh, J.R., & Movshon, J.A. (1998). Neuronal correlates of amblyopia in the visual cortex of macaque monkeys with experimental strabismus and anisometropia. *Journal of Neuroscience, 18* (16), 6411-6424.

Kiorpes, L., & McKee, S.P. (1999). Neural mechanisms underlying amblyopia. *Current Opinion in Neurobiology, 9*, 480-486.

Knierim, J.J., & van Essen, D.C. (1992). Neuronal responses to static texture patterns in area V1 of the alert macaque monkey. *Journal of Neurophysiology, 67* (4), 961-980.

Kourtzi, Z., Bulthoff, H.H., Erb, M., & Grodd, W. (2002). Object-selective responses in the human motion area MT/MST. *Nature Neuroscience, 5* (1), 17-18.

Lauwers, K., Sounders, R., Vogels, R., Vandenbussche, E., & Orban, G.A. (2000). Impairment in motion discrimination tasks is unrelated to amount of damage to superior temporal sulcus motion area. *Journal of Comparative Neurology, 420* (4), 539-557.

Lawden, M.C., Hess, R.F., & Campbell, F.W. (1982). The discriminability of spatial phase relationships in amblyopia. *Vision Research, 22* (8), 1005-1016.

Lawwill, T., & Burian, H.M. (1966). Luminance, contrast function and visual acuity in functional amblyopia. *American Journal of Ophthalmology, 62* (3), 511-520.

Ledgeway, T., & Hess, R.F. (2002). Failure of direction identification for briefly presented second-order motion stimuli: evidence for weak direction selectivity of the mechanisms encoding motion. *Vision Research, 42*, 1739-1758.

Levi, D.M., & Harwerth, R.S. (1978). Contrast evoked potentials in strabismic and anisometropic amblyopia. *Investigative Ophthalmology in Vision Sciences, 17* (6), 571-575.

Levi, D.M., & Klein, S.A. (1985). Vernier acuity, crowding and amblyopia. *Vision Research, 25* (7), 979-991.

Levi, D.M., & Klein, S.A. (1986). Sampling in spatial vision. *Nature, 320* (6060), 360-362.

Levi, M., & Harwerth, R.S. (1977). Spatio-temporal interactions in anisometropic and strabismic amblyopia. *Investigative Ophthalmology and Visual Science, 16* (1), 90-95.

Lewis, T.L., Ellemberg, D., Maurer, D., Wilkinson, F., Wilson, H.R., Dirks, M., & Brent, H.P. (2002). Sensitivity to global form in glass patterns after early visual deprivation in humans. *Vision Research, 42* (8), 939-948.

Lin, L.M., & Wilson, H.R. (1996). Fourier and non-Fourier pattern discrimination compared. *Vision Research, 36* (13), 1907-1918.

Loshin, D.S., & Jones, R. (1982). Contrast sensitivity as a function of exposure duration in the amblyopic visual system. *American Journal of Optometry & Physiological Optics, 59* (7), 561-567.

Lu, Z.L., & Dosher, B.A. (1998). External noise distinguishes attention mechanisms. *Vision Research, 38* (9), 1183-1198.

Lu, Z.L., & Sperling, G. (1995). The functional architecture of human visual motion perception. *Vision Research, 35* (19), 2697-2722.

Malik, J., & Perona, P. (1990). Preattentive texture discrimination with early vision mechanisms. *Journal of optical Society of America, 7* (5), 923-932.

Mansouri, B., Allen, H.A., & Hess, R.F. (in press). Detection, discrimination and integration of second-order orientation information in strabismic and anisometropic amblyopia. *Vision Research.*

Mansouri, B., Allen, H.A., Hess, R.F., & Dakin, S.C. (2004a). Integration of global information in amblyopia and the effect of noise. *Society for Neuroscience,* 713.14. San Diego, CA.

Mansouri, B., Allen, H.A., Hess, R.F., Dakin, S.C., & Ehrt, O. (2004b). Integration of orientation information in amblyopia. *Vision Research, 44* (25), 2955-2969.

Mansouri, B., Hess, R.F., Allen, H.A., & Dakin, S.C. (2005). Integration, segregation, and binocular combination. *Journal of Optical Society of America A: Optics, Image Sciences, and Vision, 22* (1), 38-48.

Mareschal, I., Sceniak, M.P., & Shapley, R.M. (2001). Contextual influences on orientation discrimination: binding local and global cues. *Vision Research, 41* (15), 1915-1930.

McGraw, P.V., Levi, D.M., & Whitaker, D. (1999). Spatial characteristics of the second-order visual pathway revealed by positional adaptation. *Nature Neuroscience, 2* (5), 479-484.

McIlhagga, W.H., & Mullen, K.T. (1996). Contour integration with colour and luminance contrast. *Vision Research, 36* (9), 1265-1279.

McOwan, P.W., & Johnston, A. (1996). A second-order pattern reveals separate strategies for encoding orientation in two-dimensional space and space-time. *Vision Research, 36* (3), 425-430.

Mikami, A., Newsome, W.T., & Wurtz, R.H. (1986a). Motion selectivity in macaque visual cortex. I mechanisms of direction and speed selectivity in extra-striate area MT. *Journal of Neurophysiology, 55* (6), 1308-1327.

Mikami, A., Newsome, W.T., & Wurtz, R.H. (1986b). Motion selectivity in macaque visual cortex. II Spatiotemporal range of directional interactions in MT and V1. *Journal of Neurophysiology, 55* (6), 1328-1339.

Mishkin, M., & Ungerleider, L.G. (1982). Contribution of striate inputs to the visuospatial functions of parieto-preoccipital cortex in monkeys. *Behavioural Brain Research, 6* (1), 57-77.

Morgan, M.J., Mason, A.J., & Baldassi, S. (2000). Are there separate first-order and second-order mechanisms for orientation discrimination? *Vision Research, 40* (13), 1751-1763.

Morrone, M.C., Burr, D.C., & Vaina, L.M. (1995). Two stages of visual processing for radial and circular motion. *Nature, 376* (6540), 507-509.

Movshon, J.A., Adelson, E.H., Gizzi, M.S., & Newsome, W.T. (1985). The analysis of moving visual patterns. In: C. Chagas, R. Gattass, & C. Gross (Eds.), *Pattern Recognition mechanism,* Pontificiae Academiae Scientarum Scripta Varia, 45 (pp. 117-151). Rome: Vatican Press.

Movshon, J.A., Eggers, H.M., Gizzi, M.S., Hendrickson, A.E., Kiorpes, L., & Boothe, R.G. (1987). Effects of early unilateral blur on the macaque's visual system. III. Physiological observations. *Journal of Neuroscience, 7* (5), 1340-1351.

Mussap, A.J., & Levi, D.M. (1999). Orientation-based texture segmentation in strabismic amblyopia. *Vision Research, 39* (3), 411-418.

Newsome, W.T., & Pare, E.B. (1988). A selective impairment of motion perception following lesions of the middle temporal visual area (MT). *Journal of Neuroscience, 8* (6), 2201-2211.

Nothdurft, H.C. (1991). Different effects from spatial frequency masking in texture segregation and texton detection tasks. *Vision Research, 31* (2), 299-320.

Pardhan, S. (2004). Contrast sensitivity loss with aging: sampling efficiency and equivalent noise at different spatial frequencies. *Journal of Optical Society of America A: Optics, Image Sciences, and Vision, 21* (2), 169-175.

Parkes, L., Lund, J., Angelucci, A., Solomon, J.A., & Morgan, M. (2001). Compulsory averaging of crowded orientation signals in human vision. *Nature Neuroscience, 4* (7), 739-744.

Pass, A.F., & Levi, D.M. (1982). Spatial processing of complex stimuli in the amblyopic visual system. *Investigative Ophthalmology and visual Science, 23* (6), 780-786.

Pelli, D.G. (1981). Effects of visual noise. (Cambridge, UK: University of Cambridge.

Pelli, D.G. (1997). The VideoToolbox software for visual psychophysics: transforming numbers into movies. *Spatial Vision, 10* (4), 437-442.

Pelli, D.G., & Farell, B. (1999). Why use noise? *Journal of Optical Society of America A: Optics, Image Sciences, and Vision, 16* (3), 647-653.

Pelli, D.G., & Zhang, L. (1991). Accurate control of contrast on microcomputer displays. *Vision Research, 31* (7-8), 1337-1350.

Polat, U., Sagi, D., & Norcia, A.M. (1997). Abnormal long-range spatial interactions in amblyopia. *Vision Research, 37*, 737-744.

Popple, A.V., & Levi, D.M. (2000). Amblyopes see true alignment where normal observers see illusory tilt. *Proceedings of the National Academy of Sciences of the United States of America, 97* (21), 11667-11672.

Rentschler, I., & Hilz, R. (1985). Amblyopic processing of positional information. Part I: Vernier acuity. *Experimental Brain Research, 60* (2), 270-278.

Rizzo, M., Nawrot, M., & Zihl, J. (1995). Motion and shape perception in cerebral akinetopsia. *Brain, 118 (Pt 5)*, 1105-1127.

Robson, J.G. (1975). Receptive fields: neural representation of the spatial and intensive attributes of the visual image. In: E.C. Carterette, & M.P. Friedman (Eds.), *Handbook of Perception,* 5 (pp. 81-112). New York: Academic Press.

Rosenbach, O. (1903). Ueber monokulare Vorherrschaft beim binikularen Sehen. *Munchener Medizinische Wochenschriff, 30*, 1290-1292.

Rudolph, K., & Pasternak, T. (1999). Transient and permanent deficits in motion perception after lesions of cortical area MT and MST in macaque monkey. *Cerebral Cortex, 9*, 90-100.

Salzman, C.D., Murasugi, C.M., Britten, K.H., & Newsome, W.T. (1992). Microstimulation in visual area MT: effects on direction discrimination performance. *Journal of Neuroscience, 12* (6), 2331-2355.

Schiller, P.H., & Lee, K.M. (1994). The effects of lateral geniculate nucleus, area V4 and middle temporal (MT) lesions on visually guided eye movements. *Visual Neuroscience, 11* (2), 229-241.

Schmidt, K.E., Galuske, R.A., & Singer, W. (1999). Matching the modules: cortical maps and long-range intrinsic connections in visual cortex during development. *Journal of Neurobiology, 41* (1), 10-17.

Schofield, A.J., & Georgeson, M.A. (1999). Sensitivity to modulations of luminance and contrast in visual white noise: separate mechanisms with similar behaviour. *Vision Res, 39* (16), 2697-2716.

Schroder, J.H., Fries, P., Roelfsema, P.R., Singer, W., & Engel, A.K. (2002). Ocular dominance in extrastriate cortex of strabismic amblyopic cats. *Vision Research, 42* (1), 29-39.

Simmers, A.J., & Bex, P.J. (2004). The representation of global spatial structure in amblyopia. *Vision Research, 44* (5), 523-533.

Simmers, A.J., Gray, L.S., McGraw, P.V., & Winn, B. (1999). Functional visual loss in amblyopia and the effect of occlusion therapy. *Investigative Ophthalmology and Visual Science, 40* (12), 2859-2871.

Simmers, A.J., Ledgeway, T., & Hess, R.F. (2005). The influences of visibility and anomalous integration processes on the perception of global spatial form versus motion in human amblyopia. *Vision Research, 45* (4), 449-460.

Simmers, A.J., Ledgeway, T., Hess, R.F., & McGraw, P.V. (2003). Deficits to global motion processing in human amblyopia. *Vision Research, 43* (6), 729-738.

Sireteanu, R., & Best, J. (1992). Squint-induced Modification of Visual Receptive Fields in the Lateral Suprasylvian Cortex of the Cat: Binocular Interaction, Vertical Effect and Anomalous Correspondence. *European Journal of Neuroscience, 4* (3), 235-242.

Sireteanu, R., Tonhausen, N., Muckli, L., Lanfermann, H., Zanella, F.E., Singer, W., & Goebel, R. (1998). Cortical site of the amblyopic deficit in strabismic and anisometropic subjects, investigated with fMRI. *Investigative Ophthalmology & Visual Science, 39* (4), s909.

Smith, A.T., Greenlee, M.W., Singh, K.D., Kraemer, F.M., & Hennig, J. (1998). The processing of first- and second-order motion in human visual cortex assessed by functional magnetic resonance imaging (fMRI). *Journal of Neuroscience, 18* (10), 3816-3830.

Smith, A.T., & Scott-Samuel, N.E. (2001). First-order and second-order signals combine to improve perceptual accuracy. *Journal of Optical Society of America, 18* (9), 2267-2272.

Smith, S., Clifford, C.W., & Wenderoth, P. (2001a). Interaction between first- and second-order orientation channels revealed by the tilt illusion: psychophysics and computational modelling. *Vision Research, 41* (8), 1057-1071.

Smith, S., Wenderoth, P., & Van der Zwan, R. (2001b). Orientation processing mechanisms revealed by the plaid tilt illusion. *Vision Research, 41* (4), 483-494.

Solomon, J.A., & Morgan, M.J. (1999). Dichoptically cancelled motion. *Vision Research, 39* (14), 2293-2297.

Spencer, J., O'Brien, J., Riggs, K., Braddick, O.J., Atkinson, J., & Wattam-Bell, J. (2000). Motion processing in autism: evidence for a dorsal-stream deficiency. *NeuroReport, 11*, 2765-2767.

Thomas, O.M., Cumming, B.G., & Parker, A.J. (2002). A specialization for relative disparity in V2. *Nature Neuroscience, 5* (5), 472-478.

Treutwein, B., Rentschler, I., Zetzsche, C., Scheidler, M., & Boergen, K.P. (1996). Amblyopic quasi-blindness for image structure. *Vision Research, 36* (14), 2211-2228.

Ungerleider, L.G., & Mishkin, M. (1982). Two cortical visual systems. In: D.J. Ingle (Ed.) *Analysis of Visual Behaviour* (pp. 549-586). Cambridge, Massachusetts: MIT Press.

Vaina, L.M., Lemay, M., Bienfang, D.C., Choi, A.Y., & Nakayama, K. (1990). Intact "biological motion" and "structure from motion" perception in a patient with impaired motion mechanisms: a case study. *Visual Neuroscience, 5* (4), 353-369.

Van der Zwan, R., & Wenderoth, P. (1995). Mechanisms of purely subjective contour tilt after-effects. *Vision Research, 35* (18), 2547-2557.

Van Essen, D.C., Anderson, C.H., & Felleman, D.J. (1992). Information processing in the primate visual system: an integrated systems perspective. *Science, 255* (5043), 419-423.

Vandenbussche, E., Vogels, R., & Orban, G.A. (1986). Human orientation discrimination: changes with eccentricity in normal and amblyopic vision. *Investigative Ophthalmology and Visual Science, 27* (2), 237-245.

Watt, R.J., & Andrews, D. (1981). APE. Adaptive Probit estimation of the psychometric function. *Current Psychological Review, 1*, 205-214.

Watt, R.J., & Hess, R.F. (1987). Spatial information and uncertainty in anisometropic amblyopia. *Vision Research, 27* (4), 661-674.

Watt, R.J., & Morgan, M.J. (1983). The recognition and representation of edge blur: evidence for spatial primitives in human vision. *Vision Research, 23* (12), 1465-1477.

Weiss, C., Rentschler, I., & Caelli, T. (1985). Amblyopic processing of positional information. Part II: Sensitivity to phase distortion. *Experimental Brain Research, 60* (2), 279-288.

Westheimer, G. (1990). Simultaneous orientation contrast for lines in the human fovea. *Vision Research, 30* (11), 1913-1921.

Wichmann, F.A., & Hill, N.J. (2001a). The psychometric function: I. Fitting, sampling, and goodness of fit. *Perception & Psychophysics, 63* (8), 1293-1313.

Wichmann, F.A., & Hill, N.J. (2001b). The psychometric function: II. Bootstrap-based confidence intervals and sampling. *Perception & Psychophysics, 63* (8), 1314-1329.

Wilkinson, F., James, T.W., Wilson, H.R., Gati, J.S., Menon, R.S., & Goodale, M.A. (2000). An fMRI study of the selective activation of human extrastriate form vision areas by radial and concentric gratings. *Current Biology, 10* (22), 1455-1458.

Wilkinson, F., Wilson, H.R., & Habak, C. (1998). Detection and recognition of radial frequency patterns. *Vision Research, 38* (22), 3555-3568.

Wilson, H.R., Ferrera, V.P., & Yo, C. (1992). A psychophysically motivated model for two-dimensional motion perception. *Visual Neuroscience, 9* (1), 79-97.

Wilson, H.R., & Wilkinson, F. (1998). Detection of global structure in Glass patterns: implications for form vision. *Vision Research, 38* (19), 2933-2947.

Wolf, J.M. (1986). Briefly presented stimuli can disrupt constant suppression and binocular rivalry suppression. *Perception, 15*, 413-417.

Wong, E.H., Levi, D.M., & McGraw, P.V. (2001). Is second-order spatial loss in amblyopia explained by the loss of first-order spatial input? *Vision Research, 41* (23), 2951-2960.

Zeevi, Y.Y., & Mangoubi, S.S. (1984). Vernier acuity with noisy lines: estimation of relative position uncertainty. *Biological Cybernetics, 50* (5), 371-376.

Zeki, S. (1978). Functional specialization in the visual cortex of the rhesus monkey. *Nature, 274*, 423-428.

Zhou, Y.X., & Baker, C.L., Jr. (1996). Spatial properties of envelope-responsive cells in area 17 and 18 neurons of the cat. *Journal of Neurobiology, 75* (3), 1038-1050.

Ziegler, L.R., & Hess, R.F. (1999). Stereoscopic depth but not shape perception from second-order stimuli. *Vision Research, 39* (8), 1491-1507.

Zihl, J., von Cramon, D., & Mai, N. (1983). Selective disturbance of movement vision after bilateral brain damage. *Brain, 106 (Pt 2)*, 313-340.

Appendix

Consents

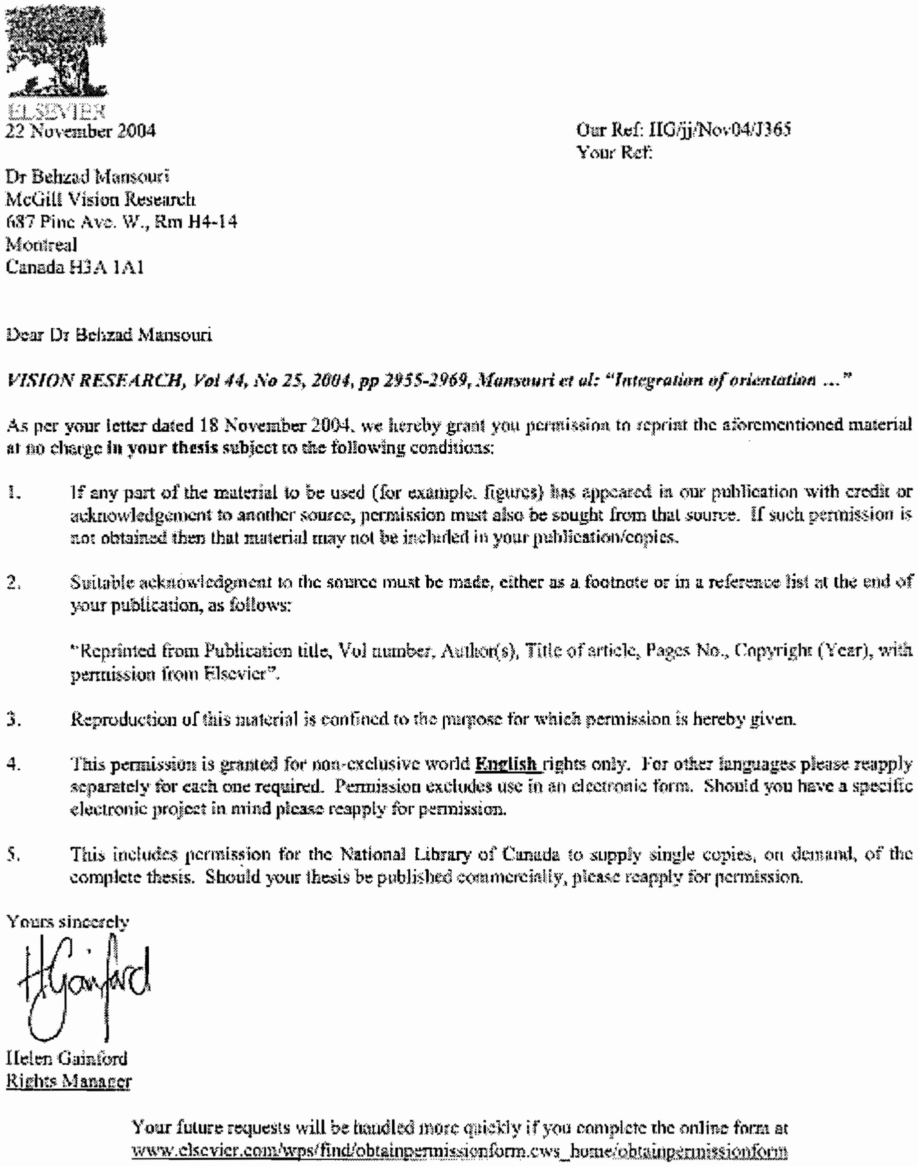

ELSEVIER

22 November 2004

Our Ref: HG/jj/Nov04/J365
Your Ref:

Dr Behzad Mansouri
McGill Vision Research
687 Pine Ave. W., Rm H4-14
Montreal
Canada H3A 1A1

Dear Dr Behzad Mansouri

VISION RESEARCH, Vol 44, No 25, 2004, pp 2955-2969, Mansouri et al: "Integration of orientation …"

As per your letter dated 18 November 2004, we hereby grant you permission to reprint the aforementioned material at no charge **in your thesis** subject to the following conditions:

1. If any part of the material to be used (for example, figures) has appeared in our publication with credit or acknowledgement to another source, permission must also be sought from that source. If such permission is not obtained then that material may not be included in your publication/copies.

2. Suitable acknowledgment to the source must be made, either as a footnote or in a reference list at the end of your publication, as follows:

   "Reprinted from Publication title, Vol number, Author(s), Title of article, Pages No., Copyright (Year), with permission from Elsevier".

3. Reproduction of this material is confined to the purpose for which permission is hereby given.

4. This permission is granted for non-exclusive world **English** rights only. For other languages please reapply separately for each one required. Permission excludes use in an electronic form. Should you have a specific electronic project in mind please reapply for permission.

5. This includes permission for the National Library of Canada to supply single copies, on demand, of the complete thesis. Should your thesis be published commercially, please reapply for permission.

Yours sincerely

H Gainford

Helen Gainford
Rights Manager

Your future requests will be handled more quickly if you complete the online form at
www.elsevier.com/wps/find/obtainpermissionform.cws_home/obtainpermissionform

ELSEVIER

22 November 2004

Our Ref: HG/jj/Nov04/J366
Your Ref:

Dr Behzad Mansouri
McGill Vision Research
687 Pine Ave. W., Rm H4-14
Montreal
Canada H3A 1A1

Dear Dr Behzad Mansouri

VISION RESEARCH, (submitted), Mansouri et al: "Detection, discrimination and integration ..."

As per your letter dated 18 November 2004, we hereby grant you permission to reprint the aforementioned material at no charge **in your thesis** subject to the following conditions:

1. If any part of the material to be used (for example, figures) has appeared in our publication with credit or acknowledgement to another source, permission must also be sought from that source. If such permission is not obtained then that material may not be included in your publication/copies.

2. Suitable acknowledgment to the source must be made, either as a footnote or in a reference list at the end of your publication, as follows:

   "Reprinted from Publication title, Vol number, Author(s), Title of article, Pages No., Copyright (Year), with permission from Elsevier".

3. Reproduction of this material is confined to the purpose for which permission is hereby given.

4. This permission is granted for non-exclusive world **English** rights only. For other languages please reapply separately for each one required. Permission excludes use in an electronic form. Should you have a specific electronic project in mind please reapply for permission.

5. This includes permission for the National Library of Canada to supply single copies, on demand, of the complete thesis. Should your thesis be published commercially, please reapply for permission.

Yours sincerely

HGainford

Helen Gainford
Rights Manager

Your future requests will be handled more quickly if you complete the online form at
www.elsevier.com/wps/find/obtainpermissionform.cws_home/obtainpermissionform

The Optical Society of America considers the below requested use of its copyrighted material to be allowed under the OSA Author Agreement submitted by the requestor on acceptance for publication of his/her manuscript. It is requested that a complete citation of the original material be included in any publication.

Susannah Lehman

Authorized Agent

Optical Society of America

From: Behzad Mansouri [mailto:bmanso1@po-box.mcgill.ca]
Posted At: Thursday, November 18, 2004 4:09 PM
Posted To: ADS
Conversation: permission to include papers in my thesis
Subject: permission to include papers in my thesis

Dear Sir/ Madam,
I am writing my PhD thesis, which includes my one published, and one in press papers in JOSA A. I would appreciate receiving permission to publish the following articles in my thesis.

1- Allen, H.A, Hess, R.F., **Mansouri, B**. & Dakin, S. (2003) Integration of first and second-order orientation.. J. Opt. Soc. Am. A. 20, 974-986

2- **Mansouri, B.**, Hess, R.F., Allen, H.A., & Dakin, S.C. (2005). Integration, segregation, and binocular combination. *Journal of Optical Society of America A: Optics, Image Sciences, and Vision, 22* (1), 38-48.

Best regards,
Behzad Mansouri M.D.
McGill Vision Research
687 Pine Ave. W., Rm H4-14
Montreal, Canada H3A 1A1
Tel: (514) 842-1231 Ext: 35307
Fax: 843-1691

Dr. Steven Dakin
Institute of Ophthalmology
University College London
11 - 43 Bath Street
London EC1V 9EL

Tel: 020 7608 6988
Email: s.dakin@ucl.ac.uk
Web: www.homepages.ucl.ac.uk/dakin

Institute of
Ophthalmology

Behzad Mansouri M.D.
McGill Vision Research
687 Pine Ave. W., Rm H4-14
Montreal, Canada H3A 1A1

10th February 2003

Dear Dr Mansouri

This letter gives my consent for you to publish from any of the following papers within your thesis:

2003	Allen, H.A., Hess, R.F., Mansouri, B., and Dakin, S.C. Integration of first- and second-order orientation information. *Journal of the Optical Society of America A*, **20**, 974-986
2004	Mansouri, B., Allen, H.A., Hess, R.F., Dakin, S.C., and Ehrt, O. Integration of orientation information in amblyopia. *Vision Research*, **44**, 2955-2969.
In Press	Mansouri, B., Hess, R.F. Allen, H.A., and Dakin, S.C. Integration, segregation and binocular combination. *Journal of the Optical Society of America A*

Sincerely

Steven Dakin

Behzad Mansouri M.D.
McGill Vision Research
687 Pine Ave. W., Rm H4-14
Montréal, H3A 1A1
Canada

I consent to the publication of the paper "Integration of orientation information in amblyopia." by Mansouri B, Allen HA, Hess RF, Dakin SC, Ehrt O. in Behzad Mansouri's thesis.

Oliver Ehrt

PD Dr. Oliver Ehrt
Department of Ophthalmology
University of Muenchen
Germany

I give you my consent to include the published papers that we are co-authored on, in their original form with suitable acknowledgements.

Harriet Allen

Brain and Behavioural Sciences
School of Psychology
University of Birmingham
Edgbaston
B15 2TT
UK

Ethics approval

Centre universitaire de santé McGill
McGill University Health Centre

Bureau d'éthique de la recherche
Office of Research Ethics

September 27, 2004

Dr. Robert F. Hess
McGill Vision Research
H4.14

REB NO. MED-B 96-259

RE: Neural Dysfunction in Human Amblyopia

Dear Dr. Hess:

Thank you for submitting the Application for Continuing Review for the research study referenced above. The report was presented for Full Board review at the convened meeting of the Biomedical-B Committee of the Research Ethics Board on September 21, 2004 was found to be acceptable for ongoing conduct at the McGill University Health Centre, and was entered accordingly, into the minutes of the meeting. The re-approval for the study was provided until September 18, 2005 and no revision to the approved consent document is required at this time.

At the MUHC, sponsored research activities that require US federal assurance are conducted under Federal Wide Assurance (FWA) 00000840.

All research involving human subjects requires review at a recurring interval. It is the responsibility of the investigator to submit an Application for Continuing Review to the REB prior to expiration of approval to comply with the regulation for continuing review of "at least once per year".

However, should the research conclude for any reason prior to the next required review, you are required to submit a Termination Report to the Committee once the data analysis is complete to give an account of the study findings and publication status. Should any revision to the study, or other unanticipated development occur prior to the next required review, you must advise the REB without delay. Regulation does not permit initiation of a proposed study modification prior to REB approval for the amendment.

Sincerely,

Leonard Moroz, MD.
Chair, Biomedical-B Committee
RVH Research Ethics Board

Centre universitaire de santé McGill
McGill University Health Centre

Bureau d'éthique de la recherche
Office of Research Ethics

September 27, 2004

Dr. Robert F. Hess
McGill Vision Research
H4.14

REB NO. MED-B 96-259

RE: Neural Dysfunction in Human Amblyopia

Dear Dr. Hess:

Thank you for submitting the Application for Continuing Review for the research study referenced above. The report was presented for Full Board review at the convened meeting of the Biomedical-B Committee of the Research Ethics Board on September 21, 2004 was found to be acceptable for ongoing conduct at the McGill University Health Centre, and was entered accordingly, into the minutes of the meeting. The re-approval for the study was provided until September 18, 2005 and no revision to the approved consent document is required at this time.

At the MUHC, sponsored research activities that require US federal assurance are conducted under Federal Wide Assurance (FWA) 00000840.

All research involving human subjects requires review at a recurring interval. It is the responsibility of the investigator to submit an Application for Continuing Review to the REB prior to expiration of approval to comply with the regulation for continuing review of "at least once per year".

However, should the research conclude for any reason prior to the next required review, you are required to submit a Termination Report to the Committee once the data analysis is complete to give an account of the study findings and publication status. Should any revision to the study, or other unanticipated development occur prior to the next required review, you must advise the REB without delay. Regulation does not permit initiation of a proposed study modification prior to REB approval for the amendment.

Sincerely,

Leonard Moroz, MD.
Chair, Biomedical-B Committee
RVH Research Ethics Board

Un hôpital de l'université McGill *A McGill University Teaching Hospital*

687, avenue des Pins ouest, H4.33, Montréal, Québec H3A 1A1 ·

ELSEVIER

22 November 2004

Our Ref: HG/jj/Nov04/J366
Your Ref:

Dr Behzad Mansouri
McGill Vision Research
687 Pine Ave. W., Rm H4-14
Montreal
Canada H3A 1A1

Dear Dr Behzad Mansouri

VISION RESEARCH, (submitted), Mansouri et al: "Detection, discrimination and integration ..."

As per your letter dated 18 November 2004, we hereby grant you permission to reprint the aforementioned material at no charge **in your thesis** subject to the following conditions:

1. If any part of the material to be used (for example, figures) has appeared in our publication with credit or acknowledgement to another source, permission must also be sought from that source. If such permission is not obtained then that material may not be included in your publication/copies.

2. Suitable acknowledgment to the source must be made, either as a footnote or in a reference list at the end of your publication, as follows:

   "Reprinted from Publication title, Vol number, Author(s), Title of article, Pages No., Copyright (Year), with permission from Elsevier".

3. Reproduction of this material is confined to the purpose for which permission is hereby given.

4. This permission is granted for non-exclusive world **English** rights only. For other languages please reapply separately for each one required. Permission excludes use in an electronic form. Should you have a specific electronic project in mind please reapply for permission.

5. This includes permission for the National Library of Canada to supply single copies, on demand, of the complete thesis. Should your thesis be published commercially, please reapply for permission.

Yours sincerely

HGainford

Helen Gainford
Rights Manager

Your future requests will be handled more quickly if you complete the online form at
www.elsevier.com/wps/find/obtainpermissionform.cws_home/obtainpermissionform

ELSEVIER

22 November 2004

Our Ref: HG/jj/Nov04/J365
Your Ref:

Dr Behzad Mansouri
McGill Vision Research
687 Pine Ave. W., Rm H4-14
Montreal
Canada H3A 1A1

Dear Dr Behzad Mansouri

VISION RESEARCH, Vol 44, No 25, 2004, pp 2955-2969, Mansouri et al: "Integration of orientation ..."

As per your letter dated 18 November 2004, we hereby grant you permission to reprint the aforementioned material at no charge **in your thesis** subject to the following conditions:

1. If any part of the material to be used (for example, figures) has appeared in our publication with credit or acknowledgement to another source, permission must also be sought from that source. If such permission is not obtained then that material may not be included in your publication/copies.

2. Suitable acknowledgment to the source must be made, either as a footnote or in a reference list at the end of your publication, as follows:

   "Reprinted from Publication title, Vol number, Author(s), Title of article, Pages No., Copyright (Year), with permission from Elsevier".

3. Reproduction of this material is confined to the purpose for which permission is hereby given.

4. This permission is granted for non-exclusive world **English** rights only. For other languages please reapply separately for each one required. Permission excludes use in an electronic form. Should you have a specific electronic project in mind please reapply for permission.

5. This includes permission for the National Library of Canada to supply single copies, on demand, of the complete thesis. Should your thesis be published commercially, please reapply for permission.

Yours sincerely

HGainford

Helen Gainford
Rights Manager

Your future requests will be handled more quickly if you complete the online form at
www.elsevier.com/wps/find/obtainpermissionform.cws_home/obtainpermissionform

From: "Lehman, Susannah" <SLEHMA@osa.org>
Subject: **RE: permission to include papers in my thesis**
Date: November 19, 2004 12:08:05 PM EST
To: bmanso1@po-box.mcgill.ca

The Optical Society of America considers the below requested use of its copyrighted material to be allowed under the OSA Author Agreement submitted by the requestor on acceptance for publication of his/her manuscript. It is requested that a complete citation of the original material be included in any publication.

Susannah Lehman

Authorized Agent

Optical Society of America

From: Behzad Mansouri [mailto:bmanso1@po-box.mcgill.ca]
Posted At: Thursday, November 18, 2004 4:09 PM
Posted To: ADS
Conversation: permission to include papers in my thesis
Subject: permission to include papers in my thesis

Dear Sir/ Madam,
I am writing my PhD thesis which includes my one published and one in press papers in JOSA A. I would appreciate receiving permission to publish the following articles in my thesis.

1- Allen, H.A, Hess, R.F., **Mansouri, B**. & Dakin, S. (2003) Integration of first and second-order orientation. . J. Opt. Soc. Am. A. 20, 974-986

2- (in press) Integration, segregation, and binocular combination
Behzad Mansouri and Robert F. Hess Harriet A. Allen Steven C. Dakin (2005)

Best regards,

Behzad Mansouri M.D.
McGill Vision Research
687 Pine Ave. W., Rm H4-14
Montreal, Canada H3A 1A1
Tel: (514) 842-1231 Ext: 35307
Fax: 843-1691

From: Harriet Allen <H.A.Allen@bham.ac.uk>
Subject: **Re: permission for publishing papers in my thesis**
Date: November 19, 2004 3:27:42 AM EST
To: Behzad Mansouri <bmanso1@po-box.mcgill.ca>

Hi Behzad

Is an email enough? If so, I give you my consent to include the published papers that we are co-authored on, in their origial form with suitable acknowledgements.

If email is not sufficient, please let me know.

Harriet

Harriet Allen
Brain and Behavioural Sciences
School of Psychology
University of Birmingham
Edgbaston
B15 2TT
UK

Behzad Mansouri wrote:

> Dear all,
> I will publish our common paper in my thesis. I have to have your written consent before that. I would appreciate if you could send me your consents.
>
> All the best,
> Behzad Mansouri M.D.
> McGill Vision Research
> 687 Pine Ave. W., Rm H4-14
> Montreal, Canada H3A 1A1
> Tel: (514) 842-1231 Ext: 35307
> Fax: 843-1691

Behzad Mansouri M.D.
McGill Vision Research
687 Pine Ave. W., Rm H4-14
Montréal, H3A 1A1
Canada

I consent to the publication of the paper "Integration of orientation information in amblyopia." by Mansouri B, Allen HA, Hess RF, Dakin SC, Ehrt O. in Behzad Mansouri's thesis.

Oliver Ehrt

PD Dr. Oliver Ehrt
Department of Ophthalmology
University of Muenchen
Germany

Dr. Steven Dakin
Institute of Ophthalmology
University College London
11 - 43 Bath Street
London EC1V 9EL

Tel: 020 7608 6988
Email: s.dakin@ucl.ac.uk
Web: www.homepages.ucl.ac.uk/dakin

UCL

Institute of
Ophthalmology

Behzad Mansouri M.D.
McGill Vision Research
687 Pine Ave. W., Rm H4-14
Montreal, Canada H3A 1A1

10th February 2003

Dear Dr Mansouri

This letter gives my consent for you to publish from any of the following papers within your thesis:

2003	Allen, H.A., Hess, R.F., Mansouri, B., and Dakin, S.C. Integration of first- and second-order orientation information. *Journal of the Optical Society of America A,* **20**, 974-986
2004	Mansouri, B., Allen, H.A., Hess, R.F., Dakin, S.C., and Ehrt, O. Integration of orientation information in amblyopia. *Vision Research,* **44**, 2955-2969.
In Press	Mansouri, B., Hess, R.F. Allen, H.A., and Dakin, S.C. Integration, segregation and binocular combination. *Journal of the Optical Society of America A*

Sincerely

Steven Dakin

McGill

McGILL VISION RESEARCH
Dept. of Ophthalmology
687 Pine Avenue West, Rm. H4-14
Montreal, Quebec, Canada H3A 1A1
Tel (514) 843-1690 Fax (514) 843-1691
Personal Line (514) 934-1934 Ext.-34757

15th December, 2004

Dear Dr Mansouri,

Re: Ph.D. Thesis seminar, 26th November 2004

On behalf of the Graduate program Committee may I congratulate you on an excellent seminar presentation. The committee's suggestions for future presentations of the work included: a slide to present the hypotheses to be tested, and some additional reference to the relevant literature. The members of the committee agreed unanimously that you have fulfilled the course requirement for presentation of the Ph.D research seminar. The other requirements of the Ph.D. degree in the program of neurological sciences have been completed except for the thesis submission.

The members of the committee agreed that you have a strong data set to write up into a PhD thesis and no further experiments are required. Please note that PhD theses including published papers should include additional sections linking ms together and an Introduction and Discussion chapter.

Yours sincerely,

Kathy Mullen, Ph.D.
(Committee Chair)

Cc. Graduate Program Office, Drs Robert Hess, Curtis Baker, and Rick Gurnsey